SED

Student Experiment Documentation

Document ID: RX-SED_REMOS-v5_0-12Jul11.doc

Mission:REXUS 9

Team Name: REMOS

Experiment Title: **RE**cession **MO**nitoring **S**ystem

Team	Name	University
Student Team Leader:	Robert Wuseni	Stuttgart
Team Members:	Christian Blank	Stuttgart
	Marcel Düring	Stuttgart
	Alena Probst	Stuttgart
	Serina Latzko	Stuttgart
	Salome Schweikle	Stuttgart
	Uwe Sauter	Stuttgart

Version:	Issue Date:	Document Type:	Valid from:
5.0	**22 July 2014**	**Spec**	**10 July 2010**

Issued by:

Experiment Scientist

Approved by:

Payload Manager

Change Record

Version	Date	Changed chapters	Remarks
0	2008-12-18	New Version	Blank Book 2010
1	21.01.2010	all	PDR
2	25.05.2010	3-6, 1.4.2	CDR Added PDR recommendations
2.1	26.06.2010	2.4, 4.6.1, 4.9.5, 6, 7.1, A	
3	11.10.2010	5.3, 3.2, 3.3, 3.4, 3.5, 4.4.2, 4.5.2, 5.1, 5.3, A.C.3	IPR
3.1	21.11.2010	1.3, 1.4.2, 4.2.2, 4.4.2, 4.7, 4.9, 5.1, 5.3, 6.1, C.1, C.3	Proof read small corrections, general actualization
4	10.02.2011	3.2, 3.3.2, 4.4.2, 6.3, D	Pre-Campaign
5	12.07.2011	3.3.2, 3.5, 7,B	Final report

Abstract: REMOS stands for REcession MOnitoring System and will be the experiment in the nosecone of a REXUS rocket flying in February 2011. The goal of the REMOS project is to develop a system enabling in situ measurements of the thickness of ablative heat-shields of re-entry vehicles by means of monitoring the material’s electric properties. It shall be tested during atmospheric re-entry of the REXUS rocket in order to prove the system's applicability to future ablative thermal protection systems.

During the down-leg of the REXUS trajectory, a probe consisting of ablator material will be exposed to the re-entry flow. It’s recession due to thermal loads is monitored using electrical and optical systems. When sensor material is ablated due to high thermal loads, the electrical properties of the sensor change, thus indicating how much of the shield was lost. A camera is foreseen for validation of the evaluated data being stored and transmitted to the ground-station directly.

The REMOS team consists of students of aerospace engineering at the University of Stuttgart and is supported by the DLR in Stuttgart.

Keywords: REXUS, REMOS, REcession MOnitoring System

CONTENTS

ABSTRACT

REMOS stands for REcession MOnitoring System and will be the experiment in the nosecone of a REXUS rocket flying in February 2011. The goal of the REMOS project is to develop a system enabling in situ measurements of the thickness of ablative heat-shields of re-entry vehicles by means of monitoring the material’s electric properties. It shall be tested during atmospheric re-entry of the REXUS Rocket in order to prove the system's applicability to future ablative thermal protection systems.

During the down-leg of the REXUS trajectory, a probe consisting of ablator material will be exposed to the re-entry flow. It’s recession due to thermal loads is monitored using electrical and optical systems. When sensor material is ablated due to high thermal loads, the electrical properties of the sensor change, thus indicating how much of the shield was lost. A camera is foreseen for validation of the evaluated data being stored and transmitted to the ground-station directly.

Space vehicles require high-performance thermal protection systems (TPS) that provide high temperature insulation capability with low weight, high strength and reliable integration with the sub-structure. Damage or failure of TPS cannot be tolerated as its integrity before each launch and re-entry is essential to the success of the mission. Consequently, knowledge of the heat-shield recession is important for the design of new reusable launch vehicles in order to reduce life-cycle cost, to increase safety margins and to improve mission reliability.

The REMOS team consists of students of aerospace engineering at the University of Stuttgart and is supported by the DLR in Stuttgart.

1 INTRODUCTION

1.1 Scientific/Technical Background

Atmospheric re-entry is one of the most challenging tasks in the design of space missions as it requires a thermal protection system (TPS) that keeps the massive amount of heat away from the spacecraft's sensible structure and on manned missions its passengers.
To do so, many TPS use the concept of ablative cooling. This means that a heat-shield usually made from ceramic or carbon phenolic materials will char, melt and sublime by the process of pyrolysis because of the high thermal loads. Thereby a lot of thermal energy is going into chemical energy. Additionally, these processes influence the boundary layer of the re-entry flow and reduce the heat flux from the surrounding plasma to the re-entry vehicle.
Ablative heat-shields are a proven and often used technology. The processes however, are still not very fully understood and heat-shield design is working with high safety margins leading to even heavier systems.
One reason for oversized TPS is the small data basis on their real behaviour during the flight. Experimental setups like plasma wind tunnel tests are very expensive and can only partly simulate real conditions.

Our idea is to develop and test a system that allows for measuring the recession rates of ablative heat-shields on a wide range of missions.
This time-resolved data from the operational phase can then be coupled with other flight data. Together, they can then provide a valuable basis for redesigning existing systems and finding more sophisticated future ablative TPS.

As temperatures during re-entry of the REXUS rocket will not be as high as for an (inter)planetary return mission, a different ablative material will be used. The main focus lies on the demonstration of the measuring principles and the measuring and monitoring system in realistic conditions. The probe material is "rolled" on a cylindrical shape in order to guarantee good flow conditions and comparable geometrical conditions.

1.2 Experiment Objectives

Objective ID	Objective	Type	Priority
OBJ1	To test a system for monitoring the change in thickness (recession) of an ablative heat-shield on the entire surface of the heat-shield	scientific	primary
OBJ2	measure electrical material characteristics for monitoring the recession	scientific	primary
OBJ3	Use video data for experiment verification	technical	primary
OBJ4	Investigate the transferability to larger scales	scientific	secondary
OBJ5	Gather video data for public relations usage	other	secondary

Table 1-1: Experiment objectives

1.3 Experiment Overview

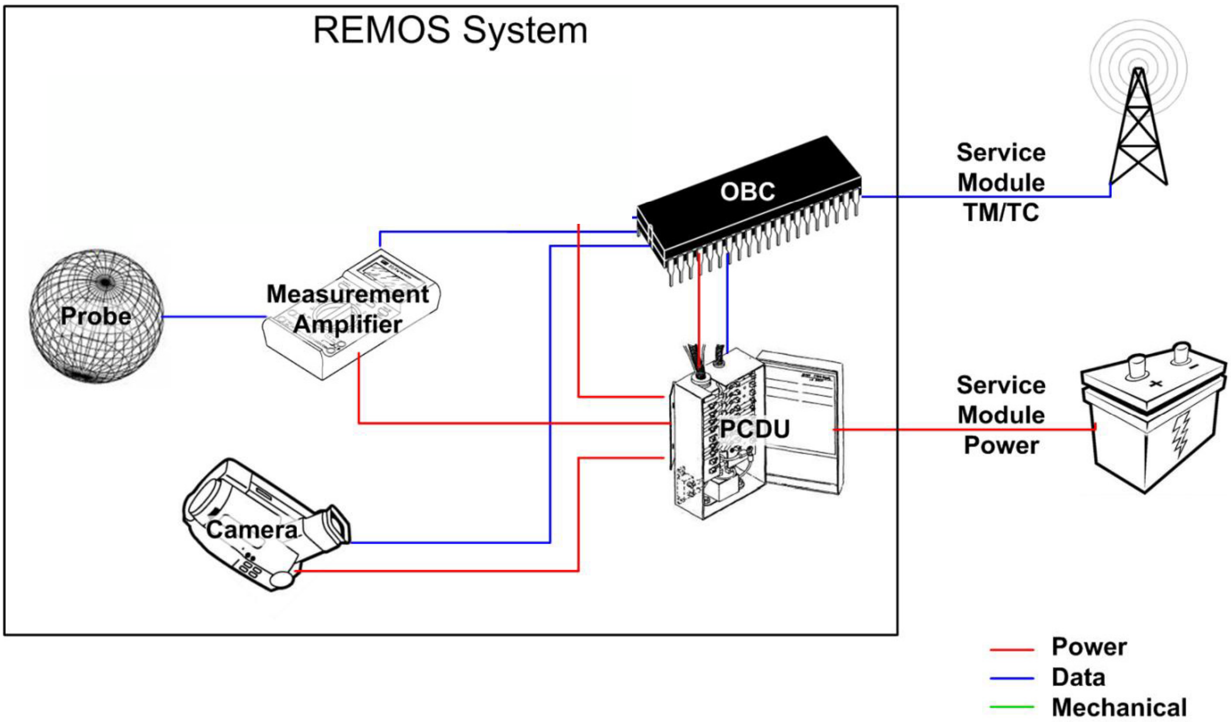

Figure 1-1: Experiment components

The REMOS experiment is located under the nosecone of the REXUS rocket. It consists of two main functional components: The probe and the monitoring system. The probe is attached to a boom in order to be in the less disturbed flow and contains the electrical sensor units. This boom is mechanically connected to a cylindrical support structure that protects the rest of the system. Inside are the two autonomous camera systems providing visual data of the probe through windows The central electronics for processing and storing the sensor data and controlling the system is also housed there and connected to the REXUS infrastructure.

During the re-entry phase the system will be active and acquire, process, save and transmit sensor data providing information about the recession rate of the probe.

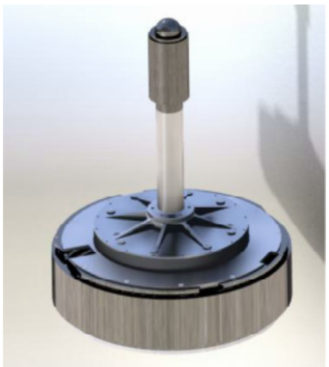

Figure 1-2: REMOS Experiment configuration

1.4 Team Details

1.4.1 Contact Point

Postal address:

DLR Institute of Structures and Design

Dr. Hannah Böhrk

Pfaffenwaldring 38-40

70569 Stuttgart

E-Mail:

Kontakt@remos-stuttgart.de Hannah.Boehrk@dlr.de

Website:

www.remos-stuttgart.de

1.4.2 Team Members

Robert Wuseni

Studies:	- University of Stuttgart, aerospace engineering
Internships:	- 6 week at VW Company Kassel
	- 2 weeks at MGM Mannheim aluminium foundry
	- 6 month at EADS Astrium Friedrichshafen, structures department
Other Experiences:	- student assistant for the fuel cell aircraft Hydrogenius at the University, responsible for cooling electronics design
	- Space Station Design Workshop (SSDW), IRS Stuttgart
REMOS position:	- project management
	- mechanical design

Serina Latzko

Studies:	- University of Stuttgart, aerospace engineering
Internships:	- DLR Stuttgart, electrical properties of ceramics
REMOS position	- probe development
	- GSE

Salome Schweikle

Studies:	- Galileo University Guatemala, (electronic) systems engineering
	- University of Stuttgart, aerospace engineering
Internships:	- 8 weeks Daimler Chrysler
	- 6 months at Astrium ST, Friedrichshafen
Other Experiences:	- student assistant for EXPERT re-entry project at the University
	- Space Station Design Workshop (SSDW), IRS Stuttgart
REMOS position	- onboard electronics
	- onboard software

Christian Blank

Studies: - University of Stuttgart, aerospace engineering

Internships: - 6 month at CNRS Orléans, France, thermal analysis on hall-effect thrusters

Other Experiences: - student assistant at the institute of Space Systems Stuttgart

- Space Station Design Workshop

REMOS position: - thermal analysis

- outreach

Alena Probst

Studies: - University of Stuttgart, aerospace engineering

Internships: - 5 months at EADS Astrium Satellites in Friedrichshafen; ProjectBepiColombo, an ESA satellite mission to Mercury in Phase B;Telemetry and Communication

- 5 months at ESA's European Astronaut Centre in Cologne; Basic Training Development and Implementation for the new ESA Astronaut Class

Other Experiences: - student assistant at the Institute of Space Systems (IRS), University of Stuttgart

- Space Station Design Workshop 2009, Stuttgart

REMOS position: - QA

- Outreach

- Risk Register

Marcel Düring

Studies: - University of Stuttgart, aerospace engineering

Final year subjects: aerodynamics, space systems

Study thesis - NASA Ames Research Center, Moffett Field, US
Topic: Investigations of Methods to Influence Resonance Characteristics of the SOFIA Telescope Cavity

Internships:	- 6 month at Airbus GmbH, Toulouse A380 Final Assembly Line
Other Experience:	- Space Station Design Workshop 2007,Sydney Australia
	- Google Lunar X-Price Student Competition, France
REMOS position:	- ground support software

Uwe Sauter

Studies:	- University of Stuttgart, aerospace engineering
Internships:	- 6 month at EADS Elbe Flugzeugwerke GmbH, Dresden, material research
Other Experiences:	- student assistant at the Institute of Flight Mechanics and Control (IFR), University of Stuttgart, X-Plane interface programming, RC model maintenance
	- student assistant at the Institute of Aircraft Design (IFB), University of Stuttgart, X-Plane model creation
	- student assistant at the High Performance Computing Center Stuttgart (HLRS) of the University of Stuttgart,
REMOS position:	- MGSE
	- Homepage

Figure 1-3: 4 Team members during final assembly in Stuttgart: Uwe Sauter, Marcel Düring, Serina Latzko, Robert Wuseni, Salome Schweikle, Christian Blank and Alena Probst (from left to right).

2 EXPERIMENT REQUIREMENTS

2.1 Functional Requirements

RQ ID	Functional Requirements	Derived from
FRQ.01	The sensing areas shall be integrated into the probe surface in such a way, that they act as part of the heat-shield	OBJ1
FRQ.02	Electric resistance of the sensing elements shall be measured at 8 locations during re-entry	OBJ2, OBJ1
FRQ.03*	Electrical capacitance between the sensing elements shall be measured at 8 locations during re-entry (This requirement has been modified, since the design of the probe is too small for 16 sensors.)	OBJ2,OBJ1
FRQ.04*	Temperatures on the Probe have to be measured at 8 locations during re-entry (This requirement has been modified, since the design of the probe is too small for 16 sensors.)	Pre-tests
FRQ.05	A camera system including a recording device has to observe the degradation of the probe	OBJ3, OBJ5
FRQ.06	All measurement and housekeeping data has to be stored on board	
FRQ.07	All measurement and housekeeping data has to be transmitted to the ground station	
FRQ.08	Housekeeping shall monitor the supply voltages	
FRQ.09	Housekeeping shall monitor the voltages behind all switchable supplies	
FRQ.10	Housekeeping shall monitor the hard wired signals	
FRQ.11	All transmitted data packets must have a unique time indication	
FRQ.12	All data storages have to survive the landing impact	
FRQ.13	Circuits must be tolerant to a short-circuit	

Table 2-1: Functional requirements

*requirement modified on 10.03.2010

2.2 Performance Requirements

RQ ID	Performance Requirements	Derived from
PRQ.01	The capacitance measurements shall have a resolution of 0.1% of the initial value	
PRQ.02	The resistance measurements shall have a resolution of 0.1% of the initial value	
PRQ.03	The measured maximum initial probe resistances must not exceed 500kOhms	
PRQ.04	The measured minimum initial probe resistances must not be below 5kOhms	
PRQ.05	The measured maximum initial probe capacitances must not exceed 1µF	
PRQ.06	The measured minimum initial probe capacitance must not be below 50pF	
PRQ.07	The temperature measurements on the probe shall be possible in a range of -100 to 500 degree centigrade	
PRQ.08	The temperature measurement on the probe shall be conducted with an accuracy within a range of +/- 2 degree centigrade	
PRQ.09	The system voltages shall be monitored with a resolution equal to or greater than +/- 0,1V	
PRQ.10	All measurements have to be done at a rate of 10 Hz	
PRQ.11	The camera frame rate shall be equal to or higher than 10Hz	

Table 2-2: Performance requirements

2.3 Design Requirements

RQ ID	Design Requirements	Derived from
DRQ.01	The experiment shall be designed for the nose section of the REXUS rocket	DLR

DRQ.02	The overall mechanical safety factor for structural failure is j=1.5	
DRQ.03	The experiment shall be designed to operate in the temperature profile of the REXUS rocket (see appendix for details)	RX User Manual 6.1
DRQ.04	The experiment shall be designed to operate in the vibration profile of the REXUS rocket (see appendix for details)	REXUS User Manual
DRQ.05	The experiment shall be designed to operate under the static acceleration loads of the REXUS rocket (see appendix for details)	RX User Manual Chap. 5.5.1
DRQ.06	For all 15l of empty volume, a venting hole with a diameter of 10mm has to be added. The hole has to be covered with a cap (see REXUS User Manual Chap. 5.4)	RX User Manual Sec.5.4
DRQ.07	The modules' internal thermal dissipation must not heat up the outer structure more than 10°C over the ambient ground temperature	RX User Manual Chap. 6.2.1
DRQ.08	The module's internal thermal dissipation must not heat up the parts close to or in contact with the feed-through cable to more than +70°C.	RX User Manual Chap. 6.2.2
DRQ.09	A module's internal thermal dissipation must not heat up parts facing other modules to more than +50°C.	RX User Manual Chap. 6.2.3
DRQ.10	The heat transport by convection must be limited in such a way that the air temperature at the module interfaces does not exceed the ambient temperature by more than 10 °C.	RX User Manual Chap. 6.2.4
DRQ.11	The electrical connector interface shall comply with the RX User Manual Chapter 7.6.1	RX User Manual Chap. 7.6.1
DRQ.12	The experiment TM/TC interface shall comply with the RS422 standard	
DRQ.13	The TM/TC protocol shall use a baud rate of 38,4kbit/s; format: 8 bits, 1stop bit, no parity	RX User Manual Chap. 7.6.2
DRQ.14	The experiment shall operate from a power supply from 24V to 36V	RX User Manual Chap. 7.6.4

DRQ.15	A short period peak power consumption shall not exceed 3 A on the RX power interface	RX User Manual Chap. 7.6.4
DRQ.16	The continuous current consumption shall not exceed 1 A	RX User Manual Chap. 7.6.4
DRQ.17	Optocouplers have to be used for the SODS, SOE and LO signals	RX User Manual Chap. 7.6.6
DRQ.18	A standard RS232 interface with 57.6kits/s, 8 data bits, 1 stop bit, no parity has to be used for the EGSE	RX user Manual Chap. 7.7
DRQ.19	All power supply cables shall be twisted	RX user Manual 7.11
DRQ.20	Data cables shall be twisted	RX user Manual 7.11
DRQ.21	Cables outside electronics boxes shall be shielded	RX user Manual 7.11
DRQ.22	The experiment shall operate under vacuum conditions	RX User Manual Chap 9.1
DRQ.23	The experiment has to be designed in such a way, that it can be classified as a category B system or lower, according to Esrange Safety Manual	Esrange Safety Manual Chap.5.2.4.2
DRQ.24	No flammable adhesives shall be used	Esrange Safety Manual

Table 2-3: Design requirements

2.4 Operational Requirements

RQ ID	Operational Requirements	Derived From
ORQ.01	The probe shall be covered after landing	
ORQ.02	The OB S/W shall be designed as a state machine	

ORQ.03	Breakout boxes shall be supplied for all electrical connections	
ORQ.04	The OB S/W shall have the capability to operate without ground support	
ORQ.05	For each flight phase a dedicated S/W mode shall exist	
ORQ.06	In a test mode all commands from GSE S/W shall be accepted	
ORQ.07	In S/W modes, that are not the test mode, only mode change commands shall be accepted (from SM only)	
ORQ.08	The data time stamp shall be synchronized before launch	
ORQ.09	The OB S/W shall be able to fly the mission only with the LO signal working	
ORQ.10	At re-entry the angle of attack shall be normal to the probe with an angle of variation of +/- 30°	

Table 2-4: operational requirements

3 PROJECT PLANNING

3.1 Work Breakdown Structure (WBS)

The work is distributed among the team members in such a way, that every member acts as an expert in a special field. The fields are:

- ☐ Project management
- ☐ Outreach
- ☐ Mechanics
- ☐ Thermal
- ☐ Electronics
- ☐ GSE
- ☐ Software

To account for interdependencies, the work is broken down into single tasks.

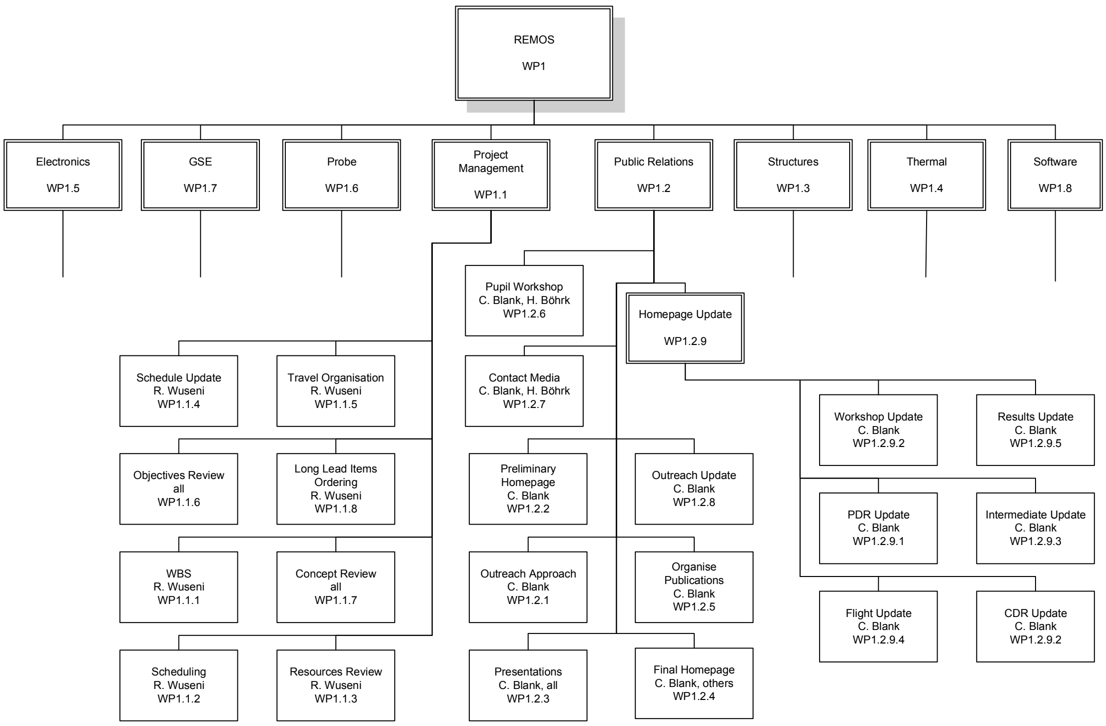

Figure 3-1: WBS top-level

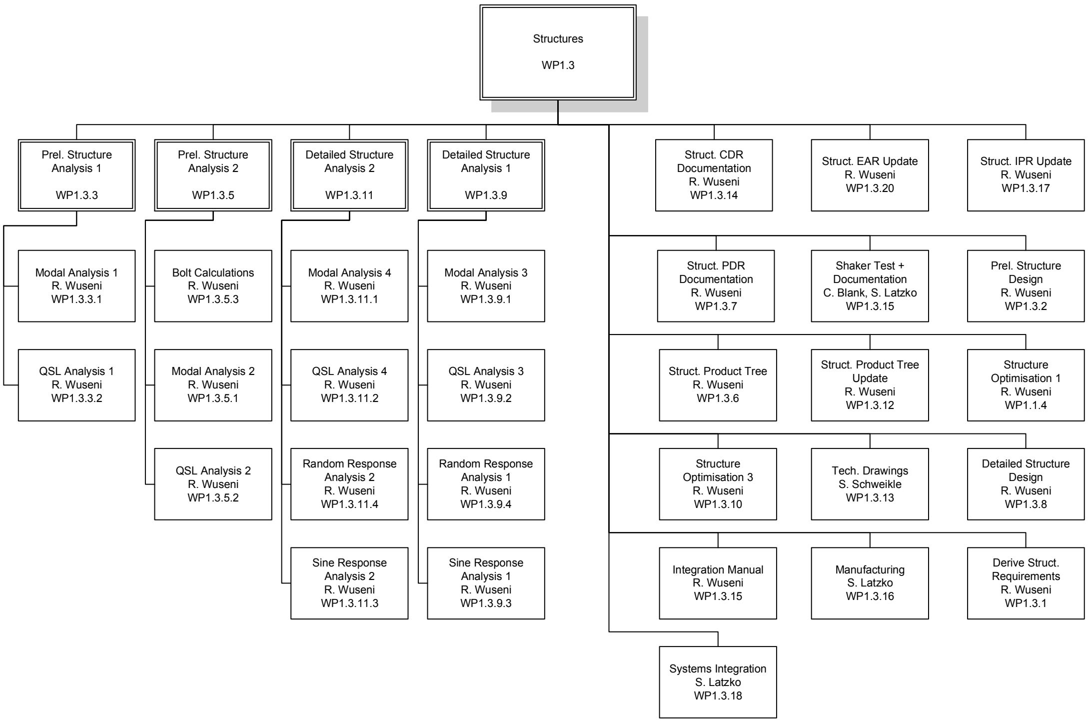

Figure 3-2: WBS structures

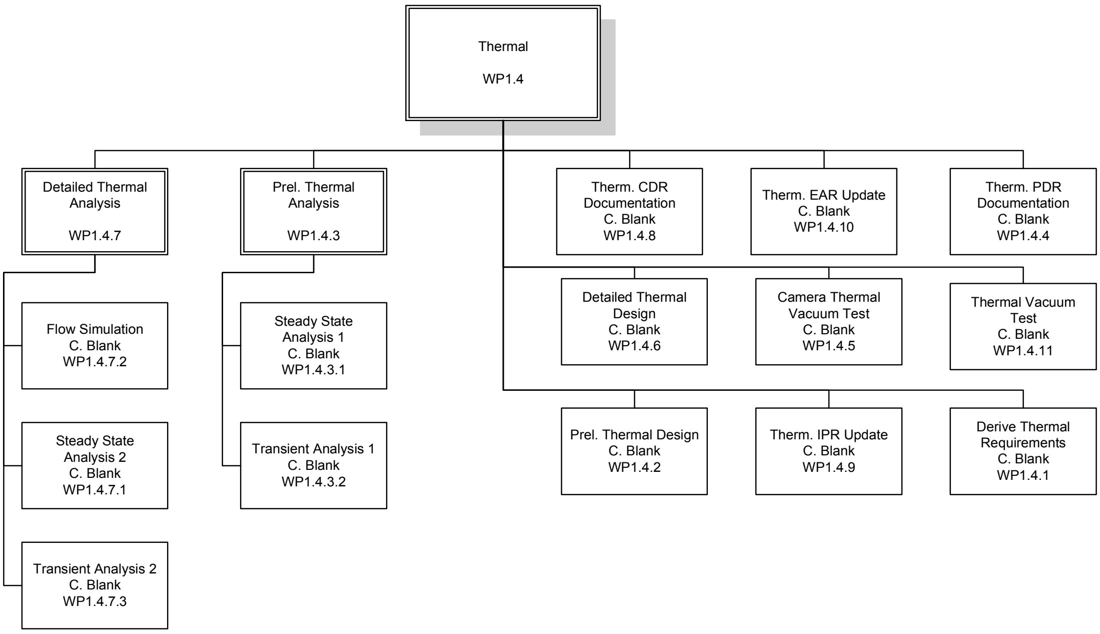

Figure 3-3: WBS thermal

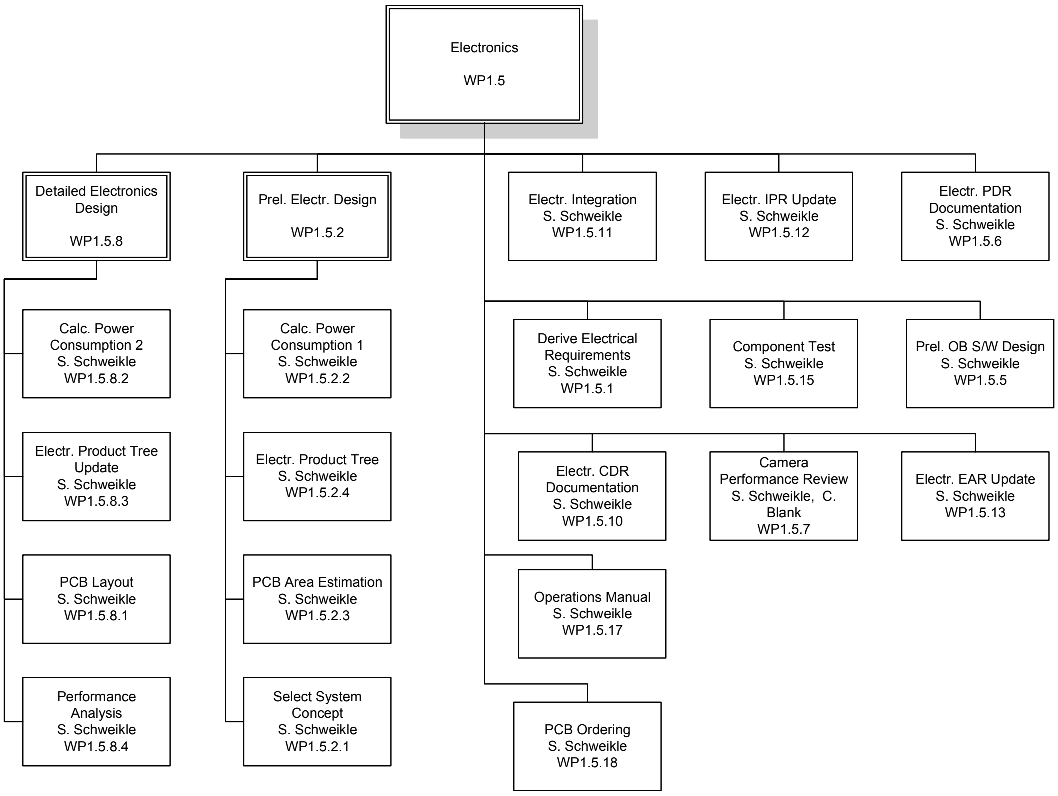

Figure 3-4: WBS electronics

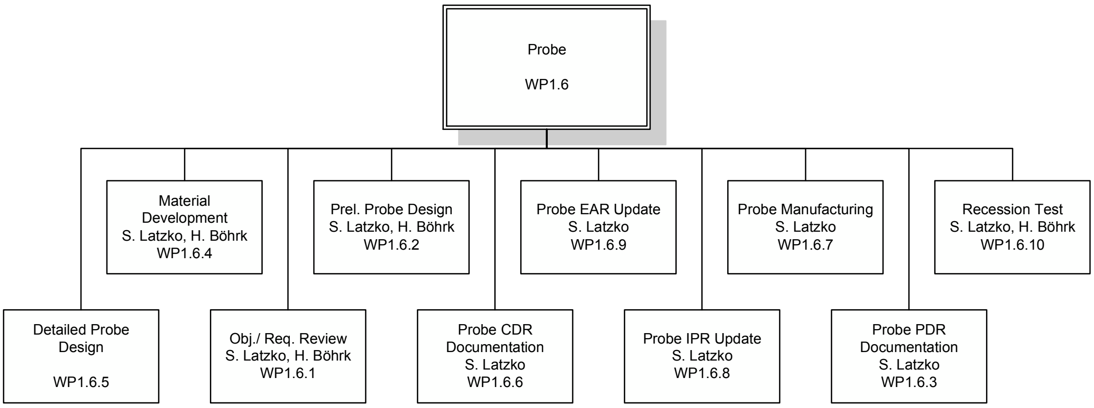

Figure 3-5: WBS probe development

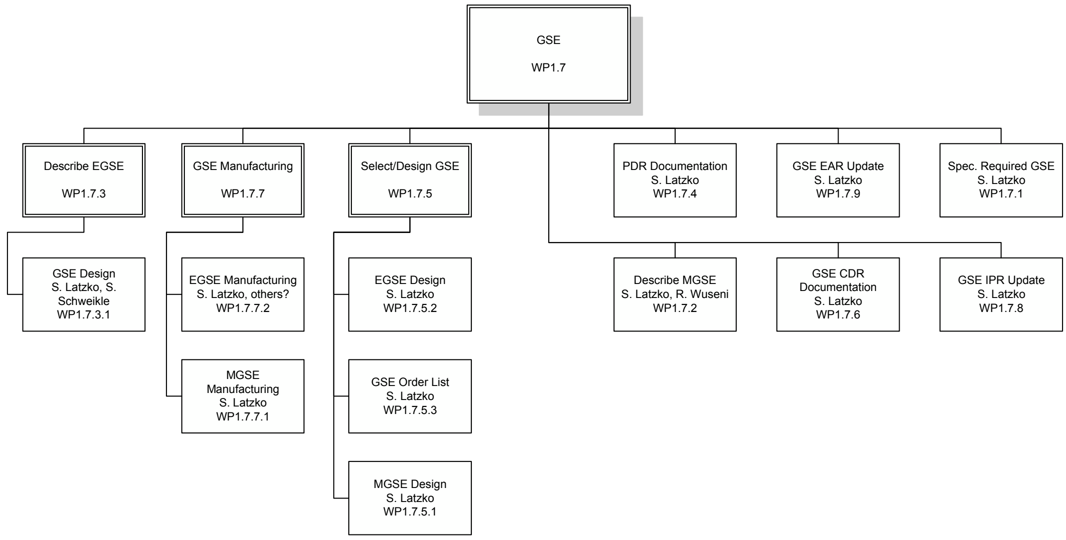

Figure 3-6: WBS GSE

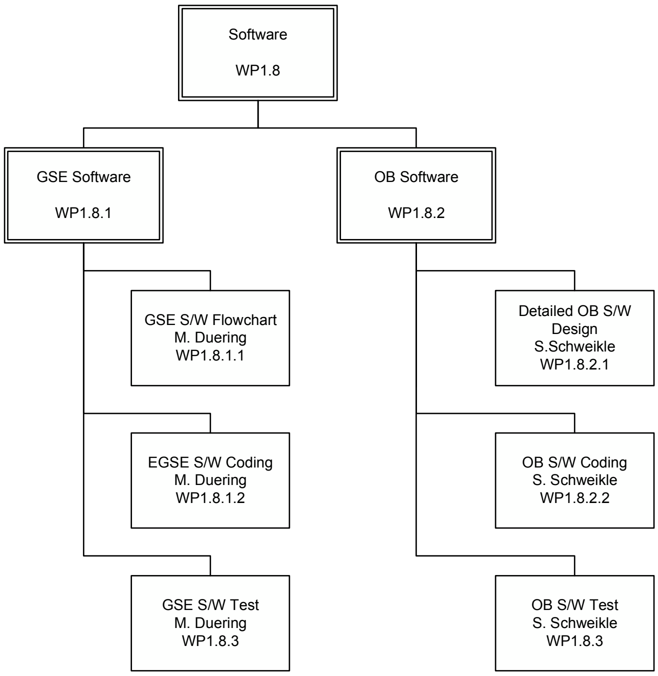

Figure 3-7: WBS software

3.2 Schedule

The following chart shows a reduced schedule. The tasks have also been listed with their WBS Code. For a more complete schedule see REMOS_project_plan_20110209_A1.pdf

(Last update: 08.02.2011)

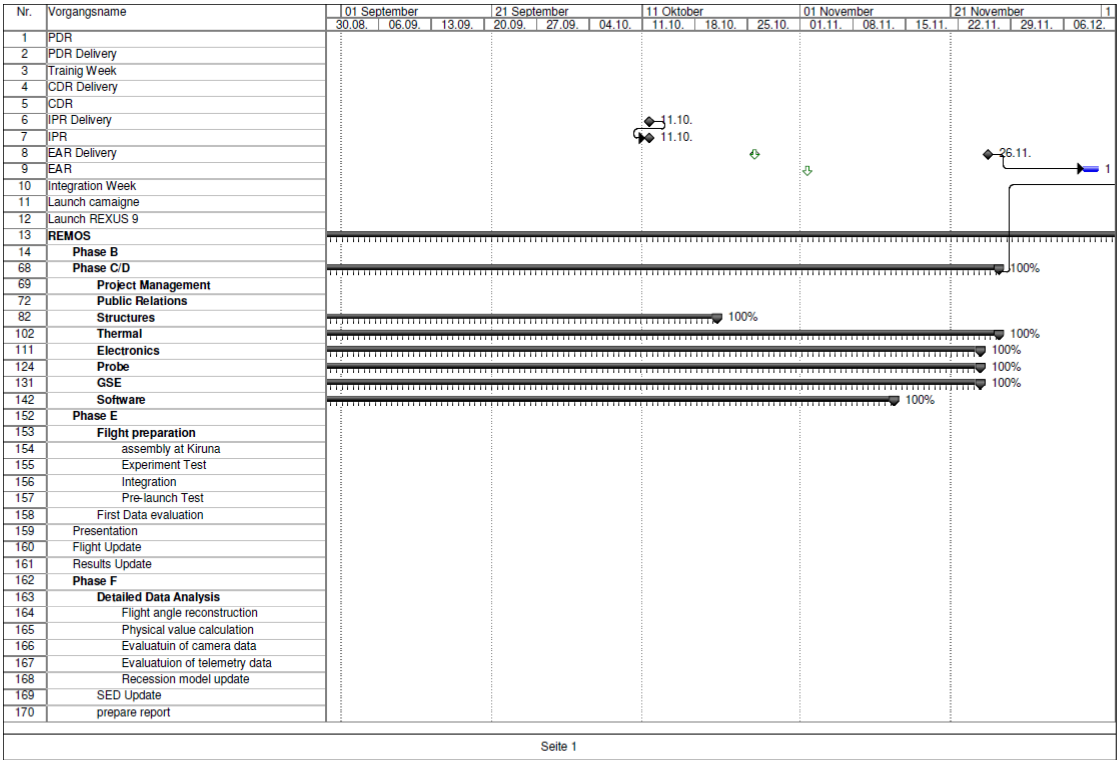

Figure 3-8: Schedule part 1

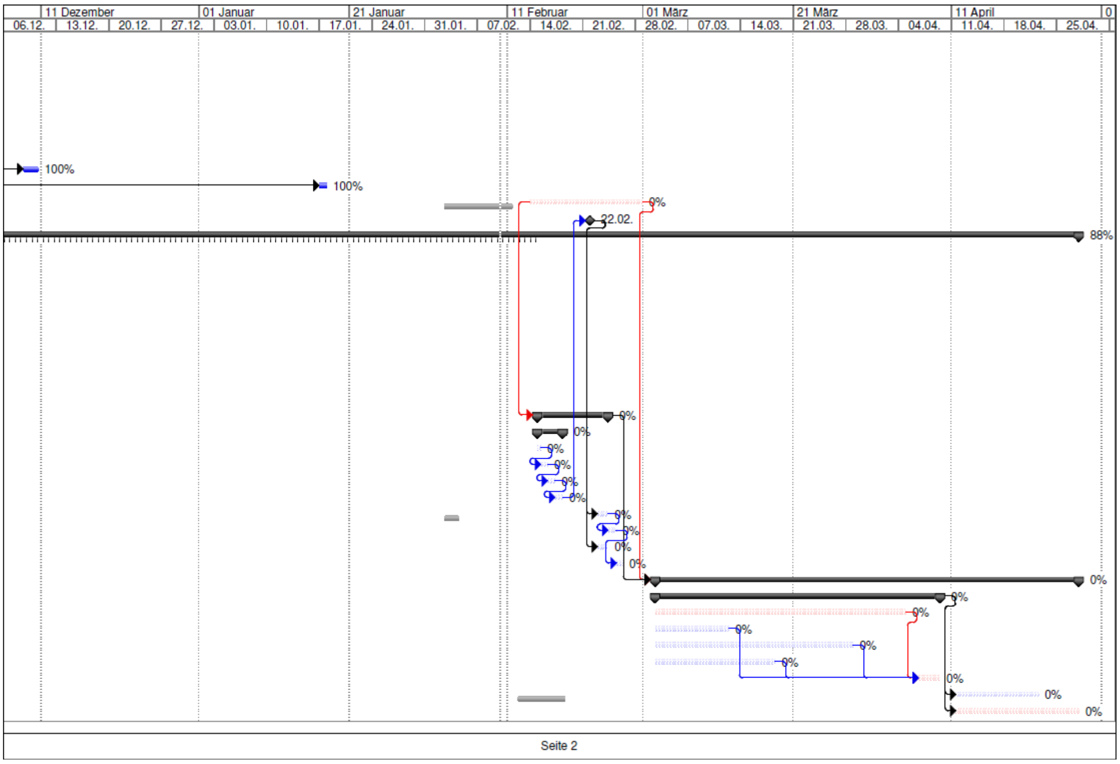

Figure 3-9: Schedule part 2

3.3 Resources

3.3.1 Manpower

Since the project is conducted in addition to regular university lectures, the workload is distribute in such a way, that the project can be performed by the six permanent team members with three to six hours per week.

<u>Team members:</u>

- ☐ Christian Blank
- ☐ Serina Latzko
- ☐ Salome Schweikle
- ☐ Robert Wuseni
- ☐ Marcel Düring
- ☐ Alena Probst
- ☐ Uwe Sauter

<u>Additional Help :</u>

- ☐ Hannah Böhrk

3.3.2 Budget

Expenditures	credit [€]	debit [€]
LBBW Sponsoring ([redacted])	[redacted]	[redacted]
PCB-POOL Platinen	[redacted]	[redacted]
Wilms Metall	[redacted]	[redacted]
Ebay Titan	[redacted]	[redacted]
Lötzubehör (Reichelt)	[redacted]	[redacted]
Alubox	[redacted]	[redacted]
Kleineisen Transportkiste	[redacted]	[redacted]
Schaumstoff Transportkiste	[redacted]	[redacted]
Conrad Kleinteile	[redacted]	[redacted]
Hornbach Klebstoffe	[redacted]	[redacted]
werbeaufkleber	[redacted]	[redacted]
	[redacted]	[redacted]

aldi_dichtungen		[redacted]
comerci_werkzeug		[redacted]
conrad_kleinteile2		[redacted]
conrad_kleinteile3		[redacted]
hohl_wasserstrahl		[redacted]
profi_markt2		[redacted]
toom_bohrer		[redacted]
TS_sicherungsscheiben		[redacted]
conrad_4		[redacted]
Sweatshirts "REMOS" (LBBW Anteil)		[redacted]
Sub total	[redacted]	[redacted]
DLR Bremen Sponsoring	[redacted]	
Shaker Adaptor		[redacted]
Cylinder Cover		[redacted]
Transportation Box interior		[redacted]
Breakoutbox (RS Elektronik)		[redacted]
Bestellliste vom 25.05. (Elektronikbox, Platinenteile, Aluteile)		[redacted]
Sub total	[redacted]	[redacted]
Bastlerzentrale Sponsoring ([redacted])	[redacted]	
Small Parts		[redacted]
Construction parts		[redacted]
Available		[redacted]
ACME Sponsoring	[redacted]	
Cameras (5 FlycamOne)		[redacted]
Micro SD Cards		[redacted]
HosttheNet Sponsoring	[redacted]	
Website		[redacted]

Atmel Corporation	[redacted]	
Tools for onboard software development		[redacted]
Kucera	[redacted]	
Color CCD Camera		[redacted]
DLR BK Stuttgart	[redacted]	
Probe Construction Materials		[redacted]
Travel Sponsoring		
Walther Blohm	[redacted]	
Studentenwerk Stuttgart	[redacted]	
Erich Becker Stiftung	[redacted]	
Bosch / Freunde der LRT	[redacted]	
Travel Expenses		
Train to Kiruna		[redacted]
Hotel Kiruna		[redacted]
Other Travel Expenses		[redacted]
Conference Fees Hyères sponsored by DLR	[redacted]	[redacted]
Conference Fees Hyères		[redacted]
Travel expenses to Hyères		[redacted]
Hotel Hyères		[redacted]
Tube material for probe cover		[redacted]
Material for mounting		[redacted]
Smal transportation box		
Stainless steel Screws		[redacted]
Team members contribution	[redacted]	
REMOS sweathirts (own contribution)		[redacted]
Total	**10668**	**10668**

Table 3-1: REMOS Budget

All costs for the experiment have been covered by REXUS/BEXUS. For all additional costs sponsorships have been acquired.

3.3.3 External Support

Sponsored homepage hosting	Hostthenet (sitorixGmbH)
Workshop	DLR Stuttgart
Test facilities	IRS Uni Stuttgart (vac. chamber) DLR Stuttgart (shaker) IEH Uni Stuttgart (EMC- chamber)
Financial Support	DLR Stuttgart LBBW Bank Foundation
Development hardware	ATMEL
Parts	Bastlerzentrale Stuttgart
Glass Fibre parts	Fibre Pipe

Table 3-2: Team support

3.4 Outreach Approach

The public outreach concept of the REMOS Project is organized in several phases – simultaneous to the overall project phases:

Until February 2010 (A,B)	Abstract, establish contact, logo, web design, operational website and mailing system
C before CDR	Website complete, Pupil workshop, first texts for print publications
D	Media coverage, Documentation, also produce Stickers/ T-Shirts,...
E During Mission operations	Livestream, Blog, Newsletter
F Post flight activity	Paper at ESA Conference, EUROAVIA

Table 3-3: Outreach timeline

Basis for contact and information is our website that consequently needs to be updated regularly. The structure as a wiki allows every team member to add news and update information very easily.

The address is www.remos-stuttgart.de . This URL also provides E-mail functionality for every team member and contact addresses for functions within the team.

An important point is documentation of our activities with pictures as well as short “diary entries” on the website (see “News”) in order to keep interested people up to date with the project.

Promotion at the University is done in close cooperation with the EXPLORE team (common presentations, newsletter articles and on the Institute’s website).

This year’s Yuri’s night in Stuttgart was organized by EXPLORE and REMOS (www.yurisnight.de). We presented our experiments, offered a space quiz, models, a rocket building workshop and had a 1:1 printout of the REXUS rocket. The teams SQUID from Sweden and FOCUS from Munich also joined the public presentation.

Additionally, a workshop with pupils in Stuttgart was organized in May 2010, where we built small “rockets” propelled with water and baking soda. We had this as an event and explained our experiment to them using our poster. (See Appendix B)

February 2010: Article in Newsletter and on university website (see Appendix)

April 2010: Yuri’s Night with articles in two newspapers

May 2010: Pupil’s workshop

Figure 3-10: Experiments for children

The integration progress can be followed on our website and facebook group.

The launch campaign was also covered by blog posts, livestreams and a newsletter to the interested public.

After the launch campaign, presentations at university institutes were given, summary articles for magazines and a paper for the ESA PAC Symposium was written. (see Appendix B).

3.5 Risk Register

There are numerous risks to be monitored. They result in tests, safety measures and design decisions trying to minimize certain risks.

They are put in the following categories:

MS	mission(operational)	occurring during the mission (after delivery)
SF	safety	threatening safety of the mission
IM	implementation and testing	occurring during or due to implementation and testing
EL	electronics and software	occurring due to electronics and software
TC	other technical	occurring due to technical reasons
PE	personnel/team	occurring due to team problems

Table 3-4: Risk categories

The P (probability) and S (severity) are determined following the following categories

Probability (P)	corresponding letter in guidelines
1. Minimum – Almost impossible to occur	A
2. Low – Small chance to occur	B
3. Medium – Reasonable chance to occur	C
4. High – Quite likely to occur	D
5. Maximum – Certain to occur, maybe more than once	E

Severity (S)
1. Negligible – Minimal or no impact
2. Significant – Leads to reduced experiment performance
3. Major – Leads to failure of subsystem or loss of flight data
4. Critical – Leads to experiment failure or creates minor health hazards
5. Catastrophic – Leads to termination of the project, damage to the vehicle or

ID	Risk & consequence if not obvious	P	S	P x S	Action
MS 10	Responsible persons fall ill or cannot be present during mission	3	2	6	Have more team members informed, write good operations instructions
TC 10	Electrical connection between probe and EB is disturbed	2	3	6	see TC 11 - 14

TC 11	Cable connectors to the probe partly fail	1	4	4	use proper connectors, check function before flight
TC 12	Cables to the probe become too hot	1	3	3	thermal calculations, heat insulation, fix cables in the center of the mast
TC 13	Signals in cables disturb other measurements	1	3	3	separate cable trees, shield separately
TC 14	Soldered contacts to probe material melt	2	4	8	further investigations!
TC 15	Probe sections in contact because of melting silver glue	3	3	9	further investigations!
TC 16	Probe sections in contact because of assembly mistakes	1	3	3	Testing
TC 20	Unexpected thermal / flow conditions during re-entry	3	3	9	
TC 21	Probe is not ablated due to low loads	2	4	8	material selection, thermal analysis
TC 22	Probe is ablated very fast due to high loads	1	2	2	
MS 30	Camera doesn't see properly	3	3	9	use three cameras
MS 31	Dirt, condensation on the glass	3	3	9	
MS 32	wrong field of view	1	4	4	Fields of view checked in CAD
MS 33	Camera destroyed during flight	1	4	4	
MS 40	Data loss	1	5	5	excessive testing
MS 41	SD Card destroyed during/after impact	1	5	5	Use TV channel
MS 42	Rocket not recovered	1	5	5	Use TV channel, downlink
MS 43	Probe mast damages experiment box during impact	2	4	8	intentional weak point
MS 44	Probe is damaged during impact	5	1	5	camera data
MS 50	Downlink failure	1	3	3	onboard data storage

MS 60	No nosecone Separation	1	4	4	
MS 61	Launch delayed, team members cannot be present	2	2	4	write good operational instructions
MS 70	Probe is damaged during final assembly	2	5	10	protective cover, spare probe, easy exchange of probe
MS 71	Water or Ice condensing inside probe material	3	2	6	Analyze severity, protect probe
IM 11	Cooperating workshops cannot manufacture a certain part	1	5	5	All Parts are integrated or ordered
IM 20	Failure during testing	3	1	3	
IM 21	Critical structural component fails during early ground test	2	2	4	Shaker test 1 successful
IM 22	REXUS specifications not met during acceptance test	1	4	4	probability lowered by pre - testing
IM 23	REXUS specifications not met during early ground tests	3	2	6	attenuate severity by early testing
IM 24	Cameras fail during testing	3	2	6	early test of cameras, spare cameras available
EL 10	Measurement signals exceed system's measuring range	1	4	4	
EL 20	Signals from Service module are not received	1	5	5	internal timer after launch signal, checks
EL 21	Failure within a software module	2	4	8	software testing, separation of modules and modes
EL 30	Water condensing inside electronics box	2	2	4	
EL 31	Failure of component on the electronics board during testing	3	2	6	early testing, spare parts, not too complex board architecture
EL 32	Failure of component on the electronics board during mission	2	4	8	tests, qualification with high margins, redundancies

PE 10	Team member renegades	1	4	4	provide motivation and beer
PE 11	Team member unavailable for several weeks	2	2	4	documentation, project planning
PE 12	No qualification for a task within the team	2	2	4	project planning, task distribution, consult experts

Table 3-5: Risk register

Retrospectively, risk monitoring and managing was a success for all risks but TC21. Electronics, Probe and GSE all worked flawlessly. Lower thermal loads were anticipated due to a lower apogee, but the probe material was not changed. Post flight thermal analysis showed that the predicted temperatures were quite realistic.

4 EXPERIMENT DESCRIPTION

This section describes the experiment, including set-up, lay-out, wiring, and the according science as well as preliminary test results.

4.1 Experiment Setup

The core of the experiment is a cylindrical burn-off probe at the end of a ca. 200mm aluminium boom extending into the sonic shock in front of the vehicle after the nose cone is ejected. Because of the large shock radius of the rocket during the flat spin re-entry, the probe should be as distant as possible from the rocket to assure an unhindered flow onto the probe.

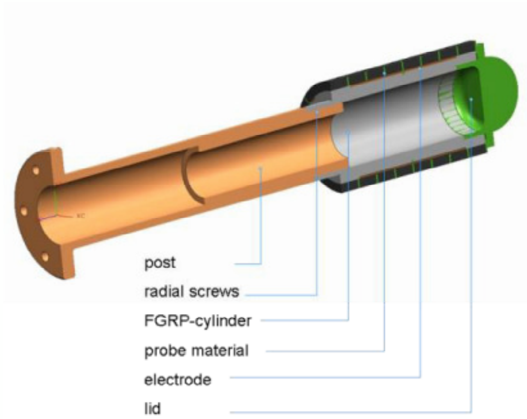

Figure 4-1: Probe layout

The connection between the boom and the fibre glass tube will be form-fit and additionally radially screwed. The probe itself is attached to the substrate of fibre glass reinforced plastics on top of the aluminium boom (see figure 4-1). For attaching the probe to the fibre glass conduit, 32 slabs of conductive foam will be glued to 2x4 foam squares in a symmetrical order, as you can see in the picture. Here, it will be important how the foam is cut because it will be necessary that the opposite areas of foam are really parallel although the material describes a bending. Therefore it will be necessary to cut a bevel at these areas as otherwise the electric field won't be sufficiently homogeneous. Between each of these foam slabs there will be thin ligaments out of Kapton foil which prevent contact serving as dielectric (displayed in green in figure 4-2).

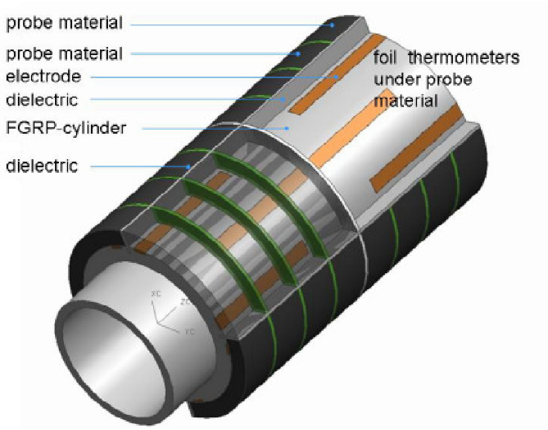

Figure 4-2: Probe Head View

Eight thin film thermometers will additionally be glued beneath each probe segment as it is essential to know the temperature during flight to give an interpretation of the results afterwards.

To provide for contact between the foam and the measurement wires, small bores will be drilled into the substrate so the copper contacts can be embedded which will be fixed to the foam using conductive adhesive with a high silver fraction. The measurement connections will also be glued to the copper contacts by conductive adhesive.

4.1.1 Probe - mechanical Layout

For the load of the probe the developing aside (fig. 4-3) is expected. The deflection was fixed at a value of 80g although it is not assumed this high during the flight. The length of the pipe is l=100mm, with g≈10m/s² an acceleration of about a=800m/s² exists. In the following it will be calculated with a small diameter of d=35mm and a big one of D=40mm (fig. 4-4). The real Diameter of D_r=50mm is not used because if calculated with D=40mm the real value of the load is smaller than the calculated one.

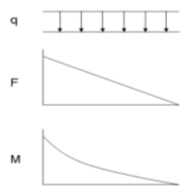

Figure 4-3: Load developing

The force G, which affects the probe in the simulated case of a=800m/s², is given by

$$G = ma\,. \tag{4.1}$$

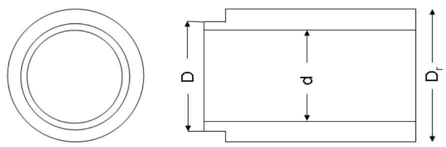

Figure 4-4: Diameters

The mass m of the pipe is equal to

$$m = \rho \cdot V\,. \tag{4.2}$$

With V=0,1dm³ and ρ=2,3kg/dm the mass is m=0,23kg. From this it follows that the force is G=184N.

The distributed load q is given by

$$G = q \cdot l\,, \tag{4.3}$$

whereas G=184N is our calculated force and l=0,1m. With these values the distributed load q results in q=1840N/m.

The maximum moment is given by

$$M = \frac{1}{2} q l^2\,. \tag{4.4}$$

With l=0,1m as the length of the pipe and q=1840N/m as the acting distributed load on the pipe the moment is M=9,2Nm.

With

$$\sigma = \frac{M}{I} e\,, \tag{4.5}$$

and

$$I = \frac{\pi (D^4 - d^4)}{64}\,, \tag{4.6}$$

the tension σ within the probe is σ=3,54MPa, with $I=5{,}2\cdot 10^{-8}m^4$.

As can be seen in Schürmann, Helmut: Konstruieren mit Faser-Kunststoff-Verbunden, Springer this value is much lower than the critical of σ=100MPa, where the elastic phase of glass fibre composites ends.

After calculating the tension manually a quick check via ANSYS was done with nearly the same results. For the check an E-Module of 20000MPa and a density of 2300g/cm³ were declared. Furthermore an acceleration of 80g was set arbitrarily. A fixed bearing at the outer face of the thinner cylinder was defined. The picture below (fig. 4-5) shows the numerical grid and the maximum tension in the principle coordinate system, whereas the deformation is shown 1200fold. The result of 5MPa including the notch effect is still uncritical to fibre glass.

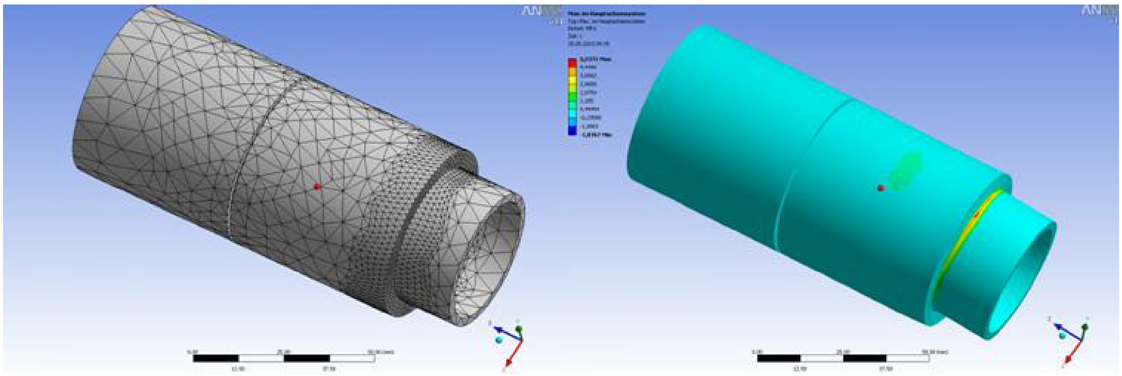

Figure 4-3: Numerical grid & maximum tension

4.1.2 Electrical

To monitor the change in capacitance and resistance of the probe while burning off during flight always two stripes of one foam square are connected on both ends, so the resistance can be measured over the length. The two other stripes will be responsible for the capacitance measurement as can be seen in the picture. The two capacitors will be connected in series to increase the capacitance. For the capacitance measurement eight cables will be used; one on each segment of the probe, while there will be 16 cables for resistance and measurements.

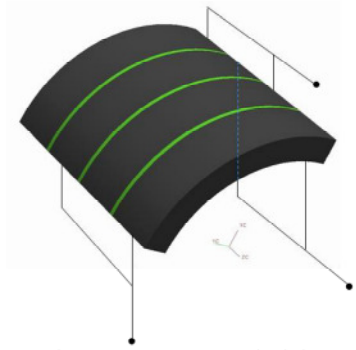

Fig. 3: Measurement Principle

Figure 4-5: Measurement Principle

For every type of measurement, i.e. temperature, there will be used an own cable harness which will be shielded so the data logging won’t be swayed.

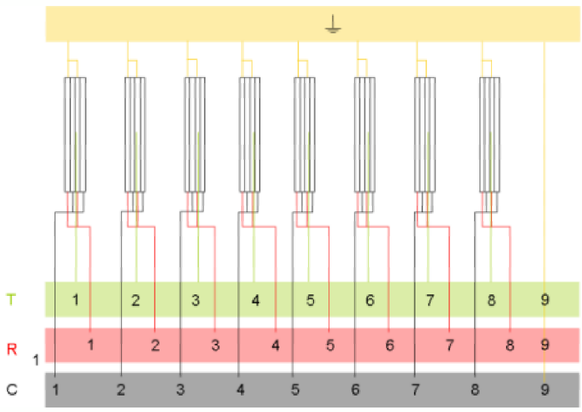

Figure 4-4: Probe Wiring

Each of the eight probe segments includes the same connection structure. Three electrical SUB-D 9pol plugs are foreseen for connecting the probe, one for the capacitance, one for the resistance and one for the temperature measurement, as indicated by colour bars in figure 4-6. Every pin of one of the three plugs leads to another segment, whereas every other part-segment is connected to the capacitance and accordingly to the resistance measurement. Resistance and capacity are measured counter “ground” potential, which has the ninth pin on every plug.

The temperature receiving element has its location in the centre of the segment. For protection against temperature, the cables will be insulated by “Altra Mat” Al_2O_3-wool against the metallic boom structure.

4.1.3 Science

The specific electrical resistance ρ is a measure of how strongly a material opposes the flow of electric current. The electrical resistance R can then be given by

$$R = \frac{l}{A}\rho, \tag{4.7}$$

where ρ is the specific electrical resistance in Ωm, l is the length of the piece of material in m, and A is the cross-sectional area of the specimen in m².

The thickness d of the material is respected in the Area A

$$A = d \cdot b, \tag{4.8}$$

with width b. Decreasing thickness d due to recession of the material results in increasing resistance as shown theoretically in figure 4-8.

However, a temperature influence is expected on the resistivity. Future work is intended to identify the temperature coefficient α of the material. When the temperature is measured simultaneously, the thickness loss Δd can be identified. The influence on the resistivity is then

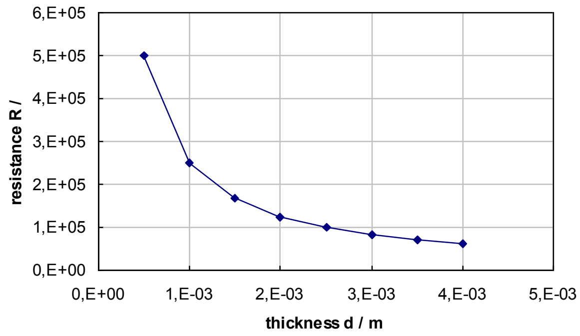

Figure 4-6: Electrical resistance due to recession

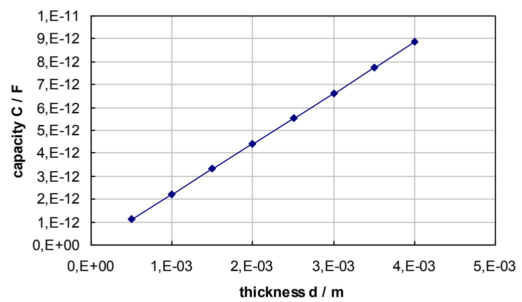

Figure 4-7: Electrical capacitance due to recession

$$\rho = \rho(T0)(1 + \alpha\Delta T). \tag{4.9}$$

The capacitance of a parallel-plate capacitor constructed of two parallel plates both of area A separated by a distance d is approximately equal to

$$C = \frac{\varepsilon_o \cdot \varepsilon_r \cdot A}{b_{dielectric}}. \tag{4.10}$$

It can be determined if the geometry of the conductors and the dielectric properties of the insulator between the conductors are known or vice versa: the thickness can be identified when the capacitance is measured. The width of the dielectric b defines the distance of the conductor plates. It needs to be small for the measurement so that it has to be ensured that the dielectric won't be too thick. The recession of the material is mirrored, again, in the plate area A with $A=dl$ according to fig. 4-9. Future work, is intended to double-check that no temperature influence occurs at capacity measurement.

4.1.4 Preliminary testing

To verify this construction preliminary tests were conducted. The results of the tests are presented below.

After preheating the hot air gun, the probe was heated as steady as possible. Measurement was taken every 10s. At the test-setup, the resistance and capacitance measurement instruments were connected in parallel because the resistance measurement instrument was expected to change the capacitance measurement by a constant value. The camera was placed in a distance of about 50cm (see fig. 4-10). After 100s, a glowing in the centre of the probe was recognized probably caused by a contact of the probe with the thermometer which had fallen out of the probe just a couple of seconds before. It felt down because the ground plate deformed due to the heat. At an anew, forced touch of the probe with the thermometer the probe began to glow again. Ablation of the foam at this spot could be recognized, the dielectric didn't ablate. Probably a bore in the ground plate played a certain role at the glowing process; in the next test it should eventually be closed and the hot air gun shouldn't be placed at the centre of the probe for too long time. The decreasing of the probe material during the ablation could not be detected by the camera. As can be seen in the drawing (fig. 4-12) the capacitance increases, while there couldn't be received a significant curve progression during the resistance measurement. At the following tests conductive silver-plated adhesive has been used to get a better connection with the probe. The results were as expected from literature.

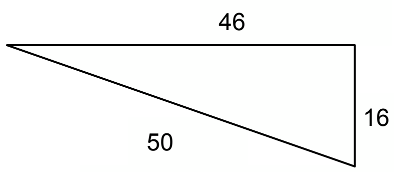

(measured values)

Fig. 4-10: Camera distance

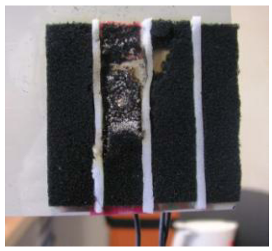

Fig. 4-11: Probe after the test

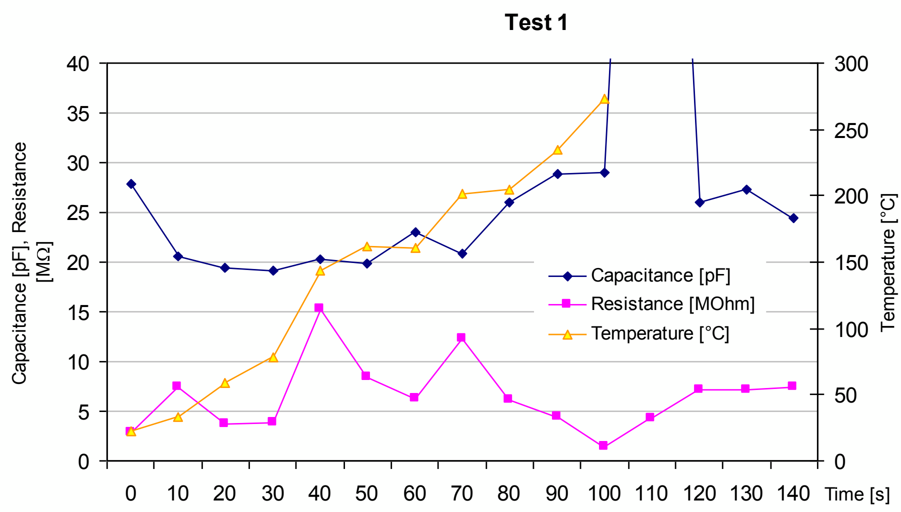

Figure 4-12: Burn test results

4.2 Experiment Interfaces

4.2.1 Mechanical

The experiment is bolted to a disc-shaped launch adapter with 16 M3x20 DIN912 screws. The launch adapter is bolted to the inner skirt of the nosecone eject mechanism from below.

To keep hot gas from entering the entire rocket experiment section a gas- and heat-shield is mounted on top of the nosecone section, just below the nose jettison mechanism (see pictures below). Only a 1mm gap remains between the inner hole of the heat-shield and the experiments outer cylinder wall.

A summary of the integration procedure is listed below. A detailed integration manual will be provided on delivery of the experiment.

1.) Bring the cylinder and adapter ring into the right position below the nosecone section ring. Take care for the rotational orientation of the experiment (orientation mark). Insert the 16 M5 screws and tighten them to defined torque.
2.) Turn around the assembly and mount the actual experiment from top side with M3 screws and given torque, again paying attention to the orientation.
3.) Bring the heat-shield into position on the top-side of the nosecone section ring and mount it with M4 screws.
4.) Integrate the entire section with the next experiment module

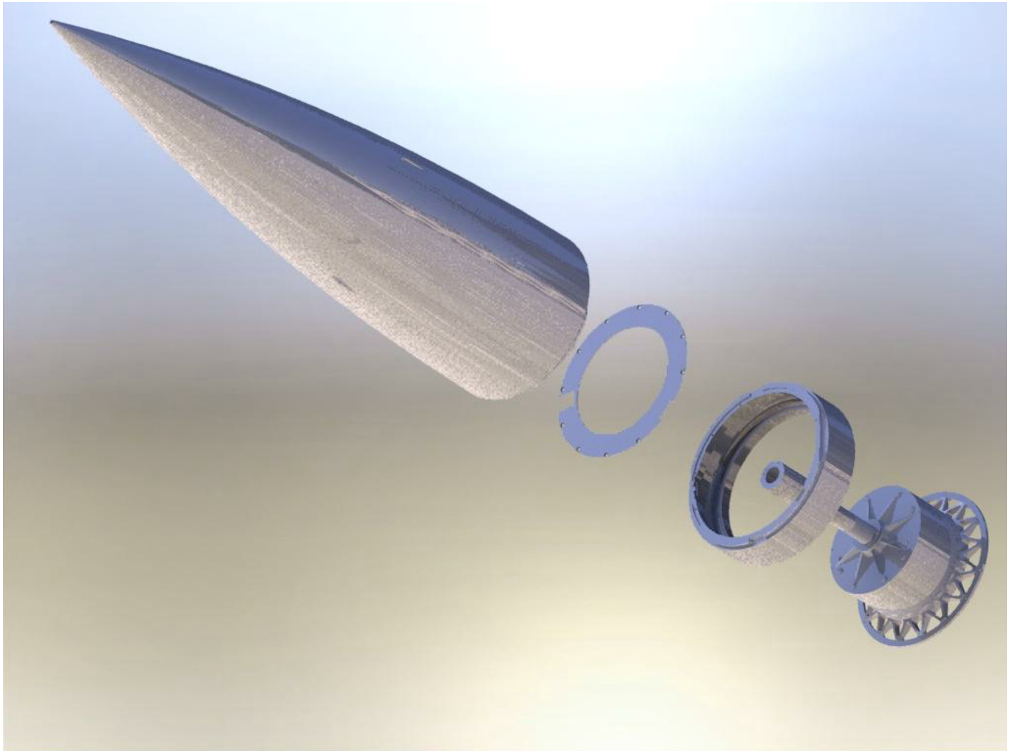

Figure 4-83: Nose section assembly

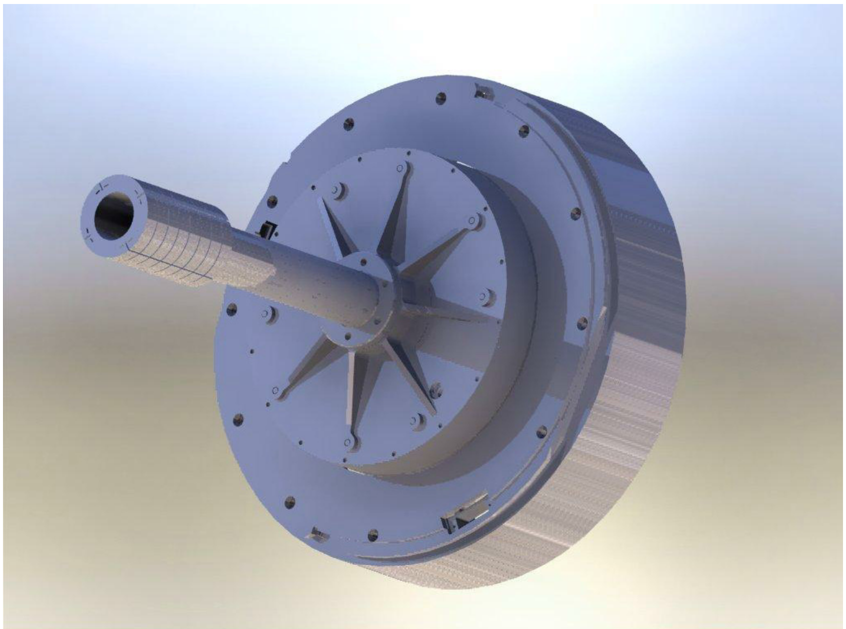

Figure 4-9: Experiment in REXUS top cylinder

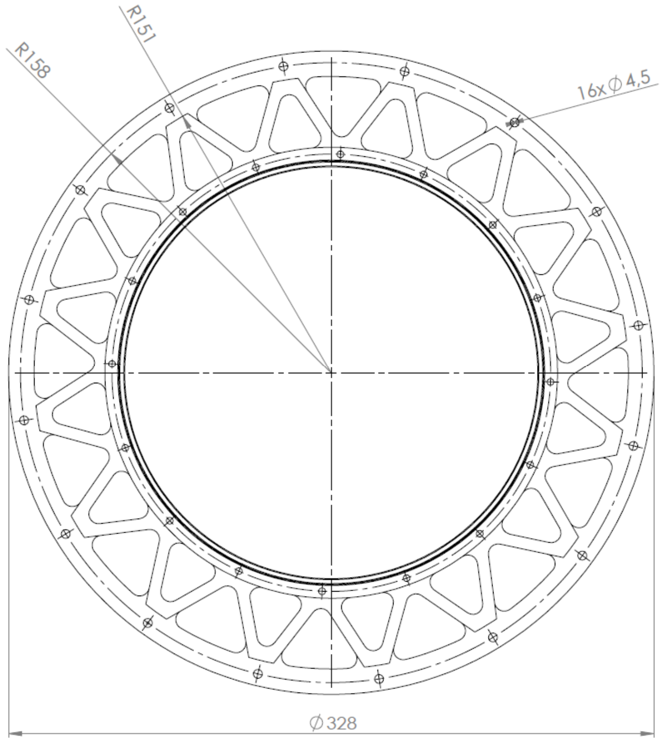

Figure 4-10: Launch adapter ring

4.2.2 Electrical

On top of the big central electronics box there is a standard SUB-D 15 pin connector. This is the main electrical interface to the REXUS service module, as specified in “RX-REXUS_user_manual-v7_0-04Dec09.pdf”

Pin Nr	Name	Remarks
1	+28 V	Battery Power (24-36V unregulated, Ipeak < 3 A)
2	spare (do not connect)	
3	SODS	Start/Stop of data storage (open collector to GND or high impedance)
4	SOE	Start/Stop of experiment(open collector to GND or high impedance)
5	LO	Lift off (open collector to GND or high impedance)
6	EXP out+	Non inverted experiment data to Service Module (RS-422)
7	EXP out-	Inverted experiment data to Service Module (RS-422)
8	28 V Ground	Power Ground
9	+28 V	Battery Power (24-36V unregulated, I_{peak} < 3 Amps)
10	28 V Charging Power	Experiment battery charging power (use 28V GND for return)
11	spare (do not connect)	
12	UTE (do not connect)	Not implemented yet (User defined Timer Event)
13	EXP in +	Non inverted Control data (commands) to Experiment (RS-422)
14	EXP in -	Inverted Control data (commands) to Experiment (RS-422)
15	28 V Ground	Power Ground

Table 4-1: REXUS electrical interface

Used signals and power timing:

The LO-, SOE- and SODS- signals are used by the onboard software for determination of the operation mode. The signals shall have the following timing: (timings are taken from REXUS 3 as reference)

Event	T	Desired Signal
System check	-300s	Power=ON
Launch	0	LO=ON (Liftoff signal on)
Nosecone separation	+60s	SOE=ON (start of experiment)
Start recording	+150s	SODS=ON (start of data storage)
Before parachute deployment	+300s	SODS=OFF (stop of data storage)
Landing	640s	SOE=OFF (end of experiment)
Experiment deactivation	Landing + 3s up to recovery	Power = OFF (all off)

Table 4-2: Signal timing for experiment

Power consumption:

Packet		prelaunch	launch	activation	measurement	recovery
		Mission phases				
OBDH		0,3	0,82	0,82	0,82	0,3
Measurement system		0	0	0,38	0,38	0
Camera system		0	0	4,5	4,5	0
PCDU		1,2	2	2	2	1,2
	required power [W]	1,5	2,82	7,7	7,7	1,5
	converter efficiency	0,8	0,8	0,8	0,8	0,8
	total drawn pwr [W]	1,875	3,525	9,625	9,625	1,875
	Measured pwr [W]}	1,4	1,456	3,36	3,64	1,4

Table 4-3: Experiment power budget

Up-and Downlink:

The data packets are laid out with respect to the recommendations of the REXUS User Manual.

Packet name	Direction	max. Size [Byte]
Telemetry	downlink	24
Measurements 1	downlink	25
Measurements 2	downlink	25
Measurement 3	downlink	25
Command	uplink	10

Table 4-4: telemetry packet summary

If data is sent on the downlink, this will be done with the measurement update rate of **10Hz.**

Since all data packets are also stored in the experiment, no confirmation of packet reception is done. Uplink only is required on 300s prior to launch via the REXUS rocket umbilical for checkout. A maximum rate of 1Hz is assumed.

The preliminary link budget is:

Link Budget

Packet	length [bytes]	Mission phases data rate in flight phase [Hz] prelaunch	launch	activation	measurement	recovery
Telemetry	18	10	10	10	10	10
Measurements 1	25	0	0	0	10	0
Measurements 2	25	0	0	0	10	0
Measurements 3	25	0	0	0	10	0
Commands	10	1	1	1	1	1
total downlink [bytes/s]		180	180	180	930	180
total uplink [bytes/s]		10	10	10	10	10

Table 4-5: Link budget

4.2.3 Radio Frequencies (optional)

No radio transmission device is used.

4.2.4 Thermal (optional)

No excessive active heat source is present. The only heat is produced by the electronics. This power of less than 28W is distributed to the entire surface of all three electronics boxes. At CDR level the electrical power consumption has dropped even below 10W.

4.3 Experiment Components

4.4 Mechanical Design

4.4.1 General Overview

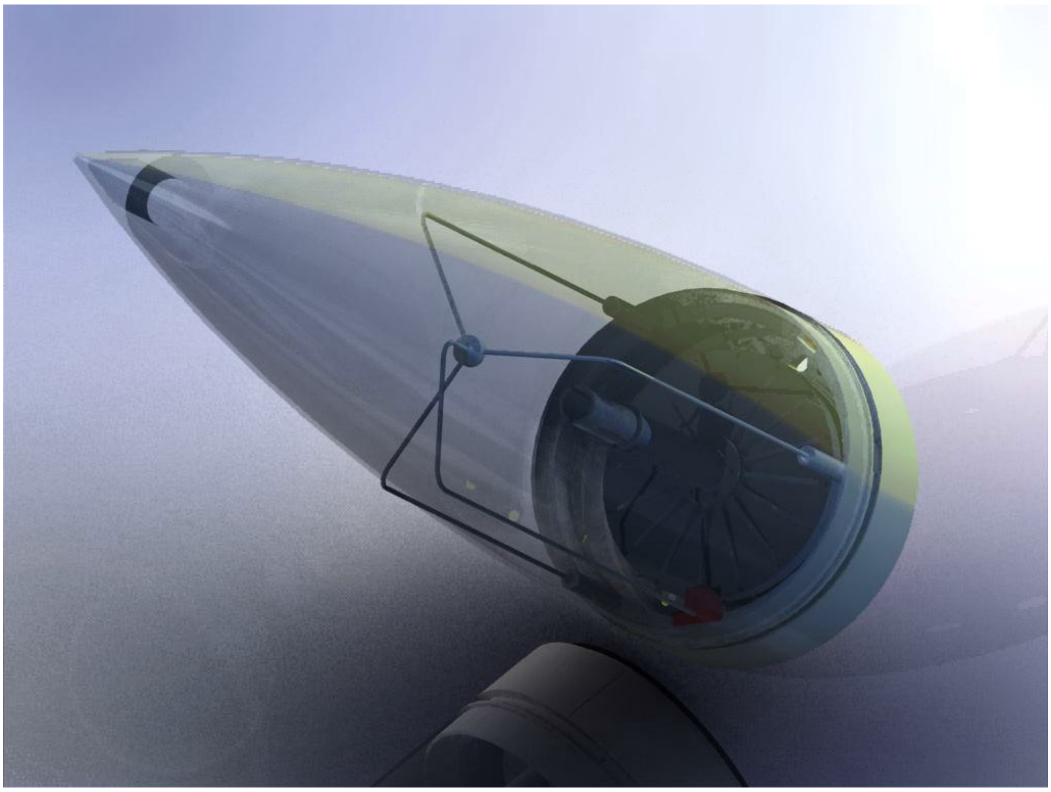

Figure 4-11: Nose section rendering

The Experiment is built up symmetrically around the central REXUS axis. A launch adapter provides a reduction of the diameter to 230mm.

On the launch adapter is 140 mm high ring section.
The top of the ring section is covered with a plate with stiffeners.
These two parts are the main structure of experiment. A heat-shield baffle has to be integrated on the top section, to prevent hot air from passing in-between the ring section and the nosecone ejection mechanism through the launch adapter.

Inside the ring section, one big and two small electronics boxes are mounted to the top plate with standoffs for mechanical and heat decoupling. All electrical consumers (except for the re-entry probe) are installed in these three boxes. Holes are drilled through the top section below the small boxes to provide an optical path for the cameras. The holes are covered with glass plates to keep out the hot air during the re-entry.

On top of the top plate is a boom with a length of 300mm. The last 100mm of the boom are covered with the ablative material. This top section forms the re-entry probe.
Inside the boom is a harness embedded into thermal protection wool.
There are no moving parts in the design!

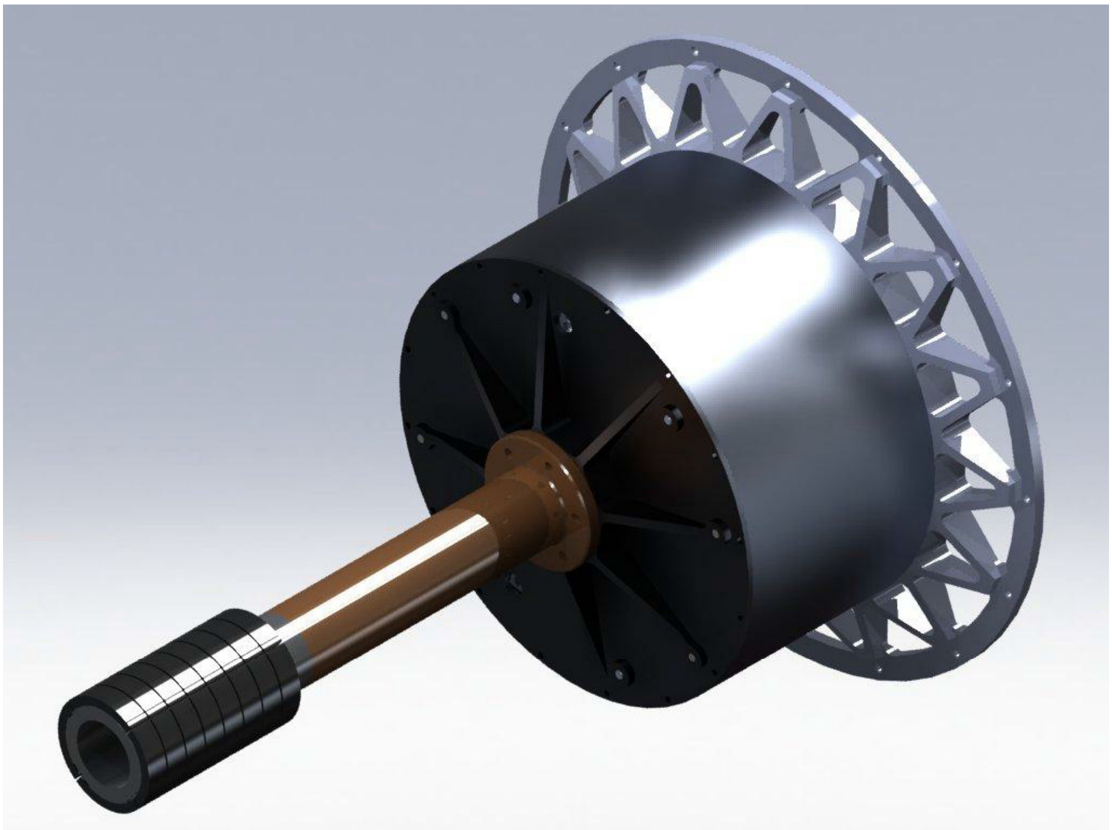

Figure 4-12: REMOS experiment rendering

All technical drawings can be found in the appendix.

4.4.2 Product Tree

Group	Part Code	Assy. Name	Part Name	Sub- Part Name	Quantity	Material/	single Mass	Total Mass	Status
						Spec	[g]	[g]	
A		launch adapter							I
	A0-001			carrier disc	1	EN AW 6082	918,1	918,1	I

	A0-002			rocket interface screws	16	Steel	3,0	48,0	I
	A0-003			experiment interface screws	16	Steel	2,0	32,0	I
	A0-004			experiment interface washers	16	Steel	0,3	4,0	-
A1			Heat-shield					0,0	I
	A1-001			Heat-shield baffle	1	EN AW 6082	174,9	174,9	I
	A1-002			Heat-shield screws	11	Steel	3,0	33,0	I
B		experiment						0,0	
B1			Support Structure					0,0	
	B1-001			outer cylinder	1	EN AW 6082	828,4	828,4	I
	B1-002			cylinder cover	1	EN AW 6082	555,6	555,6	I
	B1-003			cover screws	16	Steel	2,0	32,0	I
	B1-004			cover washers	16	Steel	2,0	32,0	I
	B1-005			electronics box standoffs	4	Titanium	6,2	24,6	I
	B1-006			camera box isolation	2	-	11,8	23,5	I
	B1-007			electronics box lock washers	4	Steel	0,5	2,0	I
	B1-008			camera box lock washers	4	Steel	0,5	2,0	I
	B1-009			electronics box screws	4	Steel	2,5	10,0	I
	B1-010			camera box screws	4	Steel	2,5	10,0	I
	B1-011			cable clamps	10	Polyester	1,0	10,0	I
	B1-012			camera windows	2	glass	5,0	10,0	I
B2			Probe						
	B2-001			AL Tube	3	EN AW 6082	372,2	372,2	P,I
	B2-002			Screws	6	Steel	3,0	18,0	I
	B2-003			washers	6	Steel	0,5	3,0	I
	B2-003			Sensor section	1	misc.	323,0	323,0	I
	B2-004			Wiring	3	-	30,0	90,0	I
	B2-005			pt100 Temperature sensors	8	-	1,0	8,0	I
	B2-006			Connector 1	1	brass	12,5	12,5	I
	B2-007			Connector 2	1	brass	12,5	12,5	I
	B2-008			Connector 3	1	brass	12,5	12,5	I
	B2-009			Thermal insulation		Al2O3 wool	50,0	0,0	I
	B2-010			Cable	3	-	100,0		I
	B2-011			D-SUB Housing	3		15,0		I
B3			Electronics box					0,0	
	B3-001			Box	1	EN AW 2018	535,6	535,6	I
	B3-002			PCDU PCB	1	-	60,0	60,0	I
	B3-003			R/T measure PCB	1	-	40,0	40,0	I

	B3-004			C measure PCB	1	-	40,0	40,0	I
	B3-005			OBC PCB	1	-	40,0	40,0	I
	B3-006			REXUS connector	1		15,0	15,0	I
	B3-007			Probe connector 1	1		12,5	12,5	I
	B3-008			Probe connector 2	1		12,5	12,5	I
	B3-009			Probe connector 3	1		12,5	12,5	I
	B3-010			Camera connector	1		12,5	12,5	I
	B3-011			D-SUB fixation kit	4	Steel	3,0	12,0	I
	B3-012			PCB guide rails	8	PVC	2,5	20,0	I
	B3-013			PCB fixations	8	PVC	2,5	20,0	I
	B3-014			PCB fixation screws	16	Steel	1,5	24,0	I
	B3-015			PCCB fixation washers	16	Steel	0,3	4,8	I
	B3-016			PCB interconnection	4	-	3,0	12,0	I
B4			Camera box					0,0	
	B4-001			Box	2	EN AW 2018	80,0	160,0	I
	B4-002			Camera system	3	-	17,0	51,0	I
	B4-003			Camera fixation	2	PVC	10,0	20,0	I
								0,0	
								0,0	
C		ground support						0,0	
C1			Break out box Sensors						
	C1-001			Box	1	ABS			I
	C1-002			D-SUB connectors male	3				I
	C1-003			D-SUB connectors female	3				I
				D-SUB Housing	3				I
				Banana jacks	27				I
C2			Break out box REXUS						
	C2-001			BOX	1	ABS			I
	C2-002			Switch	3	-			I
	C2-003			D-SUB connectors male	1				I
	C2-004			D-SUB connectors female	1				I
	C2-005			Banana jacks	2				I
	C2-006			D-SUB Housing	1				I
	C2-007			experimental PCB	1	-			I
C3			Shaker adapter						
	C3-001			Adapter Plate 0°	1	EN AW 6082			I

	C3-002			Adapter Mounting 90°	2	EN AW 6082			I
	C3-003			Base Plate	1	EN AW 6082			I
	C3-004			Adapter screws	12	Steel		0,0	I
C4			Experiment transp. box						
	C4-001			Box	1	-			I
	C4-002			Insulation	1	Foam			I
C5			Electronics transp. Box						
	C5-001			Box	1	-			-
	C5-002			ESD Insulation	1	Foam			-
								0,0	
				Total Mass flight hardware [g]				4706,2	

P: present; I: integrated; O: ordered; -: skipped during review

Table 4-6: REMOS product tree

4.4.3 Structural Analysis

For the structural analysis the REXUS User Manual has been reviewed. The contained flight data and the qualification test parameters are used as a basis for defining load cases. For CDR a static load equivalent was calculated from the static and dynamic loads and was used for quasi-static load simulations (QSL) and screw force calculations. A random-vibration analysis was simulated at acceptance level. The derived load cases and their origins are listed below:

Used load cases:

Load Case	Load	origin
1	56g axial/ 42g lateral	launch acceleration + 3*vibration loads
2	7g axial/ 7g lateral 200°C	re-entry deceleration + 1g vibration
3	6g random x 20Hz- 2000Hz	Launch vibration
4	6g random y 20Hz- 2000Hz	Launch vibration
5	6g random z 20Hz- 2000Hz	Launch vibration
0	-	Eigenvalue calculation

Table 4-7: Load case summary

These loads have been applied onto a finite element model of the structural CDR design. All surface contacts are assumed as connected. The bolt interface of the launch adapter is assumed to be infinitely rigid.

The screw forces and required mounting momentums were calculated with load case 1 and cross checked with load case 2.

FEM Results, Load case 0

In the table below the eigenfrequencies and the moving mass fraction of each frequency is listed. As can be seen, the frequencies with the highest amount of moving mass are in the range of 700Hz to 1000Hz. At the more dangerous frequencies from 220Hz to 700Hz the highest moving mass fraction only is 13%.

Mode Nr.	Eigenfrequency [Hz]	Mass fraction X [%]	Mass fraction Y [%]	Mass fraction Z [%]
1	226,21	3,8%	19,5%	0,0%
2	234,19	0,1%	12,3%	0,0%
3	236,05	13,1%	0,1%	1,0%
4	250,19	0,4%	2,4%	0,1%
5	252,5	0,9%	5,8%	0,2%
6	257,36	0,7%	5,0%	0,0%
7	353	9,1%	0,1%	0,0%
8	391,03	0,6%	0,0%	4,6%
9	392,33	3,9%	0,1%	7,9%
10	398,77	3,9%	0,1%	0,5%
11	630,96	13,0%	0,0%	0,3%
12	696,82	1,3%	0,0%	0,0%
13	705,61	10,3%	0,0%	2,6%
14	715,66	11,5%	9,7%	0,0%
15	766,91	36,4%	0,3%	63,6%
16	769,43	0,0%	35,9%	0,6%
17	887,98	28,2%	0,0%	0,0%
18	890,97	4,9%	28,5%	22,4%
19	933,22	0,1%	0,0%	0,1%
20	984,81	0,0%	8,9%	4,1%
21	991,23	1,9%	30,4%	0,0%
22	995,72	3,0%	0,1%	0,0%
23	1002,8	8,5%	82,5%	1,8%
24	1019,7	0,0%	4,7%	0,2%
25	1110,8	20,3%	5,1%	1,7%

26	1137,8	11,2%	0,1%	5,1%
27	1150,2	17,7%	0,0%	16,8%
28	1153,2	19,1%	0,6%	4,2%
29	1271,2	0,6%	1,7%	0,4%
30	1353,1	2,7%	1,0%	0,0%
31	1411,1	0,8%	0,2%	0,1%
32	1416	0,1%	0,2%	27,8%
33	1423,7	0,3%	1,2%	0,0%
34	1438,6	0,0%	2,0%	0,0%
35	1483,4	2,3%	40,5%	0,0%
36	1511,2	0,0%	0,1%	13,2%
37	1568,5	1,9%	7,8%	0,0%
38	1607,1	0,2%	0,1%	13,3%
39	1650,8	1,3%	0,8%	0,7%
40	1708,1	0,0%	23,4%	0,1%
41	1723,4	0,9%	1,8%	1,3%
42	1773,3	0,0%	2,0%	1,6%
43	1810,1	0,1%	0,9%	0,8%
44	1840,6	0,0%	0,3%	21,8%
45	1881,3	8,0%	0,0%	0,1%
46	1996,8	13,3%	0,1%	0,4%
Sum		62,3%	59,3%	79,5%

Table 4-8: Eigenfrequency analysis results

FEM Results, Load case 1

For the QSL results in x-direction, the highest stress level is 14.8 MPa. This stress is located in the reinforcements on the cylinder cover.

A similar result can be found for QSL-Y. Here the stress is 14.3MPa.

For QSL-Z, the maximum stress is 12.1 MPa.

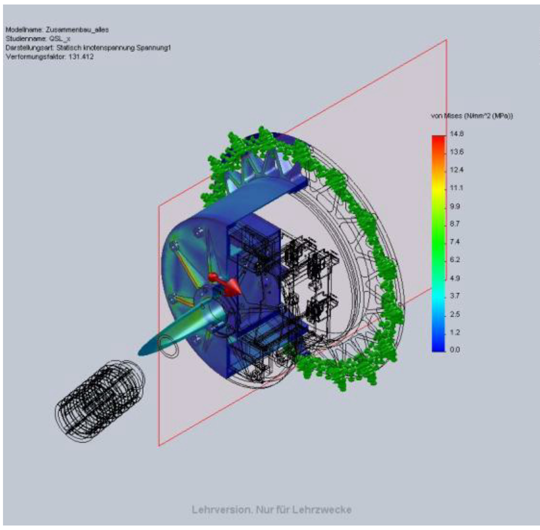

Figure 4-13: QSL results y

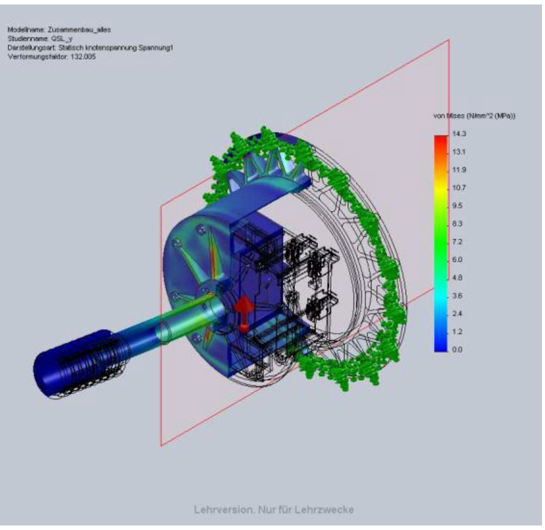

Figure 4-14: QSL results x

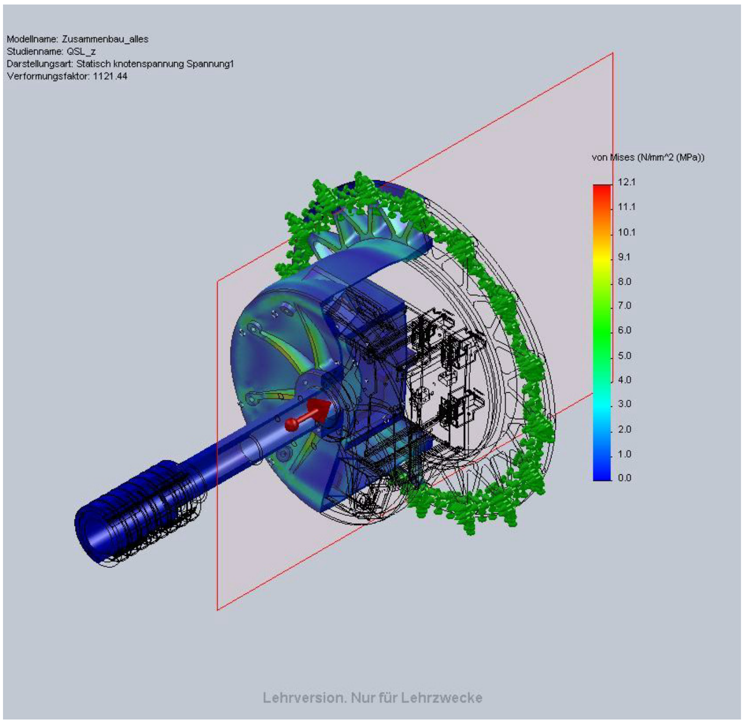

Figure 4-15: QSL results z

Results screw calculation

REMOS screw loads interfaces	delta T = 0 K Safety against rupture	delta T = 0 K Safety against gliding	delta T = 180 K Safety against rupture	delta T = 180 K Safety against gliding	required tightening momentum [Nm]
Sensor Boom	2,50	4,76	1,75	7,25	3,76
Cylinder Cover	2,20	1,54	1,56	1,92	0,93
Launch Adapter	1,88	1,56	1,46	2,24	1,02
REXUS Interface	2,67	1,56	1,76	1,98	1,84
Electronics Box	5,52	1,54	2,56	2,07	1,74
Camera Box	8,96	2,45	2,96	2,90	1,17

Table 4-9: Screw calculation results

One value is below j=1.5. But the maximum temperature of 180K above assembly temperature is not realistic for the launch adapter interface. In previous flights the inner wall temperature never exceeded 100°C. For a temperature difference of 160°C the safety already rises above 1.5.

The detailed calculations can be found in the appendix.

FEM Results, Random X

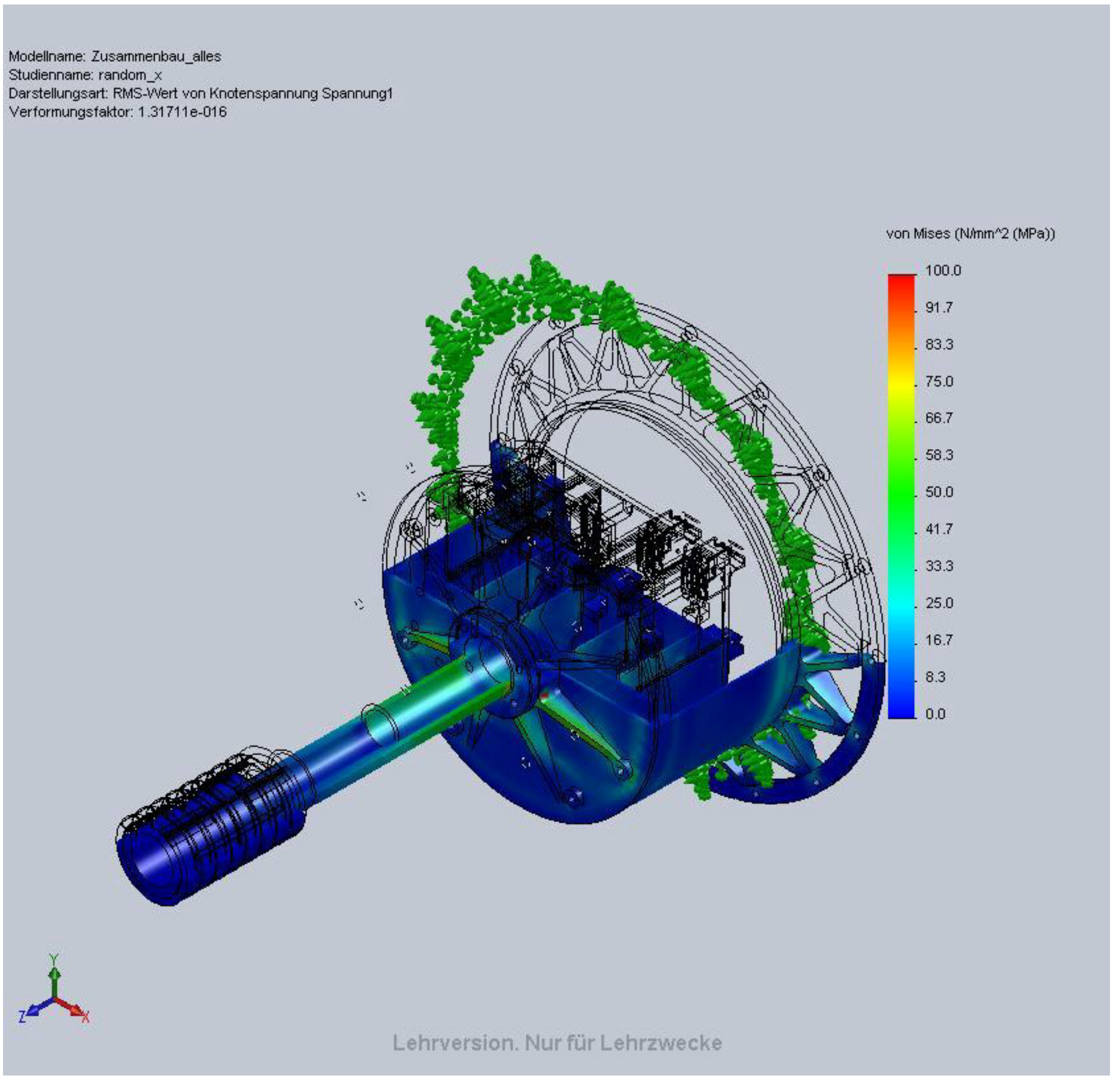

Figure 4-16: Results random x

Maximum value: 70MPa for probability distribution of 66.67%.

For probability distribution 99.97% this results in 210MPa.

FEM Results, Random Y

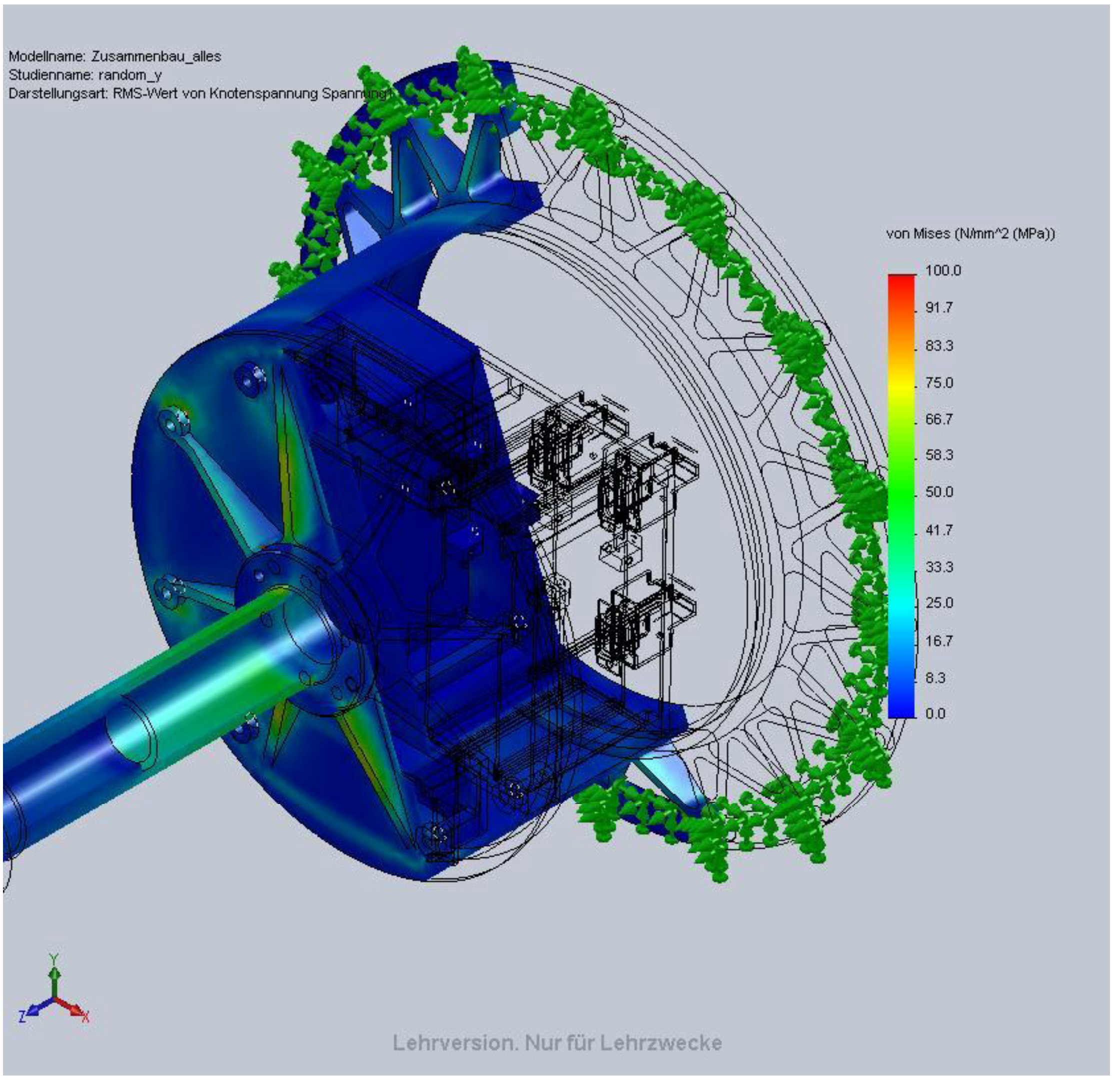

Figure 4-17: Results random y

Maximum value: 68MPa for probability distribution of 66.67%.

For probability distribution 99.97% this results in 204 MPa.

FEM Results, Random Z

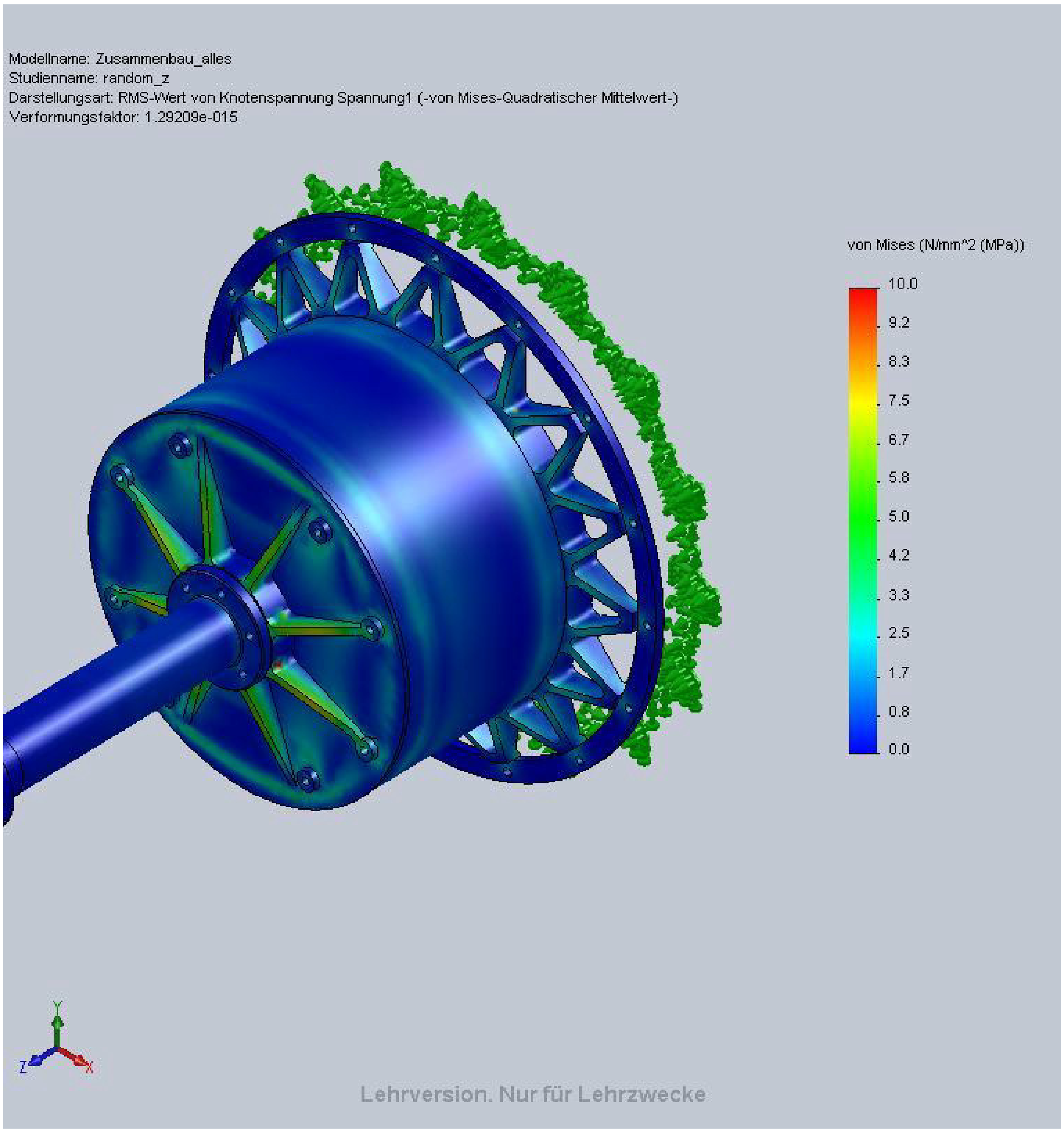

Figure 4-18: Results random z

Maximum value: 10MPa for probability distribution of 66.67%.

For probability distribution 99.97% this results in 30MPa.

4.5 Electronics Design

All Electronics are distributed in three aluminium boxes, mounted to the inward side of the cylinder cover. The two smaller boxes contain the cameras. The big central box contains all major electronics.

The electronics in the central box are distributed onto four PCBs, according to their function.

PCBs:

1. Power Conditioning and switching (PCDU)
2. Onboard data handling (OBDH)
3. Resistance and temperature measurement (R/T)
4. Capacitance measurement (C)

An integration protocol can be found in the appendix.

4.5.1 Power Conditioning and switching (PCDU)

Theory of operation:

The 28V of the REXUS supply are fed to two switching regulators, which convert the REXUS supply voltage to an intermediate supply with 7 to 8 volts. For safety reasons, they are arranged in parallel and interlinked by two load-equalizing resistors. From here on the power is distributed through post-regulators and switches to the four PCBs.

- A linear 1117 5V regulator supplies the OBDH PCB, as long as the REXUS power is switched on.
- A MAX603 5V switchable linear regulator is the power supply to all analogue electronics and measurement circuitry.
- The cameras are supplied through an additional MAX603.

On the same PCB an evaluation circuit for a thermocouple is placed. It is used to measure the temperature of the undisturbed flow at the top of the experiment boom. Although it is a measurement circuit, it was added on this PCB, as there was no free space on any other PCB.

EuroLaunch
A DLR and SSC cooperation

Schematic:

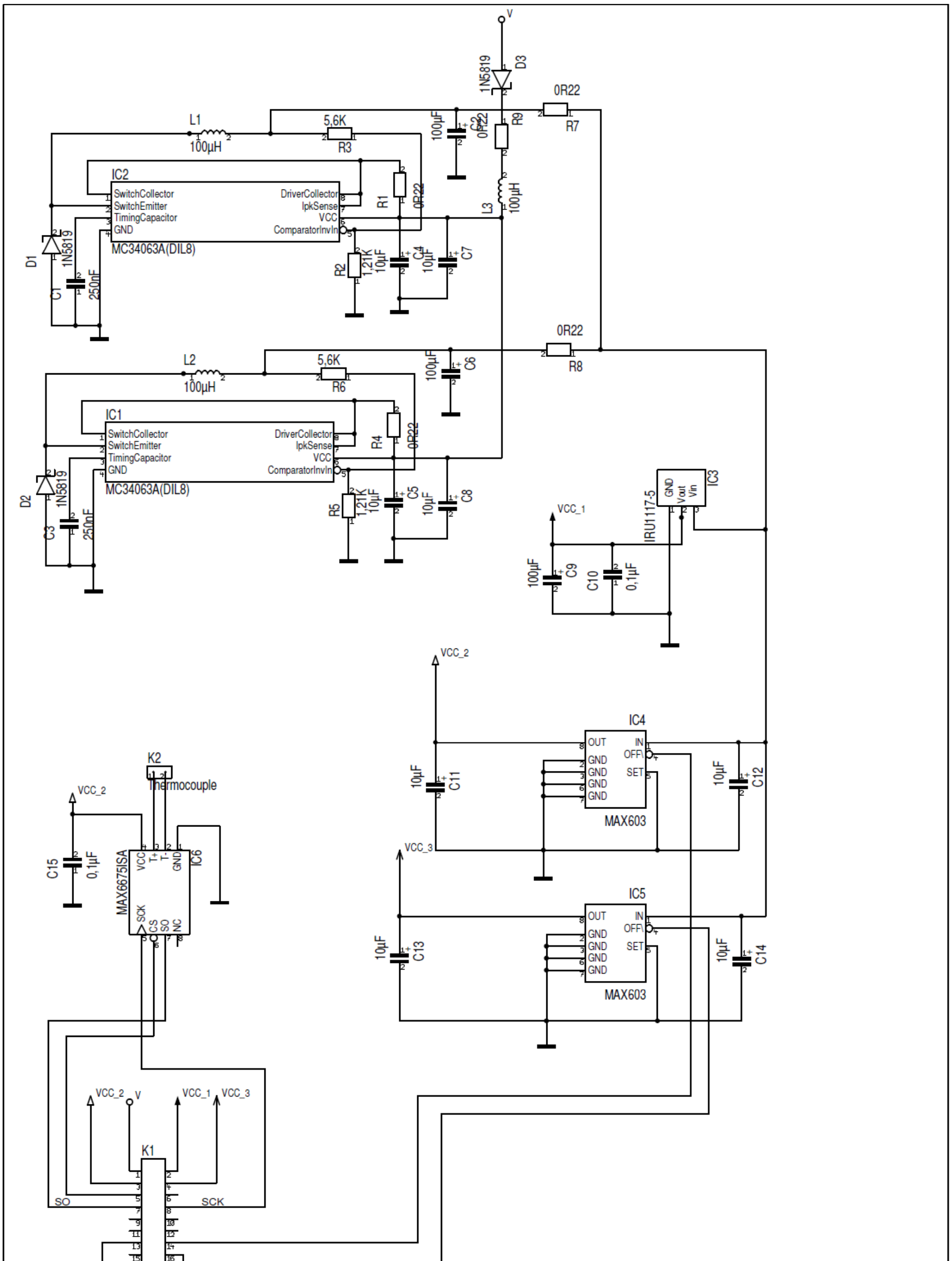

Maßstab	100,00%	Firma	Zeichner	Blatt
Änderung	26.06.10	14:34	Titel	
Ausgabe	26.06.10	18:39		
Datei	PCDU.T3001		Projekt	

Figure 4-19: PCDU schematic

PCB Design:

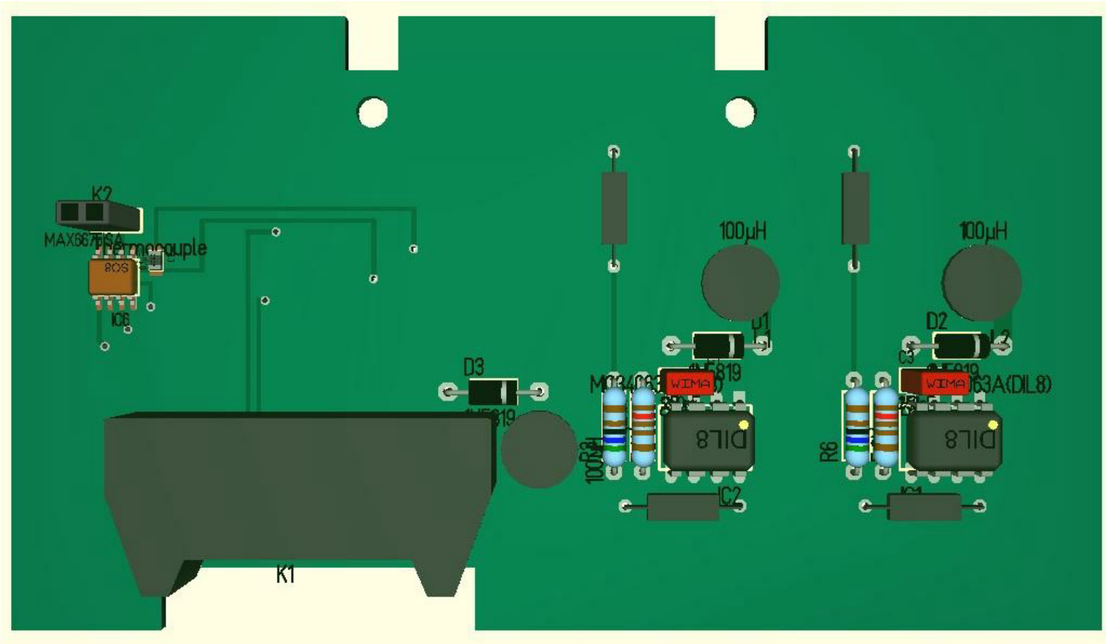

Figure 4-20: PCDU PCB top

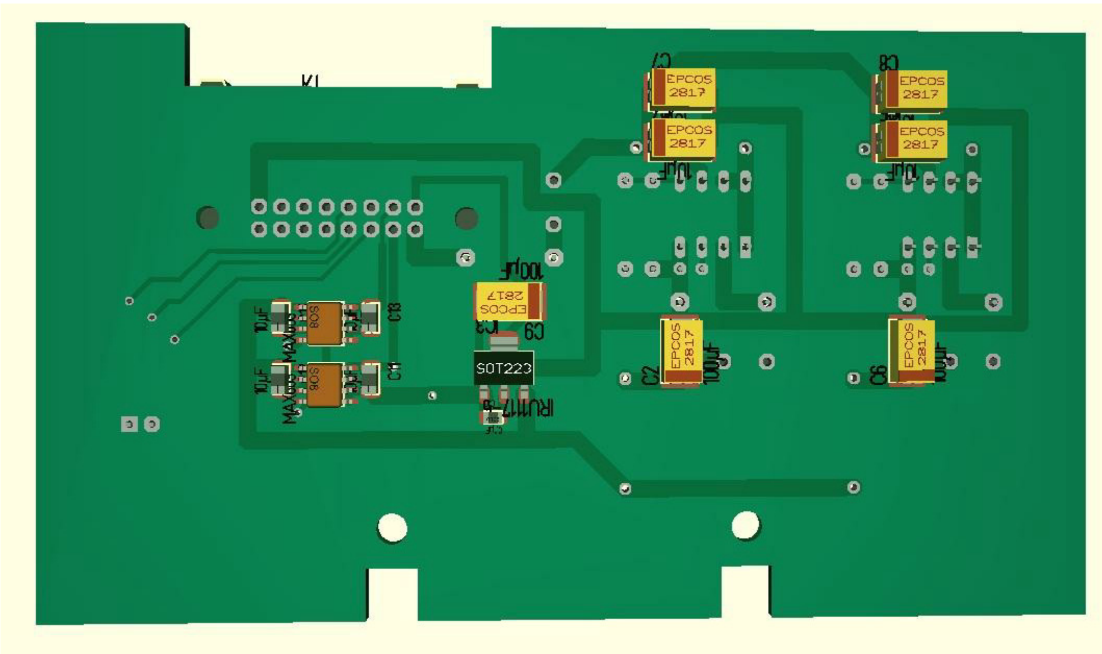

Figure 4-21: PCDU PCB bottom

4.5.2 Onboard data handling (OBDH)

Theory of operation:

The main part of the OBDH is an ATMega164, an 8bit RISC microcontroller (MCU). All onboard software runs on this device. Connected to the MCU is a standard

- RS422 interface,
- three signal lines via optocouplers
- a real time clock
- an AT45DB161 data FLASH

The OBDH PCB communicates with the other three PCBs via a serial SPI bus. For the addressing of the capacitance measurement PCB the SPI line signals are used for parallel 3bit addressing.

In comparison to the PDR version the ADC has been removed from this board and added in situ to the R/C measurement board. This is a precaution in order to eliminate a potential single point failure.

A simple temperature sensor for monitoring the temperature inside the electronics box also is connected to the internal ADC of the microcontroller.

All supply voltages are monitored as well.

Schematic:

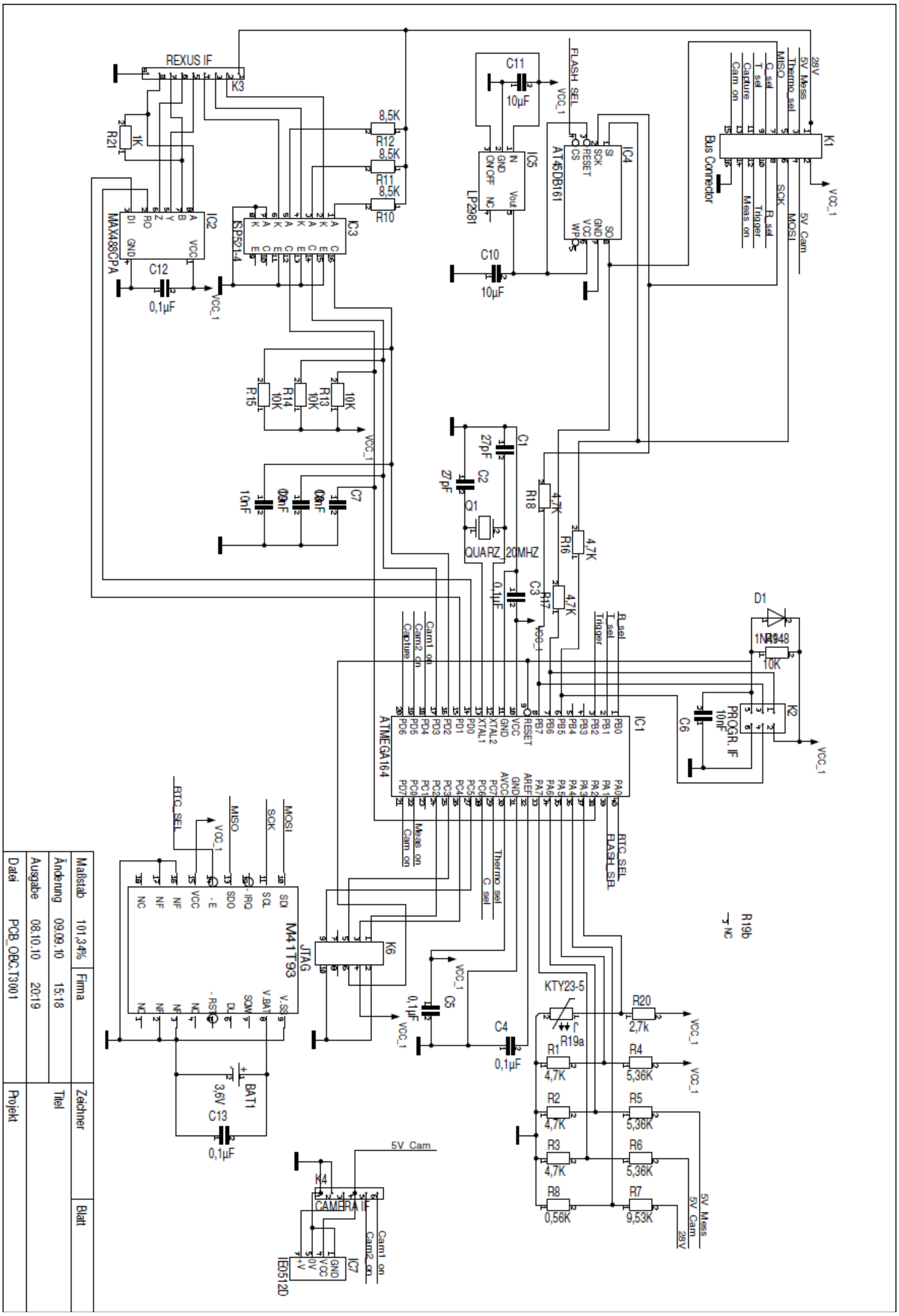

Figure 4-22: OBDH schematic

PCB Design:

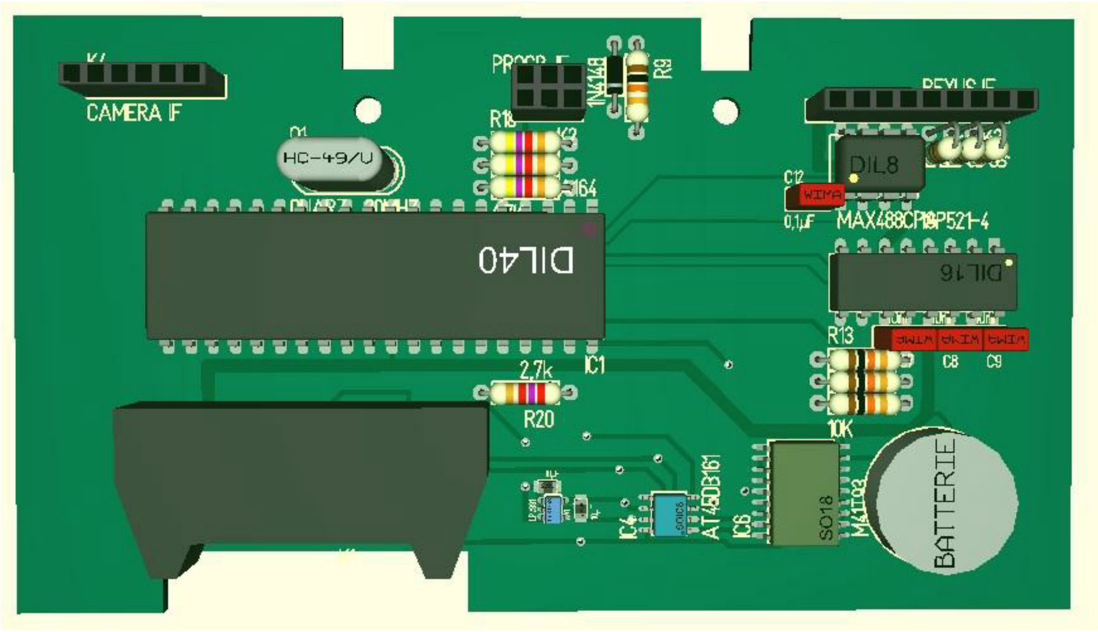

Figure 4-23: OBDH PCB top

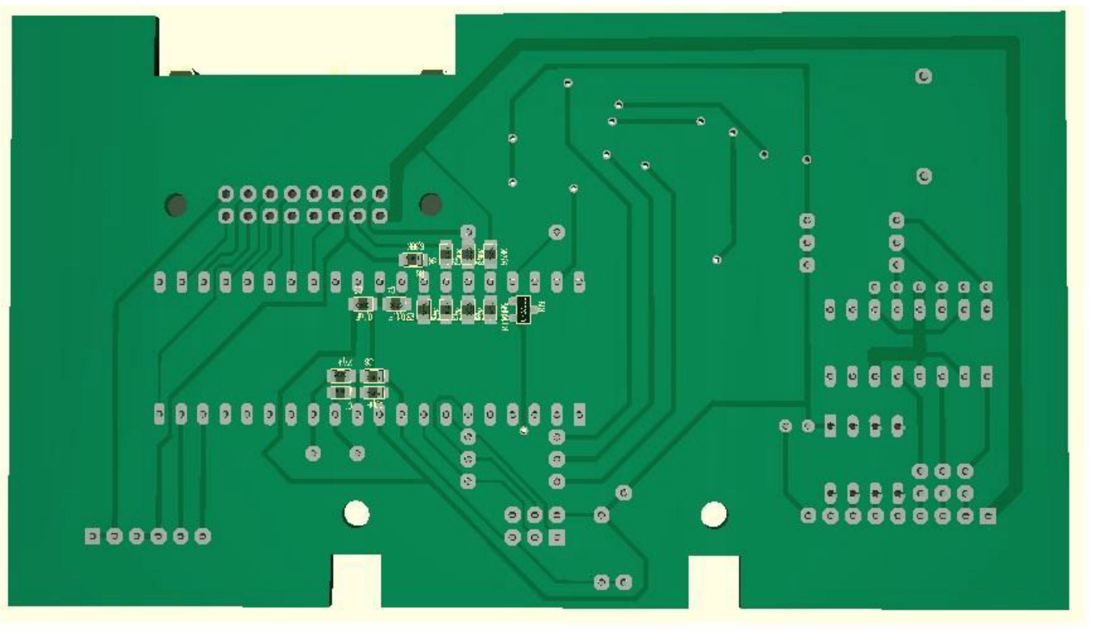

Figure 4-24: OBDH PCB bottom

4.5.3 Resistance and temperature measurement (R/T)

Theory of operation:

All 8 resistance and temperature channels are connected to this PCB.

The resistance channels are connected to the supply voltage via a resistor. When a resistance measurement is active, the desired channel is selected via a multiplexer. During a capacitance measurement, the resistor pins are pulled to ground via a transistor array, to avoid disturbances.

Each temperature channel consists of a operational amplifier (OPAMP) and a precision voltage reference, which form a constant current source. The current is fed through Pt100 temperature sensors and the voltage drop across the sensor is amplified by a second OPAMP.

The analogue voltages are fed to two A/D-converters with an SPI interface and a resolution of 12 bit.

Schematic:

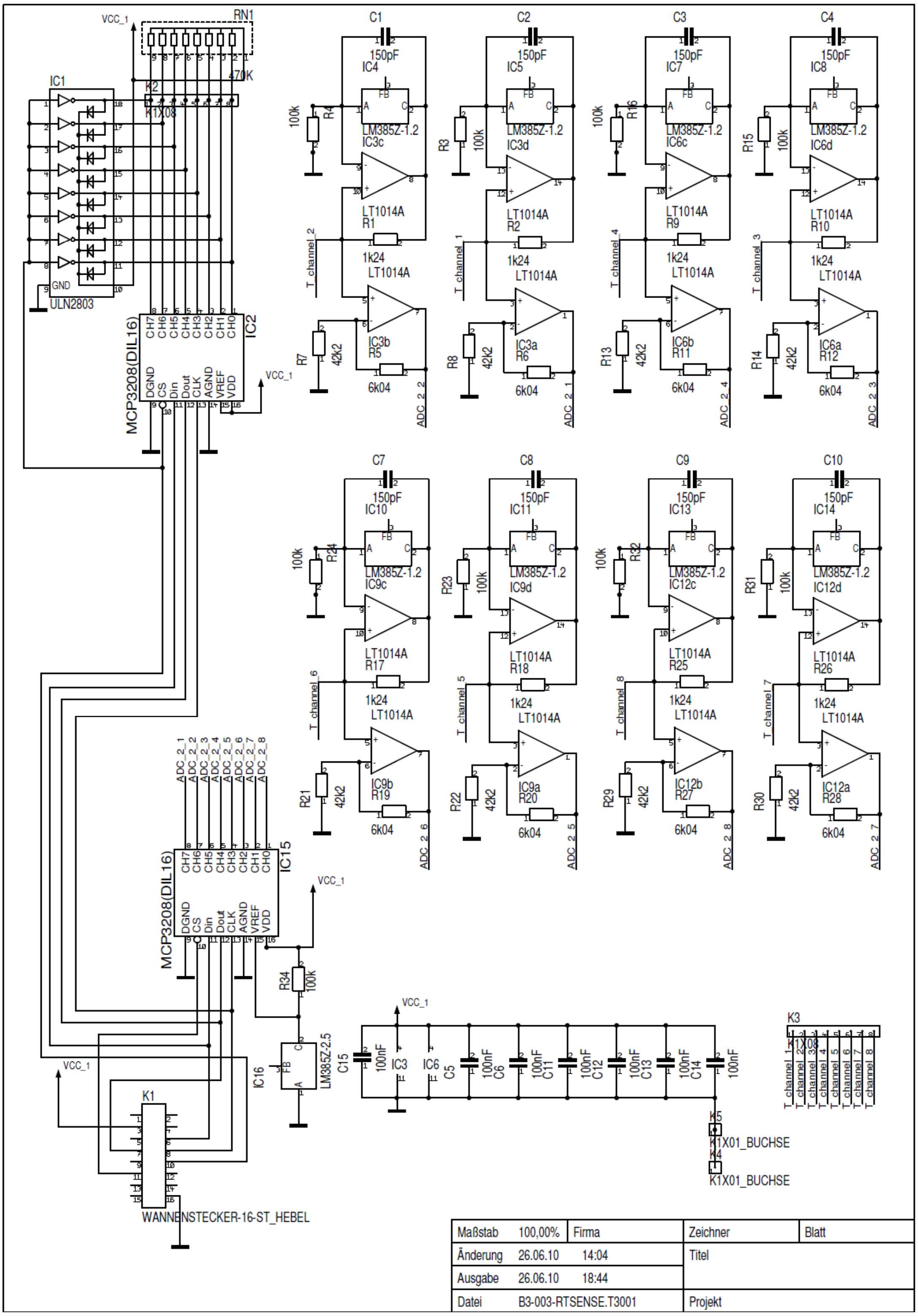

Figure 4-25: R/T schematic

PCB Design:

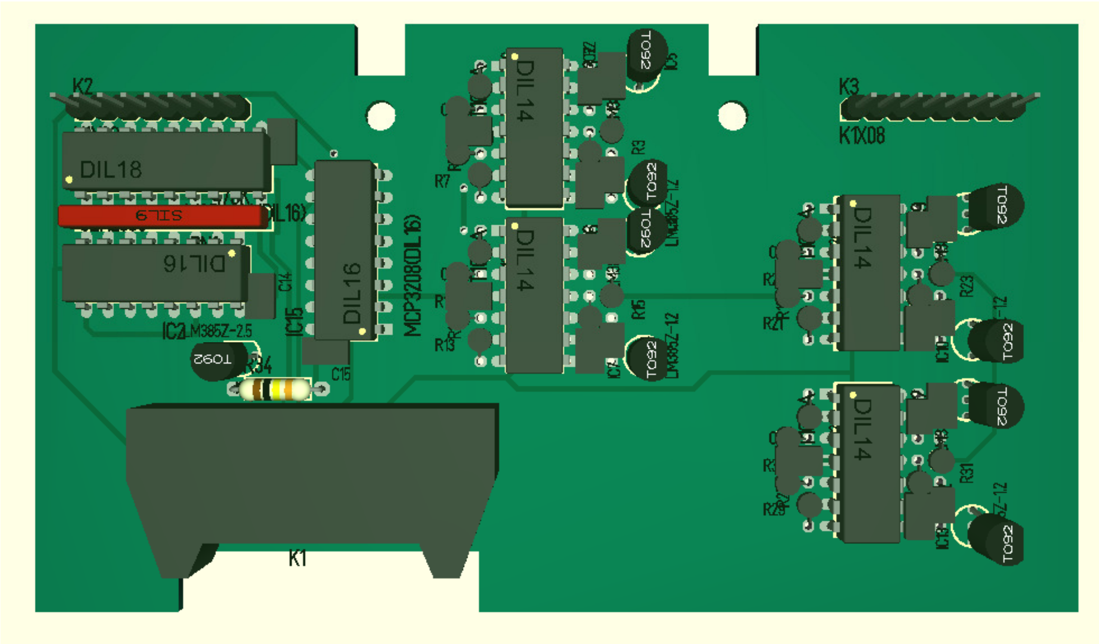

Figure 4-26: R/T PCB top

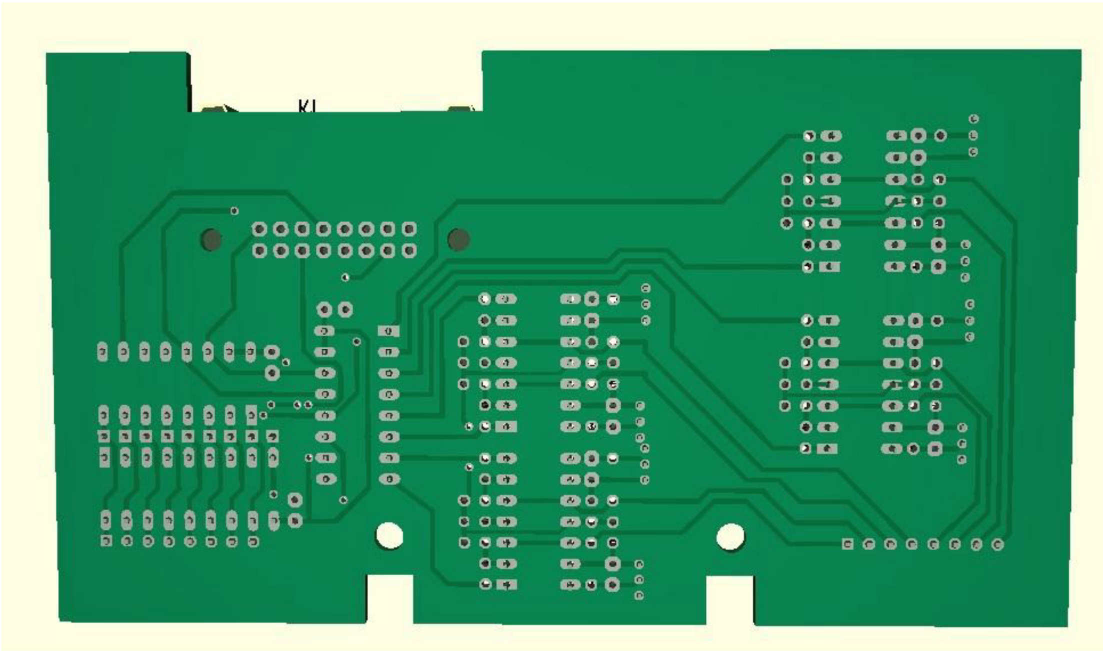

Figure 4-27: R/T bottom

4.5.4 Capacitance measurement (C)

Theory of operation:

For each capacitance channel a timing circuit and reference resistor is present. The capacitance on the probe form, together with the other parts, a mono stable RC-timer. According to the data sheet of the x556 timer, the high time of the circuit is 1.1*R*C. The desired channel can be selected by a multiplexer and a trigger pulse can be sent to start the high time. The resulting signal is rerouted to the OBC, where it is used as a gate signal for the internal high speed counter.

First test results for a similar circuit can be found in Appendix C.

Schematic:

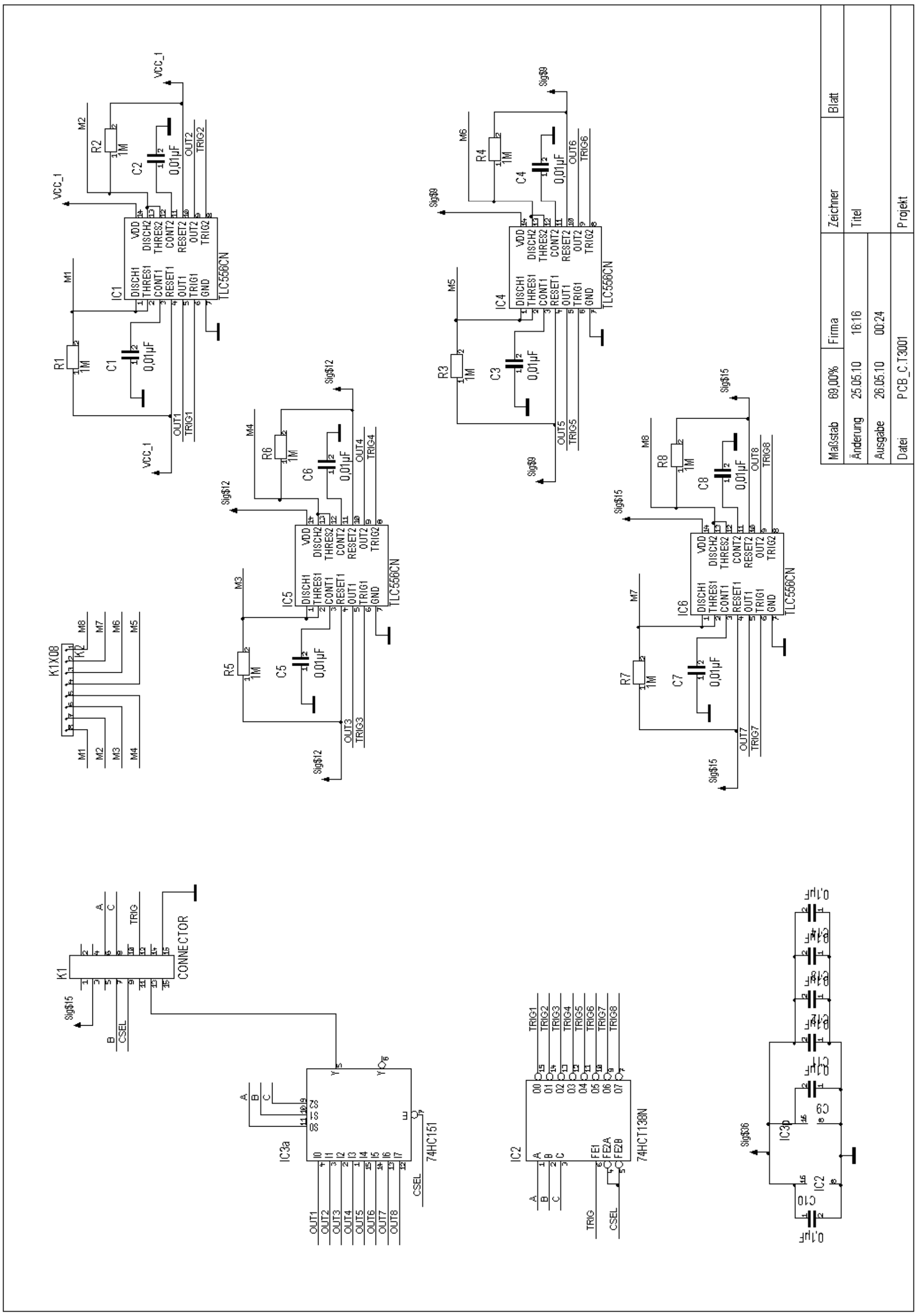

Figure 4-28: C schematic

PCB Design:

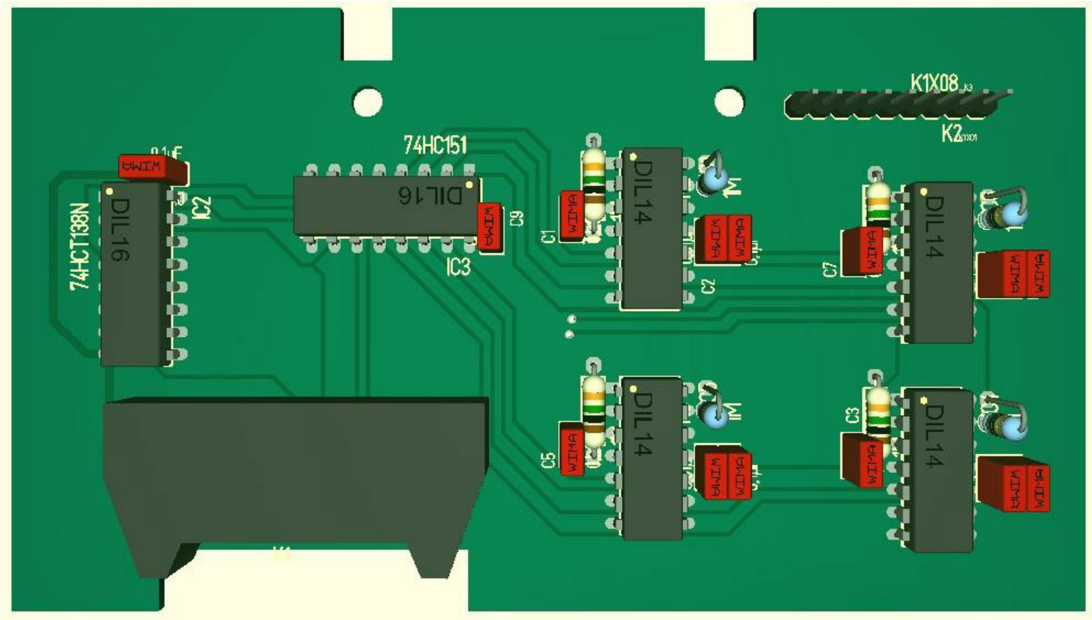

Figure 4-29: C PCB top

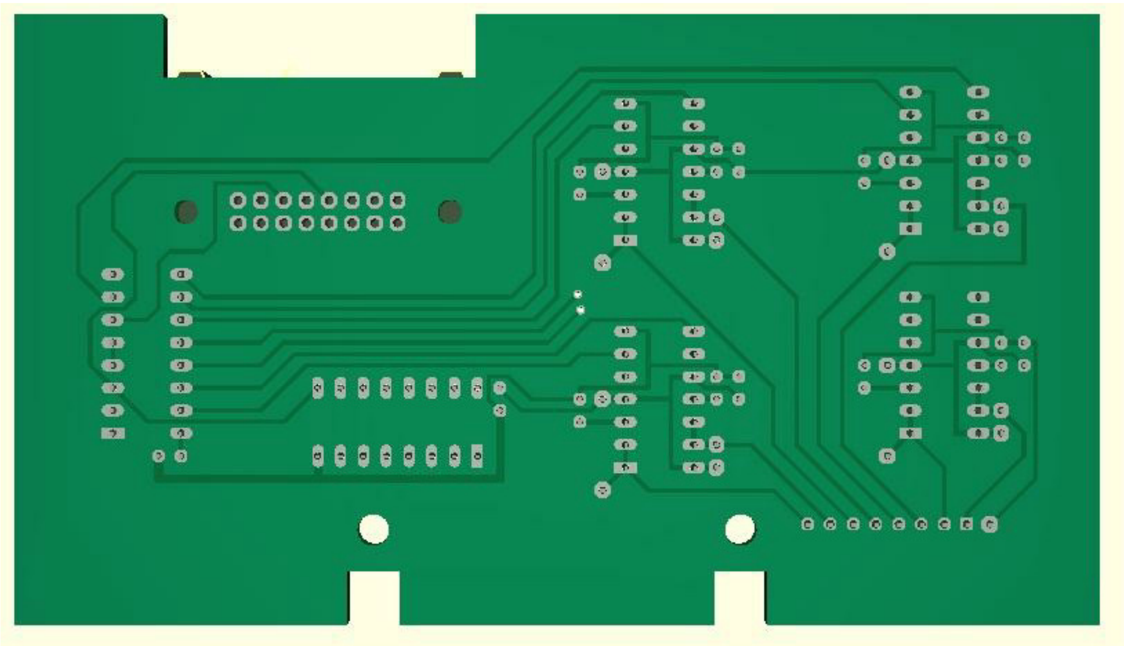

Figure 4-30: C PCB bottom

4.5.5 Camera system

The cameras are commercially available digital recording devices with a simple to use interface and low in size and mass. To verify the reliability of the cameras several investigations, including a thermal vacuum test, have been conducted prior to the beginning of the final design phase.

Digital cameras:

Two of these cameras are installed in aluminium boxes below the cylinder cover. The probe at the end of the boom is centered in the cameras fields of view.

Camera Type:	ACME FlycamOne ECO
Supply voltage.	5V
Consumption:	70mA
Storage device:	microSD
Analogue output:	no
Resolution:	VGA (640 x 480)
Frame rate:	28fps
Field of view:	53.2°
Data rate:	0,5-1 MB/s

Optional TV camera:

An optional 3rd analogue TV camera can be mounted between the experiment cylinder and the outer REXUS cylinder. It is mounted to the heat-shield with an aluminium bracket.

Camera Type:	WATEC 240VIVID
Supply voltage:	6V
Consumption:	170mA
Storage device:	no
Analogue output:	Composite video, 1Vpp (75 Ohms), PAL
Resolution:	720 x 582 pixels, 480TV lines
Frame rate:	(according to PAL standard)
Field of view:	33,4° x 25,5°

The positions and fields of view of the three cameras can be seen in the illustrations below:

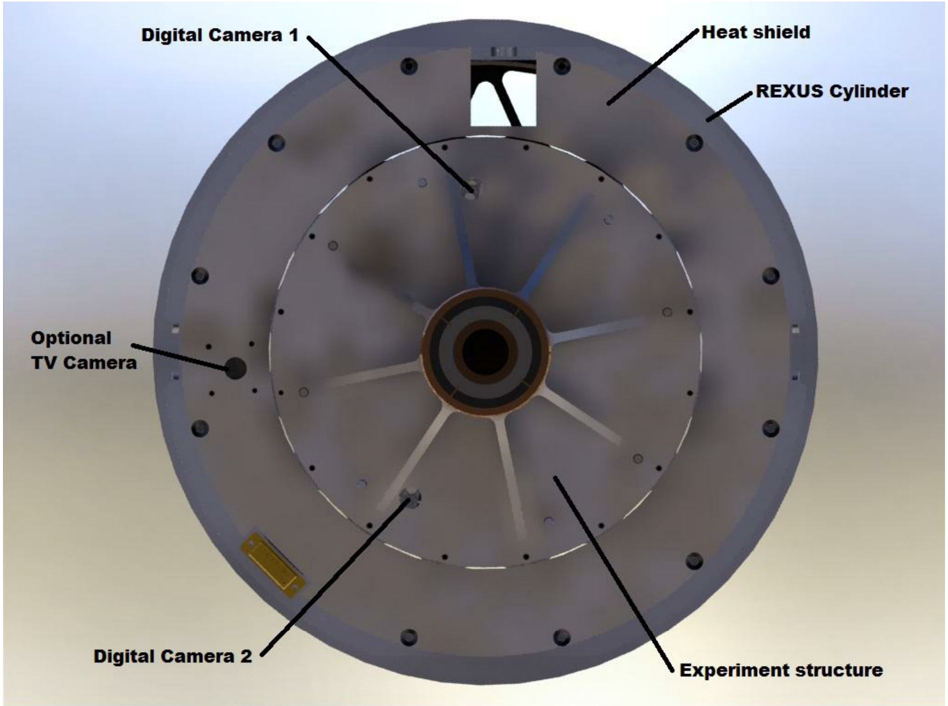

Figure 4-31: Camera positions

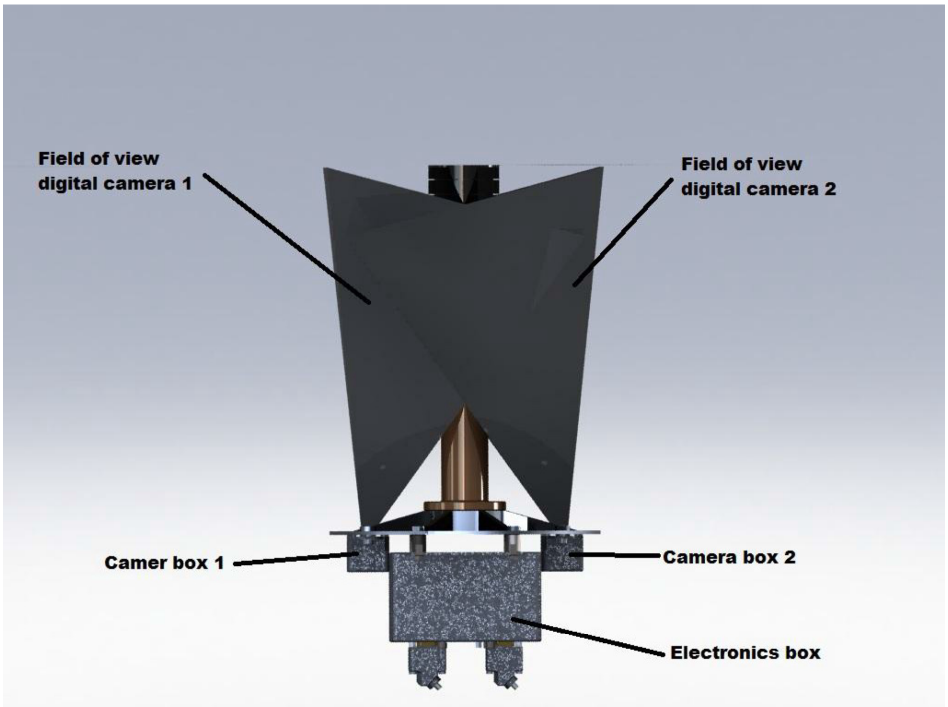

Figure 4-32: Field of view: digital cameras

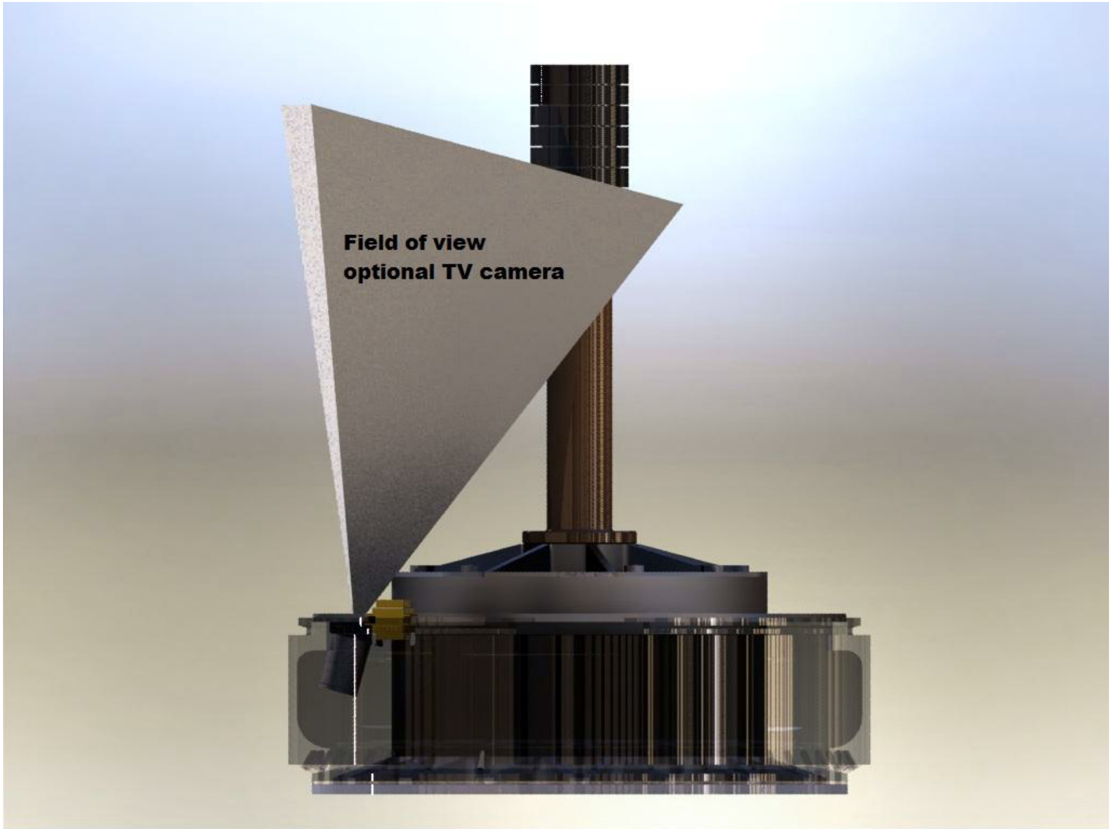

Figure 4-33: Field of view: analogue TV camera

4.6 Thermal Design

4.6.1 Thermal environment for electronics and structures

Electronics and structural components need to stay within certain temperature limits. Exact flow and temperature conditions are not important to them as long as the limits are not exceeded.

Ground operations:

There are no liquids in the experiment and the temperature range of -30°C to 30°C is manageable for all components. Long exposure to very low temperatures as well as humidity could provide some risk.

Launch and flight in high atmospheric layers:

During the launch phase the experiment is protected by the nosecone, which is separated at T = +60s. (Altitude: 57.3km).

Heat from the outer structure (wall temperature of 110°C) may heat the nosecone adaptor but will not reach the electronics.

After nosecone separation the thermal environment is cooling down to -100°C, but gas density is below 6E-5 kg/m³ (p = 4Pa) above 70km of altitude resulting in negligible heat transfer due to convection. Heat will be taken away by thermal radiation.

We assume that during this phase of the flight (until T = +200s) the temperature of the structure will be equally distributed to max. 30°C.

Atmospheric re-entry:

As density and velocity increase, Mach numbers up to 3.5 occur during this phase and thermal loads increase considerably.

Model for thermal loads:

Starting at T = +200s wall temperatures of components exposed to the re-entry flow are subjected to the thermal load profile for 150s. The temperatures are the mean value of T_w at 0° and T_w at 60°. The minimum temperature is 0° and from T = +300s to T = 350s it rises from 0°C to 10°C. (See table 4-34)

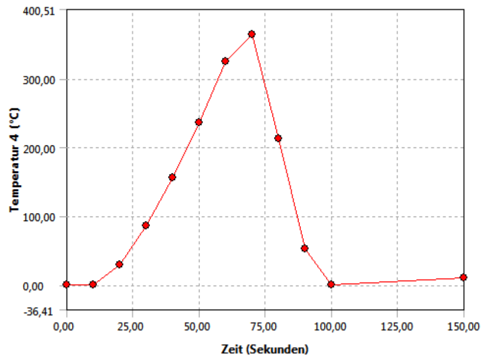

Figure 4-34: Thermal load profile

After T=+300s the rocket is falling with Ma<1, entering dense and cold atmospheric layers (altitude <9km). The structure is cooled by convection and finally reaches thermal equilibrium with the ambient temperature after landing.

Based on these assumptions, a thermal simulation has been carried out in an adiabatic environment without convection. Only the surface temperatures of the big upper surfaces are boundary conditions, because the lower part of the structure is protected against the re-entry flow from the sides by a sheet metal plate. Although the flow is only coming from one direction, the total circumference is exposed to these temperatures, whereas only a part of the cylinder cover is subjected to the same load because lower temperatures are expected there (larger radius, less exposure).

This assumption will overestimate thermal loads as maximum temperatures will only be reached on the side facing the flow and not on the entire circular structure.

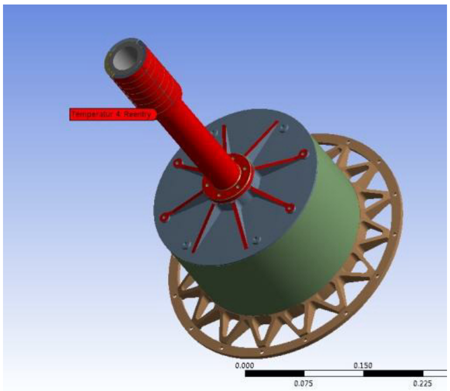

Figure 4-35: Surfaces subjected to thermal load profile

Results of thermal simulations:

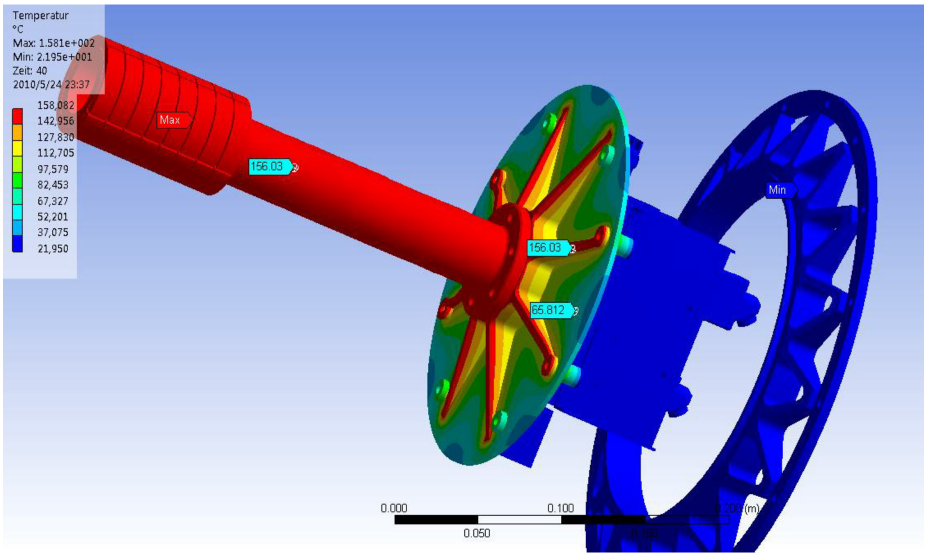

Figure 4-36: T=+240s: Probe and boom heated, structure still cold

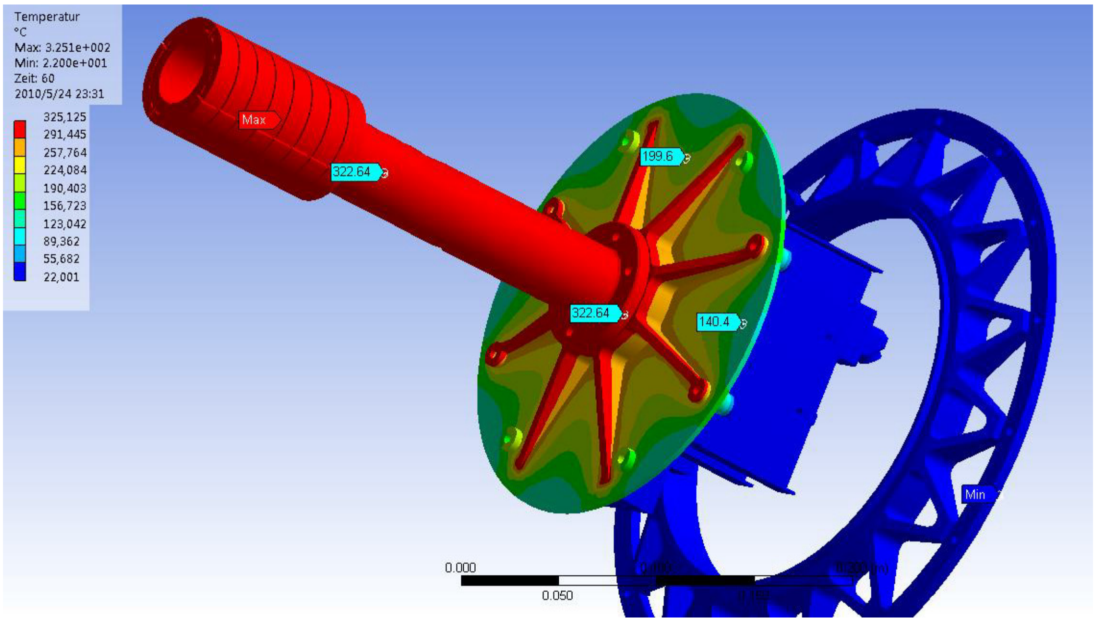

Figure 4-37: T=+260s, Peak thermal load, cylindrical cover at 140 – 200°C

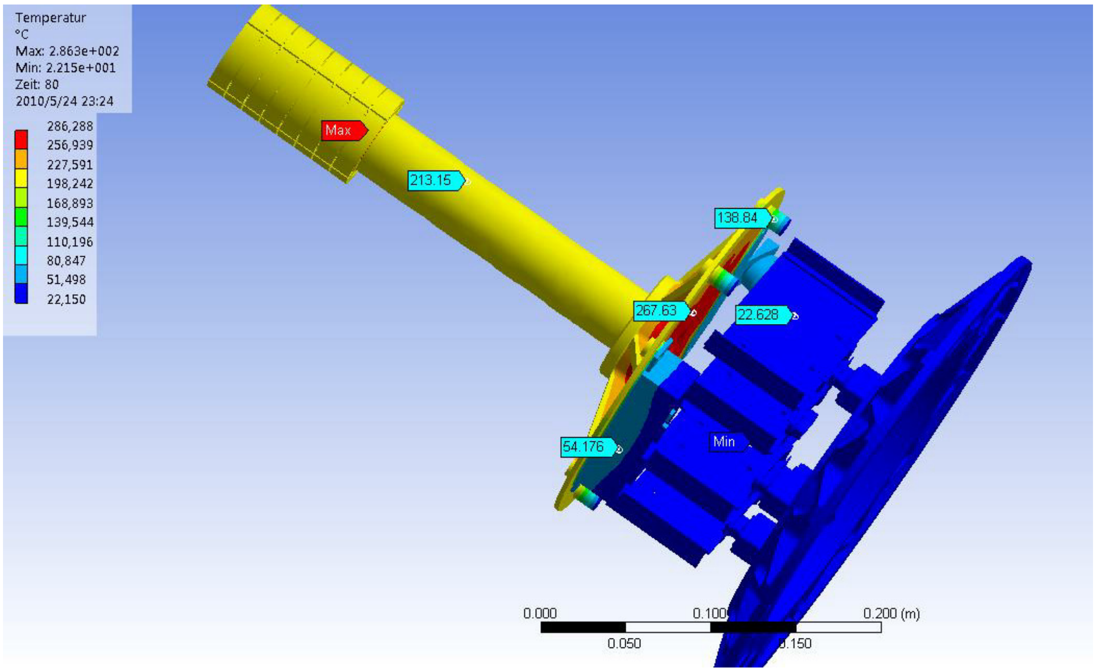

Figure 4-38: T=+280s, peak temperatures at camera boxes, thermal insulation via titanium distance pins to electronic box is very effective.

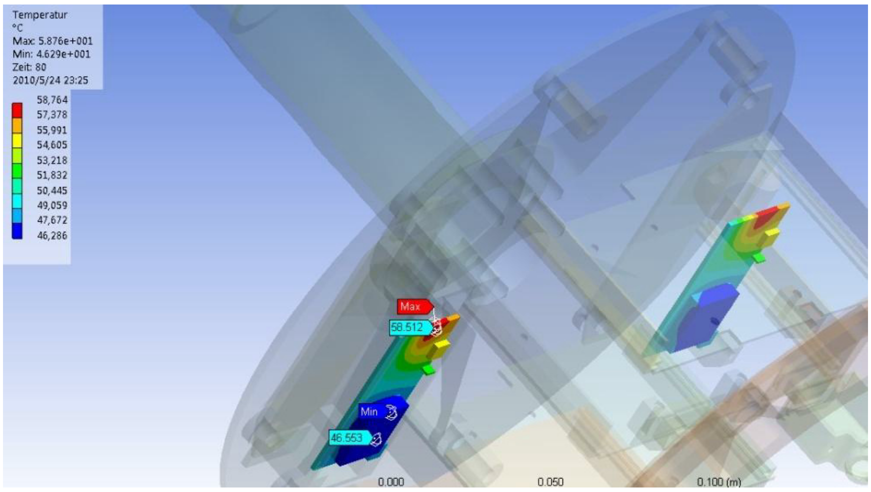

Figure 4-39: Cameras at T = +280s

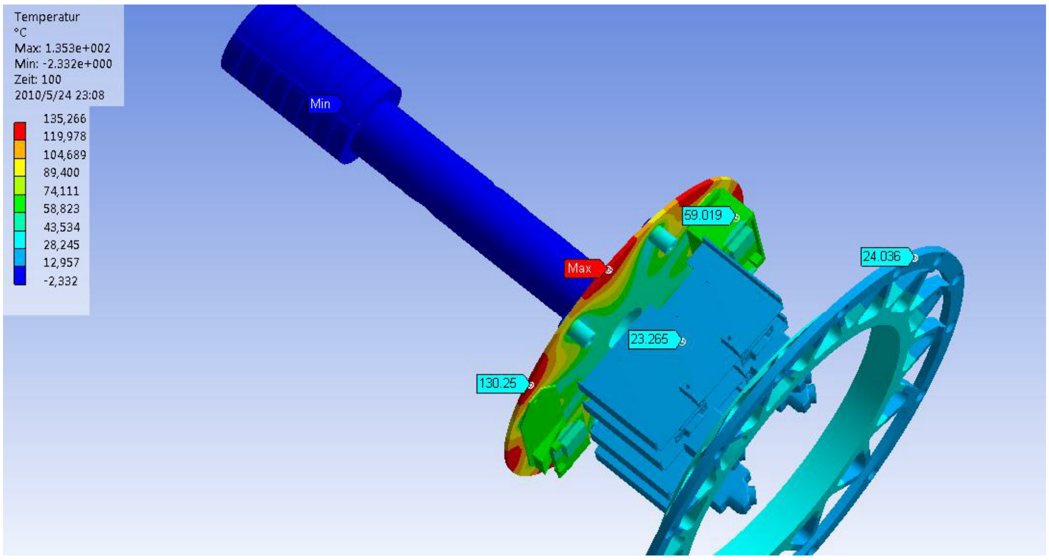

Figure 4-40: Entire Structure at T = +300s

Adaptor ring will additionally be heated from rocket structure, but this will not influence electronics temperatures.

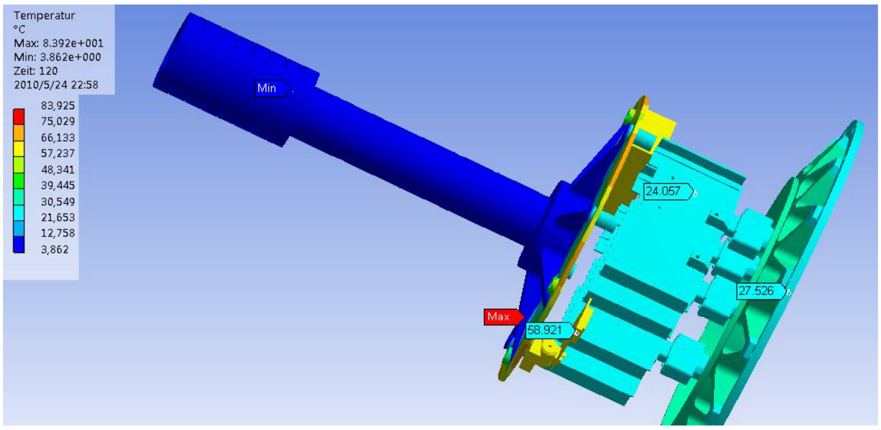

Figure 4-41: T=+320s

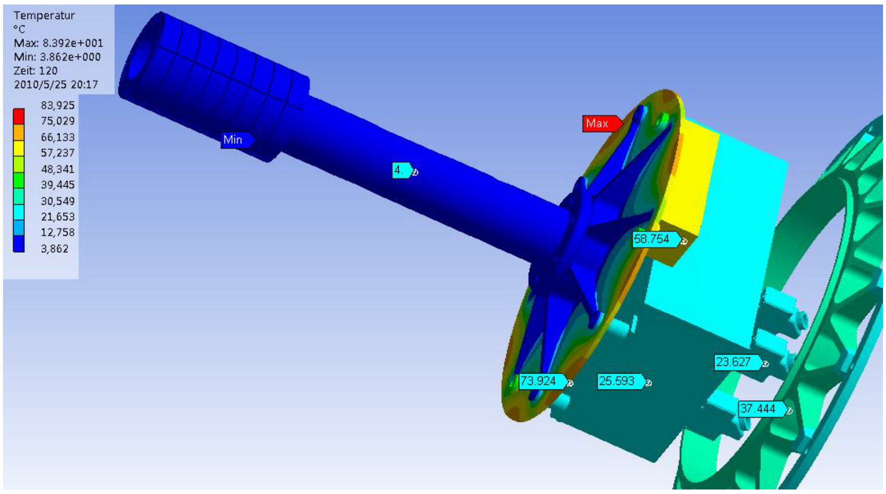

Figure 4-42: Electronics box and cover at T = +320s

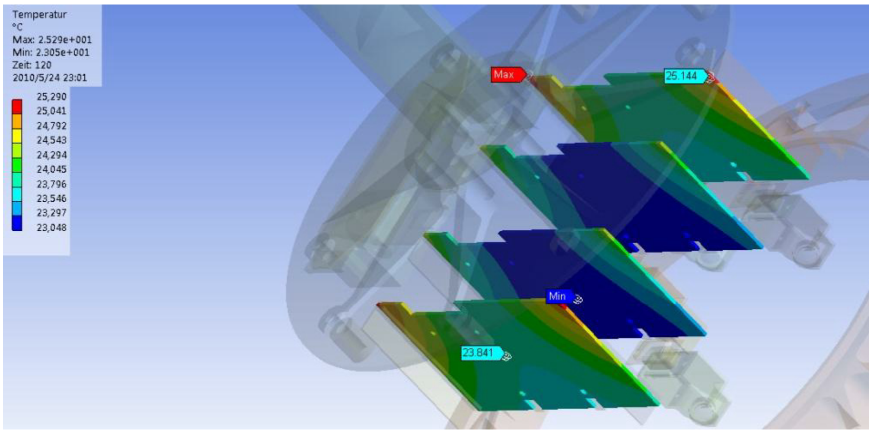

Figure 4-43: Measuring cards at T = +320s

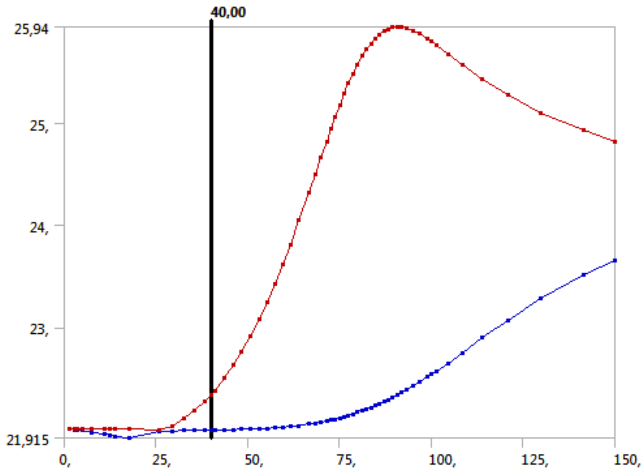

Figure 4-44: Electronics box temperatures. Red: maximum, blue: minimum trend. Timescale actually starting at +200s.

Maximum temperatures for electronics inside box from T=+200s to T = +350s

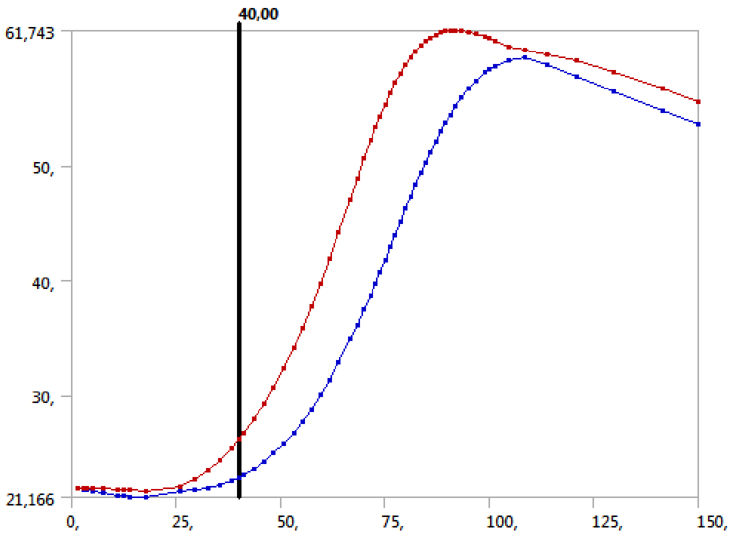

Figure 4-45: Camera box temperatures. Red: maximum, blue: minimum trend. Timescale actually starting at +200s. Maximum Temperatures for Cameras from T=+200s to T = +350s

The experiment's internal thermal dissipation is considered to be 5W at maximum. This contribution is negligible for thermal calculations. Cold conditions before launch should not affect electronics.

Thermal loads are not a structural problem. Additional heat insulation for camera boxes is realized through GFRP spacers and glass windows.

4.6.2 Thermal environment for the probe

Thermal conditions around the probe during the re-entry phase are critical for the success of the experiment. They have a strong influence on the probe material selection and should be well monitored during the actual experiment in order to be able to draw proper conclusions from the other measurement data.

The shock distance δ of the detached shock before a cylinder with the equivalent nose radius of 0.3m has been calculated.

Probe temperatures for a spherical adiabatic probe with a diameter of 0.06m were calculated on the basis of a semi-empirical heat-flux model:

Semi-empirische Wärmeflußmodelle:

Ansatz	$\dot{Q} = C \cdot \rho^N \cdot v^M$	**[W/m²]**	C **Korrelations-koeffizient**
Staupunkts-modell (SP) z.B.	$N = 1/2\ ;\ M = 3$		ρ **in** $[kg/m^3]$ v **in** $[m/s]$
	$C = 1,83 \cdot 10^{-4}\ R_N^{-\frac{1}{2}} \cdot [1 - h_W/h_{0e}]$		
	$h_W = 1004,6 \cdot T_W$	**[J/kg]**	
	$h_{0e} = 1004,6 \cdot T_\infty + \frac{1}{2}\ v_e^2$	**[J/kg]**	
Angestellte Platte	$N = 1/2\ ;\ M = 3,2$ **(laminare Strömung!)**		φ**-Anströmung**
	$C = 2,53 \cdot 10^{-5}\ \sin\ \varphi\ \sqrt{\cos\ \varphi}\ x^{-\frac{1}{2}}\ [\ 1 - \frac{h_W}{h_{0e}}\ ]$		

Where the 30° and 60° temperatures are calculated using the model for a tilted plate.

proposed by Tauber [1]

This flux is in equilibrium with the radiative flux $\sigma\varepsilon T^4$. It is solved for the wall temperature T_w at angles of attack of 0° (stagnation point model), 30° and 60°.

t_{sim} is the mean value of T_w at 0° and 60° representing the average temperature at the probe in °C used for thermal simulations. (thermal load profile (fig. 4-37).

T	Altitude	velocity	Ma	T0	gas density	T_{as}	T_w0°	T_w 30°	T_w 60°	t_{sim}	δ
[s]	[km]	[m/s]	[-]	[K]	[kg/m^3]	[K]	[K]	[K]	[K]	[°C]	[m]
200	84.0	540	1.853	211	7.53E-06	331.75	261.53	219.94	219.41	0.00	0.11
210	79.0	625	2.125	215	1.62E-05	386.68	301.02	234.39	233.30	0.00	0.09
220	72.5	690	2.308	222	4.24E-05	435.01	347.48	257.45	255.68	28.43	0.08
230	66.0	800	2.607	234	1.04E-04	527.07	422.20	298.93	296.14	86.02	0.07
240	57.5	890	2.809	250	3.18E-04	615.18	507.10	353.58	349.73	155.27	0.06
250	48.5	980	3.022	262	9.87E-04	701.09	602.84	420.07	415.09	235.82	0.06
260	38.0	1060	3.379	245	4.19E-03	734.70	698.86	502.05	495.95	324.26	0.06
270	27.5	1055	3.616	212	2.33E-02	703.18	717.54	562.90	556.99	364.11	0.05
280	19.0	800	2.763	209	9.45E-02	502.10	517.12	458.63	455.56	213.19	0.07
290	12.5	500	1.709	213	2.64E-01	312.30	335.15	317.10	315.97	52.41	0.13
300	9.0	360	1.214	219	4.47E-01	248.07	281.64	269.95	269.23	0.00	0.39

T_{as} Gas temperature after normal adiabatic shock

T_w Wall temperature of an adiabatic spherical probe, eps = 0,8, R =0,03m
calculated with semi-empirical model by

δ Shock distance before a spherical nose with R = 0,3m

Figure 4-46: Thermal environment

These calculations show that the shock caused by the body of the rocket should not interfere too much with the probe at the top of the boom.

Probe temperatures peak at 360°C and exceed 100°C for about 50s (T=+230s to T= 280s). This should allow for proper thermal conditions for ablation of the probe material.

4.7 Power System

For this experiment the REXUS service module is the only source for electrical power. The overall safety factor is j=1.5. The power consuming systems are:

System	min. load [mW]	max. load [mW]
Power control and distribution (PCDU)	1400	2054
Onboard computer (OBC)	370	822
Measurement system (RCTM)	0	358
Camera system (CAM)	0	4500

Table 4-10: Power consumption envelope

The systems are switched on and off according to chapter 4.2.2, section “Used Signals”. The power consumption per flight phase is calculated in the next table.

flight phase	used systems	calc. power consumption [mW]	meas. power consumption [mW]	maximum duration of phase [s]
pre launch	PCDU min. OBC min.	1770	1400	180
launch	PCDU min. OBC max.	2222	1456	60
activation	PCDU max. OBC max. CAM	7376	3360	90
measurement	PCDU max. OBC max. CAM RCTM	7734	3640	150
recovery	PCDU min. OBC min.	1770	0	3600

Table 4-11: Power consumption by flight phase

Considering a DC/DC converter efficiency of 0.8 and a REXUS main bus voltage of 28 V a total of 0,108 Ah is consumed from the REXUS battery.

4.8 Onboard Software Design

The onboard software is written in C. As a development platform GCC for AVR controllers in combination with ATMELs free development studio AVRStudio v4.16 is used.

The onboard software is designed as a state machine. For each phase of the flight there is a dedicated state mode. The transition from one state to another is controlled via interrupts triggered by the signals from the REXUS service module. An additional test mode exists for ground testing purposes. In the test mode all existing S/W functions can be executed separately upon request. It can only be entered from the safe mode. The functionality of the other modes is composed from the executable functions mentioned in the following. The state flow diagram can be seen below.

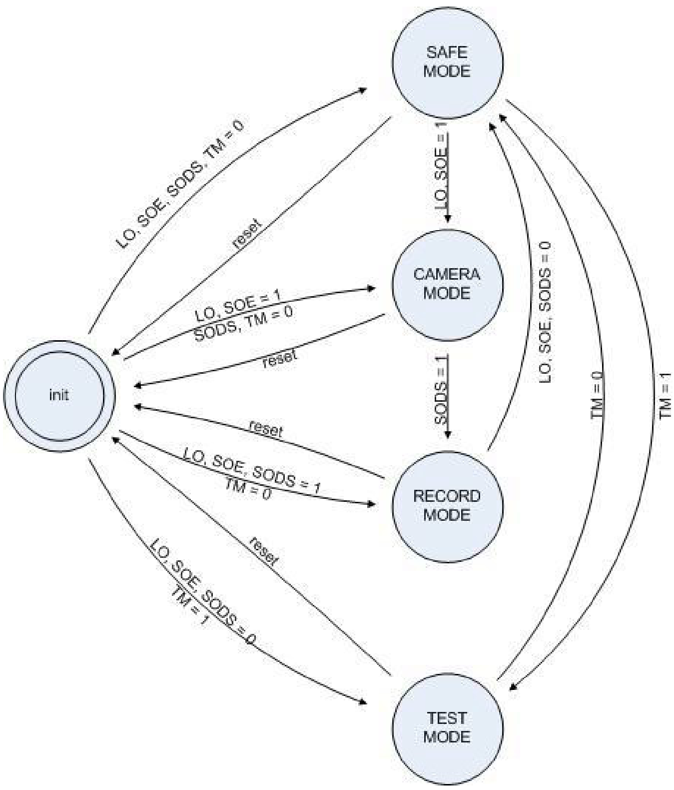

Figure 4-47: State machine

The core of the mode handling is the mode finder. It is called after every action or reset as well as by an interrupt resulting from a timer overflow. Each time the mode evaluation is executed, it determines which mode should be executed from the stored status values. These can be modified by a background thread invoked by a REXUS SM signal change as mentioned above. Once the mode is determined all required sub-functions associated to it are executed. Three essential procedures take place in each cycle of execution, which is: mode evaluation, status storage and watchdog reset. The status storage does not refer to all status parameters, but only those that change with each cycle, such as the flash memory counter. They are being stored in the external RAM of the onboard clock circuit because it has an own small watch battery and won’t lose the data in its multi-purpose RAM even in case of severe malfunctions. This is to ensure that any data collected will not be overwritten in any case.

The generalized S/W flowcharts are shown in the next figures. Also the serial data handling that is performed in background by interrupts is shown.

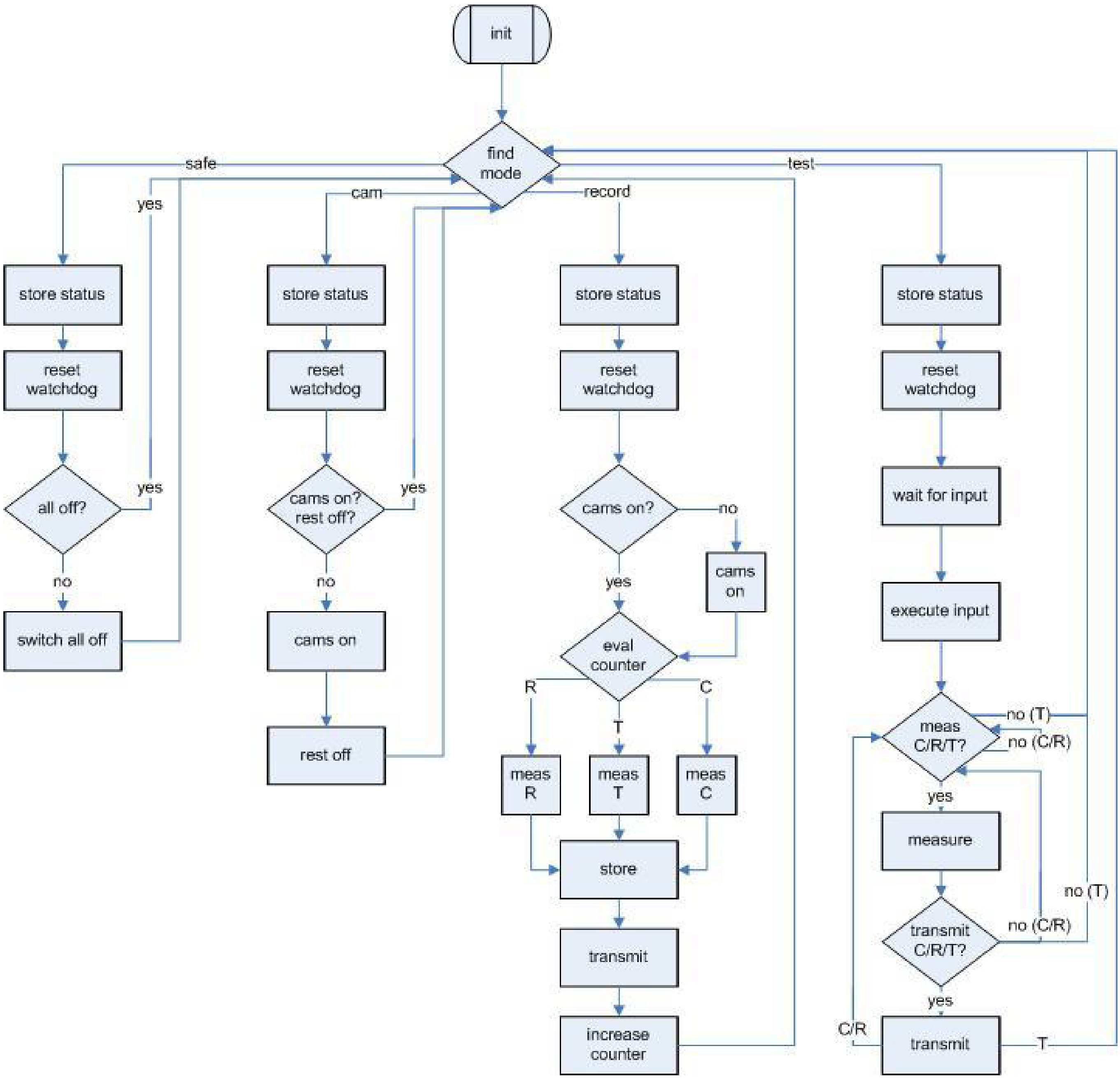

Figure 4-48: Onboard S/W flowchart

4.8.1 Modes (threads)

4.8.2 Serial data handling

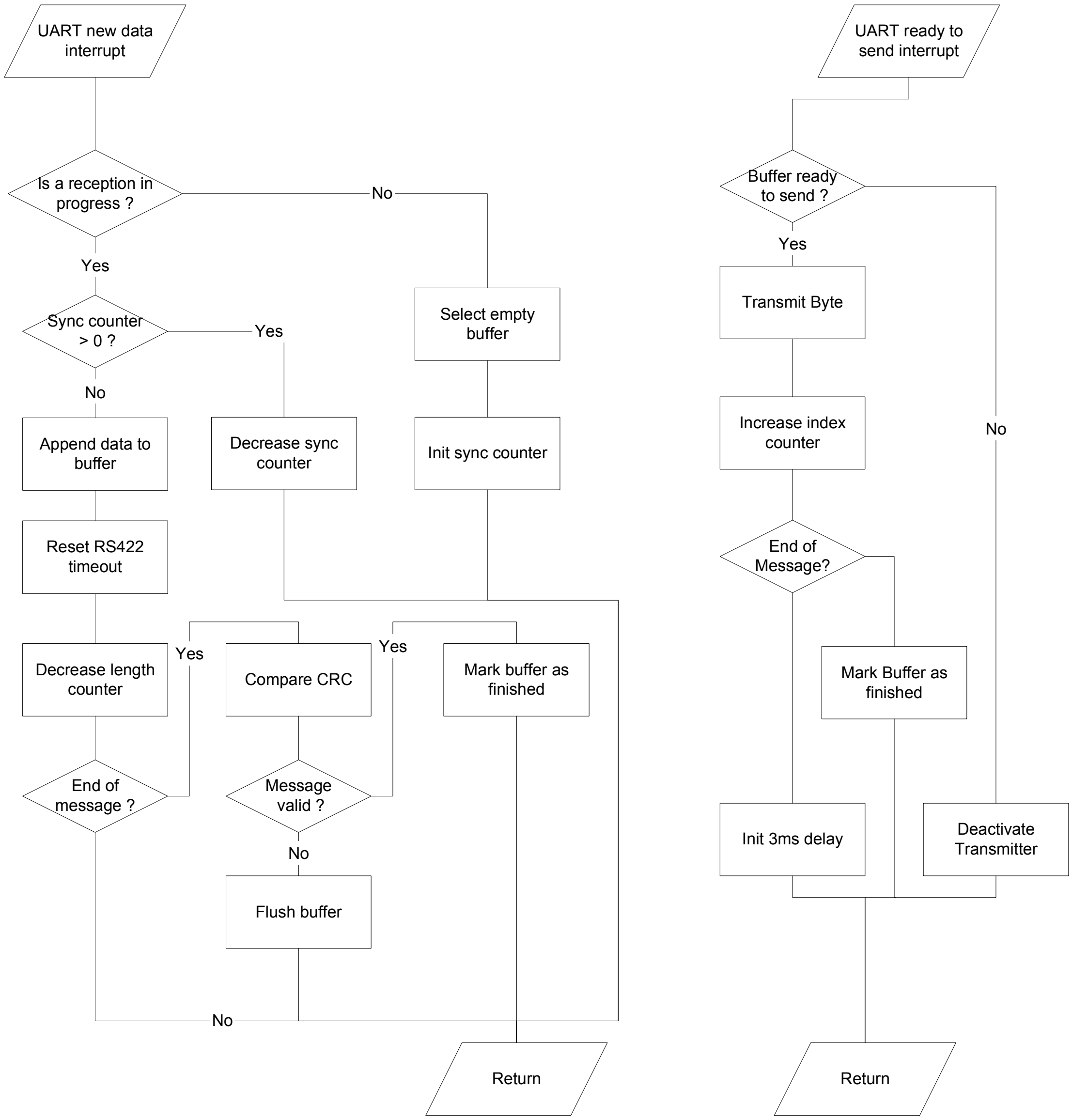

Figure 4-49: Data transmission flowchart

4.8.3 Required Storage Volume

The required storage volume can be calculated from the transmitter's data rate. The total mission duration including tests and pre-flight is assumed to be 1 hour. Since the transmission overhead is not stored, the effective maximum memory data rate reduces to 580 bytes/s with a time share of 0.4. The minimal rate is 100bytes/s with a time share of 0.6.

The required storage volume would be 580 byte/s * 3600s * 0.4+100bytes/s * 3600s * 0.6 =**1015200** bytes

The next larger storage size available is 16Mbit, which is nearly double of the required size.

4.8.4 Data Structure

All up- and downlink data has the following structure:

- sync 2 byte
- length 1 byte
- time stamp 3 byte
- ID 1 byte
- data 10 to 16 bytes
- CRC 2 byte

All data packets are followed by a 3ms delay time.

A summary of the required bandwidth can be found in 4.2.2.

4.9 Ground Control Software

The software described here is designed to maintain communication and data transmission between the REMOS onboard experiment and the Ground Control at Esrange during experiment preparation and launch.

Esrange Ground Interface

Esrange provides an electrical supply and the telemetry interface. A standard serial interface is used for the downlink. The uplink is only available during preparation phase. The data content is described below. The timing between the packages might vary due to data multiplexing in the REXUS service module.

Protocol Definition

The protocol covers the communication between the experiment and the ground control and vice versa. The connection and the data transmission depend on the operation mode of the experiment.

Link: Experiment to Ground Control

The REMOS experiment is able to send four types of data packages. Three packages containing experiment data and one for status information. The structure of the packages is listed in the tables below.

Status Message

Byte	Function	HEX value	Information
1	Sync 1	0xCC	
2	Sync 2	0xAA	
3	Packet length	0x18	
4	Packet type	0x53	‚S‘ according to ASCII code
5	Timestamp		Bit 0-3: hundredth of seconds Bit 4-7: tenth of seconds
6			Bit 0-3: seconds Bit 4-6: 10 seconds Bit 7: don’t care
7			Bit 0-3: minutes Bit 4-6: 10 minutes Bit 7: 0
8	Status 1	0x00 – 0xFF	Bit 0: Lift-Off Signal (LO) Bit 1: Start Of Experiment (SOE) Bit 2: Start Of Data Storage (SODS) Bit 3: test mode indicator Bit 4: camera 1 indicator Bit 5: camera 2 indicator Bit 6: sensor power indicator Bit 7: camera power indicator
9	Status2	0x00 – 0x3F	Bit 0: temperature sensors recording Bit 1: resistance sensors recording Bit 2: capacitance sensors recording Bit 3: temperature data transmitting Bit 4: resistance data transmitting Bit 5: capacitance data transmitting Bit 6: flash reading
10	SW-Mode		0 / 1: standby mode 14 / 15: camera mode 240 / 241: record mode 254 / 255: test mode

			Last bit shows mode integrity
11 12	Page Pointer	0x0000 – 0x0FFF	
13 14	Frame Pointer	0x0000-0x0210	
15	28V Supply	0x00–0xFF	voltage = value * const1
16	5V System	0x00-0xFF	voltage = value * const2
17	5V Sensors	0x00-0xFF	voltage = value * const3
18	5V Cameras	0x00-0xFF	voltage = value * const4
19	Electr. Temp.	0x00-0xFF	Temperature = 2. Order Polynomial interpolation
20 21	Gas temperature	0x0000 – 0x3FFF	Temperature = value * 0.25°C In case of an error: FFFF
22	Com confirm	0x00 or 0xFF	Last executed command

23
24
	CRC Checksum	0x0000 – 0xFFFF	`Initial valie for crc: crc = 0x0000`
			
			`Update function for crc:`
			`uint16_t crc_xmodem_update (uint16_t crc, uint8_t data)`
			`{`
			`int i;`
			
			`crc = crc ^ ((uint16_t)data << 8);`
			`for (i=0; i<8; i++)`
			`{`
			`if (crc & 0x8000)`
			`crc = (crc << 1) ^ 0x1021;`
			`else`
			`crc <<= 1;`
			`}`
			
			`return crc;`
			`}`

Table 4-12: Structure of the status message

Binary Code								Decimal Value	SW Mode
0	0	0	0	0	0	0	X	0, 1	Stby
0	0	0	0	1	1	1	X	14, 15	Cam
1	1	1	0	0	0	0	X	240, 241	Rec
1	1	1	1	1	1	1	X	254, 255	Test
X	X	X	X	X	X	X	(0/1)	(LSB)	Mode integrity

Table 4-13: Software mode byte breakdown

Temperature Message

Byte	Function	HEX value	Information
1	Sync 1	0xCC	
2	Sync 2	0xAA	
3	Packet length	0x19	
4	Packet type	0x54	‚T‘ according to ASCII code
5	Timestamp		Bit 0-3: hundredth of seconds Bit 4-7: tenth of seconds
6			Bit 0-3: seconds Bit 4-6: 10 seconds Bit 7: don’t care
7			Bit 0-3: minutes Bit 4-6: 10 minutes Bit 7: 0
8 9	Temp 1	0x0000- 0x0FFF	Temperature = value *const1 – const2
10 11	Temp 2	0x0000- 0x0FFF	Temperature = value *const1 – const2
12 13	Temp 3	0x0000- 0x0FFF	Temperature = value *const1 – const2
14 15	Temp 4	0x0000- 0x0FFF	Temperature = value *const1 – const2
16 17	Temp 5	0x0000- 0x0FFF	Temperature = value *const1 – const2
18 19	Temp 6	0x0000- 0x0FFF	Temperature = value *const1 – const2
20 21	Temp 7	0x0000- 0x0FFF	Temperature = value *const1 – const2
22 23	Temp 8	0x0000- 0x0FFF	Temperature = value *const1 – const2
24 25	CRC Checksum	0x0000- 0xFFFF	see above

Table 4-14: Structure of the temperature message

Resistor Message

Byte	Function	HEX value	Information
1	Sync 1	0xCC	
2	Sync 2	0xAA	
3	Packet length	0x19	
4	Packet type	0x52	‚R‘ above ASCII code
5	Timestamp		Bit 0-3: hundredth of seconds Bit 4-7: tenth of seconds

6			Bit 0-3: seconds Bit 4-6: 10 seconds Bit 7: don‘t care
7			Bit 0-3: minutes Bit 4-6: 10 minutes Bit 7: 0
8 9	R 1	0x0000- 0x0FFF	
10 11	R 2	0x0000- 0x0FFF	
12 13	R 3	0x0000- 0x0FFF	
14 15	R 4	0x0000- 0x0FFF	
16 17	R 5	0x0000- 0x0FFF	
18 19	R 6	0x0000- 0x0FFF	
20 21	R 7	0x0000- 0x0FFF	
22 23	R 8	0x0000- 0x0FFF	
24 25	CRC Checksum	0x0000- 0xFFFF	See above

Table 4-15: Structure of the resistor message

Capacity Message

Byte	Function	HEX value	Information
1	Sync 1	0xCC	
2	Sync 2	0xAA	
3	Packet length	0x19	
4	Packet type	0x43	‚C‘ according to ASCII code
5	Timestamp		Bit 0-3: hundredth of seconds Bit 4-7: tenth of seconds
6			Bit 0-3: seconds Bit 4-6: 10 seconds Bit 7: don’t care
7			Bit 0-3: minutes Bit 4-6: 10 minutes Bit 7: 0
8 9	R 1	0x0000- 0xFFFF	
10	R 2	0x0000-	

11		0xFFFF	
12 13	R 3	0x0000- 0xFFFF	
14 15	R 4	0x0000- 0xFFFF	
16 17	R 5	0x0000- 0xFFFF	
18 19	R 6	0x0000- 0xFFFF	
20 21	R 7	0x0000- 0xFFFF	
22 23	R 8	0x0000- 0xFFFF	
24 25	CRC Checksum	0x0000- 0xFFFF	see above

Table 4-16: Structure of the capacity message

<u>Link: Ground Control to Experiment</u>

This link is only used during the pre-flight operations for tests. The experiment has to be in safe or test mode to receive and handle the data. Switch to test mode is the only command accepted in safe mode, all other commands has to be executed in test mode.

Commands during test mode:

Byte	Function	HEX value	Information
1	Sync 1	0xCC	
2	Sync 2	0xAA	
3	Packet length	0x5-0x19	
4	Packet type	0x43	‚!' according to ASCII code
5	Command	See table below	
6-23	Additional required data and CRC	-	

Table 4-17: Structure of a command

Command	Bin Value	HEX Value	Additional Bytes	Comment
Exit Testmode	11111111	0xFF		
FLASH Read	0001 0011	0x13		
FLASH delete	0001 0000	0x10	2, as command	Need to be sent three

			byte	times
FLASH reset pointers	0001 0110	0x16		
FLASH set pointers	0001 1100	0x1C	4, as status 11-14	
Clock reset	0110 1100	0x6C		
Clock set	0110 0011	0x63	3, as status 5-7	
CAMs ON	0011 1111	0x3F		
CAMs OFF	0011 0000	0x30		
Record R	1100 01 11	0xC7		
Record T	1100 10 11	0xCB		
Record C	1100 11 11	0xCF		
Transmit R	1010 0111	0xA7		
Transmit T	1010 1011	0xAB		
Transmit C	1010 1111	0xAF		
Stop Recording R	1100 0100	0xC4		
Stop Recording T	1100 1000	0xC8		
Stop Recording C	1100 1100	0xCC		
Stop Transmission R	1010 0100	0xA4		
Stop Transmission T	1010 1000	0xA8		
Stop Transmission C	1010 1100	0xAC		

Table 4-18: Possible commands in test mode

Software Structure

The ground control software has only two modes, the flight mode and the test mode. The operations in each mode are:

Flight mode

- Continuous acquisition of data from downlink channel
- Handle corrupted packages and possible connection losses

Test mode (pre-flight mode)

- Sending commands to experiment (uplink)
- Run of test procedures

- System calibration

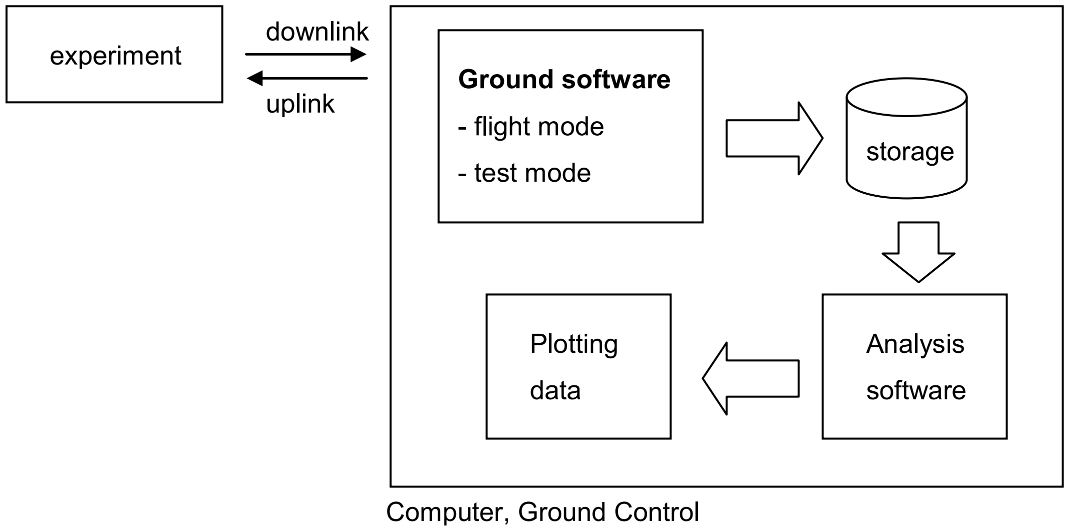

Figure 4-50: GSE S/W system overview

The generalized software structure is shown below.

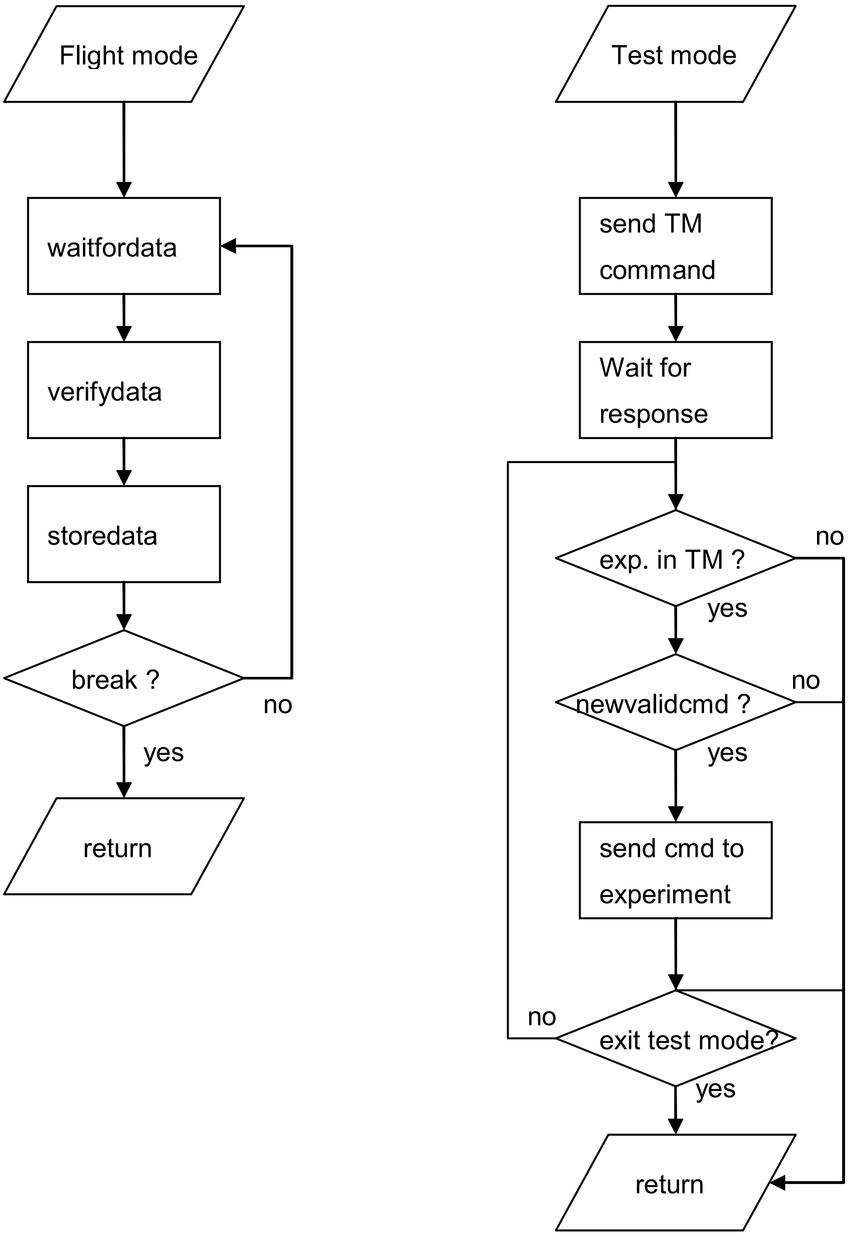

Figure 4-51: GSE S/W flowcharts

4.10 Ground Support Equipment

All GSE equipment, listed below, is manufactured and supplied by the team.

Equipment	Quantity	Location / required for
Shaker adapter	1	Stuttgart/ shaker test, EMI test
Probe breakout box	1	Stuttgart, Kiruna/ all tests + calibration
REXUS breakout box	1	Stuttgart, Kiruna / all tests + calibration
Transportation Box	1	Stuttgart, Oberpfaffenhofen, Kiruna
Transportation and integration carrier (TIC)	1	Stuttgart, Oberpfaffenhofen, Kiruna
ATMEL JTAGICE MkII	1	Stuttgart, Kiruna / onboard S/W updates
GSE Computer	1+1back up	Stuttgart, Kiruna/ Tests, calibration, flight monitoring
Locktight	10ml	Stuttgart, Kiruna
Probe Protection cover	2	Stuttgart, Kiruna

Table 4-19: Team-supplied GSE

For integration and testing prior to launch, some additional tools are required. These tools should be provided by MORABA / Esrange.

Equipment	Quantity	Location/ required for
Standard tool kit	1	Kiruna
30V 1A Power Supply	1	Kiruna
Torque wrench 0.9 Nm- 3.8 Nm	1	Kiruna
Wrench adapter for hexagon socket head cap screw (M3, M4, M5)	3	Kiruna

Table 4-20: Required GSE at Esrange

5 EXPERIMENT VERIFICATION AND TESTING

5.1 Verification Matrix

T – Test

I – Inspection

A – Analysis or similarity

R – Review of design

A – done

A – to be done

5.1.1 Functional Requirements

RQ ID	Functional Requirements	Verification
FRQ.01	The sensing areas shall be integrated into the probe surface in such a way, that they act as part of the heat-shield	R
FRQ.02	Electric resistance of the sensing elements shall be measured 8 locations during re-entry	R
FRQ.03	Electrical capacitance between the sensing elements shall be measured at 8 locations during re-entry	R
FRQ.04	Temperatures on the Probe have to be measured at 8 locations during re-entry	R
FRQ.05	A camera system including a recording device has to observe the degradation of the probe	R
FRQ.06	All measurement and housekeeping data has to be stored on board	R
FRQ.07	All measurement and housekeeping data has to be transmitted to the ground station	R
FRQ.08	Housekeeping shall monitor the supply voltages	R
FRQ.09	Housekeeping shall monitor the voltages behind all switchable supplies	R
FRQ.10	Housekeeping shall monitor the hard wired signals	R

FRQ.11	All transmitted data packets must have a unique time indication	R
FRQ.12	All data storages have to survive the landing impact	A
FRQ.13	Circuits must be tolerant to a short-circuit	T

Table 5-1: Functional requirements verification matrix

5.1.2 Performance Requirements

RQ ID	Performance Requirements	Verification
PRQ.01	The capacitance measurements shall have a resolution of 0.1% of the initial value	A
PRQ.02	The resistance measurements shall have a resolution of 0.1% of the initial value	A, T
PRQ.03	The measured maximum initial probe resistances must not exceed 500kOhms	T
PRQ.04	The measured minimum initial probe resistances must not be below 5kOhms	T
PRQ.05	The measured maximum initial probe capacitances must not exceed 1µF	A,T
PRQ.06	The measured minimum initial probe capacitance must not be below 50pF	T
PRQ.07	The temperature measurements on the probe shall be possible in a range of -100 to +500 degree centigrade	R
PRQ.08	The temperature measurement on the probe shall be conducted with an accuracy within a range of +/- 2 degree centigrade	R, T
PRQ.09	The system voltages shall be monitored with a resolution equal to or greater than +/- 0,1V	R, T
PRQ.10	All measurements have to be done at a rate of 10 Hz	R
PRQ.11	The camera frame rate shall be equal to or higher than 10Hz	R

Table 5-2: Performance requirements verification matrix

5.1.3 Design Requirements

RQ ID	Design Requirements	Verification
DRQ.01	The experiment shall be designed for the nose section of the REXUS rocket	R
DRQ.02	The overall mechanical safety factor for structural failure is j=1.5	R, A
DRQ.03	The experiment shall be designed to operate in the temperature profile of the REXUS rocket (see appendix for details)	A, T
DRQ.04	The experiment shall be designed to operate after exposure to the vibration profile of the REXUS rocket (see appendix for details)	A, T
DRQ.05	The experiment shall be designed to operate under the static acceleration loads of the REXUS rocket (see appendix for details)	A
DRQ.06	For all 15l of empty volume, a venting hole with a diameter of 10mm has to be added. The hole has to be covered with a cap (see REXUS User Manual Chap. 5.4)	R
DRQ.07	The module's internal thermal dissipation must not heat up the outer structure more than 10°C over the ambient ground temperature	A
DRQ.08	The module's internal thermal dissipation must not heat up the parts close to or in contact with the feed-through cable to more than +70°C.	A
DRQ.09	A module's internal thermal dissipation must not heat up parts facing other modules to more than +50°C.	R
DRQ.10	The heat transport by convection must be limited in such a way that the air temperature at the module interfaces does not exceed the ambient temperature by more than 10 °C.	R
DRQ.11	The electrical connector interface shall comply with the RX User Manual Chapter 7.6.1	R
DRQ.12	The experiment TM/TC interface shall comply with the RS422 standard	R

DRQ.13	The TM/TC protocol shall use a baud rate of 38,4kbit/s; format: 8 bits, 1stop bit, no parity	R
DRQ.14	The experiment shall operate from a power supply from 24V to 36V	R
DRQ.15	A short period peak power consumption shall not exceed 3 A on the RX power interface	A, T
DRQ.16	The continuous current consumption shall not exceed 1 A	R, T
DRQ.17	Optocouplers have to be used for the SODS, SOE an LO signals	R
DRQ.18	A standard RS232 interface with 57.6kits/s, 8 data bits, 1 stop bit, no parity has to be used for the EGSE	R
DRQ.19	All power supply cables shall be twisted	I
DRQ.20	Data cables shall be twisted	I
DRQ.21	Cables outside electronics boxes shall be shielded	R, I
DRQ.22	The experiment shall operate under vacuum conditions	T
DRQ.23	The experiment has to be designed in such a way, that it can be classified as a category B system or lower, according to Esrange Safety Manual	R
DRQ.24	No flammable adhesives shall be used	R

Table 5-3: Design requirements verification matrix

5.1.4 Operational Requirements

RQ ID	Operational Requirements	Verification
ORQ.01	The probe shall be covered after landing	R, I
ORQ.02	The OB S/W shall be designed as a state machine	R
ORQ.03	Breakout boxes shall be supplied for all electrical connections	R
ORQ.04	The OB S/W shall have the capability to operate without ground support	A, T
ORQ.05	For each flight phase a dedicated S/W mode shall exist	R
ORQ.06	In a test mode all commands from GSE S/W shall be accepted	R
ORQ.07	In S/W modes that are not the test mode, only mode change commands shall be accepted (from SM only)	R
ORQ.08	The data time stamp shall be synchronized before launch	R
ORQ.09	The OB S/W shall be able to fly the mission only with the LO signal working	R

Table 5-4: Operational requirements verification matrix

5.2 Test Plan

The following tests were conducted to verify the requirements.

5.2.1 Component Tests

Test number	1
Test type	vacuum
Test facility	ITLR Uni Stuttgart, vacuum chamber
Tested item	Camera system
Test procedure / level	operate the entire camera system under vacuum conditions (p < 0,05mbar) for three times the operation time
Test duration	1,5 h

Table 5-5: Test plan summary for test 1

Test number	2
Test type	Software
Test facility	Home PC, Breakout boxes
Tested item	system software
Test procedure / level	check software behavior for input signals from REXUS system, system reset (standard signal order and abnormal orders)
Test duration	2d

Table 5-6: Test plan summary for test 2

Test number	3
Test type	Electronics Power Board PCDU

Test facility	Breakout boxes, Breadboard
Tested item	Electronics
Test procedure / level	Power consumption, board interface, short circuit
Test duration	3h

Table 5-7: Test plan summary for test 3

Test number	4
Test type	Electronics R and T Measuring board
Test facility	Breakout boxes
Tested item	power consumption, board interface, measurement range
Test procedure / level	determine range of signals, out of range test
Test duration	3h

Table 5-8: Test plan summary for test 4

Test number	5
Test type	Electronics OBC board
Test facility	Breakout boxes
Tested item	Electronics
Test procedure / level	determine range of signals, out of range test, memory test
Test duration	3h

Table 5-9: Test plan summary for test 5

Test number	6
Test type	Electronics C Measuring board

Test facility	Breakout boxes
Tested item	Electronics
Test procedure / level	determine range of signals, out of range test, board interface
Test duration	5h

Table 5-10: Test plan summary for test 6

5.2.2 Functional Test

Test number	7
Test type	entire system
Test facility	Breakout boxes
Tested item	system software, electronics (peak power, power consumption
Test procedure / level	simulate an entire Flight with all signals
Test duration	2h

Table 5-11: Test plan summary for test 7

Test number	8
Test type	vibration (transient, sinusoidal) and shock
Test facility	DLR Stuttgart
Tested item	Entire system
Test procedure / level	operate the entire experiment under simulated flight conditions; pre and post inspection (functional and optical checks)
Test duration	2d

Table 5-12: Test plan summary for test 8

Test number	9

Test type	thermal vacuum
	60°C
Test facility	IRS Uni Stuttgart
Tested item	Entire system
Test procedure / level	operate the entire experiment under simulated flight conditions (decompression, vacuum recompression); pre and post inspection (functional and optical checks)
Test duration	2d

Table 5-13: Test plan summary for test 9

Test number	10
Test type	EMI
Test facility	IEH Uni Stuttgart
Tested item	Entire system
Test procedure / level	Place experiment and transmitter in correct distance. Apply Electromagnetic loads of the REXUS Transmitter. Monitor system performance
Test duration	1h

Table 5-14: Test plan summary for test 10

In addition to these tests, function checks and procedures as well as calibration tests will be necessary before the tests and before launch.

5.3 Test Results

5.3.1 Test 1: Camera Vacuum test

Camera Vacuum Test was successfully conducted.

Equipment:	Vacuum chamber, pressure sensor, temperature sensor
Test procedure:	-temperature sensor on MPEG encoder IC -Camera operating -Chamber evacuated for over 30min

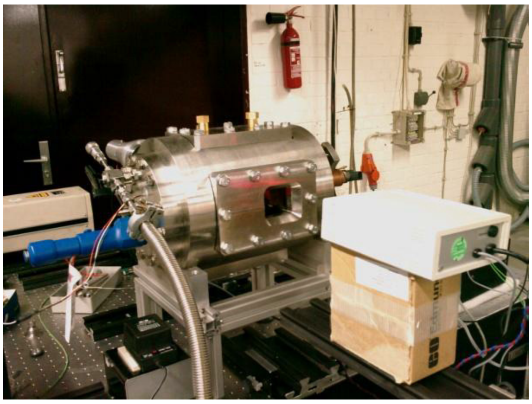

Figure 5-1: Camera vacuum test

The camera operated with no disturbances. An excessive heating of the encoder chip was not recognized.

5.3.2 Test 2: Software Test

The software test was realized in the Atmel AVR Simulator 2 which contains a detailed model of the behaviour of the processor used and is provided by its manufacturer.

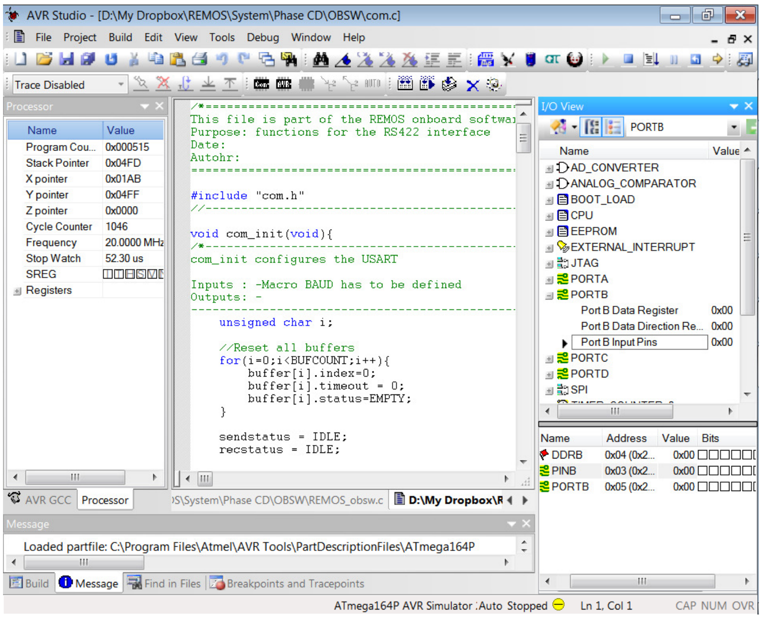

Figure 5-2: Software Test

5.3.3 Test 3: Electronics board Test

Test 3 is a functional test for the PCDU Electronic board and was completed successfully prior to manufacturing of the corresponding PCB on the full flight configuration circuit in an experimental board prototype.

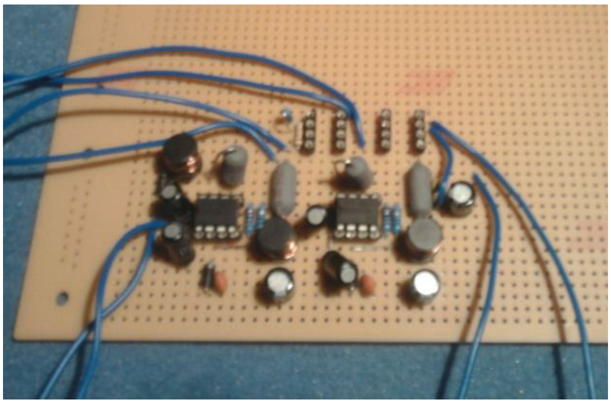

Figure 5-3:Electronics board Test

5.3.4 Test 5: OBC Test

The experiment was assembled and connected to our own GSE Service Module Simulator Box. The Simulator Box permits powering the system, setting the rocket signals and receiving telemetry via a COM Port.

This COM Port is connected to a PC via a USB adapter and there monitored by the hterm terminal software.

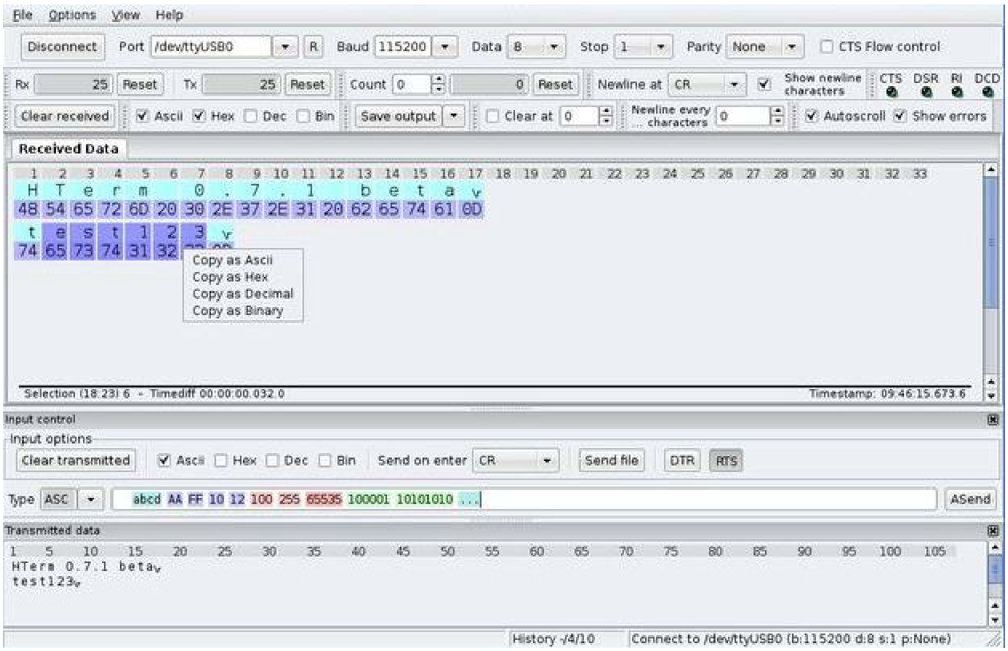

Figure 5-4:OBC Test screenshot

5.3.5 Test 6: CSENSE Test

To test the capacitance measurement channels a scope was used, to determine the high-time of capacitance-dependence timer circuit. The high-time of the signal is 1.1 * R*C, where R= 1MOhm.

Condition	Measured high-time	corresponding capacitance	Comment
No load	13,2 µs	12 pF	PCB- + Connector capacitance
27pf capacitor	45,1 µs	12pF + 29pF	within 15% capacitor tolerance
			-

Table 5-15: CSENSE test values

5.3.6 Test 7: Entire System Test

Supply range

Test condition	Voltage	Result
Minimum voltage	20 V	OK*
Maximum voltage	36 V	OK

Table 5-16: Supply range test

*without the camera system the experiment operates with supplies as low as 12V.

Inrush current test

Voltage drop across a 0.2 Ohm load resistor in the power line:

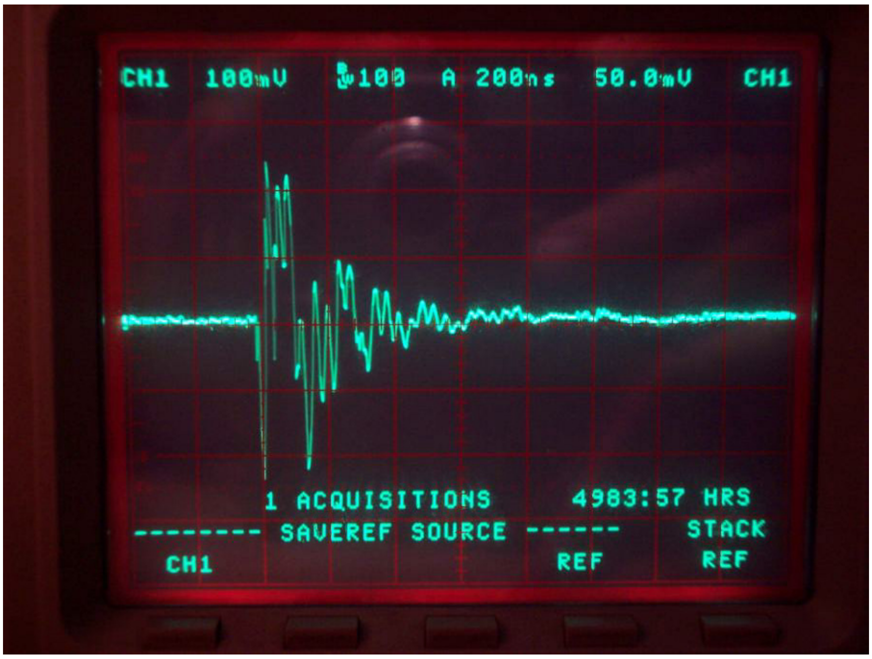

Figure 5-5:Inrush current plot

Load Resistor: R_in = 0.2 Ohm

Maximum value: U_drop = 250mV

Inrush current: I_in = U_drop / R_in = 1,25 A

The inrush current is below 3A.

Consumption

All values have been measured with a supply current of 28V.

Mode	Current [A]
Safe mode / Idle mode	0.052
Camera mode	0.120
Record mode	0.130

Table 5-17:REMOS consumptions

5.3.7 Test 8: Shaker Test

Figure 5-6: Shaker test z anx achsis

First Shaker Test without harness and with dummy-probe was successful. No structural damage was found after inspection.

Second Shaker Test was done in full flight configuration with real probe and while experiment was running. The transmitted data was monitored and analyzed and a full functional test was performed after each axis run.

Procedure:

- Each axis for 3x 1 minute at -12dB, -6dB, 0dB
- Sine- search run at 0.25g
- Loads according to REXUS user manual.

Results:

- No structural damage was found after inspection, the electronics remains functional, the measured values of the probe are not altered
- Eigenfrequencies within ± 20% range of predicted value

Details of the procedure and the results can be found in the test report in Appendix D.

5.3.8 Test 9: Thermal Vacuum Test

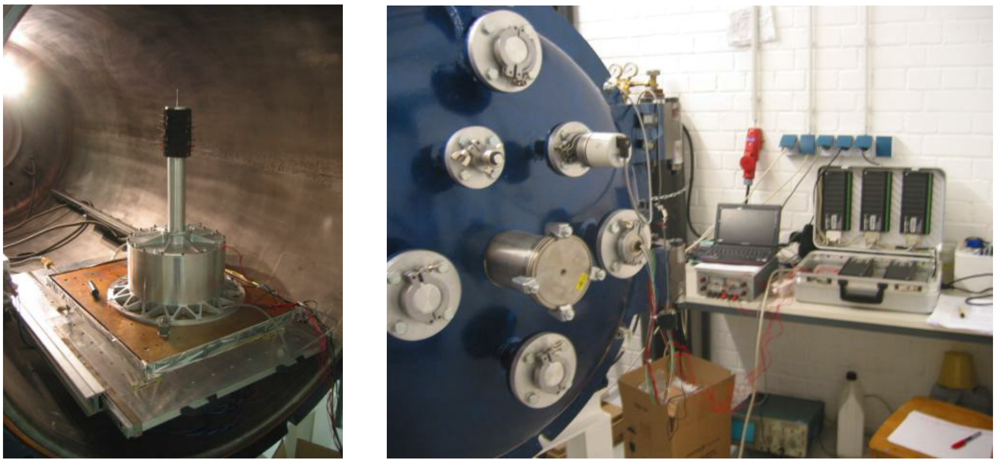

Figure 5-7: Thermal vacuum test

Thermal Vacuum Test was done in a conditioned pressure chamber. Depressurization, Cold Test, Hot Test and Pressurization were conducted with the experiment running and functional checks took place between the tests. Temperature sensors were installed to monitor the system temperature and to validate the measured temperatures.

Procedure:

- 0,5 mbar at -10°C and +45°C
- Test duration was one full flight plus an additional 15 minutes each

Results:

- The experiment was running nominally during all tests
- No function loss or damage could be detected, neither during nor after the test series

Details of the procedure (such as the full timeline) and the results can be found in the test report in Appendix D.

5.3.9 Test 10: Electromagnetic Compatibility Test

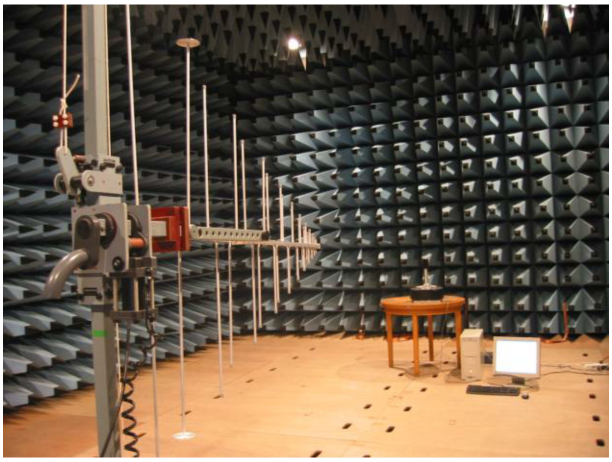

Figure 5-8: EMC test

The EMI Test was conducted under the influence of an electrical field with a constant strength.

The experiment was standing upright and the antenna was aligned horizontally for the first test and vertically for the second.

An additional third test was performed focussing on the low frequencies in order to obtain higher resolution measurement values in this range, as it is the most interesting.

Procedure:

- electrical field controlled to have a strength of 10 V/m, required transmitting power for this value ranging from 10 to 80 W
- test range 80 MHz to 1 GHz, increasing exponentially over time
- horizontal and vertical alignment

Results:

- some fluctuation in measured values could be observed during low frequencies

Details of the procedure and the results can be found in the test report in Appendix D.

6 LAUNCH CAMPAIGN PREPARATION

6.1 Input for the Flight Requirement Plan (FRP)

6.1.1 Dimensions and Mass

Experiment mass (in kg):	8,76 including REXUS module
Experiment dimensions (in m):	0,328m x 0,328m x0,446m
Experiment footprint area (in m^2):	0,0845 m^2
Experiment volume (in m^3):	0,0018 m^3
Experiment expected COG (centre of gravity) position:	x:= 0m from neutral axes REXUS y = 0m from neutral axes REXUS z = 0,077m from interface plane

Table 6-1: Experiment mass and volume

6.1.2 Electrical Interfaces

The REMOS experiment requires the service module interface and the power interface. The three status signals provided from the REXUS rocket are used to set the appropriate mode in the onboard software. An uplink during flight is not designated, but needed during integration and testing on ground. An overview of the mandatory interfaces is listed in the table below.

REXUS Electrical Interfaces		
Service module interface required? **YES**		
	Number of service module interfaces:	**1**
	TV channel required?	**YES**
Up-/Downlink (RS-422) required? **Yes**		
	Data rate - downlink:	**10 Kbit/s**
	Data rate - uplink	**Not needed during flight, but on ground for testing (1Kbit/s)**
Power system: Service module power required? **YES**		
	Peak power consumption:	**6 W**
	Average power consumption:	**3,3 W**
	Total power consumption after lift-off (until T+800s)	**0,6 Wh**
	Power ON/OFF control	**T-300s to** **T+643 (Landing + 3s)**
	Battery recharging through service module:	**No**
Experiment signals: Signals from service module required? **YES**		
	LO:	**Yes**
	SOE:	**T +60 s : ON** **T +640s: OFF (Landing)**
	SODS:	**T +150s: ON** **T +300s: OFF (parachute deployment)**

Table 6-2: Electrical interfaces applicable to REXUS

6.1.3 Launch Site Requirements

The required GSE is already listed in the 4.14.

There are no further special requirements.

6.2 Preparation and Test Activities at Esrange

Upon arrival at the launch site, each component has to be tested separately as well as the entire system. The tasks to be completed at site before launch are listed below.

REMOS Experiment	- Testing components - Verify communication - Calibration of sensors - Mounting of our experiment on REXUS - System test
Ground Control	- Setup of the computer and software - Verify communication link - System test

Table 6-3: Test activities at Esrange

6.3 Timeline for Countdown and Flight

After the experiment is mounted in the REXUS rocket, the experiment follows an autonomous program.

T – 300s	Power on. REMOS is in safe mode, sends status packages with information about software, temperature to ground control.
T-300s- T-60s	Experiment GO or NO GO.
T0, Lift-off	LO signal on. The experiment stays in safe mode. Reset for internal experiment clock.
T+60s, Nose jettison	SOE signal on. Cameras are activated.
T+150s, Reaching apogee	SODS signal on. REMOS begins data recording.
T+400 Parachute opening	SODS off, stop of data recording.

T+640s, landing	SOE off, return to safe mode.
T+ 643s	Power off

Table 6-4: Experiment timeline

6.4 Post Flight Activities

- In case that the material probe withstands the impact, the probe should be concealed and rescued for further studies.

- Disassembly of experiment

- Backup of onboard recorded data

- Packing of components

7 DATA ANALYSIS PLAN AND EXPERIMENT REPORTS

7.1 Data Analysis Plan

The post flight data analysis can be split up into four tasks. Each task can be performed by a single person. They are:

1. Post flight system analysis
    - System functionality
    - Damages
    - Occurred problems
    - Measured inside and outside flow-temperatures

2. Reconstruction of angle of attack from REXUS IMU/GPS data
    - Evaluation of deceleration vector
    - Test with a strap down algorithm
    - Comparison to GPS data
    - Comparison with camera view
3. Calculation of temperatures, capacitances and resistances from recorded/transmitted data. Cross-check with camera data.
    - Use previously recorded calibration data
4. Development of an empiric ablation model for the probe.
    - Use physical properties
    - Take probe dimensions into account
    - Combine with angle of attack
    - Create a mathematical model
    - Find model parameters for best fit to flight data

For the last task also the results from the previous tasks are required.

7.2 Launch Campaign

Launch preparations on the site included the following:

- unpacking, inspection and assembly of the entire experiment
- measurements for temperature channel calibration
- probe dimension measurements
- securing of all screws with Loctite
- several test runs
- mounting of the experiment on the rest of the payload section
- writing and completing some parts of the documentation
- removal of all protective covers

An encountered issue during the tests was a missing contact on one of the pins connecting the RT board to the ribbon cable. It was determined to be caused by corrosion due to the material combination and the severe temperature changes during transport. The corrective procedure was to disconnect the entire cable and to clean all connector pins on both sides (cable and boards). Finally, a double check of each connection via a multimeter and several test runs were performed. The problem did not reoccur.

The launch took place on the noontime of February 22nd. The weather conditions were perfect and the payload section reached a maximum height of 80,6km during the twelve minute flight. After the launch, the experiment was recovered and brought back by a helicopter within few hours. Due to the landing in deep snow, the probe did not receive any mechanical damage during the impact, thus allowing for optical inspection after the return.

7.3 Results

7.3.1 Raw Data

In the following diagrams the measured raw data is shown. The R- and C-channel values already have been calibrated before launch. For the probe temperatures only the amplification of the measurement channels are considered. For an absolute reference, data with known ambient temperature was collected prior to launch. This has to be considered during the processing of the data.

Resistance Data:

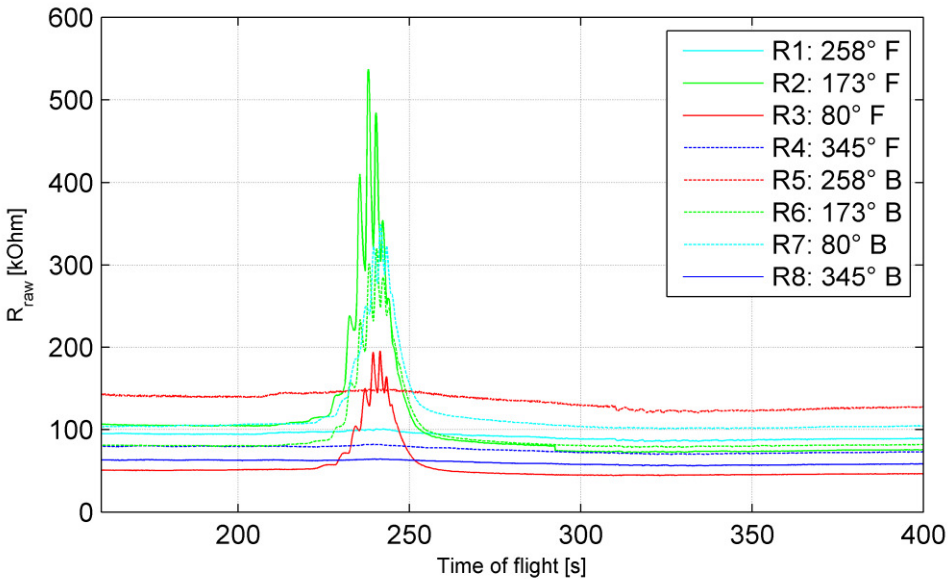

Figure 7-1: Resistance raw data

Capacitance Data:

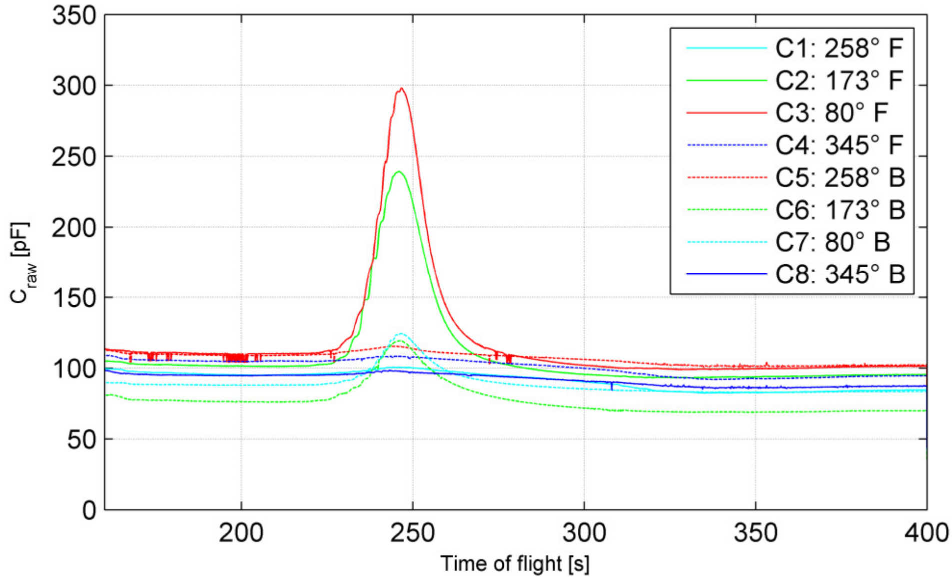

Figure 7-2:Capacitance raw data

Temperature Data:

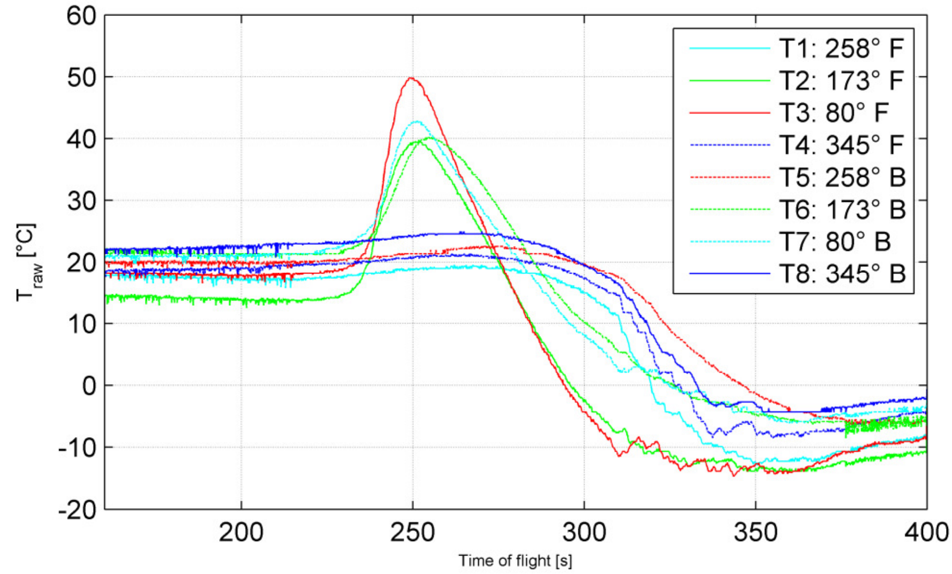

Figure 7-3: Temperature raw data

Gas Temperature Data:

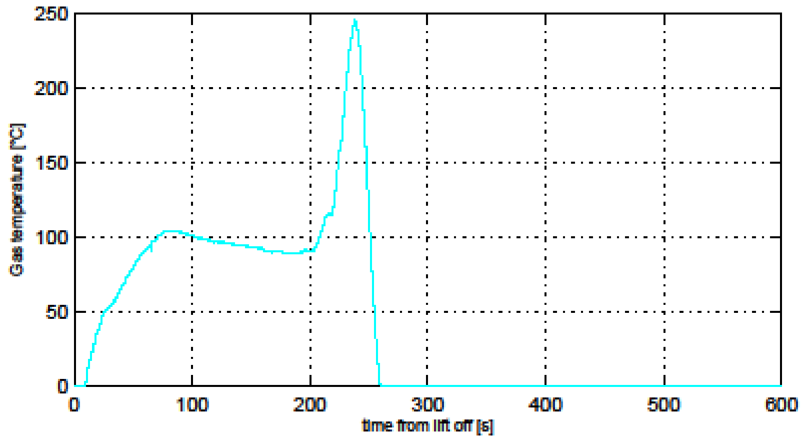

Figure 7-4: Gas temperature

7.3.2 Data Processing

Among other data the REXUS Service Module provides GPS position data and data from the Inertial Measurement Unit (IMU). REMOS relies upon IMU data for the determination of inflow vector; altitude and velocity are determined using GPS data.

The REXUS 9 reference frame is based on a Cartesian coordinate system whose X-axis defines the roll-axis of the rocket. It's Y-axis specifies the 0°-line of the perimeter while the Z-axis completes the coordinate system to be right-handed is described by two angles: the in-plane angle α, which indicates the direction within the Y-Z-plane and the out of-plane angle β. This angle shows the deviation from the plane and is positive when inclined towards the X-axis.

The angles alpha and beta are calculated with the equations:

$$\alpha = \begin{cases} \arctan 2(a_z, a_y) & : a_z \geq 0 \\ 360° - \arctan 2(a_z, a_y) & : a_z \leq 0 \end{cases}$$

$$\beta = \arctan 2\left(a_x, \sqrt{a_x^2 + a_y^2}\right)$$

where a_x, a_y and a_z are the accelerations measured in m/s^2.

For the compensation of the thermal dependency of the specific electrical conductivity and capacitance of the probe, the vertical temperature distribution within a probe section is required. The temperature below each element is measured by a sensor. To calculate the entire vertical distribution, a thermal model was developed.

The basis for the model is the equation of thermal conductivity:

$$\frac{\partial T}{\partial t} = a \cdot \Delta T + \frac{\dot{q}_i}{\rho \cdot c} \quad \text{with} \quad a = \frac{\lambda}{\rho \cdot c}$$

In the one-dimensional case the equation is reduced to $\frac{\partial T}{\partial t} = a \cdot \frac{\partial^2 T}{\partial x^2} + \frac{\dot{q}_i}{\rho \cdot c}$

The differentials of this reduced equation are approximated with the finite differences:

$\frac{\partial T}{\partial t} \approx \frac{1}{\Delta t} \cdot \left(T_i^{n+1} - T_i^n \right)$ and

$$\frac{\partial^2 T}{\partial x^2} \approx \frac{\lambda}{\rho \cdot c \cdot \Delta x^2} \cdot \left(T_{i-1}^{n+1} - 2T_i^{n+1} + T_{i+1}^{n+1} \right)$$

Inserted into the equation: $T_i^{n+1} - T_i^n = \underbrace{\frac{\lambda \cdot \Delta t}{\rho \cdot c \cdot \Delta x^2}}_{A} \left(T_{i-1}^{n+1} - 2T_i^{n+1} + T_{i+1}^{n+1} \right) + \underbrace{\frac{\Delta t}{\rho \cdot c}}_{B} \cdot \dot{q}_i^n$

Sorted and written in matrix representation:

$$\begin{bmatrix} 1+2A & -A & 0 & \cdots & 0 \\ -A & 1+2A & \ddots & & \vdots \\ 0 & \ddots & \ddots & \ddots & 0 \\ \vdots & & \ddots & 1+2A & -A \\ 0 & \cdots & 0 & -A & 1+2A \end{bmatrix} \cdot \begin{bmatrix} T_1 \\ T_2 \\ \vdots \\ T_{r-1} \\ T_r \end{bmatrix}^{n+1} = \begin{bmatrix} T_1 \\ T_2 \\ \vdots \\ T_{r-1} \\ T_r \end{bmatrix}^{n} + B \begin{bmatrix} \dot{q}_1 \\ \dot{q}_2 \\ \vdots \\ \dot{q}_{r-1} \\ \dot{q}_r \end{bmatrix}$$

Two cases are considered as boundary condition.

1.) In case of a constant temperature boundary condition the corresponding row in the matrix has to be filled with zeros, except for the position of the element, at which the temperature shall be kept constant Here a 1 is inserted.

2.) A given heat flux onto the surface of an element can be described by the use of a neighbouring imaginary element, whose temperature is adjusted in such a way, that a certain heat flux is maintained: $-\dot{q}_r = \frac{\lambda}{\Delta x}\left(T_i^{n+1} - T_r \right) \rightarrow T_r = \frac{\Delta x}{\lambda} \cdot \dot{q}_r + T_i^{n+1}$

   When inserted into the equation, the corresponding column has to be modified to: $(1 + A)T_i^{n+1} - AT_{i+1}^{n+1} = T_i^n + A\frac{\Delta x}{\lambda} \cdot \dot{q}_r$

If numerically perfect data is provided, these equations permit to directly calculate the temperature distribution. As this is not the case with the measured temperatures, the direct application of this equation leads to large distortions in the distribution, even when using filtered data.

Therefore, an estimation routine was developed, that uses the equation backwards to find the best trend of thermal flux that causes the measured temperature distribution. With this distribution and the conducted material tests, a compensation can be done.

7.3.3 Processed Data

Thermal Conditions:

During the early design of the experiment the theoretical heat flux and the resulting adiabatic surface temperature had been calculated with flight data from REXUS 6 (see chapter 4.6.2). The maximum heat flux reached a value of 10000W/m^2 for 100km apogee, resulting in a theoretical surface temperature of 717K.

After the flight, the same calculation was performed again with the actual flight profile of REXUS 9. With an apogee altitude of 80.6km the maximum heat flux reduced to 3690W/m^2, what results in a maximum adiabatic wall temperature of 540K.

The described temperature profiles can be seen in Figure 7-5. Here, the calculated Temperatures are compared to the measured Temperature at the top of the Experiment (red). The first peaks in the calculated curves result from the aerodynamic heating during launch. The sensor in the probe doesn’t heat up so quickly, because it is protected by the nose cone. Although, heated gas which found a way into the nose cone is enough, to heat up the sensor to 380K. After the separation of the nose cone, the temperature of the gas temperature sensor only drops slowly. The reasons for the slow dropping are the missing atmosphere the low coefficient of emissivity of the gas temperature sensor and its high thermal capacity. During re-entry the gas temperature fits the theoretical values very well, except for delay in the beginning of the re-entry process. This delay is caused by the sensors inertia.

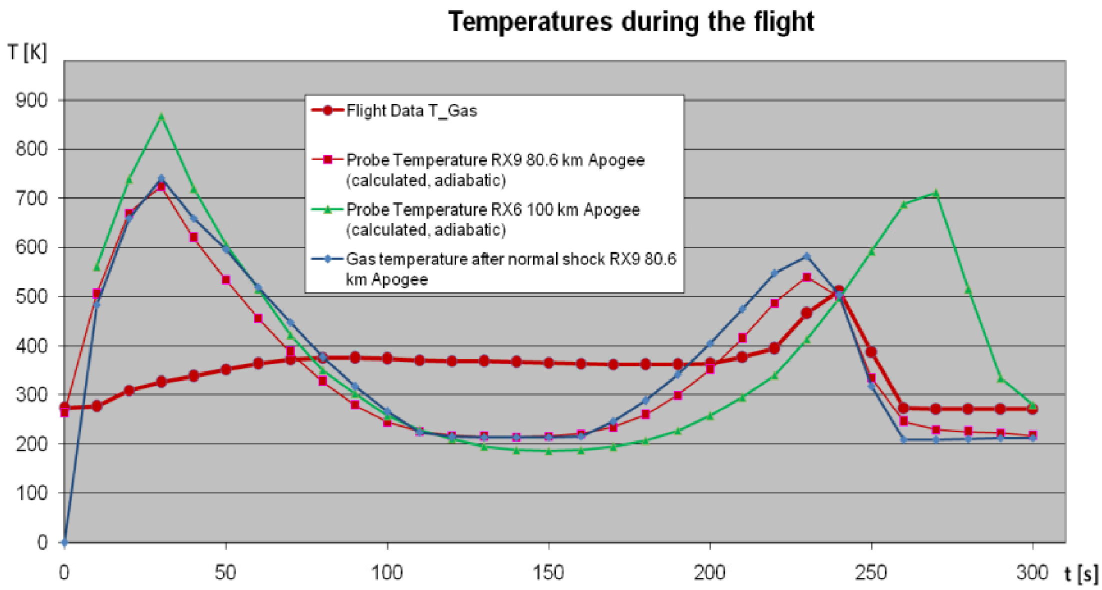

Figure 7-5: Calculated vs. measured gas temperature

When compared to the flight of REXUS 6, which was used as a design reference during the early project phases, the theoretical thermal load on REXUS 9 was reduced by a factor of 2,7. The maximum gas temperature, measured, was 248°C. The greatest heating during re-entry took place between 220s and 260s after lift-off.

Re-entry Orientation:

After the separation of the motor and the nosecone, the experiment section begins to tumble. This is a result of the small asymmetries in the separation forces, moving parts in the experiments and remaining atmosphere. With increasing atmospheric density the tumbling begins to stabilize into a flat-spin and the entire section is decelerated to subsonic speed. Below Mach 1 the tumbling increases again.

In the figure below the in-plane and out-of-plane angles during stabilisation and deceleration to Mach 1 are plotted. As can be seen, the experiment section's roll-axis (In-Plane-Angle) and pitch-axis (Out-Of-Plane-Angle) stabilize around 137°and +3°.

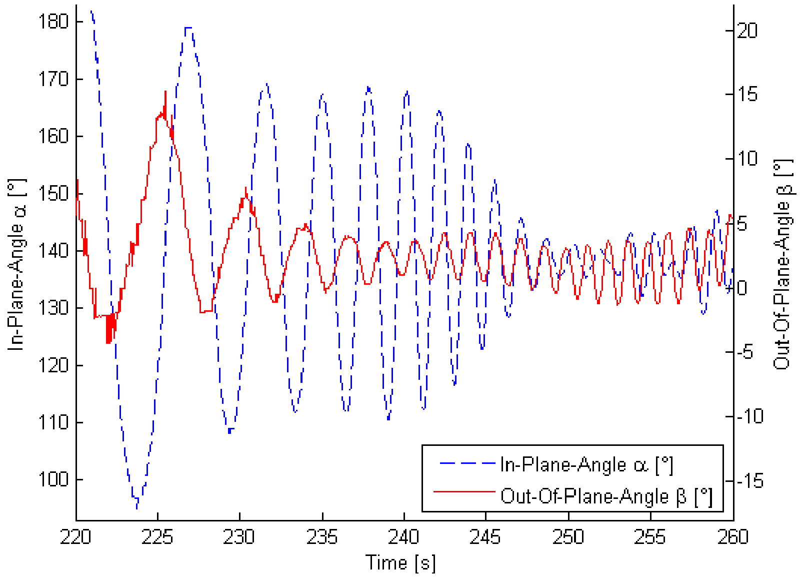

Figure 7-6: Reentry orientation

The properties of the angle of attack during the hot phase of the re-entry can be summarized, as following:

Direction	Mean Angle [°]	Deviation [°]	Frequency [Hz]
In-Plane	+140.3	+/- 40	0.3-0.63 (increasing)
Out-Of-Plane	+2.6 (nose down)	+/- 8	0.3-0.66 (increasing)

Table 7-1: Orientation properties

The orientation of the probe during the re-entry was very stable. This fact offered the best flow conditions, which were achievable with the given apogee altitude.

Heat flux and Temperature distribution:

The heat flux on each sensor element was calculated with the method described in chapter 7.3.2 and the measured temperature values as input. The used property values for the material are listed in the Table below.

Property	Value	Unit
Density	50	Kg/m^3
Thermal Capacity	1600	J/(kg*K)
Thermal Conductivity	0.05	W/m

Element Thickness	1.2	mm
Step Size	1	s

Table 7-2: Thermal mode setting

The calculated heat fluxes have been plotted over time of flight. As can be seen, the maximum heat flux occurred on element 3 with a peak of 3500W/m^2. This correlates to the theoretical heat flux, which was used to estimate the adiabatic wall temperature (see 7.3.3, subsection **Thermal Conditions**).

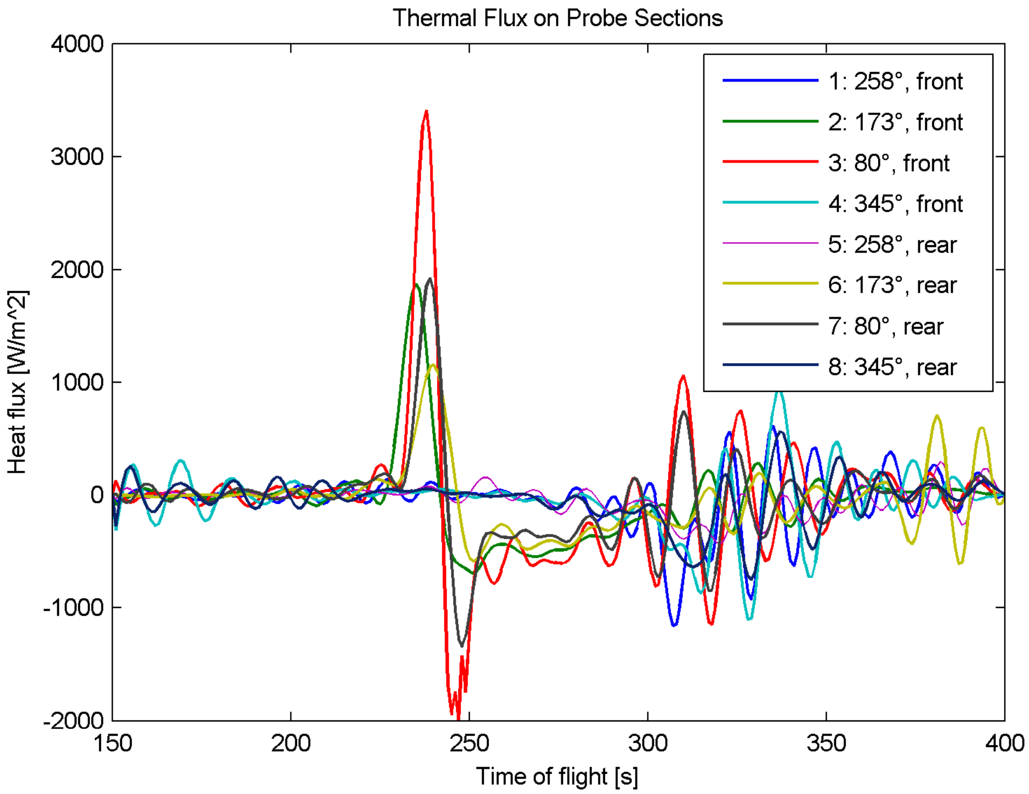

Figure 7-7: Heat flux on probe sections

As a by-product the following temperature distributions were obtained. Due to the thermal capacity of the foam material, the maximum temperature stays well below the adiabatic wall temperature.

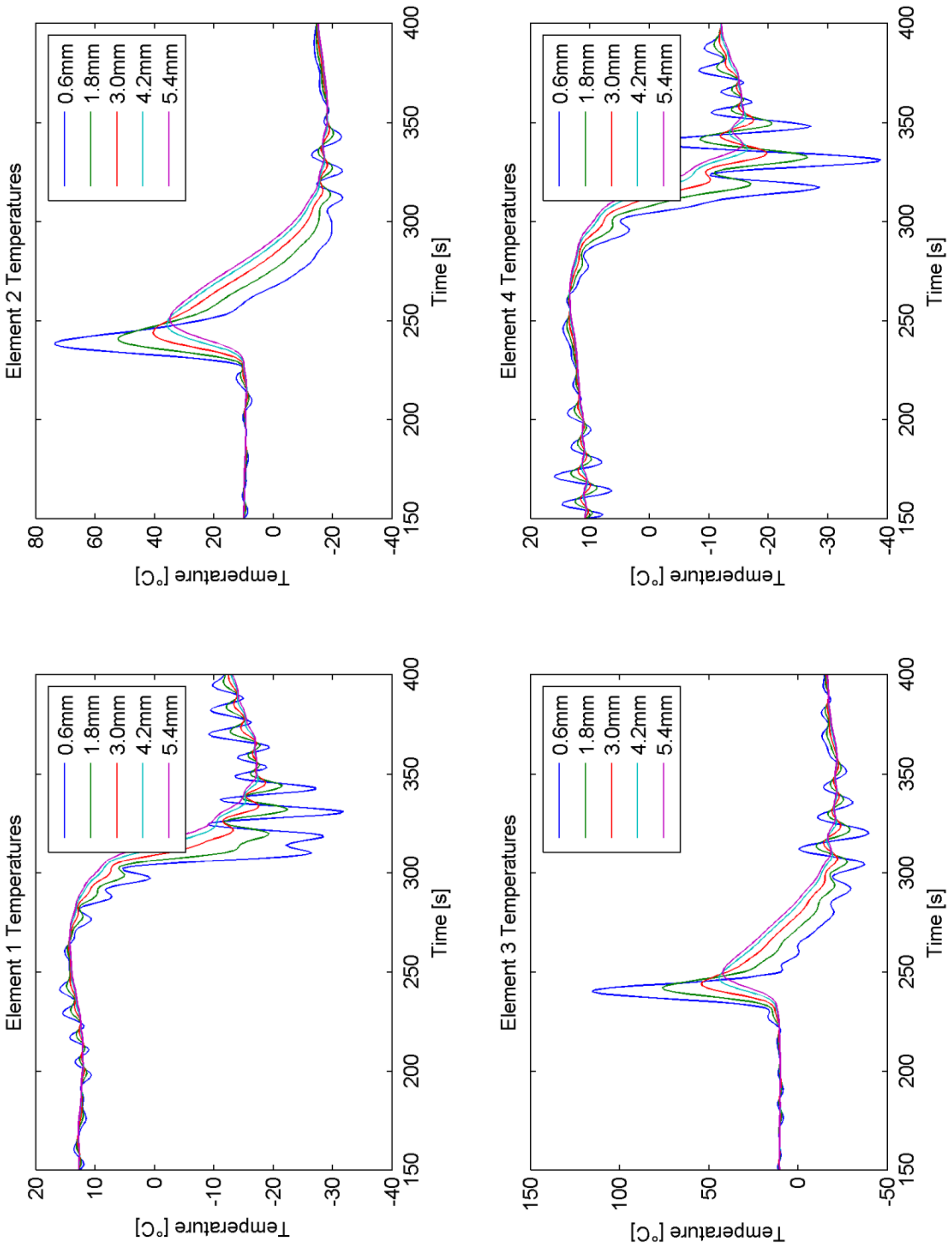

Figure 7-8: Front elements, temperature distribution

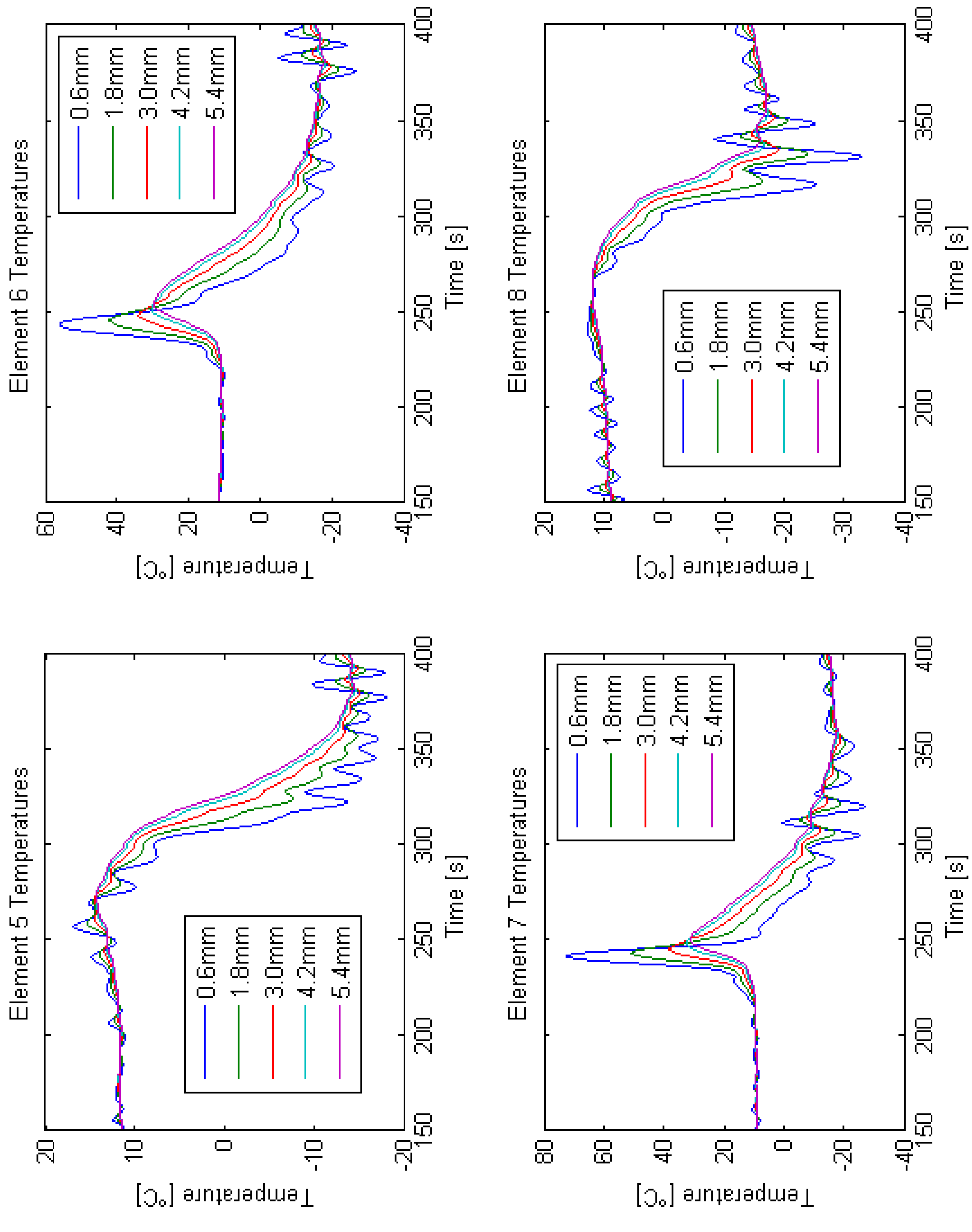

Figure 7-9: Rear elements, temperature distribution

These distributions and measurements, conducted during material tests, enabled the calculation of compensation factors for temperature drifts.

In the following subsections all corrected and compensated measurement values can be seen.

Corrected Temperatures:

The temperature channels have been calibrated, but the offset in between in the channels has to be eliminated. A time span prior to launch is taken as reference assuming the probe is in thermal equilibrium.

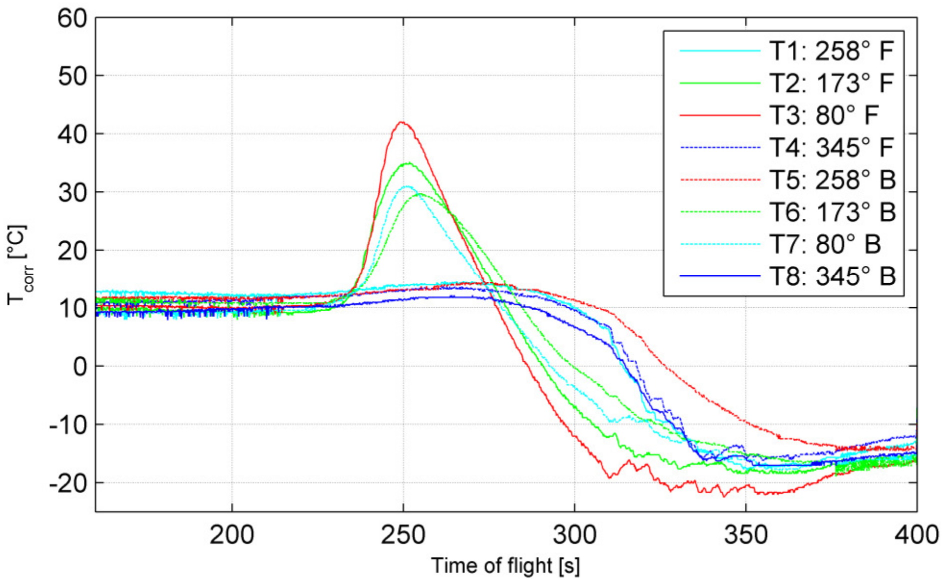

Figure 7-10 Corrected values for temperature channels

The material of the probe in the direction of 80° and 173° are heated by the flow to a maximum at 250s after lift-off. After 400s the probe is in thermal equilibrium again.

Corrected Resistance and Capacitance Channels:

A study has been carried out to assess the temperature influence on the R and C channels. The measured capacitance and resistance of the channels change due to temperature and conditions of the material either way.

In order to eliminate the temperature dependency the measurements are based on a temperature of 20°C. The correction functions are evaluated in DLR-IB 435-2010-32. The results are shown in Figure 7-11 to 7-13. The changes are purely caused by modifications in the material of the probe.

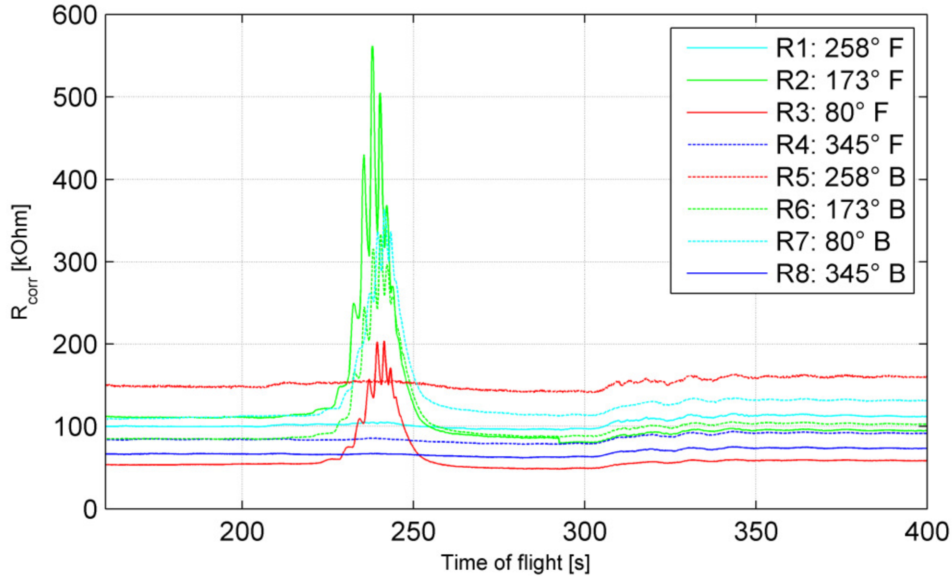

Figure 7-11 Resistance measurements with reference to a temperature of 20°C

The probe is exposed to the flow during flight and the high peaks in Figure 7-11 are caused by a compression of the material. For a further analysis of this behaviour, the normalized roll and pitch orientation have been plotted together with normalized graphs of the resistance channels 1 and 2 (Figure 7-12).

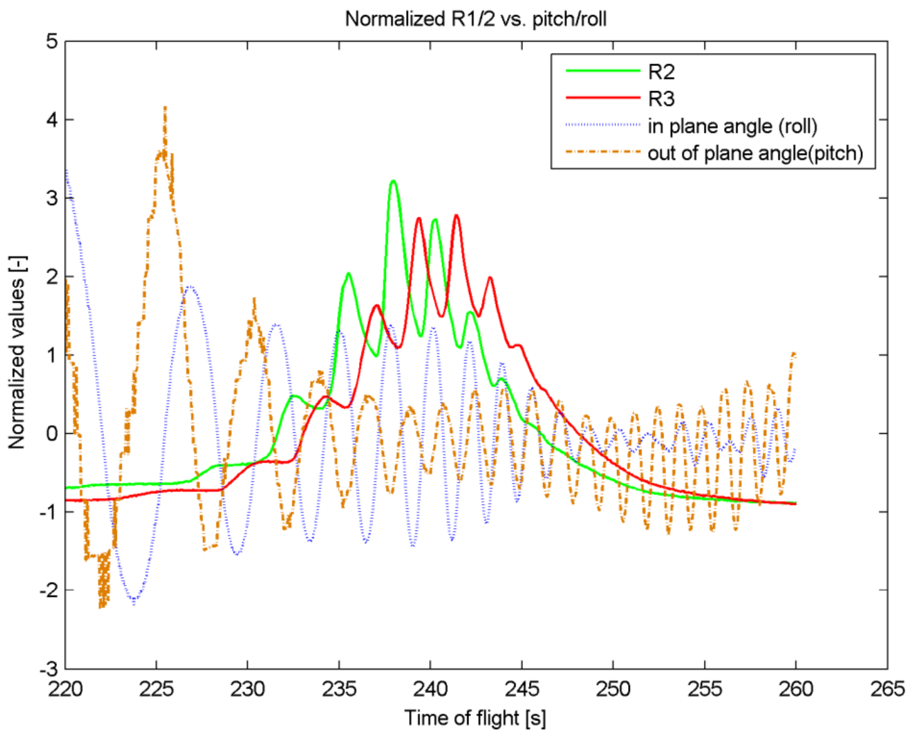

Figure 7-12: Normalized roll-, pitch-, R2- and R3 values

As can be seen, the magnitude of the resistance signal is closely linked to the roll- and pitch- orientation. The phase shift between R2 and R3 is close to 180°. This is reasonable, since the force onto an inclined surface in a flow changes with the squared cosine of its inclination. The mounting angle between R2 and R3 is 93°, what results in the phase shift. The described compression of the foam results from the travelling of the stagnation point on the surface of the probe.

A rupture in the material is indicated by a drop within a few milliseconds of the resistance of channel 2 at t = 292.4 seconds.

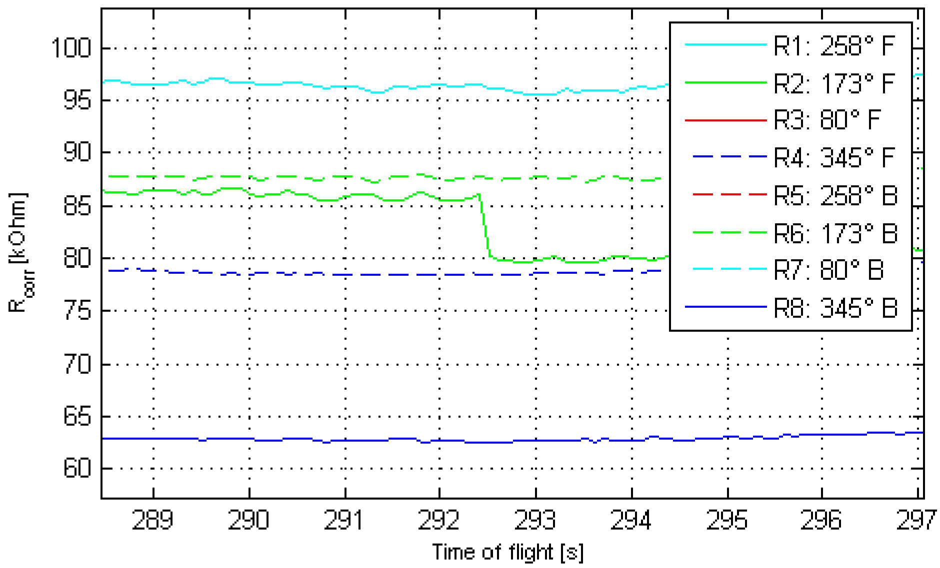

Figure 7-13 Indication of a rupture (crack) in the material in channel 2

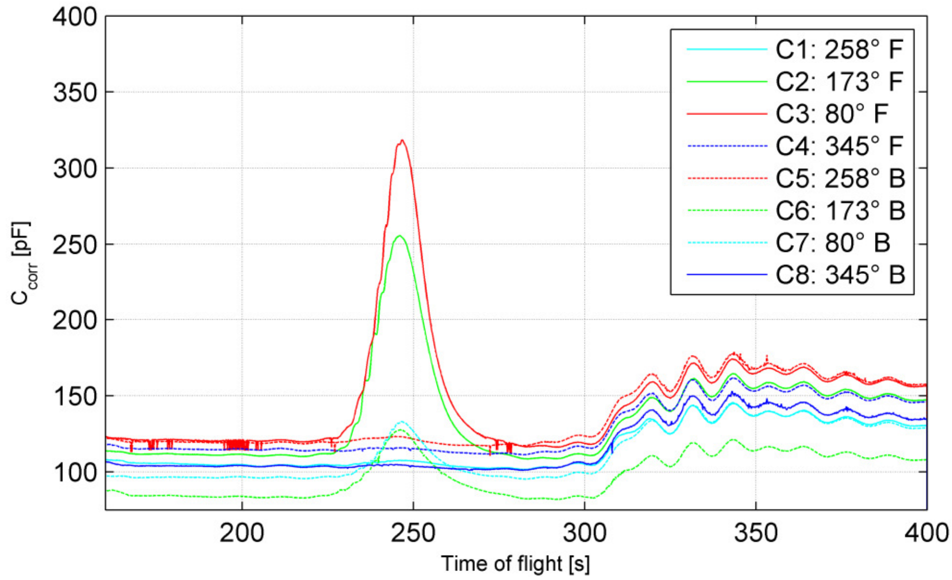

Figure 7-14 Capacitance measurements with reference to a temperature of 20°C

7.3.4 System Performance

Voltages

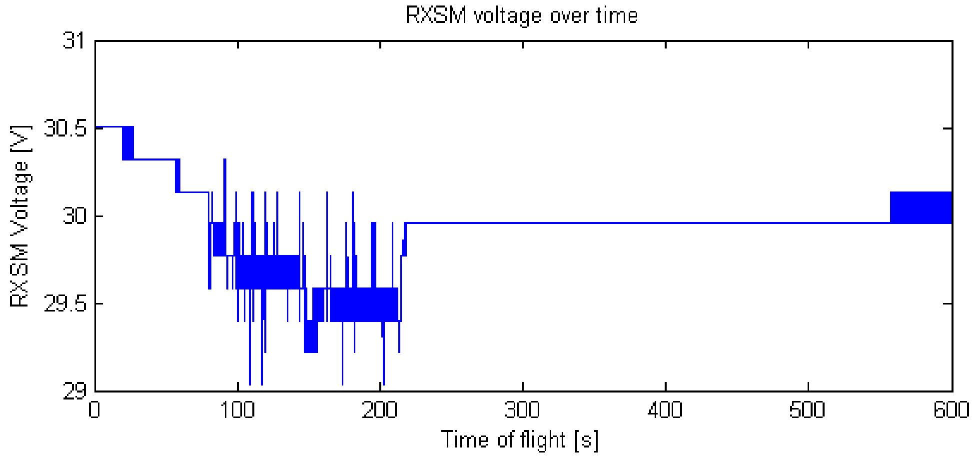

Figure 7-15: RXSM supply voltage

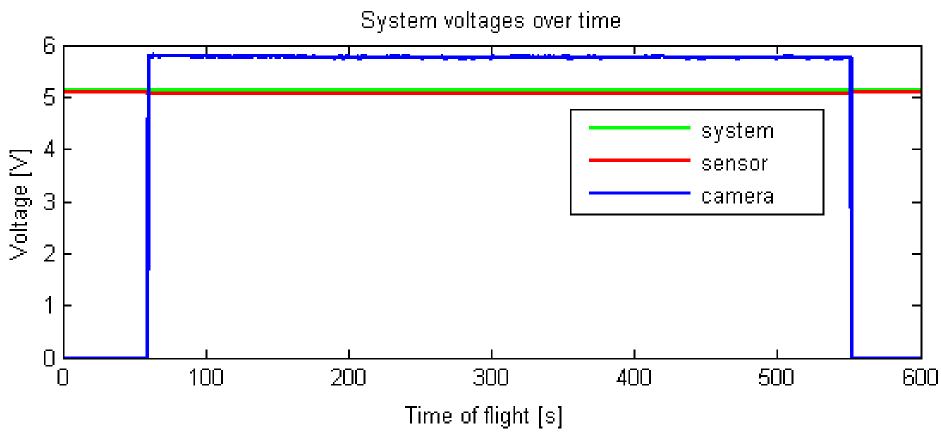

Figure 7-16: REMOS system voltages

Four different voltages were monitored during the flight and transmitted and evaluated within the status package. These are the voltage supplied by the REXUS Service Module and three regulated voltages to power the different elements of the experiment.

The system and sensors are always powered. In contrast to that, the camera voltage is provided via switchable regulators only while the cameras run. This is to reduce overall power consumption, because the cameras have a power consumption while they are in standby mode and powered.

The system voltages were within the desired tolerance of the target values and constant during the entire flight. Some minor fluctuations can be observed in the camera supply, because the regulator was dimensioned to work at 70% of its maximum load and the selected filter capacitor was rather small. Yet these deviations were accepted during the design process and are not a problem to the cameras.

Temperature

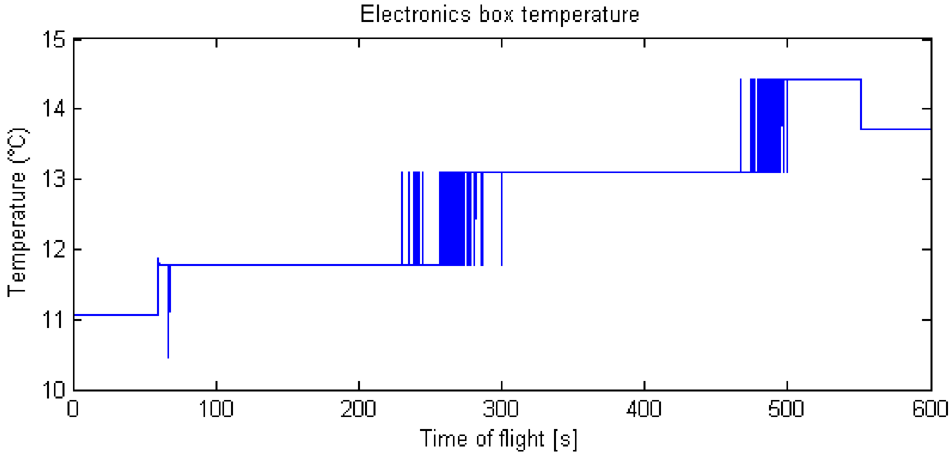

Figure 7-17: Electronics box temperature

The temperature within the electronics box increased by four degrees, as predicted by the simulation. The increase was a bit slower, though, indicating that the thermal decoupling of the electronics box was better than expected. The decrease after the flight was later and less than predicted, because the heat production by the electronics itself was neglected in the simulation.

Data loss

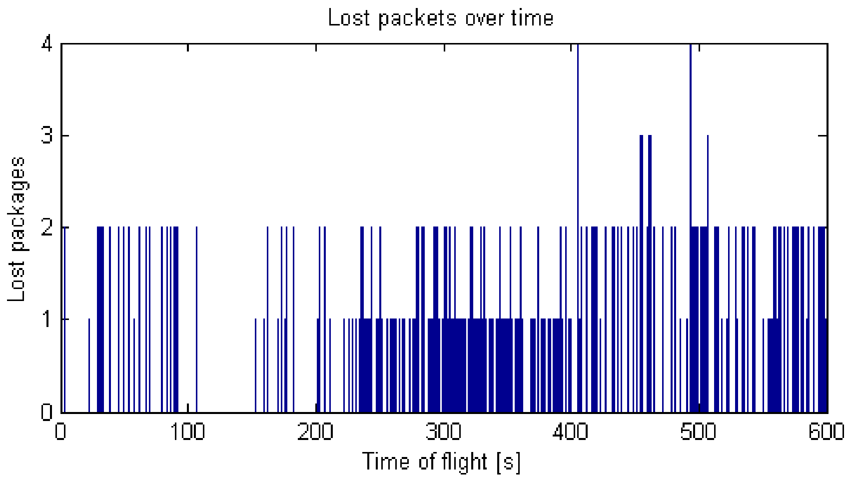

Figure 7-18: Data loss during flight

The data loss during the flight includes all packages that were not processed correctly by the ground software. This can either happen due to loss of synchronization (which always causes two consecutive packages to be dropped) or when a package is ignored because the checksum shows that error bits have occured.

The total data loss was 5% with a maximum of four lost packages in a row. Due to the high evaluation rate of 10Hz, this is not critical for the reliability of the data. The loss rate is obviously higher than during the test runs with a cable connection to the Service Module Simulator, but is remarkably less than during the test runs that included the radio transmission.

7.4 Discussion and Conclusions

The functionality of the main principle of material monitoring via electrical properties could be confirmed with this experiment.

Depending on the probe material, the system can also be able to observe changes in heat shield temperature and mechanical stress or failure. Therefore it may also be used to monitor the physical condition of non-ablating, reusable heat shields.

The systems weight and power consumption are low enough to allow for its embedding into any size of re-entry vehicle. The modularity of the measuring principle enables its integration into any kind of heat shield material that has been made electrically conductive, for example by adding carbon.

What is left to do is the quantification of the changes. Because of the temperature dependency of the material's properties and the little ablation, no accurate equation to correlate the measured changes to the absolute thickness could be developed.

7.5 Lessons Learned

7.5.1 Experiment

The probe material was too heat resistant for the application. It was selected for its electrical conductivity and because it evaporates instead of melting. For any further efforts, a quicker evaporating material with less temperature dependent electrical properties should be investigated.

The following recommendations should be considered for a similar experiment:

- Gain as much altitude, as possible! An increase in altitude from 80km to 100km will already raise the heat flux by at least a factor of 2,5.
- The heat flux onto the probe can be increased by using a shape with sharp edges. To guaranty a correct alignment with the direction of flow,

such a probe should be designed with an active orientation mechanism or as a free-flyer.

- A less temperature-dependent material should be used
- The required time for probe integration must not be underestimated, a modular probe concept that permits the assembly of single segments before attaching them to the supporting structure would be handy.
- Diligent electronics assembly is very time consuming and always takes two persons to ensure proper quality control.
- Building costly prototypes can under certain circumstances be avoided by extensive simulations of a design
- Keeping the design simple but effective and avoiding moving parts was a good idea

7.5.2 Project

The REMOS experiment was conducted in a small to medium size team. To maximize the manpower for the design and construction for the experiment itself, the administrative part should be kept was low, as possible within the team.

- Using an automated file-sharing system reduced the administrative workload a lot (Possible solutions: DLR Sharepoint Server, DropBox).
- Defining standards for design and documentation in advance kept problems with compatibility to a minimum. Used REMOS standards:

    Documents: Word98-2003, pdf (or 100% compliant)

    CAD/FEM exchange: SolidWorks 2009, STEP

    ECAD exchange: IDF-standard (compatible to used CAD system)

    Software Design: AVR GCC (onboard), C# (GSE)

- Sponsors for rocket science can be found even in times of economic crisis
- Team members scattered all across Europe can be a challenge
- Orders should be placed as soon as possible to have a time buffer in case of problems with the delivery. Sensitive components should be ordered with an adequate surplus amount.
- A clear risk identification can prevent lots of issues

7.5.3 General Experience

- Launching a sounding rocket experiment is not only educative, but also a great deal of fun
- Deadlines at ESA conferences are relative
- Kiruna is an awesome place
- PhD, Graduate and undergraduate team members can all contribute a good share to a REXUS project

8 ABBREVIATIONS AND REFERENCES

8.1 Abbreviations

ADC	Analog to Digital Converter
AIT	Assembly, Integration and Test
asap	as soon as possible
BO	Bonn, DLR, German Space Agency
BR	Bremen, DLR Institute of Space Systems
CDR	Critical Design Review
COG	Centre of gravity
DLR	Deutsches Zentrum für Luft- und Raumfahrt
EAT	Experiment Acceptance Test
EAR	Experiment Acceptance Review
ECTS	European Credit Transfer System
EIT	Electrical Interface Test
EPM	Esrange Project Manager
ESA	European Space Agency
Esrange	European Sounding Rocket Launching Range
ESTEC	European Space Research and Technology Centre, ESA (NL)
ESW	Experiment Selection Workshop
FAR	Flight Acceptance Review
FER	Final Experiment Report
FST	Flight Simulation Test
FRP	Flight Requirement Plan
FRR	Flight Readiness Review
GSE	Ground Support Equipment
HK	House Keeping
H/W	Hardware
ICD	Interface Control Document
I/F	Interface
IPR	Interim Progress Review
LO	Lift Off
LT	Local Time
LOS	Line of sight
Mbps	Mega Bits per second
MCU	Microcontroller Unit
MFH	Mission Flight Handbook
MORABA	Mobile Raketen Basis (DLR, EuroLaunch)
MUX	Multiplexer

DEMUX	Demultiplexer
OP	Oberpfaffenhofen, DLR Center
OPAMP	Operational Amplifier
PCB	Printed Circuit Board (electronic card)
PDR	Preliminary Design Review
PST	Payload System Test
REMOS	Recession Monitoring System
REXUS	Rocket Experiments for University Studfents
SED	Student Experiment Documentation
SER	Short Experiment Report
SNSB	Swedish National Space Board
SODS	Start Of Data Storage
SOE	Start Of Experiment
SSC	Swedish Space Corporation (EuroLaunch)
STW	Student Training Week
S/W	Software
T	Time before and after launch noted with + or -
TBC	To be confirmed
TBD	To be determined
TPS	Thermal Protection System
WBS	Work Breakdown Structure

8.2 References

Reference document	File name
REXUS User Manual	RX-REXUS_user_manual-v7_0-04Dec09.pdf
Esrange Safety Manual	Esrange_Safety_Manual.pdf
Esrange User Handbook	Esrange Users Handbook.pdf
ECSS standard M-ST-10C Project Management	ECSS-M-ST-10C_Rev.1(6March2009).pdf
ECSS standard Q-70-71A Space product assurance	ECSS-Q-70-71Arev1(18June2004).pdf
Optocoupler ACPL-8x7	ACPL-8x7.pdf
Analog to digital converter ADS7822	ads7822.pdf
Flash storage IC AT25DF321	AT25DF321.pdf
MCU ATMega 16	ATMega16.pdf
switching v. reg. LM2575	lm2575.pdf
OPAMP LT1014	lt1014.pdf
RS422 driver MAX3465	MAX3465-MAX3469.pdf
RTC PCF8583	pcf8583.pdf
dual CMOS Timer TLC556	tlc556m.pdf
linearv.reg with enable TPS793	tps793.pdf
counter sunk screws DIN EN ISO 7047	
inboardhexagonbolt DIN EN ISO 4762	
Flycam one eco manual	FCOe_multi.pdf
Project Plan A1 paper	REMOS_A1.pdf
Work breakdown structure in seperate document	WBS.pdf

APPENDIX A – EXPERIMENT REVIEWS

REXUS / BEXUS
Experiment Preliminary Design Review
Esrange, Kiruna, 1.-5 Feb. 2010

Flight: REXUS

Experiment: REMOS

Date: 3 Feb 2010

1. Review Panel Information

Andreas Stamminger (chair) EuroLaunch / DLR
Mark Fittock (minutes) EuroLaunch / DLR

2. General Comments

- PDR presentation

Well-liked
Overtime though
Text almost too small to read
Watched the board

- SED content

Images and simulations well-coloured
Some figures and numbers
References method
Use appendices rather than referenced files
Logo in the SED… but already changed
More clarity on team description
Good document, well done
Verification matrix missing
Risk register and mech interface and design, EFA good

3. Panel remarks

- Mechanical

How will you cope with the stresses?
SD card for camera, how will it be secured? Team - slot and glued
Wall thickness is large on your structure
Base structure is heavy and could be reduced
Issues foreseen with the coverplate which normally sits to cover the nosecone adaptor, solution must be determined by both parties
Is base possible to reduce so that the balancing weights can be added? Team to analyse
How many cameras and how? Two cameras currently planned,
Payload mass estimated to be 40 kg… this is incorrect, you need to consider all systems that will reenter together as the payload
Team - Size of screws to attach to nosecone adaptor and thread inserts? To be passed from EuroLaunch
Concerns over force transfer from probe… consider sacrificial joints, so that the probe breaks in a good way
What do you expect for temperature on the probe? Team – maximum of 250 or 300, it is definitely uncertain
Beware mechanical deformation for destruction, Team – want to transfer all data down
Consider heating up the experiment to 400oC, Team – material selected for test of monitoring of

sufficient degradation to prove monitoring system
Team – spare probe for testing and transport

- Electrical

Supplied schematics is good
Some design error in the interface to REXUS, optocouplers good, positive part of optocoupler connected to ground
Impressed by double failsafe design for converters, redundancy on power supply… perhaps team doesn't trust the power supply from EuroLaunch, beware coupling between converters
Be careful with contacts for sd cards
Be careful with contacts inside post and insulation
Regulator powering on system is difficult, think of using diodes so that they don't feed the wrong way
Switching regulators should have filtering on the inputs
Team – currently a simplified schematic
Can send your final schematics to Pinzer (ASAP)
Can't attach the outputs from the regulators together without resistors, capacitors will buffer the regulator voltage a bit, diode acts to cause a voltage drop
Linear output from regulators an issue? One regulator will act as master, a resistor on one output can reduce the issue
Load sharing resistor can prevent a regulator from being over-loaded
USB interface only for testing? Team – yes, and don't need access after delivery
Monitoring your voltages with resistor devices… Zener diode is useful there… stops hiccups on the input
Optocouplers for inputs, you go straight from transistor to ucontroller, small capacitors stop hiccups from hurting the ucontroller

- Thermal

How can you remove heat from the electronic box? Team – don't but think it's not a problem
Thermally isolating with spacers could cause problems with vibration
Do you measure heat in the elec box? Team – no but we could

- Software

Software is good. Quite good. Well-liked.
p.17 software not on top level of WBS
Ground support software
State machine is quite good
Flow diagrams should have main blocks of software identified
Telemetry format is very good
Uplink during flight why? Team – uplink is nice for if there is an error but maybe possible to not, watchdog also there to catch errors, can skip if it isn't desired
Data structure on the downlink, LO, SOE and SODS good in housekeeping data, Team – housekeeping determines status
Cameras – make sure you can reach them, plan for accessability
Connectors also need to be accessible

- Testing

Component testing to be added to the project planning, Team – know this, will do this
Verification matrix missing!
Remember testing can be done at Bremen
Can also test at Oberpfaffenhofen

- Operations

Do you deliver your GSE? Team – yes
Camera – TV channel, can you really see anything in your cameras, Team – will see smoke, need to validate and know what happens, Board - please define time when you need the camera, Team – from 80 km to 20 km
What higher resolution do you need to go to? Test this first to make sure it will do the job that you need
You need to define all your camera requirements, Team – don't have money for a more expensive camera, Board – define it anyway, perhaps then EuroLaunch can help
Think of an infrared camera to view the heat

- Safety and Risks

Probe being pushed in or transferring forces to the payload

- Planning, Organization and Outreach

Manpower budget is way too low
Outreach in SED not so good, much better in presentation
Used for your theses? Team – no, used for credit points
Add the other members to your team officially (can use a half member system if that is preferable to you)

- Final Board Comments

N/A

- Student Questions

Power on/off control means? Board – 10 mins before launch turned on, 10 mins after landing turned off, this section refers to requirements you may have, tell EuroLaunch and we can switch off after you go to safe mode

4. Final remarks

- Major Actions Required

Design of a safe probe
Review electronic design

- Result

PDR passed

- Next Required SED Version

SED V2.0 two weeks before the CDR

REXUS / BEXUS
Experiment Critical Design Review

Flight: REXUS-09

Payload Manager: A. Stamminger

Experiment: REMOS

Location: DLR-OP **Date:** 08-06-10

1. Review Board

Olle Persson	SSC	Mark Uitendaal	SSC
Hans Henricson	SSC	Mikael Inga	SSC
Andreas Stamminger (chair)	DLR-RY	Koen de Beule	ESA
Mark Fittock (secretary)	DLR-RY	Helen Page	ESA
Adam Lambert	ESA	Markus Pinzer	DLR-MORABA
Martin Siegl	ESA	Marcus Hoerschgren	DLR-MORABA

2. Participating Payload Team members

Robert Wuseni, Salome Schweilke, Serina Latzko, Marcel Düring

Hannah Böhrk DLR-BK, Jonathan Gräßer DLR-BK

3. General Comments

- Presentation
  - Timing was good
  - Slides were clear and concise
  - Don't have to be so nervous with the board
- SED
  - Some of mechanics could be made clearer otherwise good section
  - Reviews missing
  - Not vers 3 it is version 2.0
  - Some figure number missing
  - Chapter 7 is missing about Post Flight Analysis
  - Verification matrix added and is good
  - **Content and format as discussed in the SED section needs to be updated**

4. Panel Comments and Recommendations

- Requirements
  - Functional 3 and 4 were for 16 locations and are now reduced to 8, this should be explained why it was changed
  - Operations reqs, should have requirements for re-entry stability orientation for it to be complete
- Mechanics
  - Good mechanical design
  - Difficult to see from documentation how it is mounted in the nosecone adaptor
  - Structural and dynamic analysis very nice
  - Payload will most likely have a spinning/tumbling motion, suggest to correlate with

attitude data, make sure you are covering the temperatures generated in this case
    - Experiment probe will quite likely be damaged on landing but can you work on it if it returns in one piece? Response: nice but of no great benefit
    - Where is the camera positioned? Response: in two smaller aluminium boxes to the right and left of the experiment
    - **Need to make experiment mechanical interfaces and assembly much more clear**
    - **Needs to be sealed to the next experiment to stop gas feeding through,** should leave a small gap for vibration (1mm or less)
    - Can probe damage other experiments by pushing it through? Response: no probe will act as shock absorber

- Electronics & Power
    - Do you have a temperature sensor in the electronics box? Response: was planned, is possibly missing
    - An EMC test may be a good idea for the experiment considering the probe and electronics
    - Can do a check using a similar transmitter to look at effects
    - **Because DCDC redundancy design might cause problems, sharing resistors were meant to have been implemented, not found in SED, must be amended**
    - **Interface to REXUS optocoupler device, must also be fixed in SED**
    - Take care of RF interferences to analog channels, interference on cables could affect results, test it
    - You requested TV channel, can be provided for one of the two cameras
    - Can the camera memory be controlled or how? Response: just on and off
    - Can you send via TV channel and save data onboard? Response: no
    - **Need to define the TV solution for the option of one TV channel**
    -

- Thermal
    -

- Software
    - Signals, requested an SODA signal, change to SODS
    - **Need to clarify the signals on p.43**
    - Software was quite good
    - Time-event list is lacking before and after flight considerations
    - **You should transmit a signal to show that the experiment is operational before lift-off**
    - Test what you fly and fly what you test, test software that you will use for flight rather than testing test software

- Verification & Testing
    - EMC test suggested
    - p.88 and p.91, you have 10 tests that take 15 minutes, consider your set-up and cleaning up time as well
    - colour scheme in the verification matrix is very very good
    - should describe location of tests as well as equipment

- Launch & Operations (incl. ground support)
    - No special requests
    - **Bring a pair of prepared computers (with ground control software), list this in GSE**
    - Budget for GSE is in the wrong location

- Safety & Risk Analysis
    - Risk analysis updated
    - Analysis is a little bit too good
    - What are you most worried about? Response: main risk is the flow conditions of the reentry

- Project Planning & Outreach
    - **Need to arrange dates for meeting, integration and testing**

- Can attend the RXBX Experiment Results Symposium dinner
    - WBS good
    - Gantt not totally clear from SED but looking like progress is better than displayed
    - Is division (geographically) an issue for the team? Using skype to maintain communication
    - Good that outreach included as appendix in SED
    - Please upload to the media folder
    - Can broaden outreach to other media types such as radio
    - WBS could stick to one format style
    - Producing stickers is a good way to draw more of an audience

- Student Questions
    - We would like components manufactured, how will this work? Response: submit CAD files, Stamminger gets quotes and then gets the components produced for you, beware of leaving it too late
    - Will attitude be provided to everyone? Response: rates, accelerations available but during re-entry attitude is not possible with REXUS sensors, on teamsite RX7 and RX8 flight data is available, think to timestamp in comparison to the camera
    - How accurate are the rate sensors of REXUS? Response 3 milli degrees per second

5. Final remarks

- Summary of main actions for the experiment team
    - **Content and format as discussed in the SED section needs to be updated**
    - **Need to make experiment mechanical interfaces and assembly much more clear**
    - **Needs to be sealed to the next experiment to stop gas feeding through**
    - **Because DCDC redundancy design might cause problems, sharing resistors were meant to have been implemented, not found in SED, must be amended**
    - **Interface to REXUS optocoupler device, must also be fixed in SED**
    - **Need to define the TV solution for the option of one TV channel**
    - **Need to clarify the signals on p.43**
    - **You should transmit a signal to show that the experiment is operational before lift-off**
    - **Bring a pair of prepared computers (with ground control software), list this in GSE**
    - **Need to arrange dates for meeting, integration and testing**

- CDR Result
    - Not passed

- Next SED version
    - 16 July 2010

- Planning for IPR and EAR
    - TBD

APPENDIX B – OUTREACH AND MEDIA COVERAGE

Stuttgarter Studenten forschen im Weltraum

Zwei Studententeams aus Stuttgart, wurden vom Deutschen Zentrum für Luft- und Raumfahrt (DLR) ausgewählt, auf der Forschungsrakete REXUS im März 2011 ihre Experimente zu fliegen. Bis zu drei Minuten Schwerelosigkeit stehen EXPLORE hierbei zur Verfügung, um den Flüssigkeitstransfer zwischen Testkammern zu untersuchen. REMOS überwacht während des Wiedereintritts die Ablation von Hitzeschutzmaterialien. Im Rahmen einer Trainingswoche im Esrange Space Center in Kiruna meisterten beide Teams im Februar 2010 das offizielle Review mit Experten und werden nun bis November die Flughardware integrieren.

EXPLORE

EXPeriment for Liquid On-orbit RE-fueling (EXPLORE)
Das Experiment EXPLORE simuliert in einem Betankungsvorgang unter Schwerelosigkeit kritische Technologien für zukünftige Missionen zu Zielen wie Mond und Mars. Das Team besteht aus den sechs Studierenden der Luft- und Raumfahrttechnik an der Universität Stuttgart: Christine Hill, Andreas Fink, Johannes Weppler, Robert Schelling, Emil Nathanson, Jürgen Schlutz; sowie dem Offenburger Elektro- und Informationstechnik-Studenten Daniel Störk (nicht im Bild).

Das EXPLORE Team neben der TEXUS Rakete im IRS

Untergebracht in einem Nutzlastmodul der REXUS Rakete besteht EXPLORE aus der Betankungsanlage, der Steuerungs- und Aufzeichnungselektronik sowie der strukturellen Befestigung. In der Betankungsanlage bedruckt ein zentraler Gasdrucktank zwei gleiche Flüssigkeitstanks, von denen wiederum die Flüssigkeit über Massenflussregler und entsprechende Ventile und Leitungen in die sechs Testkammern geleitet wird. Das Geschwindigkeitsprofil der Strömung wird für jede Kammer variiert, um optimale Bedingungen zu identifizieren und maximale Füllstände zu erreichen. Dabei muss eine Trennung zwischen der flüssigen und gasförmigen Phase in der Testkammer erreicht werden, um den wertvollen Treibstoff nicht zu verschwenden. Die Elektronik besteht aus einem Mikrocontroller zur Ansteuerung und zur Erfassung der Sensordaten. Im Verlauf des Experiments werden Druck-, Temperatur- und Video-Bilddaten aufgezeichnet, die den Befüllungsvorgang charakterisieren.

EXPLORE wird in der Umsetzung vom IRS mit seiner Expertise und Testeinrichtungen unterstützt.

REcession MOnitoring System (REMOS)
REMOS ist ein Experiment zur Flugerprobung eines Systems, das den Zustand von Hitzeschilden zukünftiger Raumkapseln überwachen kann. Ziel ist es, während des Wiedereintritts – das heißt dann, wenn das Hitzeschild nach und nach abbrennt und verglüht (ablatiert) – den Verlauf der Ablation aufzuzeichnen. Das Team besteht aus den Stuttgarter Studierenden Salome Schweikle, Robert Wuseni, Serina Latzko, Alena Probst, Marcel Düring und Christian Blank.

REMOS wird in der Nasenspitze der REXUS Rakete fliegen und nach dem Abwurf der Nasenkappe direkt der Umgebung ausgesetzt sein. Wenn die Rakete wieder in die dichtere Erdatmosphäre eintritt, wird ein Mast mit einer Materialprobe und der Sensorik der Strömung ausgesetzt. Während die Probe durch die steigenden thermischen Lasten ablatiert, zeichnet REMOS ständig die sich ändernden elektrischen Eigenschaften

Mitglieder des REMOS Team am Esrange Space Center

auf und schickt sie zusammen mit Videomaterial an die Bodenstation der Studenten. Die so gewonnenen Daten sollen dazu dienen, zukünftige Thermalschutzsysteme bezüglich Gewicht, Kosten und Zuverlässigkeit zu optimieren.

Dabei wird das Team vom DLR Stuttgart – besonders durch Dr. Hannah Böhrk – sowie durch das IRS und das ITLR unterstützt.

Das REXUS/BEXUS Programm
Das REXUS/BEXUS Programm ermöglicht Studierenden von Universitäten und höheren Bildungseinrichtungen in Europa wissenschaftliche und technologische Experimente auf Forschungsballons und -raketen zu fliegen. Jedes Jahr starten je zwei Raketen und Ballons, die insgesamt bis zu 20 Experimente tragen, jedes Einzelne entworfen und gebaut von Studententeams.

Kontakt und weitere Informationen:
www.explore-rexus.de
www.remos-stuttgart.de
www.rexusbexus.net

Article on the homepage of the Institute of Space Systems (IRS) of the University Stuttgart:

Home | Institut | Lehre | Forschung | Aktuelles

Institut für Raumfahrtsysteme

News

Zum Newsarchiv

Stuttgarter Studenten forschen im Weltraum

Zwei Studententeams aus Stuttgart wurden vom Deutschen Zentrum für Luft- und Raumfahrt (DLR) ausgewählt, auf der Forschungsrakete REXUS im März 2011 ihre Experimente mitfliegen zu lassen. Bis zu drei Minuten Schwerelosigkeit stehen EXPLORE hierbei zur Verfügung, um den Flüssigkeitstransfer zwischen Testkammern zu untersuchen. REMOS überwacht während des Wiedereintritts. die Ablation von Hitzeschutzmaterialien. Im Rahmen einer Trainingswoche im schwedischen Kiruna besuchten die Studierenden Anfang Februar 2010 das Esrange Space Center, von wo die Forschungsraketen gestartet werden. Neben detaillierten Einführungen in die Systeme der Rakete wurden hier auch die Entwürfe von Experten analysiert und in einem offiziellen Review für die nächsten Projektphasen freigegeben. Ein Meilenstein, den beide Teams erfolgreich meistern konnten.

EXperiment for Liquid On-orbit REfueling (EXPLORE)

EXPLORE

Das Experiment EXPLORE simuliert einen Betankungsvorgang unter Schwerelosigkeit. Dies ist für viele Explorationsmissionen wichtig, die enorme Transportkapazitäten zu Zielen wie Mond und Mars aufbringen müssen. So ist Wiederbetankung von orbitalen Transferstufen auch als eine wichtige Technologie im Rahmen der neuen Schwerpunkte der amerikanischen NASA herausgehoben. EXPLORE wurde bereits im Herbst 2009 von den sechs Studierenden Christine Hill, Andreas Fink, Johannes Weppler, Robert Schelling, Emil Nathanson und Jürgen Schlutz der Luft- und Raumfahrttechnik an der Universität Stuttgart initiiert und wird von diesen im Laufe des Jahres 2010 realisiert.

Das Experiment wird in einem Nutzlastmodul der REXUS Rakete untergebracht sein und besteht aus der Betankungsanlage, der Steuerungs- und Aufzeichnungs¬elektronik sowie der strukturellen Befestigung. In der Betankungsanlage bedruckt ein zentraler Gas¬druck¬tank zwei gleiche Flüssigkeitstanks, von denen wiederum die Flüssigkeit über Massenflussregler und entsprechende Ventile und Leitungen in die sechs Testkammern geleitet wird. Das Geschwindigkeitsprofil der Strömung wird für jede Kammer variiert, um optimale Bedingungen zu identifizieren und maximale Füllstände zu erreichen. Dabei muss eine Trennung zwischen der flüssigen und gasförmigen Phase in der Testkammer erreicht werden, um den wertvollen Treibstoff nicht zu verschwenden. Die Elektronik besteht aus einem Mikrocontroller, der zum Einen die Regler und Ventile der Betankungsanlage steuert, zum Anderen aber auch die Sensordaten erfasst und speichert. Im Verlauf des Experiments werden Druck-, Temperatur- und Video-Bilddaten aufgezeichnet, die den Befüllungsvorgang charakterisieren.

EXPLORE arbeitet in erster Linie mit einfachen Komponenten und Mitteln, um ein komplexes Experiment zu verwirklichen. Hierzu zählt nicht nur die eigentliche Funktionalität des Aufbaus und der Elektronik, aber auch die Qualifizierung des ganzen Experiments für den Flug. Vibrationen beim Start, Vakuum im Flug und extreme Temperaturen von etwa -30°C im Norden Schwedens sind nur einige der Herausforderungen, die das Team in den nächsten Monaten in Ihrem Entwurf berücksichtigen und in der Umsetzung nachweisen müssen. Das IRS unterstützt dabei mit seiner Expertise und Testeinrichtungen.

REcession MOnitoring System (REMOS)

REMOS ist ein Experiment zur Flugerprobung eines Systems, das den Zustand von Hitzeschilden zukünftiger Raumkapseln überwachen kann. Ziel ist es, während des Wiedereintritts – das heißt dann, wenn das Hitzeschild nach und nach abbrennt und verglüht (ablatiert) - den Verlauf der Ablation aufzuzeichnen. Ein Einsatzgebiet wäre zum Beispiel das derzeit in Europa projektierte Hitzeschutzsystem für das ATV. Das Team besteht aus den Stuttgarter Studierenden Salome Schweikle, Robert Wuseni, Serina Latzko, Alena Probst und Christian Blank.

REMOS wird in der Nasenspitze der REXUS Rakete fliegen und nach dem Abwurf der Nasenkappe direkt der Umgebung ausgesetzt sein. Wenn die Rakete wieder in die dichtere Erdatmosphäre eintritt, wird eine Materialprobe, in die die Sensoren integriert sind, der Strömung ausgesetzt. Durch die steigenden thermischen Lasten ablatiert sie nach und nach. REMOS zeichnet ständig die sich ändernden elektrischen Eigenschaften auf und schickt sie zusammen mit Videomaterial an die Bodenstation der Studenten. Die so gewonnenen Daten sollen dazu dienen, zukünftige Thermalschutzsysteme besser an die extremen Umweltbedingungen anzupassen. Sie müssen derzeit mit sehr hohen Sicherheitsreserven ausgelegt werden, da über ihr genaues Abbrandverhalten nur sehr wenig bekannt ist und Simulationen nur schwer durchführbar sind. Mit REMOS könnte bei einer Vielzahl von Flügen eine Datenbasis aus realen Missionen erzeugt und mit weiteren Messdaten kombiniert werden.
Dieses detaillierte Wissen über das Verhalten ablativer Hitzeschilde während des Wiedereintritts ist überaus wertvoll für deren Entwicklung und Verbesserung. Es hilft, Gewicht einzusparen, Kosten zu senken und die Zuverlässigkeit zu erhöhen.

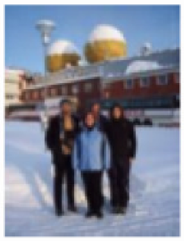

Das Experiment besteht aus dem Überwachungssystem, das sich in einer zylindrischen Box auf dem Nasenadapter der Rakete befindet. Daran ist ein Mast mit der eigentlichen Probe und den Sensoren befestigt. Bis Juni erfolgt das detaillierte Design bevor dann bis November die Montage und Tests folgen. Dabei wird das Team vom DLR in Stuttgart sowohl finanziell als auch fachlich – besonders durch Hannah Böhrk - unterstützt. An der Uni Stuttgart stellen das IRS und das ITLR Einrichtungen zur Verfügung.

Das REXUS/BEXUS Programm

Das REXUS/BEXUS Programm ermöglicht Studierenden von Universitäten und höheren Bildungseinrichtungen in Europa wissenschaftliche und technologische Experimente auf Forschungsballons und -raketen zu fliegen. Jedes Jahr starten je zwei Raketen und Ballons, die insgesamt bis zu 20 Experimente tragen, jedes Einzelne entworfen und gebaut von Studententeams.

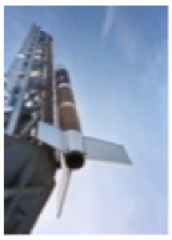

- REXUS Experimente werden auf einer ungesteuerten, spin-stabilisierten Rakete gestartet, die von einem verbesserten Orion Motor mit 290 kg Festtreibstoff angetrieben wird. Sie kann bis zu 40 kg an Experimentmodulen in eine Höhe von 100 km bringen. Die Rakete hat eine Länge von etwa 5,6 m und einen Durchmesser von 35,6 cm.
- BEXUS Experimente werden von einem Höhenforschungsballon mit einem Volumen von 12 000 m auf eine Maximalhöhe von 35 km getragen, abhängig von der absoluten Experimentmasse (40-100 kg). Der Flug dauert zwischen 2 und 5 Stunden.

Das REXUS/BEXUS Programm wird in einem bilateralen Abkommen zwischen dem Deutschen

Zentrum für Luft- und Raumfahrt (DLR) und dem Swedish National Space Board (SNSB) realisiert. Der schwedische Nutzlastanteil wird dabei über eine Zusammenarbeit mit der Europäischen Raumfahrtagentur (ESA) Studierenden aus anderen Europäischen Ländern zugänglich gemacht. EuroLaunch, eine Kooperation zwischen dem Esrange Space Center der Swedish Space Corporation (SSC) und der Mobilen Raketenbasis (MORABA) des DLR, ist für das Management der Kampagne sowie für den Betrieb der Fahrzeuge verantwortlich. Experten der ESA, des SSC und des DLR leisten technische Unterstützung für die Studententeams im Projektverlauf.

Mehr über das REXUS/BEXUS programm ist auf der REXUS/BEXUS Projektseite zu finden: www.rexusbexus.net

Kontakt und weitere Informationen:

EXPLORE	REMOS
IRS, Universität Stuttgart	DLR Institut für Bauweisen und Konstruktionsforschung
http://www.explore-rexus.de	http://www.remos-stuttgart.de
info@explore-rexus.de	kontakt@remos-stuttgart.de

Bilder

EXPLORE

highres-version

Die stilisierte Bilderserie des EXPLORE Logos zeigt eine Rakete für die Raumtransportsysteme zur Erforschung ferner Planeten. Wiederbetankung steht zwischen den beiden, EXPLORE ist Ziel und Lösung zugleich (Bild: EXPLORE)

highres-version

Das EXPLORE Team (v.l.n.r): Johannes Weppler, Christine Hill, Andreas Fink, Emil Nathanson, Robert Schelling, Jürgen Schlutz (Bild: EXPLORE)

highres-version

Andreas Fink und Johannes Weppler inspizieren das REXUS Experimentmodul für den mechanischen Einbau von EXPLORE (Bild: EXPLORE)

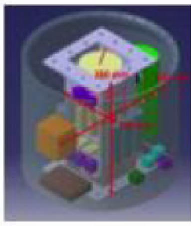

highres-version

3D-Ansicht des EXPLORE Aufbaus (Bild: EXPLORE)

REMOS

highres-version

Das REMOS Logo mit der Probe während

highres-version

REMOS montiert auf

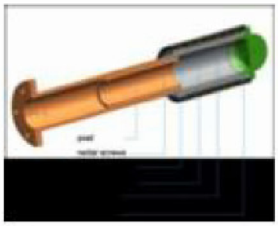

highres-version

Aufbau der Probe mit dem

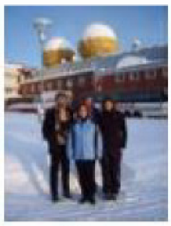

highres-version

Das REMOS Team in Kiruna: Robert Wuseni, Salome

des Wiedereintritts und den Teammitgliedern (Bild: REMOS)	den Nasenadapter der REXUS Rakete (Bild: REMOS)	Ablatormaterial (schwarz) und den integrierten Sensoren (Bild: REMOS)	Schweikle, Christian Blank und Alena Probst (v.l.n.r). nicht auf dem Bild: Serina Latzko (Bild: REMOS)

REXUS

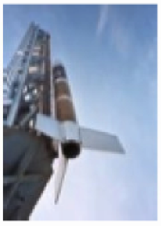

highres-version

Forschungsrakete REXUS auf der Startrampe (Bild: DLR)

highres-version

REXUS Start vom Esrange Space Center in Kiruna, Schweden (Bild: DLR)

- **News** Neuigkeiten aus dem Institut
- **News-Archiv** Ältere Neuigkeiten aus dem Institut
- **Highlight-Archiv** Alle Highlights in umgekehrter chronologischer Reihenfolge
- **Highlight-Liste** Thematische sortierte Liste aller Highlights seit Mai 2003
- **Pressespiegel** Materialien vom und über das Institut für Raumfahrtsysteme
- **Veranstaltungen** Termine rund um das Institut
- **Faltblätter** Informationsmaterial über das Institut und seine Forschungsaktivitäten
- **Bildergalerie** Bilder zu Forschungsthemen des Instituts

letzte Änderung: 02.03.2010 | email | © Universität Stuttgart | Impressum

Yuri's Night in Stuttgart; together with Team SQUID, EXPLORE and FOCUS:

Web-Article:

Yuri's Night – Stuttgart, Deutschland

Yuri's Night Stuttgart 2010

Am Sonntag, dem **11. April 2010** feierte Stuttgart mit der Yuri's Night den 49. Jahrestag von Gagarins legendärem Raumflug. Der **Tag der Raumfahrt** im Herzen der Landeshauptstadt zog Groß und Klein in seinen Bann, als **hunderte Besucher** die **Ausstellung, Vorträge und Aktivitäten** im Stuttgarter Planetarium erkundeten. Die **World Space Party** in der SkyBar/SkyBeach sorgte für einen gelungenen Ausklang am Abend.

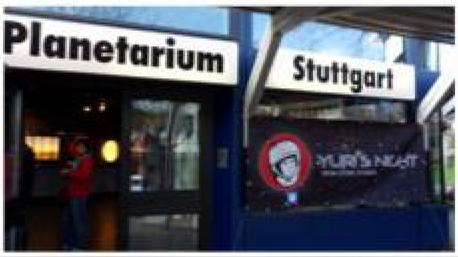

Raumfahrt Hautnah Erleben im Planetarium Stuttgart

Im Planetarium Stuttgart und gemeinsam mit Partnern wie dem Institut für Raumfahrtsysteme (IRS), der europäischen Raumfahrtagentur ESA, dem Deutschen Zentrum für Luft- und Raumfahrt (DLR), Space Travellers, Astos Solutions und Anderen bot die Yuri's Night am 11. April 2010 ein umfassendes und abwechslungsreiches Informationserlebnis rund um die Raumfahrt! Die Veranstaltung richtete sich in erster Linie an Familien und Kinder, konnte jedoch auch interessierte Besucher anderer Altersgruppen locken und faszinieren. Dabei wurde Raumfahrt nicht nur beschrieben, sondern auch praktisch und direkt für jeden erfahrbar gemacht:

Raumfahrt zum Anfassen und Staunen bot eine umfangreiche Ausstellung von Raketen, Raumstationen und Raumfahrzeugen sowie vielen interessanten Schautafeln. Sie führte die Besucher in die Technologien und Systeme der Raumfahrt ein und vermittelte die Herausforderungen und Möglichkeiten der Weltraumforschung und -erkundung. Teile der Ausstellung waren z.B.:

- historische amerikanische und russische Trägersysteme (Wostok, Proton, Soyuz, Mercury-Redstone, Mercury-Atlas, Gemini-Titan, Ariane 4, Ariane 5, Space Shuttle, Saturn V, N1)
- die Raumstationen MIR und ISS sowie das Versorgungsfahrzeug ATV
- die Mars Rover Spirit und Opportunity
- das Hubble Weltraumteleskop
- ESA Satellitenmissionen Cluster II und Venus Express

Yuri's Night Stuttgart www.yurisnight.de info@yurisnight.de

Yuri's Night – Stuttgart, Deutschland

Die Ausstellung wird noch **bis zum 30. April 2010 im Foyer des Planetariums** zu bewundern sein.
Neben den Modellen gab es aber noch zahlreiches anderes Infomaterial wie Broschüren, Zeitschriften, Aufkleber, und und und, das alle Besucher gerne mit nach Hause nahmen.

Im Keplersaal des Planetariums bot die Yuri's Night im Laufe des Nachmittags **eindrucksvolle Vorträge zu ausgewählten Themen,** welche die Besucher mit einfachen Einführungen und aktuellem Hintergrundwissen in die spannende Welt der Raumfahrt eintauchen ließen.
Das Vortragsprogramm im Einzelnen:

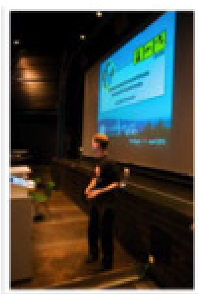

- **13:45 Uhr: Faszination Raumfahrt**
  Warum feiern wir Yuri's Night? Wie funktioniert eine Rakete? Was ist Schwerelosigkeit? Wie nutzen wir Raumfahrt jeden Tag? Einen kurzweiligen Exkurs in die Besonderheiten und Errungenschaften der Raumfahrt bereitete Jürgen Schlutz vom Institut für Raumfahrtsysteme der Universität Stuttgart und Koordinator der Yuri's Night.
- **15:45 Uhr: Schwerelosigkeitsexperimente von und für Studierende**
  Studentische Teams der Forschungsrakete REXUS berichteten über ihre Erfahrungen und Herausforderungen. Mit dabei waren die Teams EXPLORE (Stuttgart), REMOS (Stuttgart), FOCUS (München) und SQUID (Stockholm), die im März 2011 ihre Experimente auf REXUS 9/10 an die Grenze zum Weltraum schicken.
- **17:45 Uhr: Marsmission auf Erden**
  Die Schweizer Astronomin Barbara Burtscher nahm uns mit auf ihre Expedition in der Mars Desert Research Station der Mars Society in Utah, USA. Ein umfangreiches wissenschaftliches Programm beschäftigte die internationale Crew genauso wie gruppendynamische und alltägliche Herausforderungen beim Zusammenleben auf engstem Raum.

Der Keplersaal mit seinen ca. 150 Plätzen war für alle Vorträge gut gefüllt und erlaubte den Zuhörern auch, eigene Fragen an die Experten zu stellen.

Yuri's Night – Stuttgart, Deutschland

Highlight der Yuri's Night 2010 waren sicherlich die vielfachen Aktivitäten, die zum Mitmachen und Ausprobieren einluden. **Raumfahrt zum Selbermachen** war die Devise, und Möglichkeiten hierzu gab es ausreichend: Ein Raketenbastelworkshop erlaubte auch den Kleinsten, eine eigenes Raketenmodell aus vorgefertigten Bausätzen der Firma machtWissen.de zu gestalten und dann direkt vor der Tür des Planetariums im Schlossgarten mit Hilfe von kleinen Treibsätzen zu starten. Die Mini-Raketen erreichten dabei eine Flughöhe von bis zu 100m, fielen dann gebremst zur Erde zurück und konnten wiederverwendet oder als Souvenir mit nach Hause genommen werden. Die regelmäßigen Raketenstarts sorgten im Schlossgarten Stuttgart bei gutem Wetter für viele interessierte Zuschauer!

Parallel konnten unter Anleitung von Astos Solutions begeisterte Raketenfans am Zielschiessen mit Luftdruckraketen teilnehmen und spielerisch Prinzipien hinter Antrieb und Flugbahnen erlernen.

Auch unter dem Dach des Planetariums boten der Mini-Fallturm und ein Planeten-Dart abwechslungsreiche Betätigung. Auf eine Fallstrecke von etwas mehr als zwei Metern erreicht eine kleine Kapsel am Mini-Fallturm Schwerelosigkeit und kann so physikalische Prinzipien ohne Schwerkraft demonstrieren. Dazu gehören z.B. Kapillarkräfte, das Mischungsverhalten von Flüssigkeit und Gas sowie Magnetismus. Beim Planeten-Dart konnten durch Identifizierung und „Abschießen" der Himmelskörper unseres Sonnensystems Kleinpreise gewonnen werden.

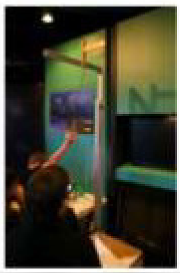

Yuri's Night Stuttgart www.yurisnight.de info@yurisnight.de

Yuri's Night – Stuttgart, Deutschland

Eingebettet in die Yuri's Night 2010 fand in Stuttgart auch der **1. REXUS Public Day** statt, an dem sich studentische Teams der REXUS Forschungsrakete gemeinsam den Besuchern und der Presse präsentierten. Insgesamt vier Teams aus **Stuttgart, München und Stockholm** begeisterten interessierte Zuhörer mit ihren Vorträgen, Demonstrationen und viel Hintergrundwissen rund um aktuelle Forschungsfragen und die Umsetzung von Raketenexperimenten.

EXPLORE untersucht den Transfer von Flüssigkeiten unter Schwerelosigkeit, REMOS wird beim Wiedereintritt die Abbrandrate des Hitzeschutzmaterials bestimmen, FOCUS revolutioniert den Bau grosser Strukturen im Weltraum und SQUID macht wichtige Messungen des Strahlungs- und Teilchenumfelds in der Atmosphäre. Alle Experimente werden noch in diesem Jahr fertiggestellt und im Frühjahr 2011 auf der REXUS Rakete fliegen.

Am ganzen Nachmittag forderte ein „**Raumfahrt-Quiz**" die Besucher, ihre neu erlernten Kenntnisse über das Sonnensystem, Yuri Gagarin, die aktuellen Raumfahrtmissionen und REXUS Experimente zu testen und mit der Teilnahme **attraktive Preise rund um die Raumfahrt** zu gewinnen. Dank unseren Sponsoren warteten insgesamt 15 tolle Preise auf ihre Gewinner und lockten viele zur Verlosung in den Keplersaal. Die Preise der Yuri's Night 2010 sind im Anhang zu finden.

Eine **Space Bar mit Snacks, Getränken und Cocktails** bot allen Raumfahrtfans die Möglichkeit, sich mit passenden Leckereien zu stärken. Faszinierende Getränke wie „Earthrise", „Sternschnuppenregen" oder „Yuri's Delight" sind nur eine Auswahl der umfangreichen Erfrischungskarte.

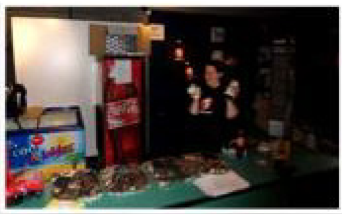

Raumfahrt und ihre Technologien sind auch eng mit Science Fiction verbunden, die oftmals Anregungen bringt und es auf ganz besondere Weise versteht, Menschen allen Alters zu faszinieren. Umso mehr freuen wir uns, dass auch die **Arma**

Yuri's Night Stuttgart www.yurisnight.de info@yurisnight.de

Yuri's Night – Stuttgart, Deutschland

Candida, ein deutscher Arm der 501st Legion, die Yuri's Night in Stuttgart unterstützte. Der Kostümklub rund um die imperialen Streitkräfte aus dem Kinoklassiker „Krieg der Sterne" schickte drei Vertreter, die in ihren **eindrucksvollen Uniformen und Rüstungen** ständig für Aufmerksamkeit und tolle Erinnerungsfotos sorgten.

Im Laufe des Nachmittags sorgte auch die Big Band des **All-mand Chaoten Orchesters** für **Live-Musik** am Planetarium und konnte bei strahlendem Sonnenschein mit ihrer Musik die Gäste begeistern.

Der Ansturm der Besucher auf das Angebot, die leuchtenden Kinderaugen, die interessierten Nachfragen und das durchweg positive Feedback waren ein klares Zeugnis für eine äußerst gelungene Veranstaltung, die ihre Vorgänger sicher in den Schatten stellt. Von Beginn um 13 Uhr an riss der Strom an Gästen nicht ab und sorgte bei den Modellraketen, an der Bar und bei allen Aktivitäten für andauernde Schlangen. In der Tat übertraf der Besucheransturm mit sicherlich mehr als 500 Gästen im Durchlauf unsere Erwartungen bei Weitem!

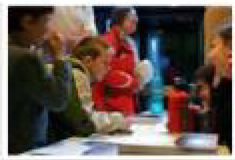

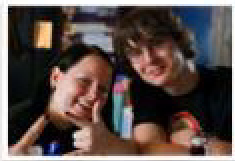

Raumfahrt Feiern über den Dächern der Stadt

Nach den informativen Veranstaltungen am Nachmittag lud die Yuri's Night 2010 am Abend mit der „**World Space Party**" auf die Dachterrasse der Stuttgarter SkyBar/SkyBeach. Ein Live-DJ sowie coole Drinks, beste Atmosphäre und tolle Ausblicke über die Stadt sorgten für einen entspannten Ausklang des Tages!

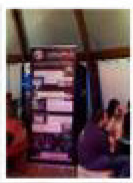

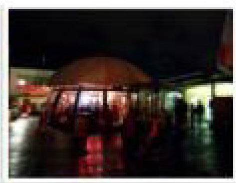

Yuri's Night Stuttgart www.yurisnight.de info@yurisnight.de

Yuri's Night – Stuttgart, Deutschland

Yuri‘s Night 2010 in Deutschland

Neben der Stuttgarter Veranstaltung sorgten auch weitere Yuri's Night Events anderswo in Deutschland für Aufsehen und Andrang. Insgesamt fünf Veranstaltungen in Rostock, Berlin, Heidelberg, München und Stuttgart feierten um den 12. April 2010.

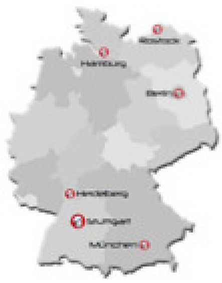

Die Yuri's Night 2010 sorgte in Deutschland für ein deutliches Medienecho und konnte dadurch Ihren Zweck, die Kommunikation der Raumfahrtaktivitäten gegenüber einem breiten Publikum, vollkommen erfüllen. Veranstalter, Partner, Sponsoren und auch Besucher können sicherlich zufrieden auf diesen Erfolg zurückblicken und frohen Mutes die neue Herausforderung der Yuri‘s Night 2011 wagen, zum 50. Jubiläum von Yuri Gagarins Raumflug!

Ein paar Beispiele aus dem Medienspiegel sind ebenfalls angehängt!

Yuri's Night Stuttgart www.yurisnight.de info@yurisnight.de

Newspaper Articel 1 about Yuri’s Night in Stuttgart:

Raketen-Countdown im Schlossgarten

Hunderte beim Tag der Raumfahrt – Stuttgarter Studenten planen 2011 Projekt in Schweden

VON JENS NOLL

STUTTGART. Sarah hat eine Rakete gebaut. Natürlich möchte sie auch beim Start dabei sein. Sie gibt die Startzündung, ein „Achtung" ertönt, und schon steigt die Rakete zischend in die Höhe. Das Besondere an dem Fluggerät: Es ist selbst gebastelt, aus einem einfachen Bausatz aus Kartonteilen.

Mit zahlreichen Aktionen, Informationen und Anschauungsmaterial lockte am Sonntag die „Yuri's Night 2010" die Besucher in das Planetarium und auf einen mit Absperrband markierten Bereich des Schlossgartens. Die Raketen starteten zu Ehren des russischen Kosmonauten Juri Gagarin, der am 12. April 1961 als erster Mensch im Weltall die Erde umkreiste. „Wir möchten den Menschen die Raumfahrt näherbringen", sagt Jürgen Schlutz, wissenschaftlicher Mitarbeiter am Institut für Raumfahrtsysteme der Universität Stuttgart. Er ist der Organisator der Veranstaltung, die seit 2001 in Stuttgart stattfindet. „Tatsächlich ist Yuri's Night ein internationales Ereignis", so Schlutz, „es ist der Tag der Raumfahrt."

195 Veranstaltungen in 64 Ländern finden um den 12. April herum statt, der auch durch den Start des ersten Space Shuttles der amerikanischen Raumfahrtbehörde Nasa 1981 zu einem besonderen Tag der Raumfahrt wurde. An diesem Tag faszinierte die Raumfahrt auch das Stuttgarter Publikum: „Ich bin beeindruckt von dem Andrang", so Schlutz. „In den letzten Jahren hatten wir rund 300 Besucher, heute sind es weitaus mehr."

Zu den Besonderheiten der Ausstellung im Foyer des Planetariums gehörte ein Modell im Maßstab 1:20 der Ariane 5, der Trägerrakete der europäischen Weltraumbehörde Esa. Sie wurden mit weiteren Modellen eigens aus Darmstadt nach Stuttgart gebracht. Eine anschauliche Erklärung von Schwerelosigkeit bot ein Mini-Fallturm: Eine kleine Plattform wird aus einer Halterung ausgeklinkt und fällt zu Boden. Eine kleine Kamera zeichnet ein darauf stehendes Wasserglas auf. Läuft das Video in Zeitlupe ab, so kann man während des Falls im Wasserglas die Entstehung einer Wasserblase beobachten – der Hinweis auf einen kurzen Moment der Schwerelosigkeit.

Mit dem Phänomen der Schwerelosigkeit befasst sich derzeit eine Gruppe von Luft- und Raumfahrtstudenten der Universität Stuttgart: Sie nehmen an einem deutsch-schwedischen Programm des Deutschen Instituts für Luft- und Raumfahrt teil – und stellten ihre Arbeit in Stuttgart vor. Im März 2011 werden sie dabei sein, wenn in Nordschweden eine Höhenforschungsrakete mit selbst geplanten und gebauten Messungsmodulen zu einem Parabelflug startet. „Wir möchten die Dicke von einem Hitzeschild messen", erklärt Christian Blank, Student der Luft- und Raumfahrttechnik. „Das Tolle dabei ist: Wir können bei dem Projekt von Anfang bis Ende dabei sein."

Auf sein Wissen und das seiner Kommilitonen, darunter auch schwedische Studenten, bauten die Kinder eifrig, die für das Quiz an diesem Tag Antworten auf viele Fragen suchten. Leider hatten nicht alle Raumfahrtfans in Stuttgart die Gelegenheit, ihre eigene Rakete – so wie Sarah – starten zu lassen. Denn die Zahl der Bausätze reichte nicht für den Ansturm aus.

Fasziniert betrachtet Luca Kovacevic bei der Ausstellung zu Ehren Juri Gagarins im Planetarium ein Modell der Raumfähre Discovery
Foto: Franziska Kraufmann

Newspaper Articel 2 about Yuri's Night in Stuttgart:

Kinder fliegen für einen Nachmittag ins All

Juri's Night Im Planetarium haben Raumfahrer in spe über die Grenzen des Weltalls nachgedacht. *Von Michael Schoberth*

Der 12. April ist ein wichtiger Tag für die Raumfahrt. Denn an diesem Tag flog im Jahr 1961 der sowjetische Kosmonaut Juri Gagarin als erster Mensch ins All, und genau 20 Jahre später startete das erste US-amerikanische Space Shuttle. Daher solle die Juri's Night auch ein Tag der Verständigung zwischen den beiden Supermächten sein – so sagte Jürgen Schlutz, der Koordinator für den Aktionstag in Stuttgart, gestern im Planetarium. In 64 Ländern findet in diesen Wochen ein Tag der Raumfahrt statt, in Stuttgart bereits zum vierten Mal. Juri's Night will mit Experimenten und Vorträgen alle Facetten der Raumfahrt zeigen.

Schlutz erklärt sich die Faszination des Universums so: „Der Weltraum ist die letzte Grenze des Menschen." Begeistert hatte sich auch der zwölfjährige Dennis die Ausstellung und die verschiedenen Modelle der Raketentypen angesehen. „Das All ist noch nicht erkundet, das ist interessant", sagte er. Aber Astronaut will er auf keinen Fall werden, eher Bankdirektor. Dann könne er vielleicht genug Geld verdienen, um später als Weltraumtourist zum Mond oder zum Mars zu fliegen: „Und Steine von dort mitbringen." Die ebenfalls zwölfjährige Simone hat zwar in der Schule die Planeten durchgenommen, aber ansonsten wenig Interesse an der technischen Seite der Raumfahrt. Sie blickt eher philosophisch auf das All: „Die Erde ist im Universum, aber man weiß ja nicht, wo das Universum eigentlich ist. Darum wissen wir nicht, wo wir eigentlich genau sind." Raketen und Satelliten könnten das Ende des Alls nicht erreichen.

Die Frage, wo das Weltall anfängt und aufhört, hat sich auch die siebenjährige Phila gestellt. Aber selbst ihr Vater konnte ihr keine befriedigende Antwort geben. Dafür bastelte er unter ihrer Anleitung eine 20 Zentimeter große Rakete aus Pappe, die später mit Hilfe eines Feuerwerkkörpers abgeschossen wurde. Sie selbst will jedoch nicht mit einer Rakete fliegen. „Da wird mir bestimmt schlecht", sagte Phila.

Außer den jungen Weltraumexperten stellten auch angehende Luft- und Raumfahrttechniker ihre Forschungsarbeiten vor. Bei dem deutsch-schwedischen Rexus-Projekt haben Studenten die Möglichkeit, ihre Experimente ins All zu bringen und die Daten dann auszuwerten. Das siebenköpfige Team der Universität Stuttgart will herausfinden, wie Weltraumtransporter im All betankt werden könnten.

Auch die Kleinsten haben schon großes Interesse an der Raumfahrt. Foto: Michael Steinert

Poster about REMOS for Outreach Events like Yuri's Night:

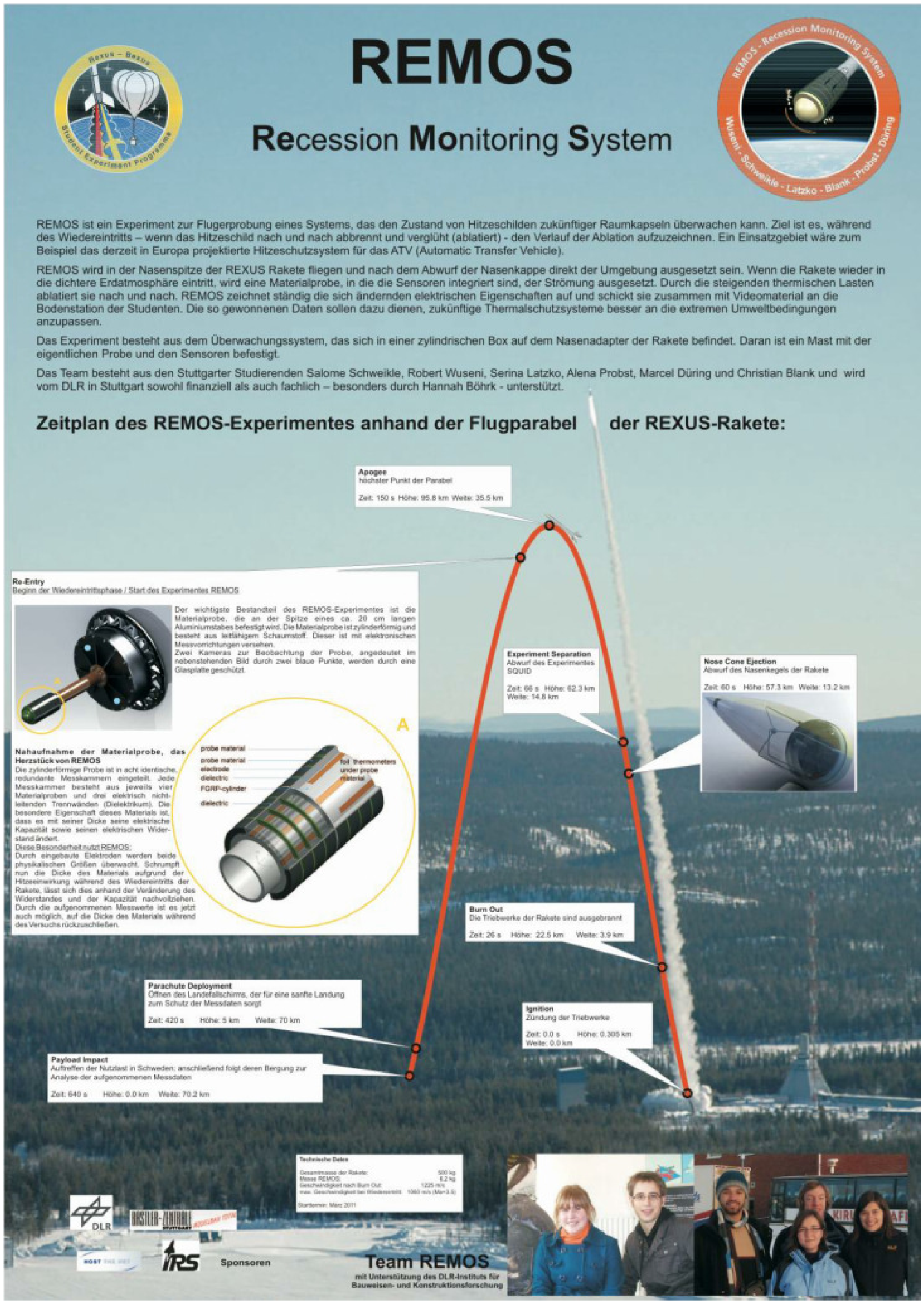

Kinder- & Jugendakademie Stuttgart (Academy for Children and Youngsters):

We organized an afternoon for school children at our university, on which they get to know the physics of rockets on the basis of physics they have already learned in school. They built small “rockets” out of film cans, magnesium tablets and water and learned how to calculate the altitude of the flight parabola. On this basis they could easily follow the physical concept of a sounding rocket.

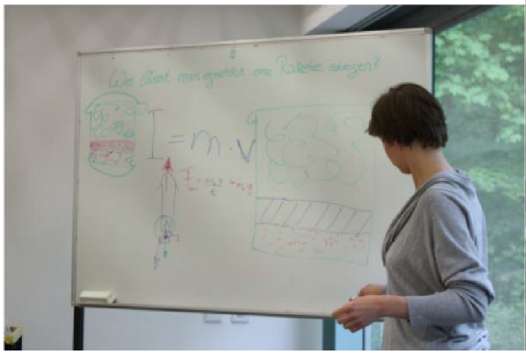
I=m·v


REMOS

Article in the EURAOAVIA News (Member Magazine of EUROAVIA):

REMOS on REXUS 9: A Student Experiment flying atop a Sounding Rocket to the Border of Space in northern Sweden

By Christian Blank, EA Stuttgart

c.blank@remos-stuttgart.de

On February 22 2011 at 13:50 local time the REMOS student experiment was launched on top of the REXUS 9 sounding rocket and reached an altitude of 80.6 km above the ESRANGE facility at the polar circle in northern Sweden. REMOS stands for REcession MOnitoring System and was built by a group of eight students of aerospace engineering from the University of Stuttgart within the framework of the REXUS/BEXUS program. The goal of the REMOS project was to develop a system enabling realtime measurements of the state of ablative heatshields for reentry vehicles by means of monitoring the material's electric properties. It was tested during the atmospheric reentry of the REXUS 9 rocket in order to prove the system's applicability to future ablative thermal protection systems.

REXUS 9 leaving the ESRANGE launch pad at Kiruna and shooting towards space.

The REMOS Logo: www.remos-stuttgart.de

How can students get a ride on a sounding rocket?

This possibility is given to students within the REXUS program once a year. REXUS stands for "Rocket Experiments for University Students" and provides students with the opportunity to carry out scientific and technological experiments on sounding rockets. Each year, two rockets are launched from ESRANGE Space Center in Kiruna, northern Sweden.

The REXUS/BEXUS program is realized under a bilateral Agency Agreement between the German Aerospace Center (DLR) and the Swedish National Space Board (SNSB). The

Swedish share of the payload has been made available to students from other European countries through a collaboration with the European Space Agency (ESA). Experts from ESA, SSC and DLR provide technical support to the student teams throughout the project.

For current projects and applications see www.rexusbexus.net

The origins of the REMOS Experiment

In October 2009, we handed in the first concept ideas for our experiment and were then invited to present them at a selection workshop at the DLR in Cologne: We wanted to design a system that is able to monitor the state of an ablative heatshield by measuring the material's electric properties. This is interesting because space vehicles require high-performance thermal protection systems (TPS) that provide high temperature insulation capability with low weight, high strength and reliable integration with the sub-structure. Damage or failure of TPS cannot be tolerated as its integrity before each launch and reentry is essential to the success of the mission. Consequently, knowledge of the heatshield recession and state is important for the design of new reusable launch vehicles in order to reduce life-cycle cost, to increase safety margins and to improve mission reliability.

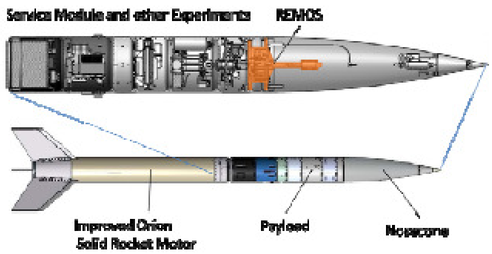

Sketch of the REXUS 9 rocket and its Payload.

The REXUS 9 rocket

The REXUS 9 rocket is propelled by an Improved Orion solid rocket motor originating from the Hawk anti aircraft missile with 290 kg of propellant. The total mass is 540 kg and its length 6 m with a diameter of 356 mm. It reaches an apogee of 80.63 km on its parabola with a ground range of 35 km. The nosecone of the spin stabilized rocket is ejected after leaving the atmosphere and a Yo-Yo system stops the rotation in order to generate good microgravity conditions for around three minutes. During the entire flight, a service module provides power and telecommunications to the experiments. After reentering the Earth's atmosphere, a parachute system is decelerating the payload before the impact after a total flight time of 15 minutes. The payload emits a radio signal and is recovered by a helicopter.

The REMOS team in front of the assembled rocket.

The REMOS Experiment Design

As a sounding rocket reenters the Earth's atmosphere with a much lower speed than an orbital spacecraft, the temperatures that are encountered during the "hot phase" are much smaller. This is why we did not use ceramic TPS materials but electrically conductive polyurethane foam. We calculated that during the down leg of the trajectory temperatures of up to 260°C will occur behind the detached sonic shocks around the probe boom.

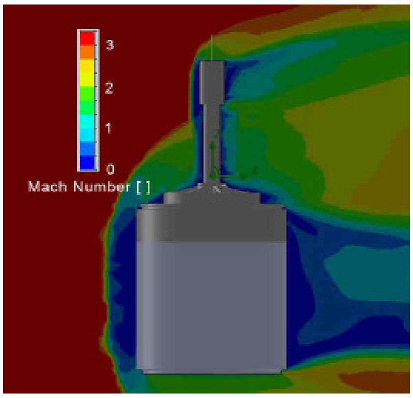

Map of the flow Mach number around the experiment (flow from the left) at an altitude of 20 km.

We knew that the experiment module is tumbling in a flat spin motion during this phase of the flight and the flow is basically coming from the side. So we decided to design a probe boom that reaches out of the wake of the experiment module and is rotation symmetric. It hosts eight segments of ablative foam: each of them consists of four foam stripes. The stripes of each segment are insulated against each other with a Kapton dielectric and interconnected in pairs to enable capacitance and resistance measurement between them. The segments are distributed equally around the boom and allow for recording spatial information. This means we can monitor, where and how the state of the material changes.

As it is essential for the interpretation of these measured values to know the temperature during flight, each segment hosts a thin film thermometer below its surface. An additional thermocouple was placed at the tip of the probe to measure the gas temperature.

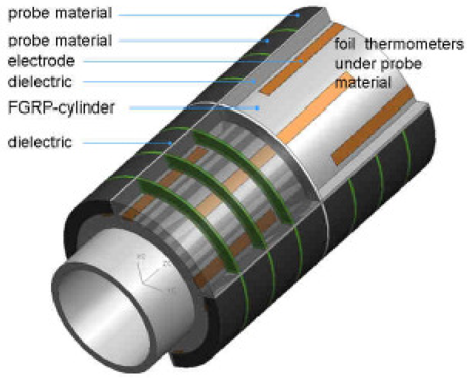

Design of the probe at the tip of the boom with two segments cut away.

PDR at ESRANGE

After being selected our team of seven graduate and undergraduate students started more detailed calculations and did preliminary design studies that were reviewed by a board of experts at the Preliminary Design Review (PDR) at ESRANGE near Kiruna – the place where the rocket would eventually be launched one year later – in February 2010.

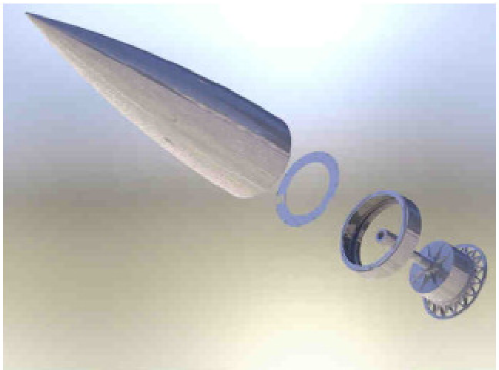

The REMOS experiment under the nosecone of the REXUS 9 rocket.

During this training week we got a lot of information on the rocket, the interfaces with the rocket's service systems and the conditions occurring during the flight. Additionally we got to know the people launching the rocket, building the other experiments and the places where the final assembly would take place.

Aurora in the sky above ESRANGE.

For sure we had a lot of fun getting to know the other teams and the extraordinary surroundings: visiting the numerous launch pads and radar stations, cross country skiing, visiting the ice hotel and watching auroras during the icy nights was a great reward and motivation for the work to come in the following months.

Detailed Design and Experiment Assembly

After the PDR we started the detailed design: One analogue and two digital cameras observe the probe during reentry to correlate video data with the calculated thickness values. They are protected from the hot gas by a baffle that also serves as mount for the analogue camera.

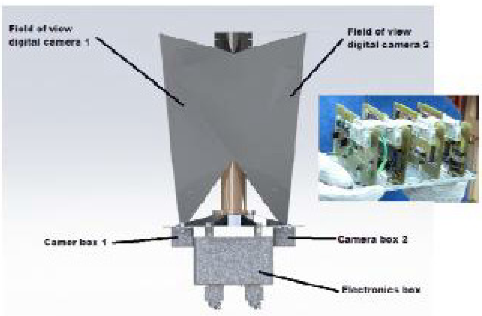

Fields of view of the digital cameras and the position of the electronics box protected under the metal cover.

The evaluation of data takes place on four custom-built PCBs, each one dedicated to a specific task. These are power conditioning and distribution, onboard data handling, capacitance measurement and resistance- and temperature measurement. Unlike resistance and temperature, the capacitances can only be measured indirectly by using them to form triggerable single-pulse oscillators whose wavelength can be evaluated with a high-speed counter. The total of 25 sensor channels and five housekeeping channels are evaluated at a rate of 10Hz.

Robert holding the assembled electronics with the four custom built PCBs in his hands.

In June 2010 we passed the Critical Design Review (CDR) at Oberpfaffenhofen and started building the experiment: With the support of the DLR and the sponsors that we had acquired we bought PCBs, silver glue, cameras, electronic boxes but also ground support equipment to test and ship the experiment. The ground control software was written and we stressed our experiment: shaker tests, thermal vacuum tests and EMV tests were conducted to make sure that everything is working properly not only under space conditions but also when standing on the launch pad at -40°C or during ascent at accelerations of up to 18 G.

Marcel and Uwe integrating the experiment.

As an additional incentive for meeting the project deadlines, Olle Person, the SSC REXUS project manager had promised a flight in his Piper Super Cup plane to the team that delivers a flight ready experiment first - we were doing night shifts in order to be that team!

Launch Campaign in Kiruna

The REMOS tag in powder snow on "Radar Hill" at ESRANGE.

After the REMOS experiment had been tested it was shipped to northern Sweden in a container. When the REMOS team arrived, we needed to become acclimatized first: -30°C during the day and -40°C during the nights was quite cool. A side effect of these temperatures is extremely humid air provoking static electricity discharges on almost anything you touch. This is why we had to be extremely careful when handling the experiment and the electronics. Getting a spare electronics component to this remote place is quite difficult!

Removing the protective cover from the probe.

During the first days we assembled the experiment modules and connected everything to the service module. In parallel the solid rocket motor, the nosecone ejection and the parachute system were integrated. In "bench tests" we simulated the flight and made sure that there is no interference between the experiments.

The REMOS Team around the integrated payload.

Finally, there was a test countdown: Serina, Marcel and Christian were sitting in the science center monitoring the parameters while running through all the procedures of the real launch.

February 22 was the day we had worked for more than a year then: With the launch scheduled for 10:00 local time we got up really early, went through the weather and security briefings and set up all our ground support equipment. One hour prior to the launch, the evacuation of the area started. Because of a problem with the mechanics of the launcher system, we had a hold of two hours. Everybody in the control room was excited and nervous. A gearbox of the launcher system responsible for adjusting the launcher elevation was blocked because of the cold. Another attempt was started and finally the experiment payload module was turned on. This was the moment when we could see, if REMOS was still “alive”: housekeeping data was transmitted and we went through our checklists to be sure it was ready for flight. These checks help to let you sleep during the nights because when designed properly they give certainty that everything is in “nominal” condition. From that point on, the only thing you can do is hope that everything will work as expected.

The Flight of REXUS 9

During the final minutes of the hot countdown, all the area had to keep radio silence when the rocket motor is finally armed and the sirens warned even the reindeer in the impact area of the upcoming launch. After the last seconds of the countdown we could see the overwhelming flash followed by the sound of the rocket shooting towards space at an incredible speed.

Everything was happening exactly as during the simulations we had run a dozen times before, but the camera image was showing space instead of a workbench!

At an altitude of approximately 52 km our cameras were activated and recorded the nosecone separation at an altitude of 62 km.

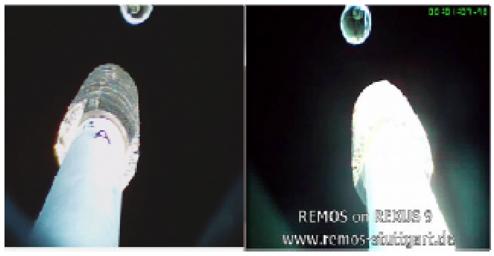

Images of cameras A (left) and B (right) right after the nosecone was jettisoned.

From this point on the probe was exposed to the flow. The three measurement channels were activated shortly after reaching the apogee of 80.63 km and REMOS shut down after 400 s before the final descent on a parachute.

Camera B looking at the probe towards the sun at an altitude of 70 km above the Earth with its tiny atmosphere on the left.

A critical phase for our experiment was the impact, because the tip of our experiment would hit the ground first. Luckily, it hit an area with a lot of snow and when the helicopter brought the payload back, there was no damage except for some snow inside the module. So we could extract the SD cards containing the video data and start analyzing the capacitance, resistance and temperature data.

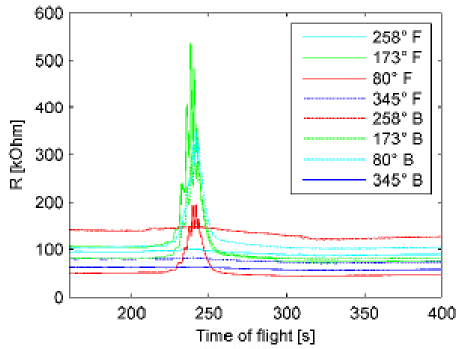

The resistance values of the probe segments exposed to the flow raised considerably during the reentry phase.

After the successful launch of the second rocket on the next day, all teams prepared their performances for the campaign party and after being sober again we has our plane ride over Kiruna before flying back to Germany.

Conclusion

At the ESA PAC Symposium in Hyères we met a lot of friends again and received our REXUS diplomas.

But work was not finished after the successful launch: evaluating the data and writing a paper for an ESA conference in southern France kept us pretty busy until summer 2011.

The REMOS experiment for monitoring the electrical properties of an electrically conductive material operated flawlessly during the REXUS 9 flight. It turned out to be a reliable and space-proven system that can be integrated and operated at low cost and weight. Complete and consistent data sets illustrating the changes in electric material properties as well as housekeeping data were recorded in the ground software. The temperature, resistance and capacitance values of the probe sections have the potential to reveal the realtime state of the material. The system is thereby ready to be flown on rockets with higher apogees and other probe materials.

Find more information about REMOS and see the videos at www.remos-stuttgart.de

Finally, I want to strongly encourage all EUROAVIA members to have a look at www.rexusbuxus.net and to form teams for the next turn (apply by October 2011). This is once in a lifetime opportunity to be part of a space project from the design to the launch and a great experience - even Bachelor and undergraduate students can participate!

Paper and Presentation at the ESA PAC Symposium in Hyères 2011

REMOS - RECESSION MONITORING SYSTEM: EXPERIMENT CONCEPT AND RESULTS OF THE FLIGHT ON REXUS 9

Christian Blank[1], Hannah Boehrk[2], Marcel Duering[1], Serina Latzko[1], Uwe Sauter[1], Salome Schweikle[1], and Robert Wuseni[1]

[1]*REMOS, info@remos-stuttgart.de*
[2]*DLR Institute of Structures- and Design Suttgart, Germany, hannah.boehrk@dlr.de*

ABSTRACT

REMOS stands for REcession MOnitoring System and is a student experiment launched on the REXUS 9 rocket in February 2011 from Kiruna. The goal of the REMOS project is to develop a system enabling in-situ measurements of the thickness of ablative heatshields of reentry vehicles by means of monitoring the material's electric properties. The system is tested during atmospheric reentry of the REXUS rocket in order to prove its applicability to future ablative thermal protection systems based on conductive materials. REMOS electronics are sensing resistance, capacitance and temperature in the probe sections. When probe material is ablated due to high thermal loads, the electrical properties of the probe sections change, thus providing temporal and spatial information on material thickness. Video data of three cameras is used for validation of the sensor data being stored and transmitted directly to the ground station. The data gathered by the service system's inertial measurement unit and GPS-receiver was evaluated to compute the inflow vector. In the present paper, the architecture and implementation of the REMOS flight experiment will be presented. The results from pre-flight tests, the launch campaign and post-flight analysis will be compared.

Key words: REMOS, DLR, REXUS, REXUS 9, TPS.

1. INTRODUCTION

Space vehicles require high-performance thermal protection systems (TPS) that provide high temperature insulation capability with low weight, high strength and reliable integration with the supporting structure. Damage or failure of TPS cannot be tolerated as its integrity before each launch and reentry is essential to the success of the mission. Consequently, knowledge of the heatshield recession is important for the design of new reentry vehicles in order to reduce life-cycle costs, to increase safety margins and to improve mission reliability. The goal of the REMOS project is to develop a system enabling real-time measurements of the thickness of ablative heatshields of reentry vehicles by means of monitoring the material's electric properties. It shall be tested during atmospheric reentry of the REXUS rocket in order to prove the system's applicability to future ablative TPS. The primary (p) and secondary (s) objectives of this experiment are:

- Measure electrical material characteristics. (p)
- Use video data for experiment verification. (p)
- Investigate the transferability to larger scales. (s)
- Gather video data for public relations usage. (s)

The REXUS rocket is a single-stage, spin-stabilised sounding rocket with a nominal diameter of 356 mm. It is capable of transporting a payload of 80 kg to an altitude of 90 km on a parabolic trajectory.An exploded view of the nose section can be seen in Figure 1.

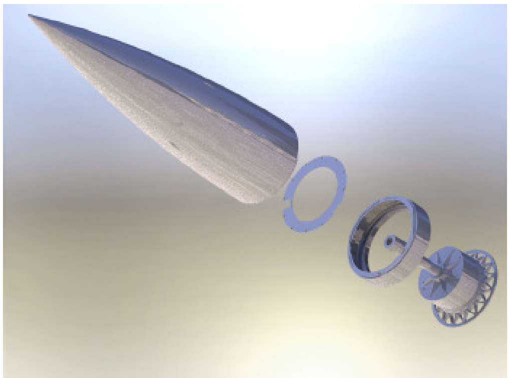

Figure 1. REXUS Nosecone section

At the beginning of this document the flown trajectory and a method for the extraction of the direction of flow as well as the predicted in-flight temperatures will be described. Following, the basic idea of the measurement principle and the entire structural and electronial design of the experiment are introduced. Finally, the measured and evaluated data is discussed and conclusions are derived.

2. MISSION

The experiment was on standby, protected by the nosecone during launch and activated 60 s after lift-off at an altitude of approximately 52 km. The cameras recorded the nosecone separation at an altitude of 62 km at t = 74 s. From this point the probe was exposed to the flow. The three measurement channels were activated shortly after reaching the apogee of 80.63 km of altitude at t = 138 s. The experiment shut down after 400 s before final descent on a parachute. The hot phase along with the maximum deceleration occurs during descent between 220 and 250 s after lift-off, as depicted in Figure 2.

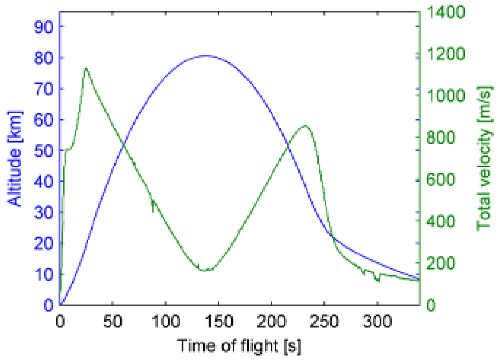

Figure 2. Altitude and total velocity over time

2.1. Determination of Inflow Direction

Among other data the REXUS Service Module provides GPS position information and data from the Inertial Measurement Unit (IMU). REMOS relies upon IMU data for the determination of the inflow vector; altitude and velocity are determined using GPS data.

Coordinate System and Conventions

The REXUS 9 reference frame is based on a cartesian coordinate system whose X-axis defines the roll-axis of the rocket. It's Y-axis specifies the 0°-line of the perimeter while the Z-axis completes the coordinate system to be right-handed, as displayed in Figure 3.

The inflow direction is described by two angles: the in-plane angle α, which indicates the direction within the Y-Z-plane and the out-of-plane angle β. β shows the deviation from the plane and is positive when inclined towards the X-axis.

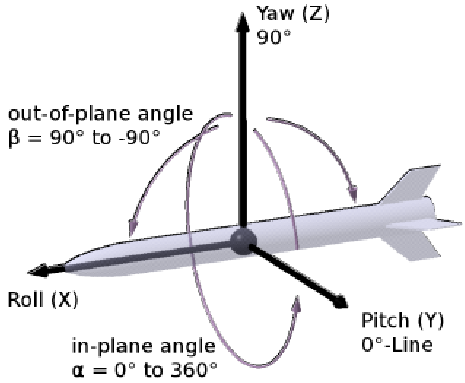

Figure 3. Body frame coordinate system

Calculation of angles α and β is done as follows:

$$\alpha = \begin{cases} \operatorname{atan2}(a_z, a_y) & : \ a_z >= 0 \\ 360° + \operatorname{atan2}(a_z, a_y) & : \ a_z < 0 \end{cases} \quad (1)$$

$$\beta = \operatorname{atan2}\left(a_x, \sqrt{a_y^2 + a_z^2}\right) \quad (2)$$

where a_x, a_y and a_z are the accelerations measured in m/s^2.

2.2. Aerothermodynamics

On the tip of the REXUS 9 rocket the REMOS experiment is directly exposed to the flow. During the supersonic phase of the launch it is protected by the nosecone. After nosecone separation the thermal environment is cooling down to -100°C, but gas density is below $6 \cdot 10^{-5}$ kg/m^3 (p = 4 Pa) above 70 km resulting in negligible heat transfer due to convection. Heat is predominantly exchanged via thermal radiation. Coming from the apogee of 80.63 km, the total velocity increases to up to 854 m/s (Ma = 2.7; t = 232 s) during the hot phase in an altitude of 20 km. The calculated curves turn out to be a good guess for the actually measured temperature profile. For the originally assumed apogee of 100 km, higher velocities and resulting thermal loads would have been encountered (see Figure 5). The entire hot phase of the reentry is characterised by supersonic flow conditions: A detached shock forms in front of the experiment module. Assuming a flow from the side, the shock distance is a function of the probe radius. The fluid is decelerated to subsonic speed and the gas temperature increases. A map of the Mach number distribution is given in Figure 4. It is the result of a numerical simulation of the reentry flow around the experiment module. For orientation Figure 5 also contains the calculated gas temperatures T_{AS} after a normal adiabatic shock calculated from the flight data. Calculations for the probe temperature were done

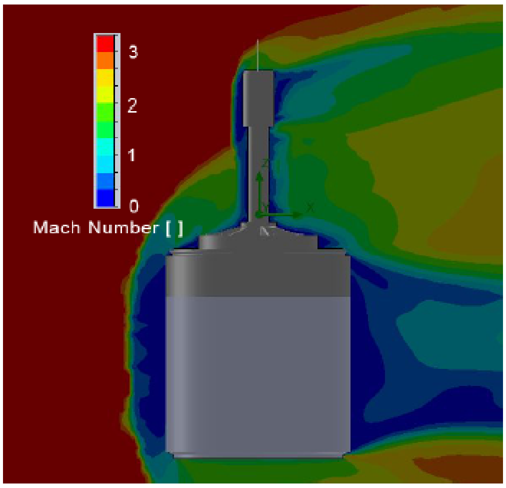

Figure 4. Map of the Mach number around the experiment module at an altitude of 20 km

based on a semi-empirical heat flux model of Equation 3 by Tauber [3]

$$\dot{Q} = C * \rho^N * v^M \tag{3}$$

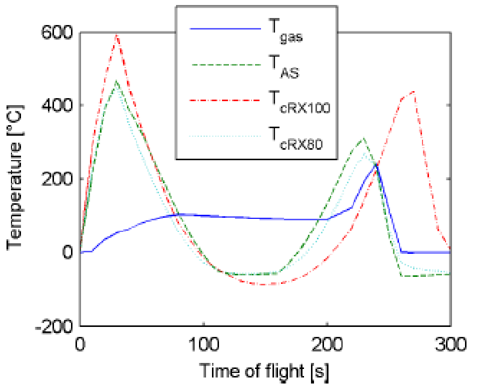

Figure 5. Calculated gas and probe surface temperatures as a function of the time of flight compared to the data recorded during real flight

with the heat flux $\dot{Q}$, the density ρ, the velocity v and the empirical constants C, N and M. Assuming a radiative heat exchange to thermal equilibrium this results in a first guess for the expected probe surface temperatures. Figure 5 shows that this temperature peaks at $T_{cRX80} = 267°C$ and $\dot{Q} = 3.6\,\mathrm{kW/m^2}$ for the $80.63\,\mathrm{km}$ apogee. For the originally assumed apogee at $100\,\mathrm{km}$, a value of $T_{cRX100} = 439°C$ and $\dot{Q} = 11.5\,\mathrm{kW/m^2}$ was calculated.

3. RECESSION MEASUREMENT

The goal of this experiment is to demonstrate the feasibility of an in-situ measurement system for ablative heatshield thickness. To reduce the amount of required modifications of existing designs, it was chosen to monitor electric properties of the heatshield material. This would reduce the required changes to the conditioning of its ohmic resistance, which can be achieved by changing the amount of uncombined carbon and/or other additives. This modification still allows for any shape, dimension and thicknesses of the heatshield tiles.
In the next section the theoretical background for such a heatshield material monitoring system is described. Since the REXUS flight is only suborbital and only reaches a fraction of the thermal loads of an orbital reentry, an appropriate material for the demonstrator has to be chosen, which is described after the introduction to the theory. Finally, the design process of the flight hardware is described briefly. This process was driven by requirements derived from the previously defined objectives and [1]. These requirements are grouped into four types. Altogether this resulted in

- 13 functional requirements
- 11 performance requirements
- 24 design requirements
- 10 operational requirements.

These requirements were used for verification in all phases of the systems engineering process.

3.1. Measurement Principle and Probe Setup

The conductive foam probe material is attached to a substrate of fibre glass reinforced plastics (GFRP) on top of the aluminium boom. Four foam slabs form a single probe section. These slabs are interconnected by conduits, as shown in Figure 6. Between each of these foam slabs there are thin ligaments of Kapton foil preventing electric contact and serving as dielectric material depicted in green in Figure 7. One Pt100 thermometer is glued beneath each probe segment in order to measure the temperature of the foam elements. For ensuring contact between the foam and the measurement wires, the contacts are glued to the foam with conductive adhesive.
To monitor the change in capacitance and resistance of the probe two stripes of one foam square are connected on both ends. The two other stripes are responsible for the capacitance measurement. The two capacitors are connected in parallel to increase the capacitance. For the capacitance measurement eight wires are used while there are 16 wires for resistance and temperature measurements.
Every type of measurement is realised via a separately shielded harness so that the data logging isn't swayed.

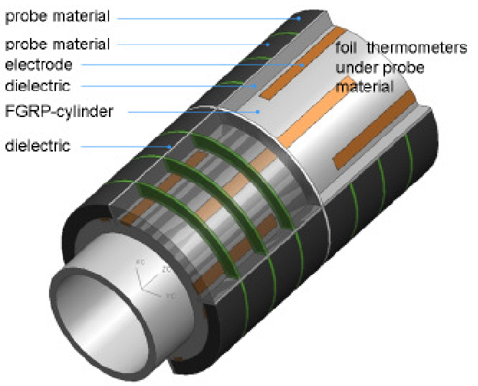

Figure 6. Probe assembly

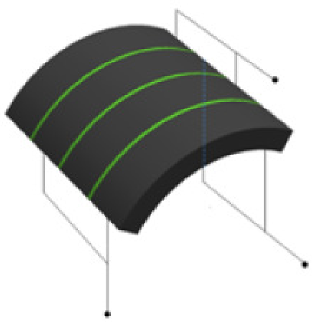

Figure 7. Measurement principle

Each of the eight probe segments include the same connection structure. Three SUB-D 9 pole plugs were used for connecting the probe: one for the capacitance, one for the resistance, and one for the temperature measurement. Considering the predicted temperature profile (see Figure 5), an electrically conductive polyurethane foam was selected. The disintegration temperature for this material is below the expected peak temperature of 260°C.

3.2. Mechanical Structure

The front section of REXUS 9 consists of the nosecone adapter and the nosecone itself. The usable space in this section of the REXUS rocket is limited by the following constrains:

- Due to required space for possible mounting of balancing masses, the maximum diameter is limited to 250 mm.
- The maximum usable height is limited to 500 mm by the separation mechanism in the ejectable nosecone.

An exploded view of all major parts can be seen in Figure 1. In addition to the geometric restrictions the experiment has to be designed to the requirements posed by the flightload envelope of the REXUS rocket. The foreseen procedure of verification in [1] is a random vibration test with the experiment operating as it will be during the actual launch. It is recommended to perform the test in all axes at the levels given in Table 1.

Table 1. Random Vibration Spectrum [1]

Axes	Frequency	Level	PSD
Longitudinal	20-2000	6.0	0.018
Lateral	20-2000	6.0	0.018
	Hz	g_{RMS}	g^2/Hz

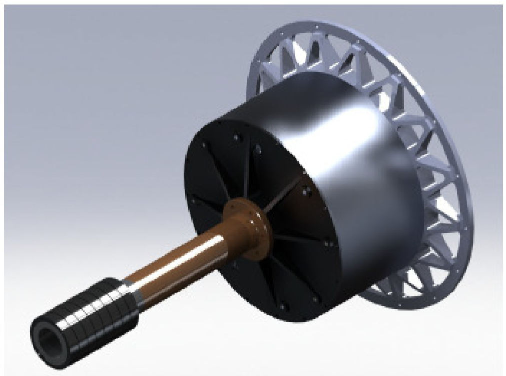

Figure 8. REMOS Experiment

As a result of the refinement of the systems engineering process the design shown in Figure 8 was developed. It shows the four major structural components of the experiment, which are described below in detail:

- The launch adapter bridges the gap between the REXUS interface and the inner cylinder. For reduction of mass it is designed as a truss structure.
- The inner cylinder serves as a spacer between the launch adaper and the cylinder cover. It's height is determined by the required space for the electronics boxes.
- The cylinder cover is the central structural part of the entire experiment. It provides interfaces for all required systems on the inward side and the mechanical interface to the sensor boom.
- The sensor boom is the supporting structure of the sensing elements, which are mounted onto a GFRP-pipe at the tip. It is mounted concentrical to the roll-axis of the rocket onto the cylinder cover. The length of the boom was limited by manufacturing capabilities. Although, it still is long enough, to provide

undisturbed flow conditions at the sensing elements (see Figure 4).

All supporting subsystems are mounted to the inward side of the cylinder cover with thermal insulating materials. It accommodates the central electronics box and two digital camera systems, one at each side of the box. The central focus for the entire structural design was the reduction of mass. An overall safety factor of $j = 1.5$ was selected. Due to limitations in manufacturing, requirements of electrical shielding and handling, this factor was overachieved at several locations.

During the early design phases the margins of safety were calculated analytically. In later design phases these calculations were supplemented by calculations with the finite element method (FEM). The applied load cases can be seen in Table 2.

Table 2. Load caseses for FEM

Load Case	Load	Origin
0	-	Eigenvalue calculation
1	56 g axial / 42 g lateral	Launch acceleration and 3 times vibration loads
2	7 g axial / 7 g lateral / 200° reentry	
3	6 g random x	Launch vibration
4	6 g random y	Launch vibration
5	6 g random z	Launch vibration

Load case 0 is not an actual load case, since only the systems eigenfrequencies and eigenmodes are calculated. These intermediate results provide a good reference for the following shaker test. As calculated by the FEM, the first vertical eigenmode appeared at $f_{v1} = 766$ Hz, the first lateral mode at $f_{l1} = 226$ Hz. Load case 1 was derived from the static flight loads plus three times the maximum dynamic loads occurring during the flight. This quasi-static load case primarily served for calculation of bolt forces. The random load cases were set up according to [1]. To confirm flight-readiness, a final shaker test with random loads at acceptance level was performed. The calculated eigenfrequencies could be confirmed with $f_{v1} = 550$ Hz, which represents a deviation of -28% and $f_{l1} = 190$ Hz, which represents a deviation of -16% to the FEM results. These deviations can be explained by the damping of the shaker adapter and the entire harness with its thermal insulation in the sensor boom, which had to be modeled in the FE-model as a distributed mass without damping.

3.3. Experiment Electronics

To fulfil the experiment's goals in terms of gathering flight data, the required electronic functionality can be summarised as follows:

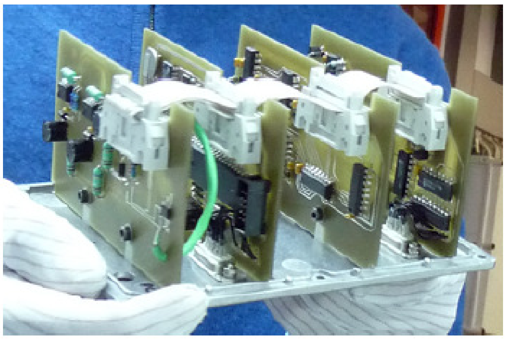

Figure 9. Electronics box

- Provide preconditioned power supply for the different systems of the experiment
- Sense resistances of the probe elements
- Sense capacitances of the probe elements
- Sense temperatures below the probe elements
- Sense temperature of the surrounding flow
- Store data onboard
- Transmit data via the service module to the ground station
- Record videos of the flight

The electronics are located in three aluminium enclosures to provide shielding from electromagnetic distortions. The smaller enclosures contain FlycamOne ECO cameras, which are used for imaging the probe during the flight. They provide sufficient time for recording onto microSD cards at VGA resolution, while weighing only 17 g. A third camera for direct TV downlink is installed in the nosecone adapter's cover.
The central electronics box accommodates four PCBs, each one dedicated to a specific task. These are power-conditioning and distribution (PCDU), onboard data handling (OBDH), capacitance measurement (C-SENSE) and resistance- and temperature measurement (RT-SENSE). Due to the special requirements, all PCBs were custom-built. The PCDU conditions the unregulated 28 V main-bus of the REXUS to an intermediate voltage by the use of a redundant configuration of two DC/DC-converters. For a better reduction of noise on the supply lines, the following continuous supply for the OBDH and the switchable supplies for the sensors and cameras are conditioned with linear regulators. The OBDH consists of an 8-bit Atmel RISC microcontroller (MCU) with a serial interface to a 16 Mbit FLASH storage, a real-time clock for synchronization, an RS422 interface to the REXUS service module and an interface to the sensing systems.

Table 3. Sensor characteristics of REMOS

Value	Type	Nr.	Range	Accuracy
		SENSORS		
T	Thermocouple	1	0 – 1024°C	±0.5°C
T	Pt100	8	-50 – 300°C	±0.2°C
R	Voltage divider	8	100 – 10^6 Ω	±2.9 %
C	x556 timer	8	0.5 – 500 pF	±0.05 pF
		HOUSEKEEPING		
T	KTY23-5	1	-50 – +150°C	±0.3°C
V	Voltage divider	4	0 – 46 V	±0.6 %

The capacitances of the probe elements are measured indirectly by using them to form triggerable single-pulse oscillators, whose wavelengths are used as a gating time for the OBDH's high-speed counter. The theoretical resolution of this system is 0.05 pF. The measurement of the resistances is done by simple voltage dividers, whose voltages are input to a 12bit ADC. The measurement of the temperatures is done by Pt100 sensors, which are supplied by constant current sources. The levels are amplified and fed to a second 12-bit ADC. A thermocouple in the tip of the sensor boom provides measurements of the temperature of the undisturbed flow. All measurements are done at a rate of 10 Hz. The entire system consumes less than 3.7 W of peak power (see Table 4).

The software, running on the MCU, is thread-oriented and was completely written in C. Depending on its operational mode, which is selected by hardwired timing signals from the RXSM, it takes care of the digitalisation of measurement data, their formatting for transmission and storage, as well as the processing of housekeeping data.

To confirm the functionality in the space environment a thermal-vacuum test was conducted. The entire experiment was placed in a vacuum chamber, where it was cooled down and heated up in the range of the qualification temperatures. Several simulations of an entire flight cycle were performed at different temperatures. Since a number of transmitters are operating next to the experiment in flight, it had to be confirmed, that these transmitters have no influence on the measurement system. This was accomplished by an electromagnetic interference test (EMI-test). As a result, small distortions of the signals were found in the frequency range of 150 MHz to 300 MHz. As these distortions stayed below 2% of the average measurement value and since the EMI-test was conducted at field strengths several magnitudes higher, than the expected values in flight, no distortions by the transmitters were expected.

Table 4. Power characteristics of REMOS

Mode	Running systems	Consumption
Standby	housekeeping	1.46 W
Camera	+ cameras	3.36 W
Record	+ sensors	3.64 W

Table 3 lists the measurement performance of REMOS. Constant deviations are given in the corresponding unit, quantity-dependant ones in %.

4. RESULTS

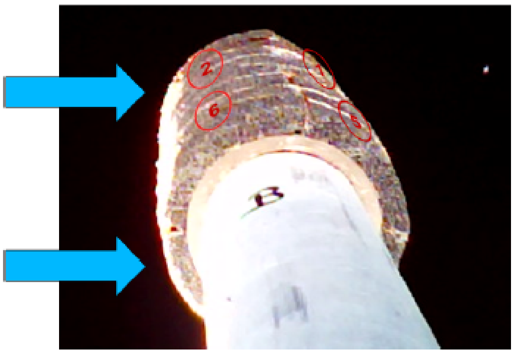

Figure 10. Image of the camera video looking at the boom with the probe

No major problems occurred during preparation of the flight. The experiment operated perfectly from power-up at t = −600 s to power-down at t = 600 s. The ground software operated as expected. Due to a switching problem only 7 s of analog video were transmitted to the control centre. Since the digital cameras recorded the preselected part of the flight, which could be secured after landing, the malfunction had no impact on the amount of usable video material. See Figure 10 for an example image from the video. Altogether, the experiment can be declared a success.

The following sections describe the in-flight performance of the system and present the measured temperature, resistance and capacitance results of the probe.

4.1. System Performance

The acquisition and transmission of all data worked as expected. The lost data packets during flight stayed below 5%, what was declared as an acceptable value for randomly distributed losses. The maximum amount of lost packets in series never exceeded 4 packages, what equals to 0.4 s. Although the outside temperature varied between -20°C at launch and +250°C at reentry, the electronics temperature only chilled down to +11°C and didn't exceed +14.5°C during flight. These values confirm, that a good thermal decoupling of the electronics box from the structure was achieved. All supply voltages stayed at their nominal values with less than 1% of variation during switching of loads.

4.2. Attitude and inflow vector

Figure 11 shows the altitude and the total acceleration during t= 150 s upto 300 s. The total acceleration during the down-leg reaches a_{total} = 0.2 g at t = 220 s in an altitude of 48 km. This value is a reasonable choice to begin the analysis of the inflow vector.

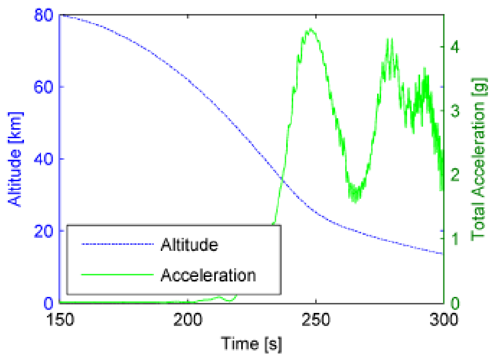

Figure 11. Altitude and total acceleration a_{total} at $t = 150s \ldots 300s$

After de-spin and nosecone seperation during ascent REXUS 9 begins an unstable tumbling movement. Athmospheric influence slows this tumbling down to a dynamically stable flat spin. The flat spin results in nutational movements which can be seen in a coupling of the in-plane and out-of-plane angle, depicted as shown in Figure 12. The oscillating inflow is reflected in the measurements of temperatures in individual probe sections.

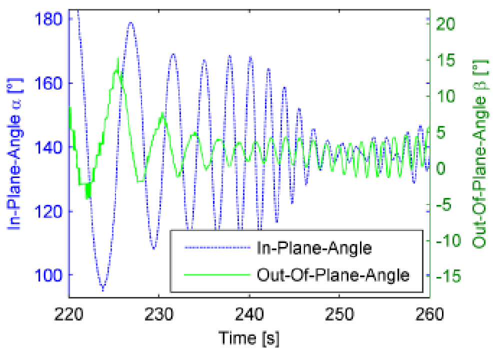

Figure 12. Coupling of α and β at $t = 220s \ldots 260s$

4.3. Flow Temperature

The ambient gas temperature T_{gas} was measured at the tip of the probe and during ascent it rose to 100°C due to the heat absorbed by the nosecone (Figure 5). After nosecone separation, the thermocouple is slightly cooling due to radiation but its thermal inertia is too big as to be able to measure the actual T_{gas} at altitudes above 60 km. During the hot phase, the value peaks at 241°C which is 35 K lower than the predicted surface probe temperature peak. Figure 4.3 shows the evolution of the

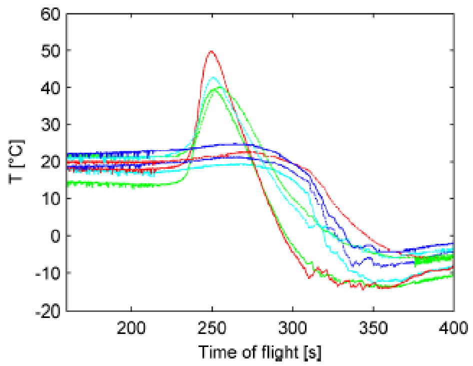

Figure 13. Temperatures measured under the 8 probe segments during reentry phase.

temperatures that were measured under each of the eight probe segments during the reentry phase. It is obvious that the probe segments in the direction of 80° and 173 ° are exposed to the highest heat flux. This is found for the segments in front as well as the ones in the back and confirming the observation that the flow is constantly coming from the 140° direction (see Figure 12). The segments on the opposite side are not even heated up entirely as gas density and consequently the heat flux is very low in the shadow of the probe. The peaks in probe segment temperatures are observed at t = 250 s; for T_{gas} this peak already occurs at t = 238 s. Looking at the amplitude of the peaks, one notes that the foam is a good thermal insulator and its thermal capacity is not negligible. Finding a suitable model for the average foam temperature based on these values remains an issue of investigation that is a prerequisite for eliminating the influence of the temperature on the resistance and capacitance measurements.

4.4. Capacitance and Resistance Data

The electrical properties, in particular the resistance and capacitance, for each channel are shown in Figure 14 and 15. The elements located in the direction of 80° and 173° (back and front) are effected by the flow, whereas the channels located on the downstream side are not affected.

The change is due to the increased temperature, which is predictable by Formula 4:

$$R = \rho(T)\frac{l}{A} \tag{4}$$

$\rho(T)$ is the density. The length l and the area A are geometric properties of each element. The fluctuating behaviour of the R channels correlates to the roll orientation and is not caused by signal noise. The measurement is highly sensitive to mechanical influences. Here it acts as an indicator for the stagnation point. E.g. it can be used for detecting cracks in the material.

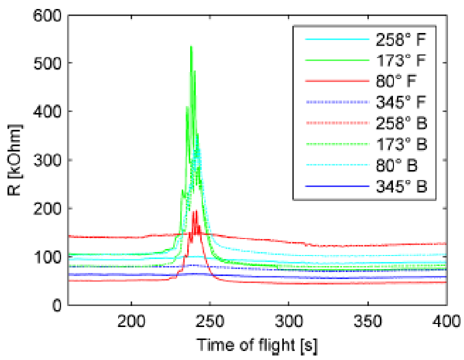

Figure 14. Measured data from resistance channels.

The magnitude of the change in capacitance differ from one channel to the other, since it also depends on the initial value. This is related to the manufacturing and the properties such as the thickness of the dielectric material and the size of the foam material vary for each channel.

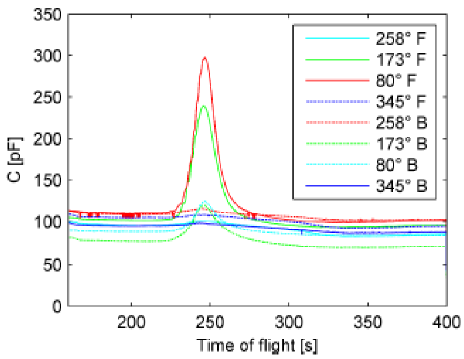

Figure 15. Measured data from capacitance channels

Looking at the values on the beginning of the measurement and at the final time, there is a shift, which is caused by modifications in the material. This was measured in previous tests on ground and verfied by the flight [4].

4.5. Conclusions & Outlook

The REMOS experiment for monitoring the electrical properties of an electrically conductive material operated flawlessly during the REXUS 9 flight. It turned out to be a reliable and space-proven system that can be integrated and operated at low cost and weight. Its design is modular and flexible: The probe can be exchanged and the measuring range allows for using it with other probe materials. The sampling rate of 10 Hz and the telemetry concept allow for realtime evaluation of the electric parameters. Complete and consistent data sets illustrating the changes in electric material properties as well as housekeeping data were recorded in the ground software. The temperature, resistance and capacitance values of the probe sections correlate well with the position data from the IMU. They have the potential to reveal the realtime state of the material. The system is thereby ready to be flown on rockets with higher apogees and other probe materials. A modular electronics system was developed and tested for a wide range of operation temperature, in vacuum conditions and under electromagnetic radiation. Its modules can be used for other applications, too.

ACKNOWLEDGEMENTS

We want to cordially thank the REXUS/BEXUS Program organizers and everyone involved. Furthermore, REMOS was supported by the DLR BK Stuttgart, ACME, Atmel, Bastler-Zentrale Stuttgart, Erich-Becker-Stiftung, Hostthenet, IEH, IRS, ITLR, Kucera, LBBW, Studentenwerk Stuttgart and Walter-Blohm-Stiftung.

REFERENCES

[1] EuroLaunch, 2009, REXUS User Manual v7.0

[2] RX09_11-02-10 REXUS-09 FRP

[3] M.E. Tauber et al.: Aerothermodynamics of Transatmospheric Vehicles. Journal of Aircraft, Vol. 24, September 1987

[4] Resistance and capacitance investigation of the probe material for REMOS DLR-IB 435-2010/32

APPENDIX C – ADDITIONAL TECHNICAL INFORMATION

C.1 Technical Drawings

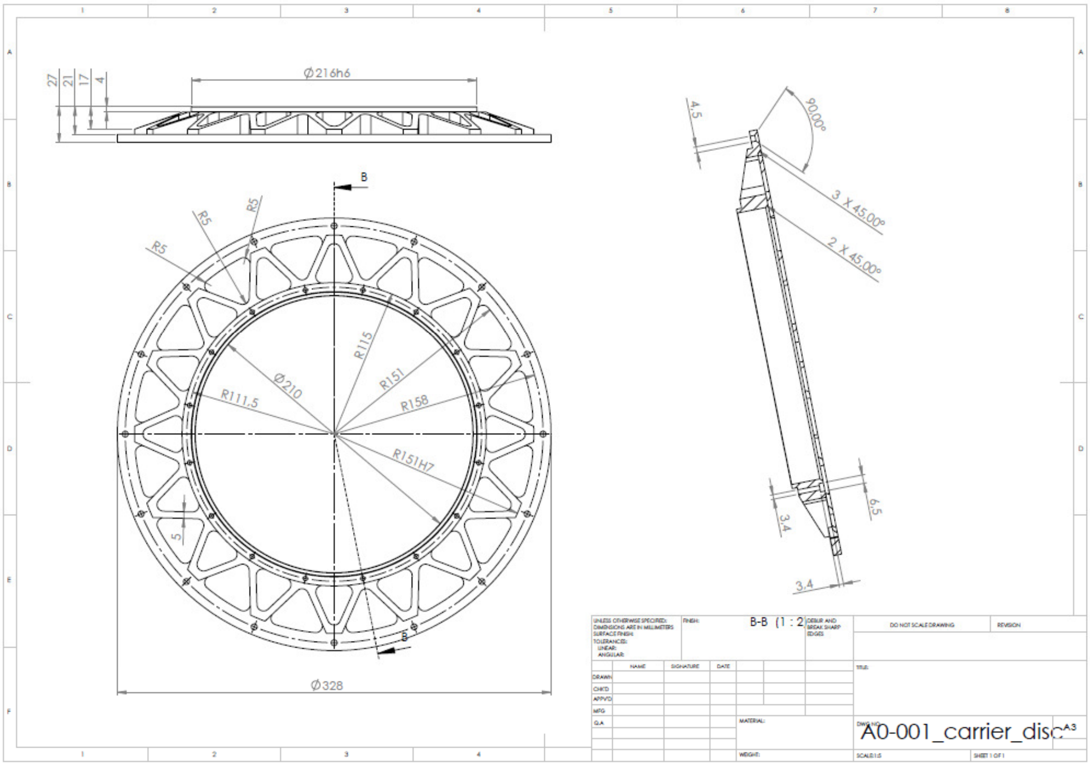

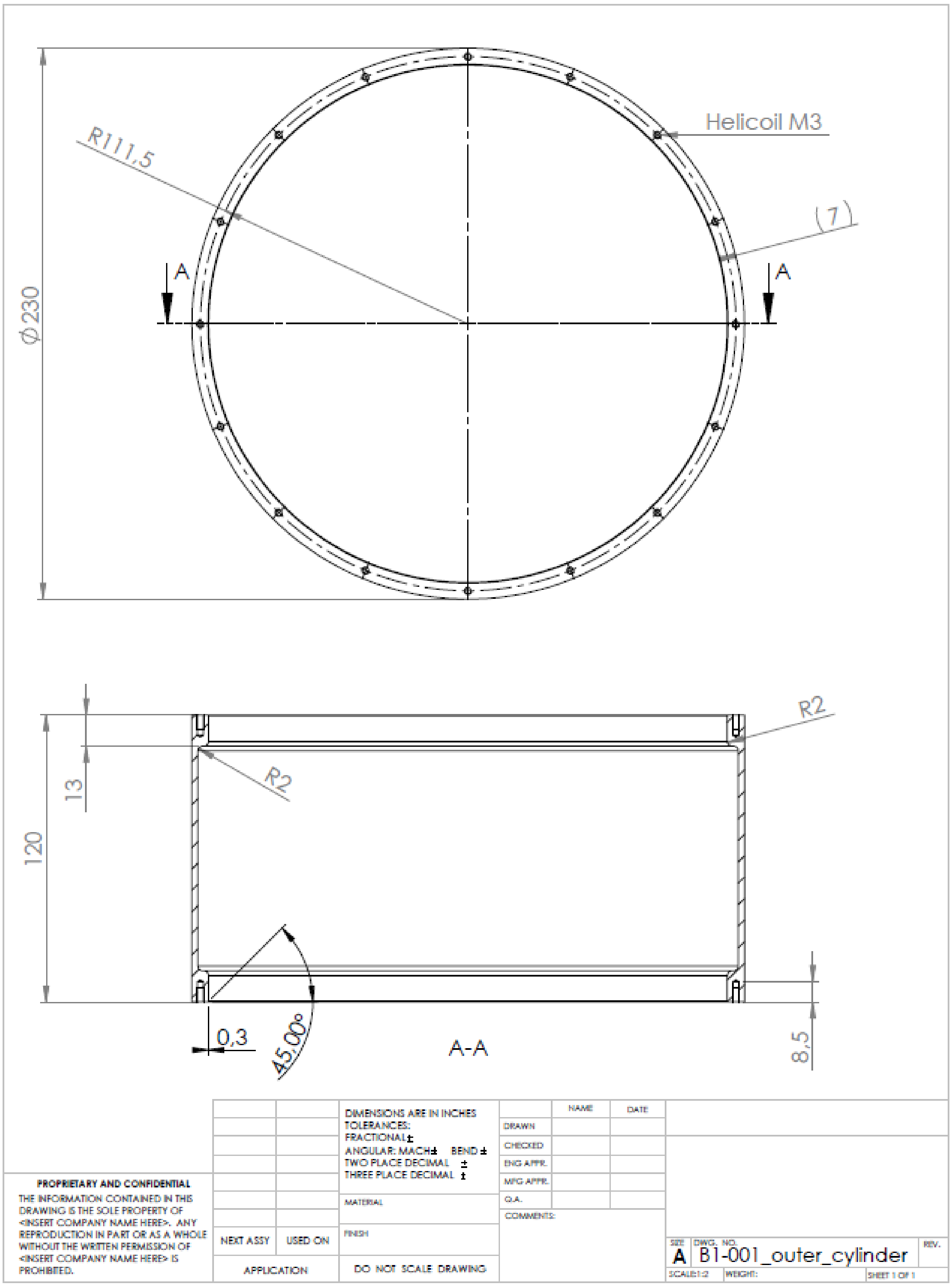
Helicoil M3
R111,5
(7)
A
A
Ø230
R2
R2
13
120
0,3
45,00°
A-A
8,5
DIMENSIONS ARE IN INCHES
TOLERANCES:
FRACTIONAL ±
ANGULAR: MACH ± BEND ±
TWO PLACE DECIMAL ±
THREE PLACE DECIMAL ±
NAME
DATE
DRAWN
CHECKED
ENG APPR.
MFG APPR.
Q.A.
COMMENTS:
MATERIAL
FINISH
NEXT ASSY
USED ON
APPLICATION
DO NOT SCALE DRAWING
PROPRIETARY AND CONFIDENTIAL
THE INFORMATION CONTAINED IN THIS DRAWING IS THE SOLE PROPERTY OF <INSERT COMPANY NAME HERE>. ANY REPRODUCTION IN PART OR AS A WHOLE WITHOUT THE WRITTEN PERMISSION OF <INSERT COMPANY NAME HERE> IS PROHIBITED.
SIZE
DWG. NO.
REV.
A
B1-001_outer_cylinder
SCALE:1:2
WEIGHT:
SHEET 1 OF 1

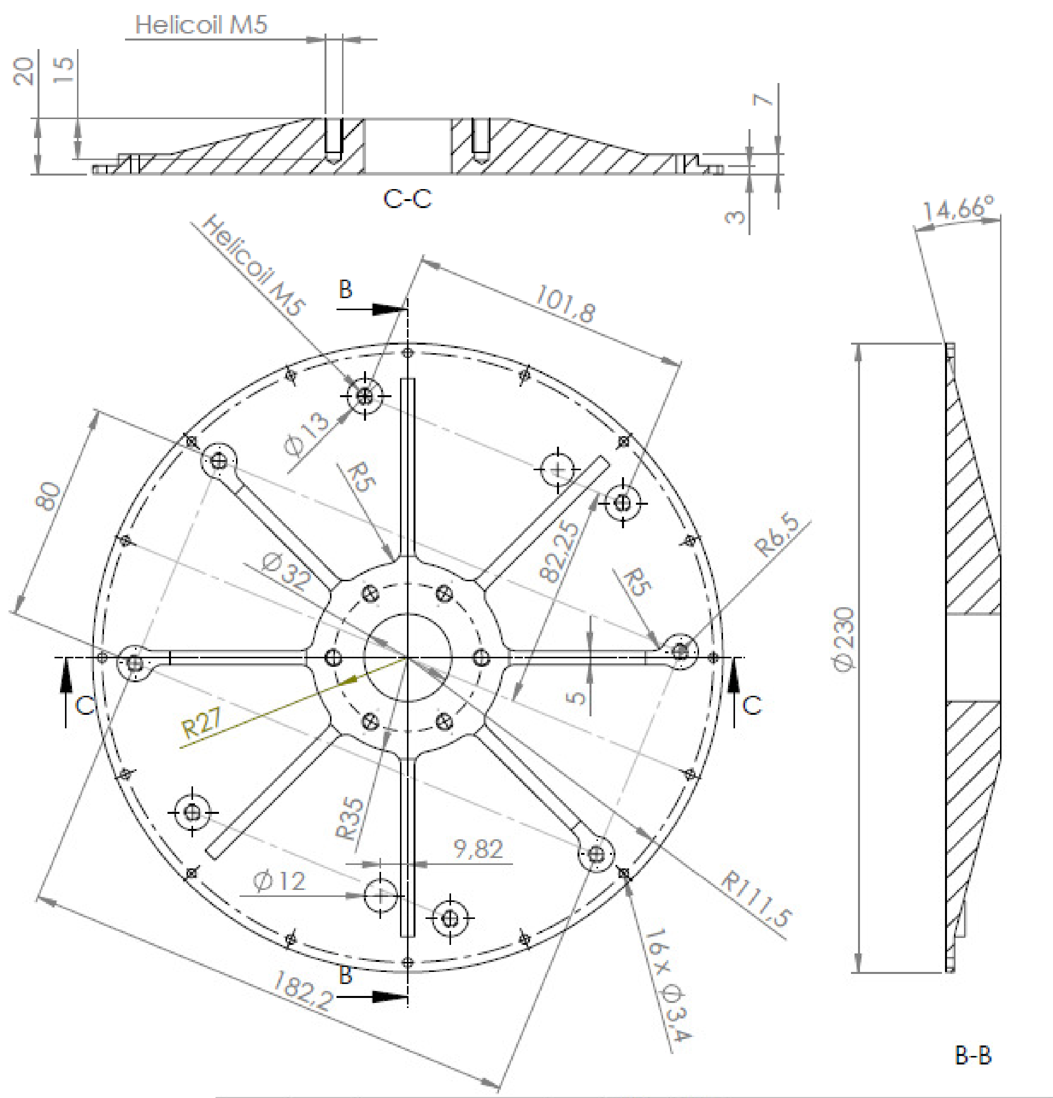

		DIMENSIONS ARE IN INCHES TOLERANCES: FRACTIONAL ± ANGULAR: MACH ± BEND ± TWO PLACE DECIMAL ± THREE PLACE DECIMAL ±		NAME	DATE
			DRAWN		
			CHECKED		
			ENG APPR.		
			MFG APPR.		
		MATERIAL	Q.A.		
		FINISH	COMMENTS:		
NEXT ASSY	USED ON				
APPLICATION		DO NOT SCALE DRAWING			

PROPRIETARY AND CONFIDENTIAL

THE INFORMATION CONTAINED IN THIS DRAWING IS THE SOLE PROPERTY OF <INSERT COMPANY NAME HERE>. ANY REPRODUCTION IN PART OR AS A WHOLE WITHOUT THE WRITTEN PERMISSION OF <INSERT COMPANY NAME HERE> IS PROHIBITED.

SIZE	DWG. NO.	REV.
A	B1-002_cylinder_cover	
SCALE:1:2	WEIGHT:	SHEET 1 OF 1

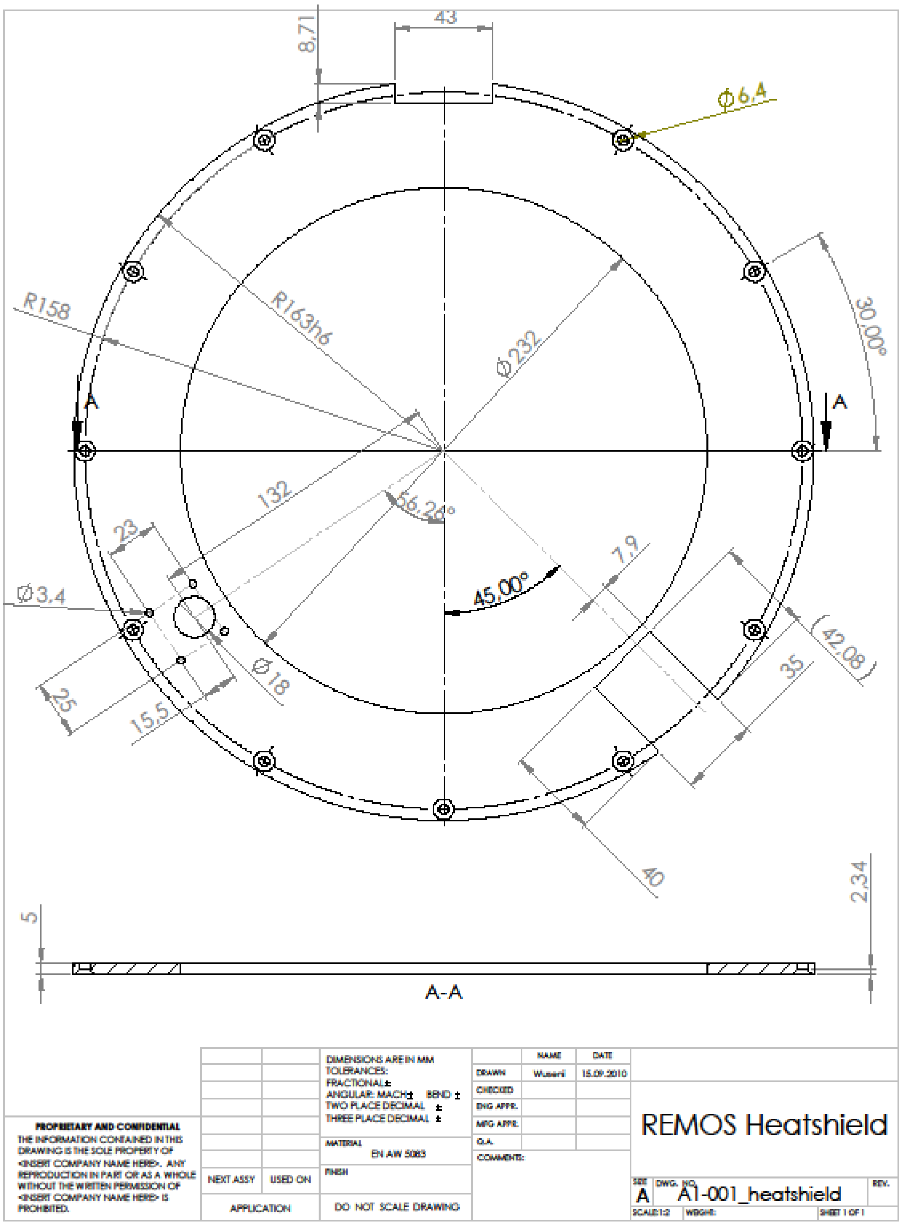
43
8,71
Ø6,4
R158
R163h6
Ø232
30,00°
A
A
132
56,26°
23
Ø3,4
45,00°
7,9
42,08
35
Ø18
25
15,5
40
5
2,34
A-A
DIMENSIONS ARE IN MM
TOLERANCES:
FRACTIONAL±
ANGULAR: MACH± BEND ±
TWO PLACE DECIMAL ±
THREE PLACE DECIMAL ±
MATERIAL
EN AW 5083
FINISH
NEXT ASSY
USED ON
APPLICATION
DO NOT SCALE DRAWING
NAME
DATE
DRAWN
Wuseni
15.09.2010
CHECKED
ENG APPR.
MFG APPR.
Q.A.
COMMENTS:
REMOS Heatshield
SIZE
A
DWG. NO.
A1-001_heatshield
REV.
SCALE:1:2
WEIGHT:
SHEET 1 OF 1
PROPRIETARY AND CONFIDENTIAL
THE INFORMATION CONTAINED IN THIS DRAWING IS THE SOLE PROPERTY OF <INSERT COMPANY NAME HERE>. ANY REPRODUCTION IN PART OR AS A WHOLE WITHOUT THE WRITTEN PERMISSION OF <INSERT COMPANY NAME HERE> IS PROHIBITED.

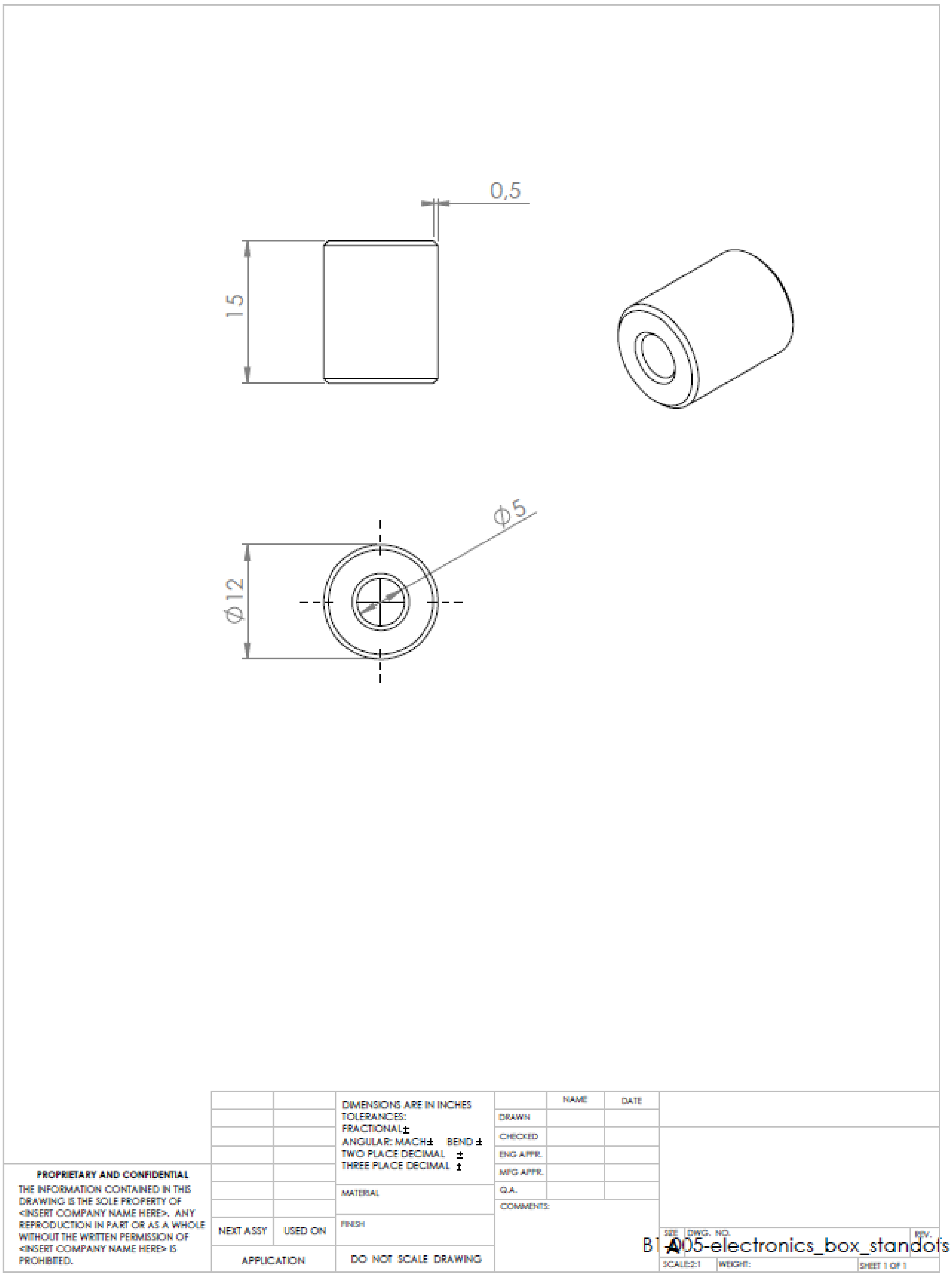
0,5
15
ϕ5
ϕ12
PROPRIETARY AND CONFIDENTIAL
THE INFORMATION CONTAINED IN THIS DRAWING IS THE SOLE PROPERTY OF <INSERT COMPANY NAME HERE>. ANY REPRODUCTION IN PART OR AS A WHOLE WITHOUT THE WRITTEN PERMISSION OF <INSERT COMPANY NAME HERE> IS PROHIBITED.
NEXT ASSY
USED ON
APPLICATION
DIMENSIONS ARE IN INCHES
TOLERANCES:
FRACTIONAL ±
ANGULAR: MACH ± BEND ±
TWO PLACE DECIMAL ±
THREE PLACE DECIMAL ±
MATERIAL
FINISH
DO NOT SCALE DRAWING
NAME
DATE
DRAWN
CHECKED
ENG APPR.
MFG APPR.
Q.A.
COMMENTS:
SIZE
DWG. NO.
REV.
B
A005-electronics_box_standofs
SCALE:2:1
WEIGHT:
SHEET 1 OF 1

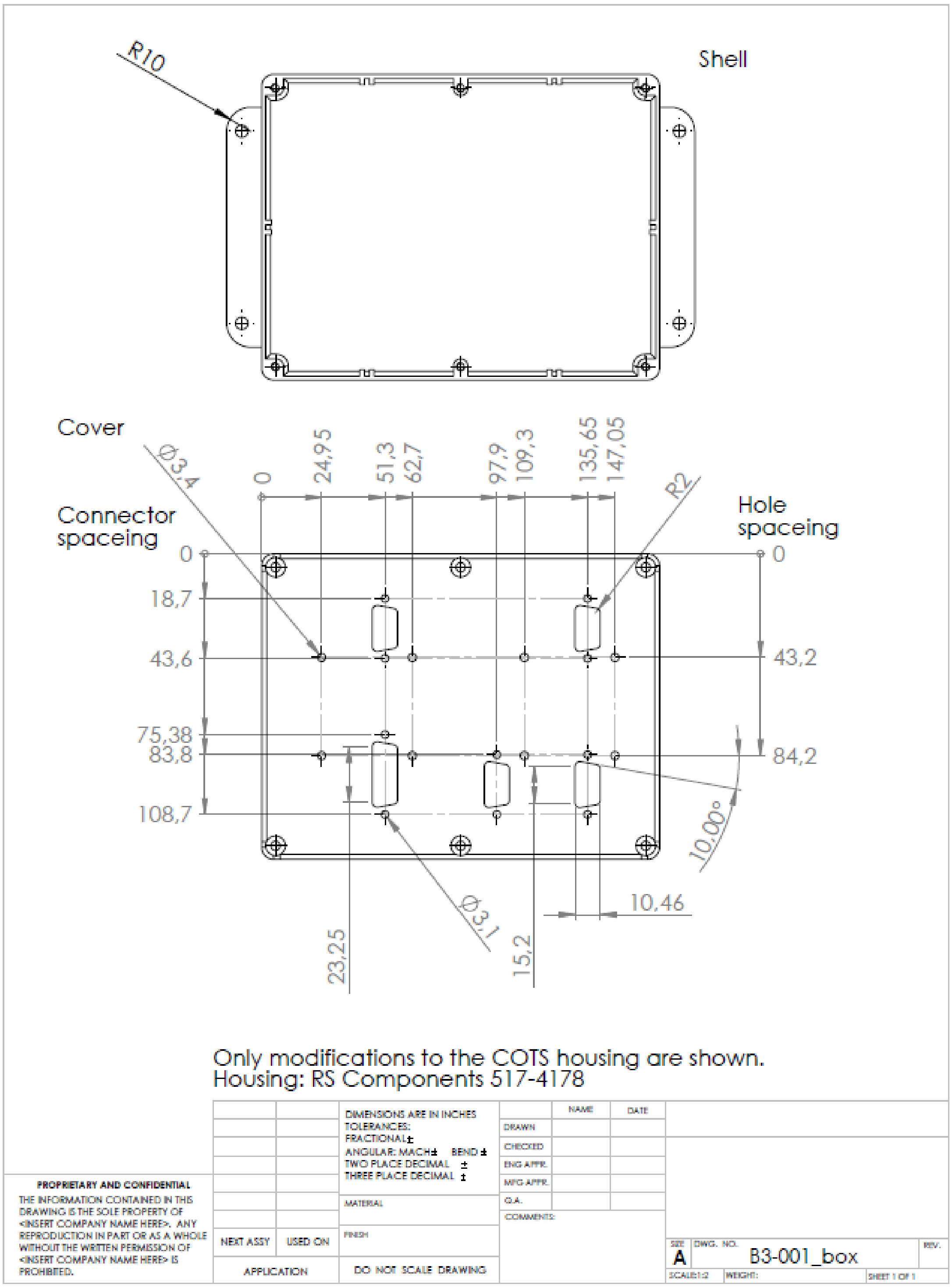
R10
Shell
Cover
Ø3,4
0
24,95
51,3
62,7
97,9
109,3
135,65
147,05
R2
Connector
spaceing
Hole
spaceing
0
18,7
43,6
75,38
83,8
108,7
0
43,2
84,2
10,00°
10,46
Ø3,1
23,25
15,2
Only modifications to the COTS housing are shown.
Housing: RS Components 517-4178
DIMENSIONS ARE IN INCHES
TOLERANCES:
FRACTIONAL ±
ANGULAR: MACH ± BEND ±
TWO PLACE DECIMAL ±
THREE PLACE DECIMAL ±
NAME
DATE
DRAWN
CHECKED
ENG APPR.
MFG APPR.
Q.A.
COMMENTS:
MATERIAL
FINISH
NEXT ASSY
USED ON
APPLICATION
DO NOT SCALE DRAWING
PROPRIETARY AND CONFIDENTIAL
THE INFORMATION CONTAINED IN THIS DRAWING IS THE SOLE PROPERTY OF <INSERT COMPANY NAME HERE>. ANY REPRODUCTION IN PART OR AS A WHOLE WITHOUT THE WRITTEN PERMISSION OF <INSERT COMPANY NAME HERE> IS PROHIBITED.
SIZE
A
DWG. NO.
B3-001_box
REV.
SCALE:1:2
WEIGHT:
SHEET 1 OF 1

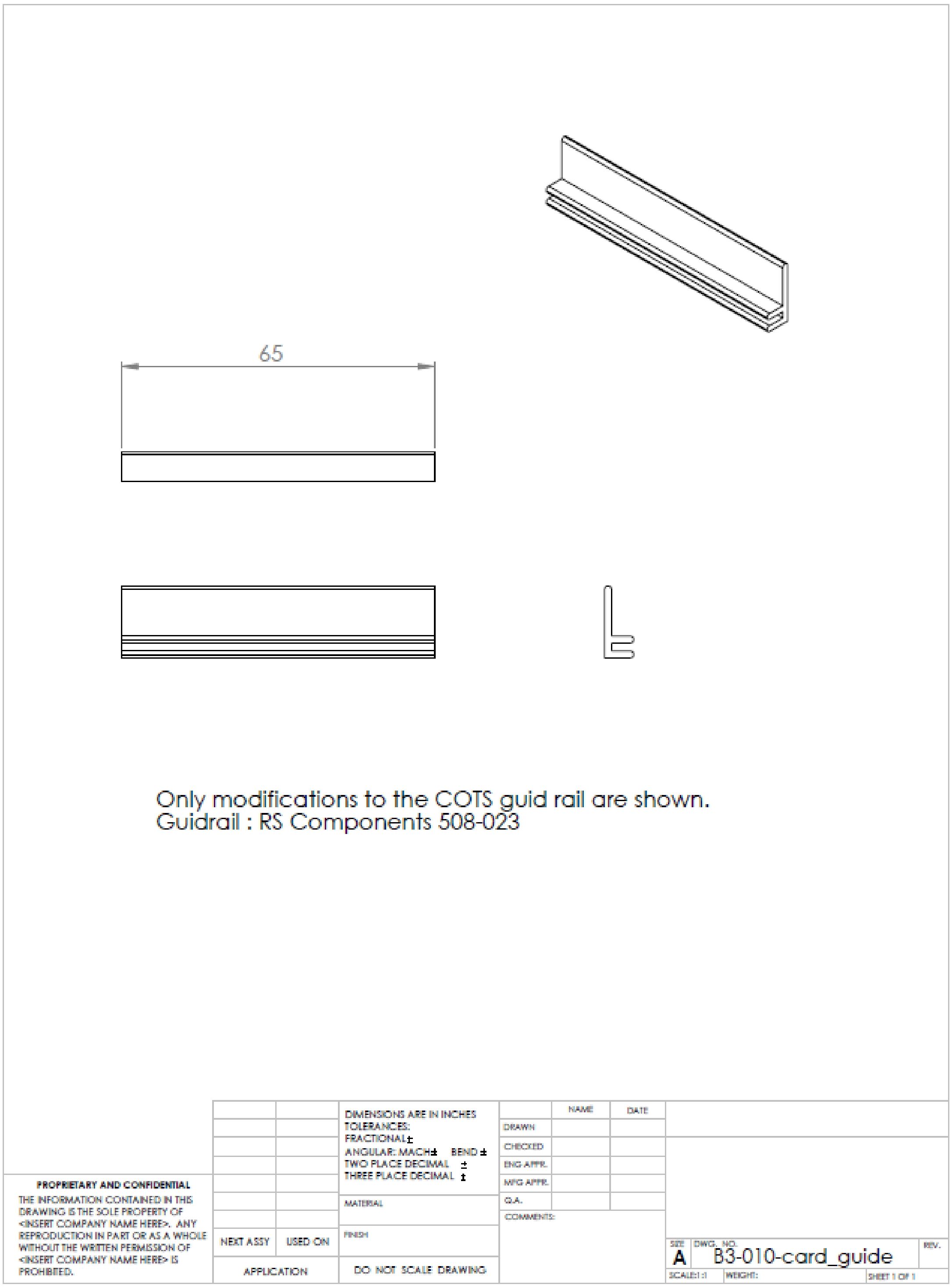
65
Only modifications to the COTS guid rail are shown.
Guidrail : RS Components 508-023
DIMENSIONS ARE IN INCHES
TOLERANCES:
FRACTIONAL ±
ANGULAR: MACH ± BEND ±
TWO PLACE DECIMAL ±
THREE PLACE DECIMAL ±
NAME
DATE
DRAWN
CHECKED
ENG APPR.
MFG APPR.
Q.A.
COMMENTS:
MATERIAL
FINISH
NEXT ASSY
USED ON
APPLICATION
DO NOT SCALE DRAWING
PROPRIETARY AND CONFIDENTIAL
THE INFORMATION CONTAINED IN THIS DRAWING IS THE SOLE PROPERTY OF <INSERT COMPANY NAME HERE>. ANY REPRODUCTION IN PART OR AS A WHOLE WITHOUT THE WRITTEN PERMISSION OF <INSERT COMPANY NAME HERE> IS PROHIBITED.
SIZE
A
DWG. NO.
B3-010-card_guide
REV.
SCALE:1:1
WEIGHT:
SHEET 1 OF 1

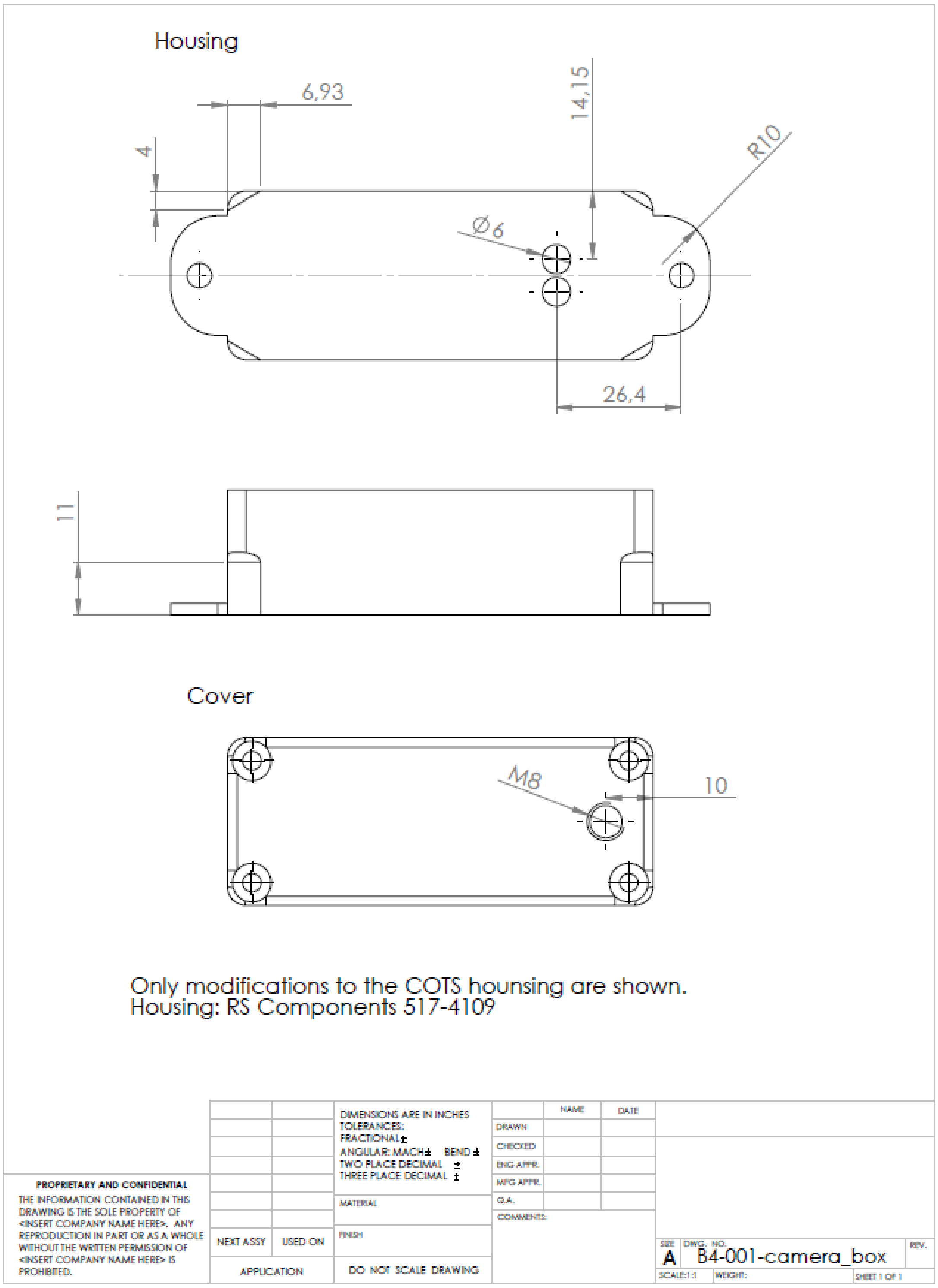
Housing
6,93
14,15
R10
4
Ø6
26,4
11
Cover
M8
10
Only modifications to the COTS hounsing are shown.
Housing: RS Components 517-4109
DIMENSIONS ARE IN INCHES
TOLERANCES:
FRACTIONAL ±
ANGULAR: MACH ± BEND ±
TWO PLACE DECIMAL ±
THREE PLACE DECIMAL ±
NAME
DATE
DRAWN
CHECKED
ENG APPR.
MFG APPR.
Q.A.
COMMENTS:
MATERIAL
FINISH
NEXT ASSY
USED ON
APPLICATION
DO NOT SCALE DRAWING
PROPRIETARY AND CONFIDENTIAL
THE INFORMATION CONTAINED IN THIS DRAWING IS THE SOLE PROPERTY OF <INSERT COMPANY NAME HERE>. ANY REPRODUCTION IN PART OR AS A WHOLE WITHOUT THE WRITTEN PERMISSION OF <INSERT COMPANY NAME HERE> IS PROHIBITED.
SIZE
DWG. NO.
REV.
A
B4-001-camera_box
SCALE:1:1
WEIGHT:
SHEET 1 OF 1

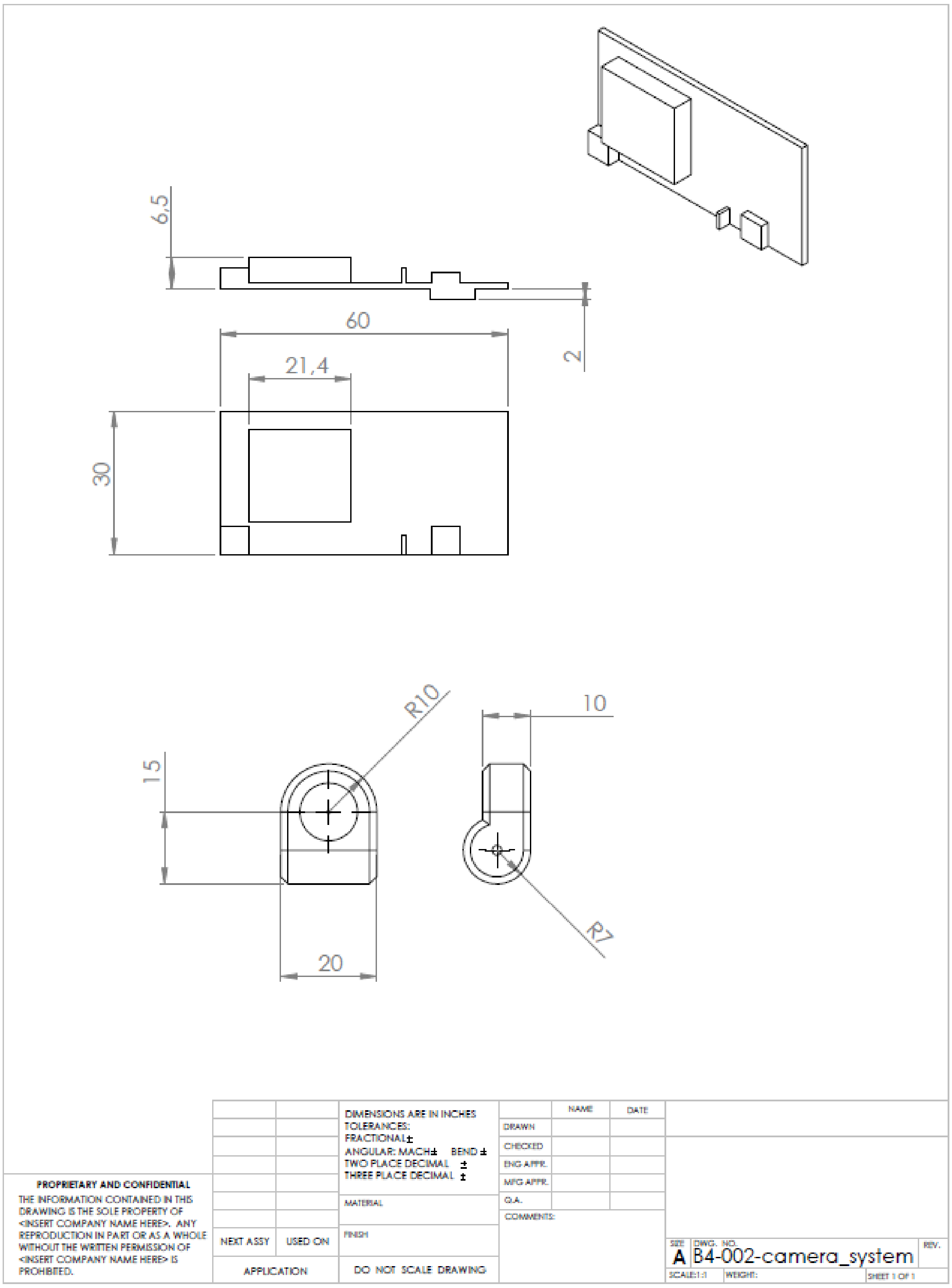
6,5
60
21,4
2
30
R10
10
15
20
R7
DIMENSIONS ARE IN INCHES
TOLERANCES:
FRACTIONAL±
ANGULAR: MACH± BEND ±
TWO PLACE DECIMAL ±
THREE PLACE DECIMAL ±
NAME
DATE
DRAWN
CHECKED
ENG APPR.
MFG APPR.
Q.A.
COMMENTS:
MATERIAL
FINISH
NEXT ASSY
USED ON
APPLICATION
DO NOT SCALE DRAWING
PROPRIETARY AND CONFIDENTIAL
THE INFORMATION CONTAINED IN THIS DRAWING IS THE SOLE PROPERTY OF <INSERT COMPANY NAME HERE>. ANY REPRODUCTION IN PART OR AS A WHOLE WITHOUT THE WRITTEN PERMISSION OF <INSERT COMPANY NAME HERE> IS PROHIBITED.
SIZE
A
DWG. NO.
B4-002-camera_system
REV.
SCALE:1:1
WEIGHT:
SHEET 1 OF 1

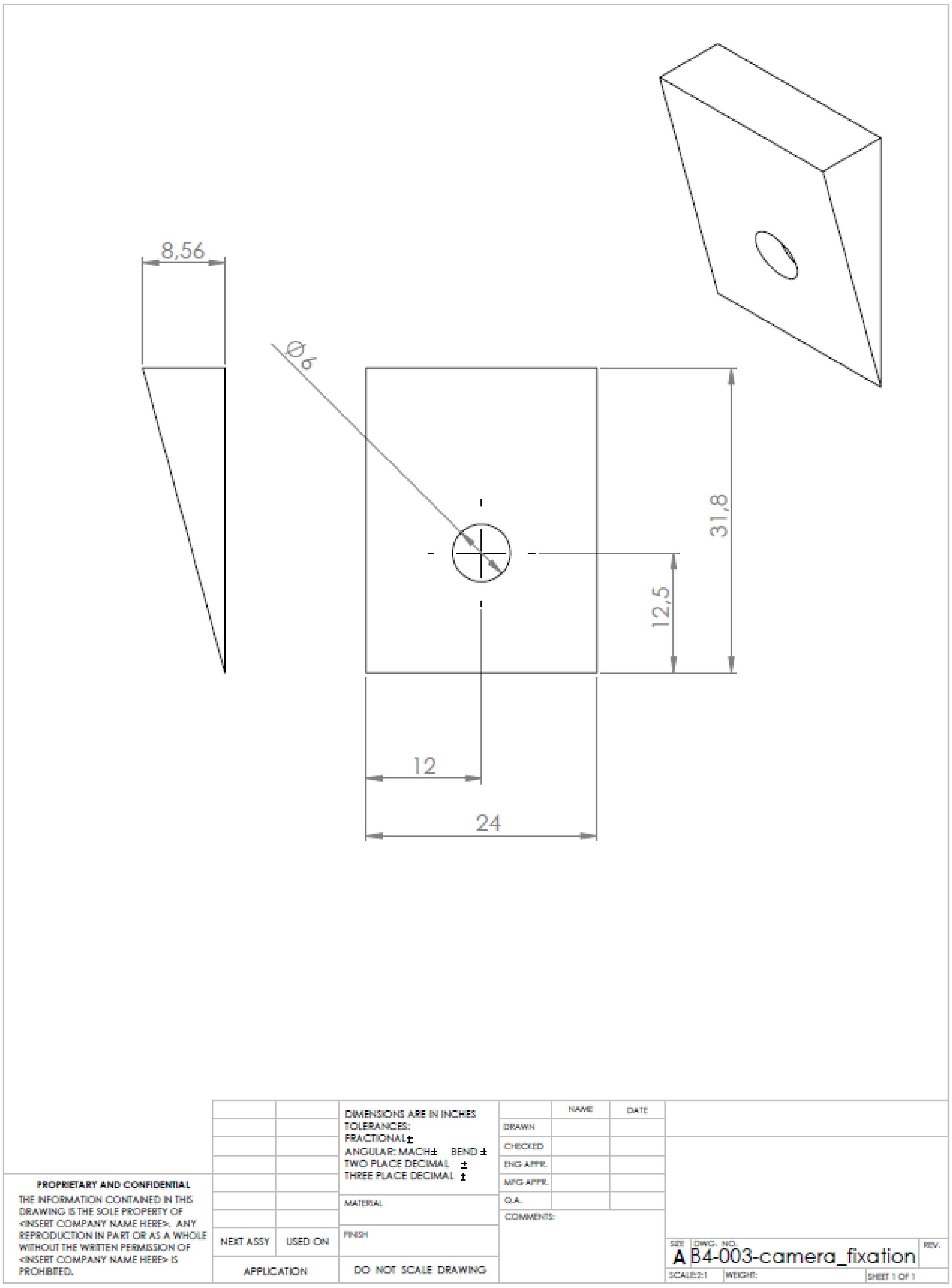
8,56
Ø6
31,8
12,5
12
24
PROPRIETARY AND CONFIDENTIAL
THE INFORMATION CONTAINED IN THIS DRAWING IS THE SOLE PROPERTY OF <INSERT COMPANY NAME HERE>. ANY REPRODUCTION IN PART OR AS A WHOLE WITHOUT THE WRITTEN PERMISSION OF <INSERT COMPANY NAME HERE> IS PROHIBITED.
NEXT ASSY
USED ON
APPLICATION
DIMENSIONS ARE IN INCHES
TOLERANCES:
FRACTIONAL ±
ANGULAR: MACH ± BEND ±
TWO PLACE DECIMAL ±
THREE PLACE DECIMAL ±
MATERIAL
FINISH
DO NOT SCALE DRAWING
NAME
DATE
DRAWN
CHECKED
ENG APPR.
MFG APPR.
Q.A.
COMMENTS:
SIZE
DWG. NO.
A
B4-003-camera_fixation
REV.
SCALE:2:1
WEIGHT:
SHEET 1 OF 1

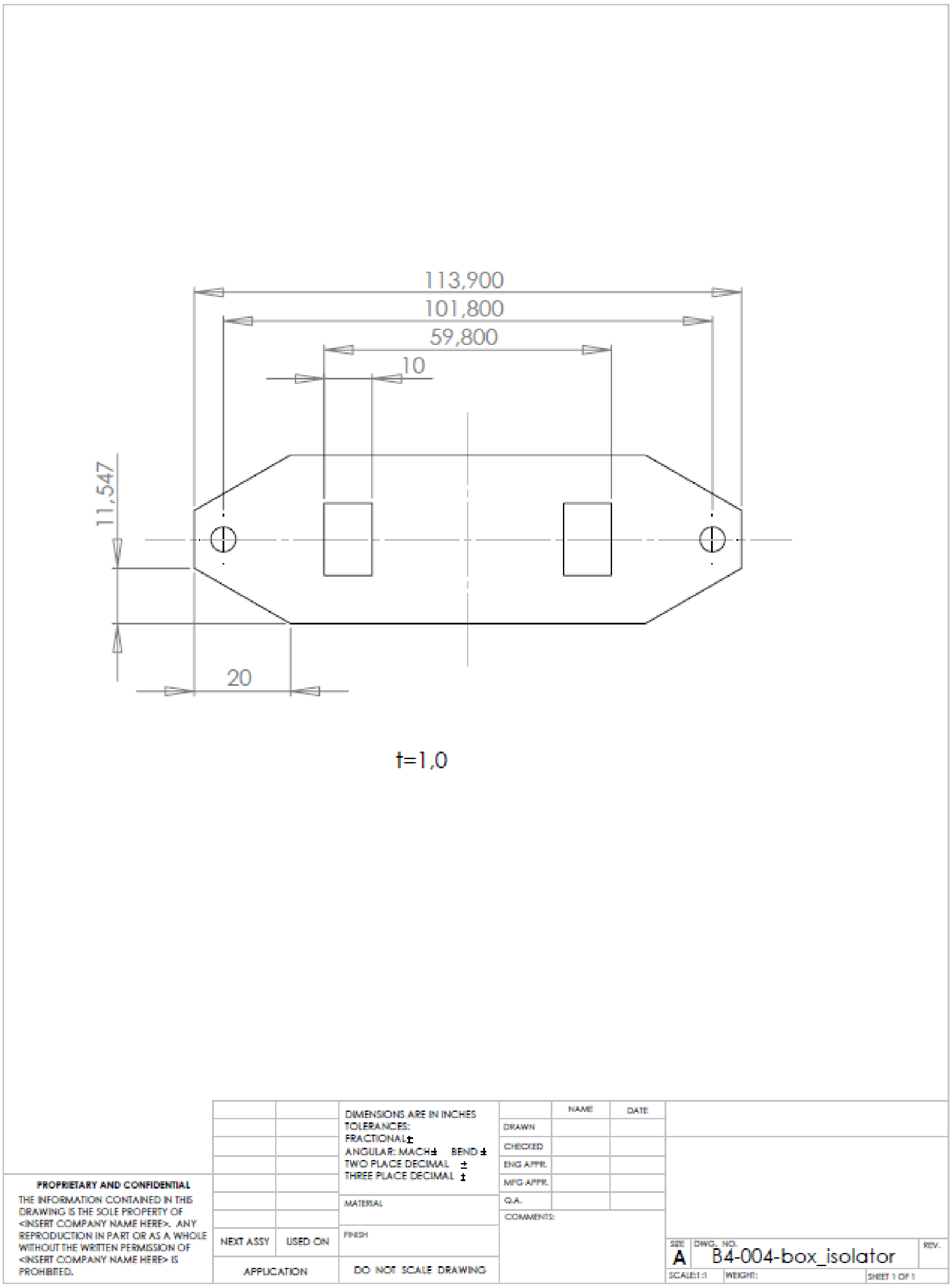
113,900
101,800
59,800
10
11,547
20
t=1,0
DIMENSIONS ARE IN INCHES
TOLERANCES:
FRACTIONAL±
ANGULAR: MACH± BEND ±
TWO PLACE DECIMAL ±
THREE PLACE DECIMAL ±
MATERIAL
FINISH
DO NOT SCALE DRAWING
NAME
DATE
DRAWN
CHECKED
ENG APPR.
MFG APPR.
Q.A.
COMMENTS:
PROPRIETARY AND CONFIDENTIAL
THE INFORMATION CONTAINED IN THIS DRAWING IS THE SOLE PROPERTY OF <INSERT COMPANY NAME HERE>. ANY REPRODUCTION IN PART OR AS A WHOLE WITHOUT THE WRITTEN PERMISSION OF <INSERT COMPANY NAME HERE> IS PROHIBITED.
NEXT ASSY
USED ON
APPLICATION
SIZE
A
DWG. NO.
B4-004-box_isolator
REV.
SCALE:1:1
WEIGHT:
SHEET 1 OF 1

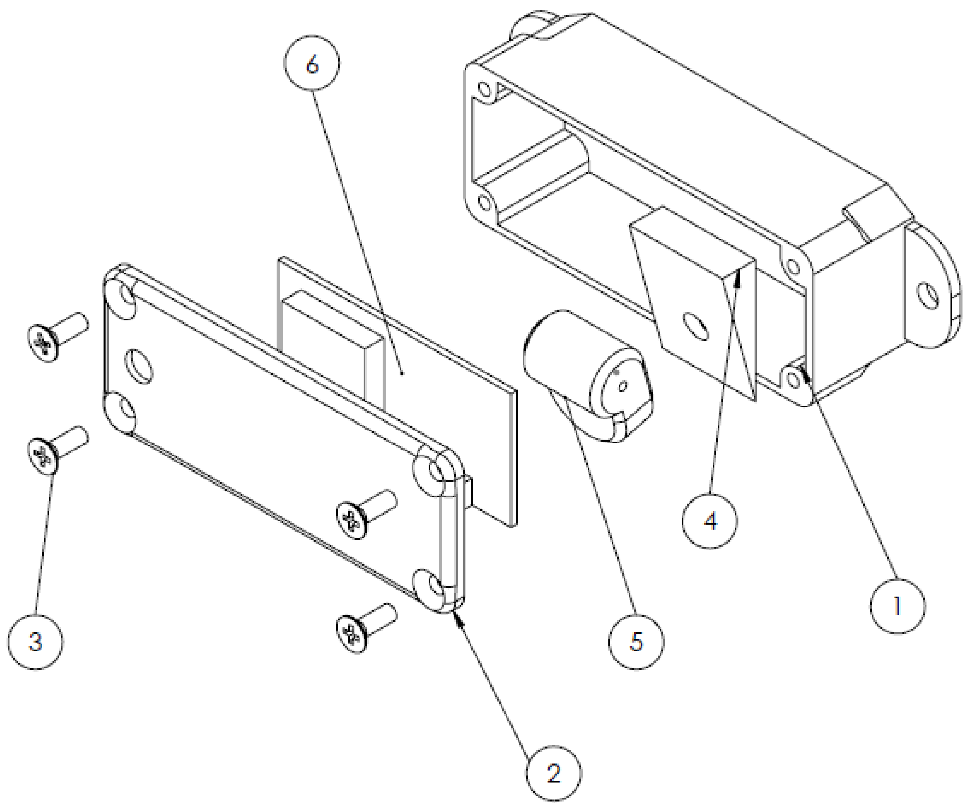

POS-NR.	NAME	NOTE	QUANT.
1	B4-001a-camera_housing		1
2	B4-001b-camera_cover		1
3	B4-001c-B18.6.7M - M3.5 x 0.6 x 10 Type I Cross Recessed FHMS --10N		4
4	B4-003-camera_fixation		1
5	B4-002-camera_system2		1
6	B4-002-camera_system1		1

PROPRIETARY AND CONFIDENTIAL
THE INFORMATION CONTAINED IN THIS DRAWING IS THE SOLE PROPERTY OF <INSERT COMPANY NAME HERE>. ANY REPRODUCTION IN PART OR AS A WHOLE WITHOUT THE WRITTEN PERMISSION OF <INSERT COMPANY NAME HERE> IS PROHIBITED.

NEXT ASSY | USED ON
APPLICATION

DIMENSIONS ARE IN INCHES
TOLERANCES:
FRACTIONAL ±
ANGULAR: MACH ± BEND ±
TWO PLACE DECIMAL ±
THREE PLACE DECIMAL ±

MATERIAL

FINISH

DO NOT SCALE DRAWING

	NAME	DATE
DRAWN		
CHECKED		
ENG APPR.		
MFG APPR.		
Q.A.		

COMMENTS:

SIZE A | DWG. NO. B4-camera_box | REV.
SCALE:1:1 | WEIGHT: | SHEET 1 OF 1

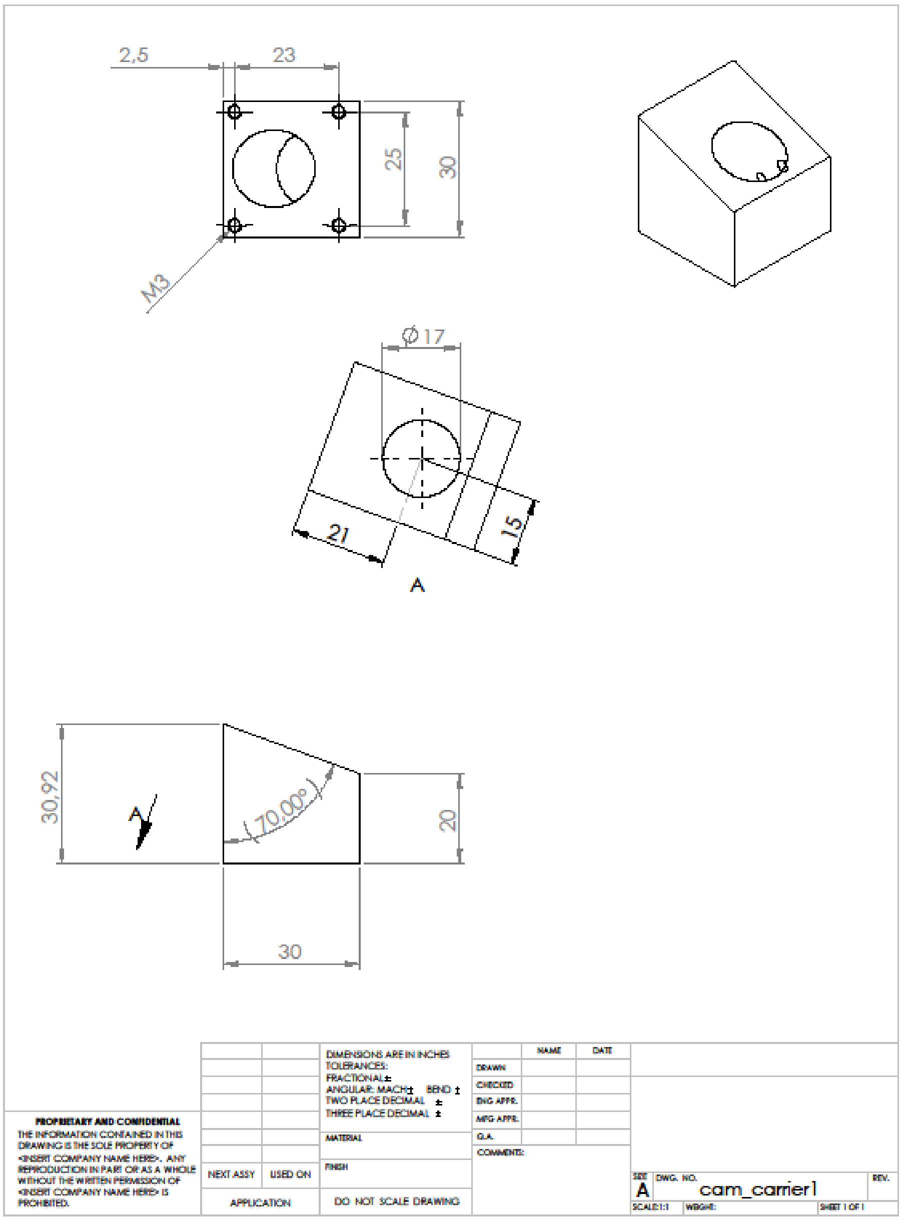
2,5
23
25
30
M3
Ø17
21
15
A
30,92
A
70,00°
20
30
PROPRIETARY AND CONFIDENTIAL
THE INFORMATION CONTAINED IN THIS DRAWING IS THE SOLE PROPERTY OF <INSERT COMPANY NAME HERE>. ANY REPRODUCTION IN PART OR AS A WHOLE WITHOUT THE WRITTEN PERMISSION OF <INSERT COMPANY NAME HERE> IS PROHIBITED.
NEXT ASSY
USED ON
APPLICATION
DIMENSIONS ARE IN INCHES
TOLERANCES:
FRACTIONAL ±
ANGULAR: MACH ± BEND ±
TWO PLACE DECIMAL ±
THREE PLACE DECIMAL ±
MATERIAL
FINISH
DO NOT SCALE DRAWING
NAME
DATE
DRAWN
CHECKED
ENG APPR.
MFG APPR.
Q.A.
COMMENTS:
SIZE
A
DWG. NO.
cam_carrier1
REV.
SCALE:1:1
WEIGHT:
SHEET 1 OF 1

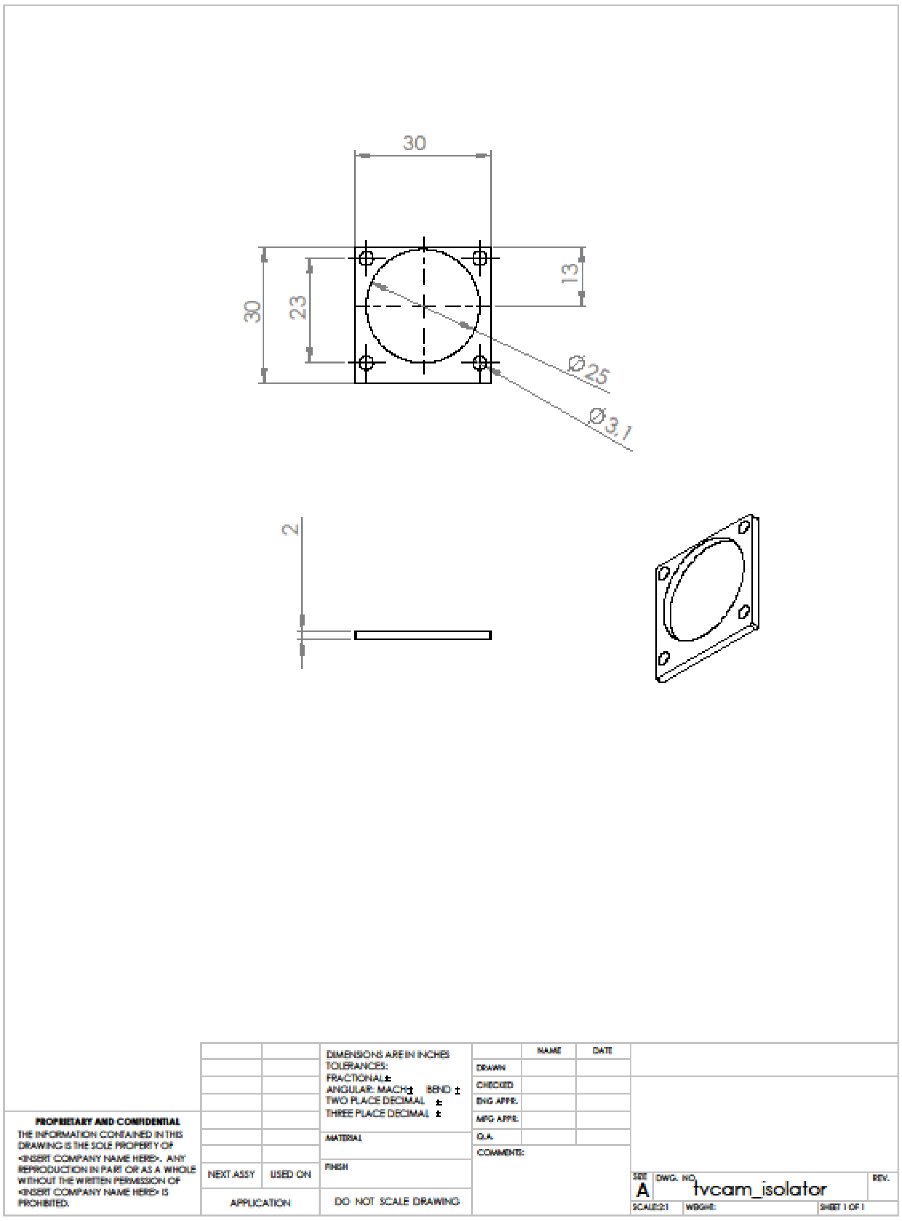
30
30
23
13
Ø25
Ø3.1
2
DIMENSIONS ARE IN INCHES
TOLERANCES:
FRACTIONAL±
ANGULAR: MACH± BEND ±
TWO PLACE DECIMAL ±
THREE PLACE DECIMAL ±
MATERIAL
FINISH
DO NOT SCALE DRAWING
NEXT ASSY
USED ON
APPLICATION
NAME
DATE
DRAWN
CHECKED
ENG APPR.
MFG APPR.
Q.A.
COMMENTS:
PROPRIETARY AND CONFIDENTIAL
THE INFORMATION CONTAINED IN THIS DRAWING IS THE SOLE PROPERTY OF <INSERT COMPANY NAME HERE>. ANY REPRODUCTION IN PART OR AS A WHOLE WITHOUT THE WRITTEN PERMISSION OF <INSERT COMPANY NAME HERE> IS PROHIBITED.
SIZE
A
DWG. NO.
tvcam_isolator
REV.
SCALE:2:1
WEIGHT:
SHEET 1 OF 1

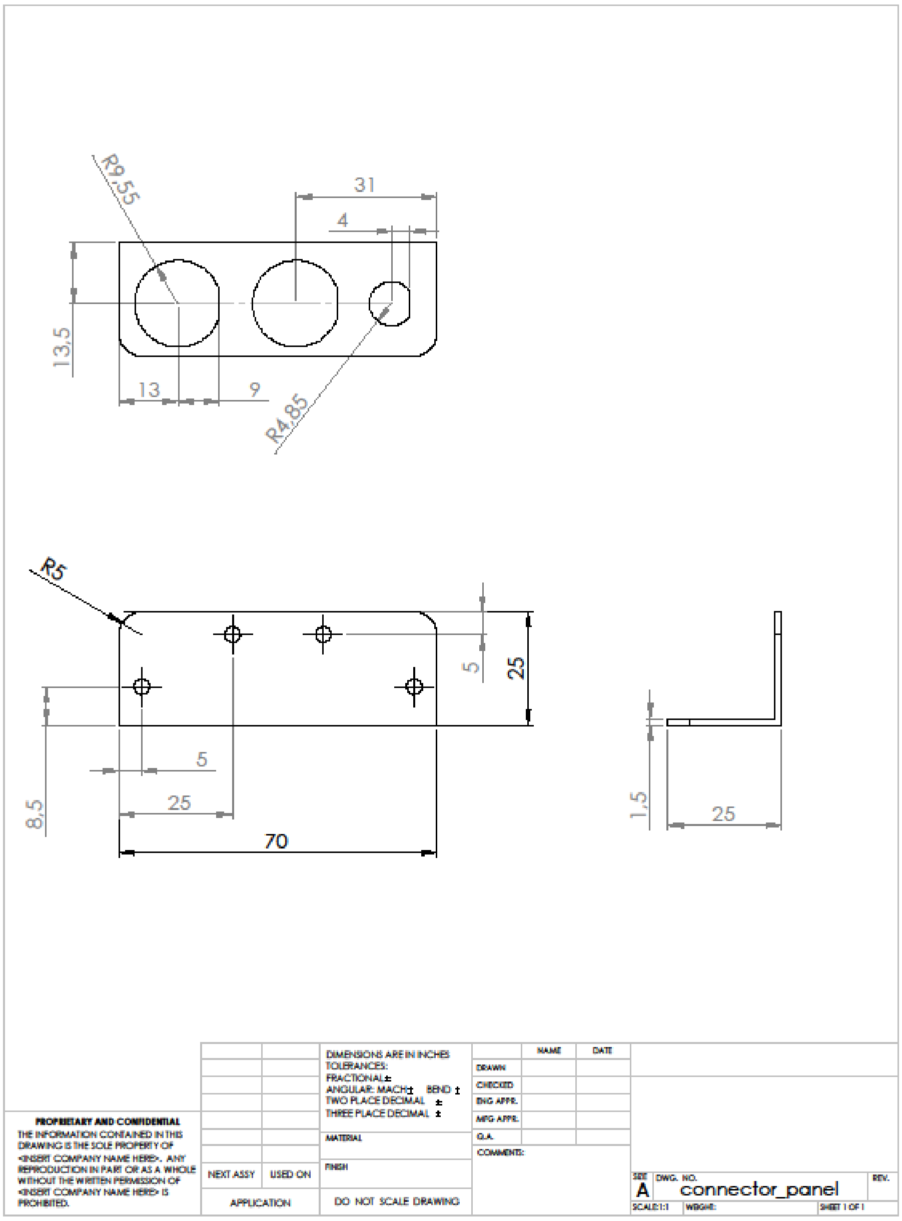
R9,55
31
4
13,5
13
9
R4,85
R5
5
25
8,5
5
25
70
1,5
25
PROPRIETARY AND CONFIDENTIAL
THE INFORMATION CONTAINED IN THIS DRAWING IS THE SOLE PROPERTY OF <INSERT COMPANY NAME HERE>. ANY REPRODUCTION IN PART OR AS A WHOLE WITHOUT THE WRITTEN PERMISSION OF <INSERT COMPANY NAME HERE> IS PROHIBITED.
NEXT ASSY
USED ON
APPLICATION
DIMENSIONS ARE IN INCHES
TOLERANCES:
FRACTIONAL±
ANGULAR: MACH± BEND ±
TWO PLACE DECIMAL ±
THREE PLACE DECIMAL ±
MATERIAL
FINISH
DO NOT SCALE DRAWING
NAME
DATE
DRAWN
CHECKED
ENG APPR.
MFG APPR.
Q.A.
COMMENTS:
SIZE
A
DWG. NO.
connector_panel
REV.
SCALE:1:1
WEIGHT:
SHEET 1 OF 1

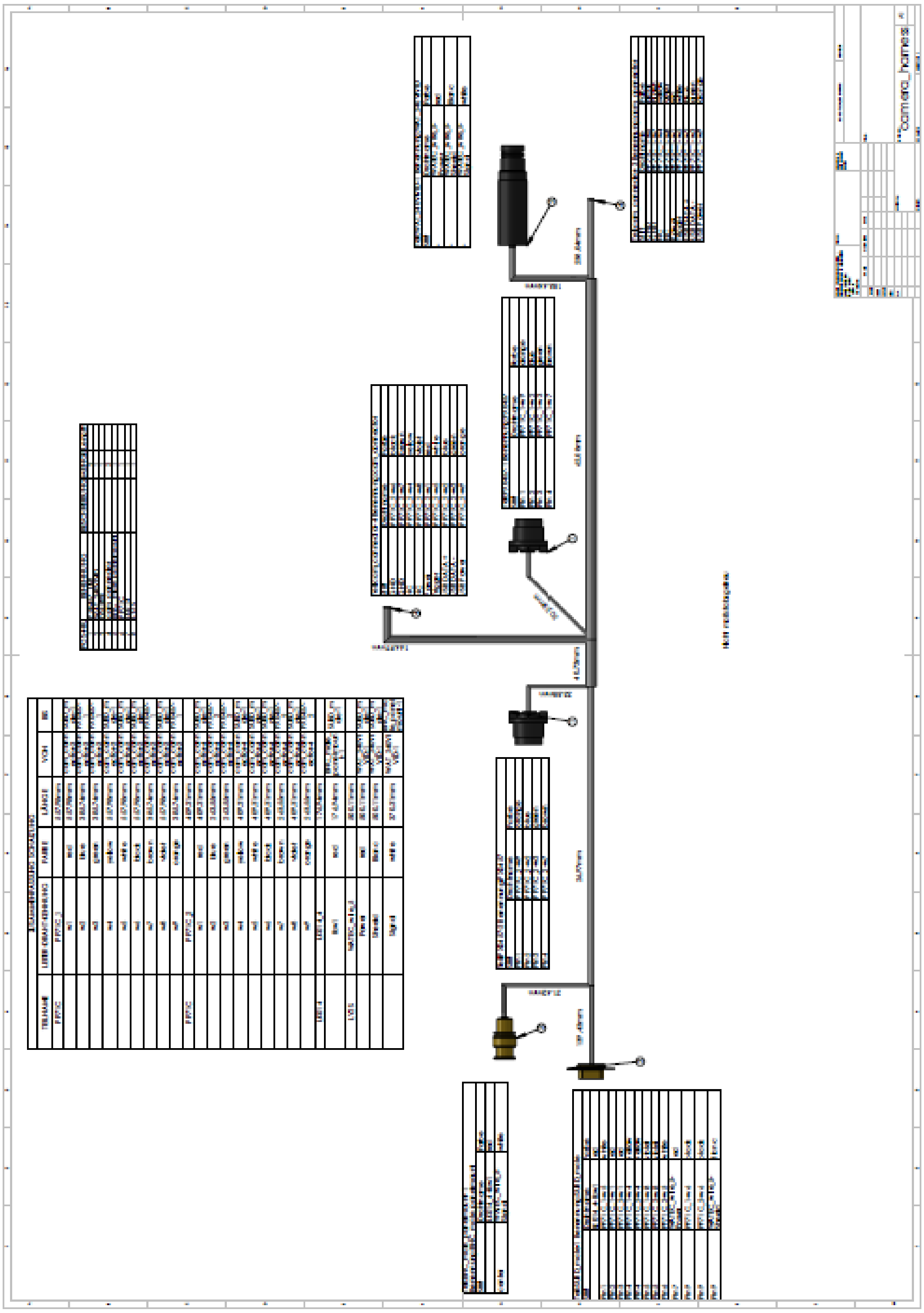

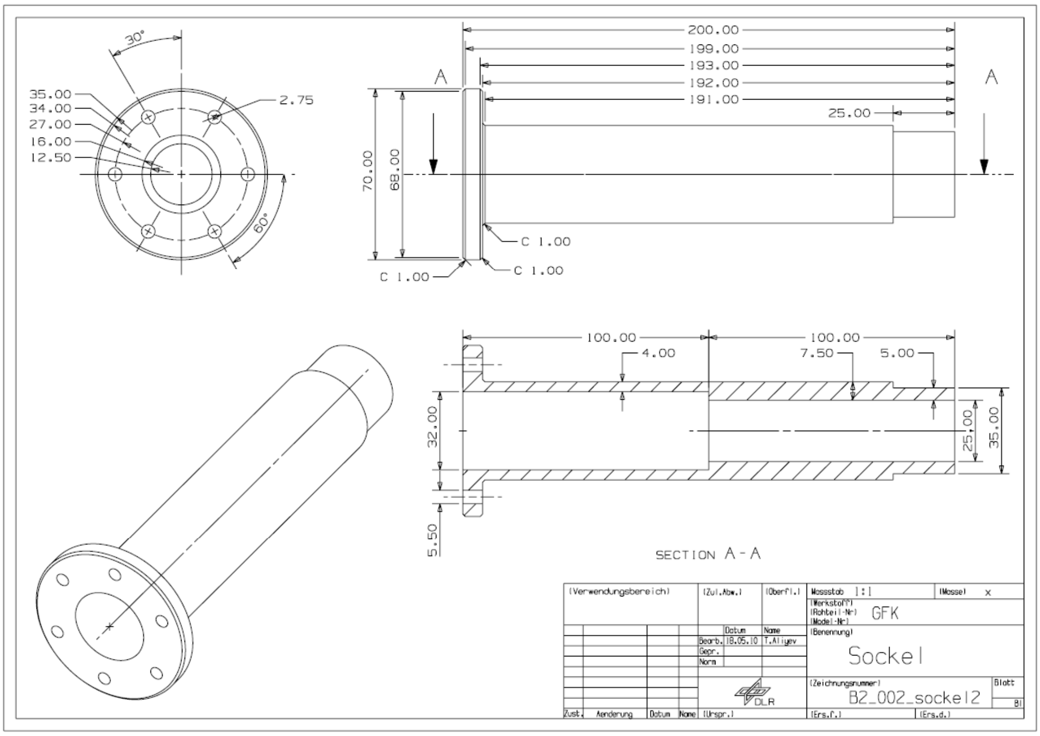
SECTION A-A
GFK
Sockel
B2_002_sockel2

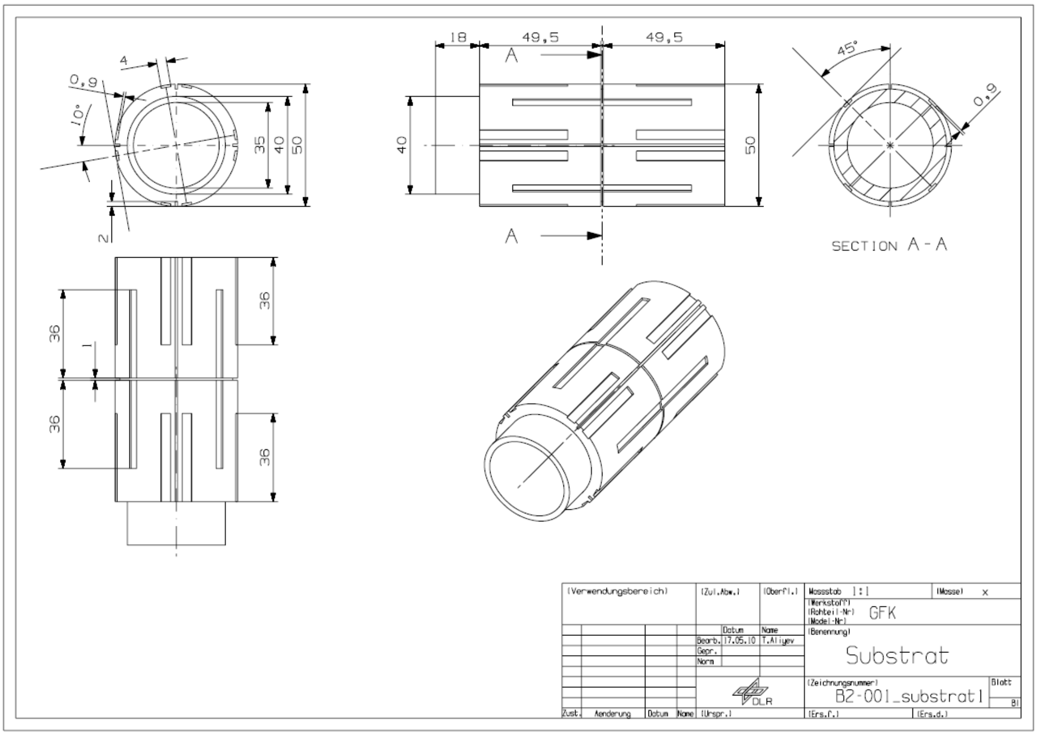
SECTION A-A
GFK
Substrat
B2-001_substrat1

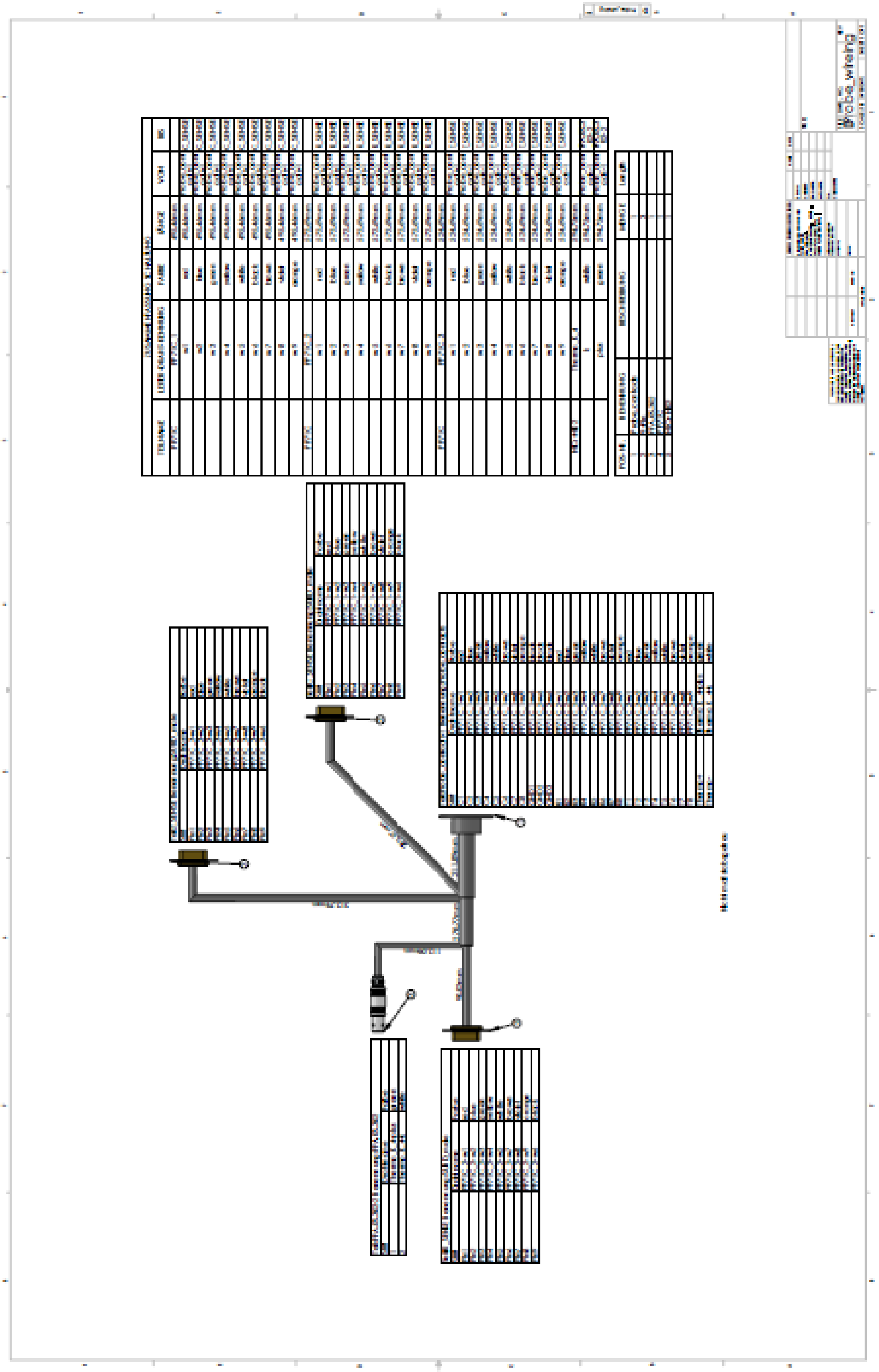

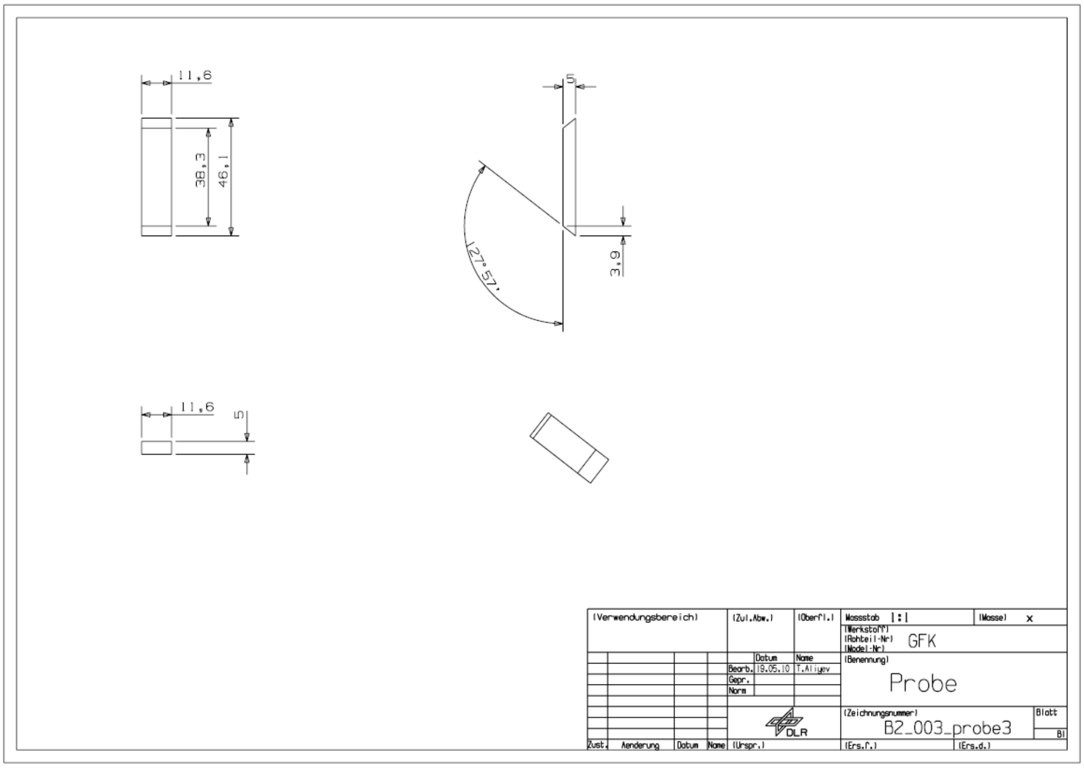
11,6
38,3
46,1
5
3,9
127°57'
11,6
5
(Verwendungsbereich)
(Zul.Abw.)
(Oberfl.)
Massstab 1:1
(Masse) x
(Werkstoff)
(Rohteil-Nr)
(Model-Nr)
GFK
Datum
Name
Bearb. 19.05.10 T.Aliyev
Gepr.
Norm
(Benennung)
Probe
(Zeichnungsnummer)
B2_003_probe3
Blatt
Bl
DLR
Zust.
Aenderung
Datum
Name
(Urspr.)
(Ers.f.)
(Ers.d.)

C.2 Screw Calculations

REMOS screw calculations (according to VDI 2230)

1. System design

The overall safety factor is $j := 1.5$

Compensation for uncertaties in Loads $j_{ext} := 1.3$

Reliability for random loads is 99.97%. This results in $j_{rand} := 3.0$

Gliding coefficient on aluminium: $\mu_K := 0.2$ $\mu_G := 0.2$

Tightening facor for momentum torque wrench: $\alpha_A := 1.6$

Young's modulus of aluminium: $E_{Alu} := 70GPa$

Thermal expansion factors: $\alpha_{Alu} := 23.2 \cdot 10^{-6} \frac{1}{K}$

$\alpha_{St} := 13 \cdot 10^{-6} \frac{1}{K}$

1.1 Interface, mass and COG specifications

All distances are referred to the coordinate system at the REXUS interface. The z-axis points toward launch direction. Other axes are according to coord. def. in REXUS User Manual.

1.1.1 Sensor Boom interface

Mass: $m_{sensors} := 0.696kg$

COG: $cog_{sensors} := \begin{pmatrix} 0.0 \\ 0.0 \\ 324.6 \end{pmatrix} mm$

Interface position: $z_{sensors} := 163mm$

Number of gaps: $q_{F\_sb} := 1$

Tightening length: $l_{k\_sb} := 6mm$

1.1.2 Cylinder Cover interface

Mass: $m_{cover} := 2.92kg$

COG: $cog_{cover} := \begin{pmatrix} 0.851 \\ -0.11 \\ 177.47 \end{pmatrix} mm$

Interface position: $z_{cover} := 143mm$

Number of gaps: $q_{F\_cc} := 1$

Tightening length: $l_{k\_cc} := 3.5mm$

1.1.3 Launch Adapter interface

Mass: $m_{launch} := 3.113kg$

COG: $cog_{launch} := \begin{pmatrix} 0.626 \\ -0.081 \\ 152.485 \end{pmatrix} mm$

Interface position: $z_{launch} := 23mm$

Number of gaps: $q_{F\_la} := 1$

Tightening length: $l_{k\_la} := 15mm$

1.1.4 REXUS rocket interface

Mass: $m_{rexus} := 4.066kg$

COG: $cog_{rexus} := \begin{pmatrix} 0.48 \\ -0.06 \\ 119.806 \end{pmatrix} mm$

Interface position: $z_{rexus} := 0mm$

Number of gaps: $q_{F\_r} := 1$

Tightening length: $l_{k\_r} := 4mm$

1.1.5 Electronics Box interface

Mass: $m_{ebox} := 0.802kg$

COG: $cog_{ebox} := \begin{pmatrix} 2.566 \\ -0.305 \\ 84.231 \end{pmatrix} mm$

Interface position: $z_{ebox} := 143mm$

Number of gaps: $q_{F\_eb} := 1$

Tightening length: $l_{k\_eb} := 17.5mm$

1.1.6 Camera Box interface

Mass: $m_{cbox} := 0.1kg$

COG: $cog_{cbox} := \begin{pmatrix} 15.22 \\ 80.67 \\ 127.41 \end{pmatrix} mm$

Interface position: $z_{cbox} := 143mm$

Number of gaps: $q_{F\_cb} := 1$

Tightening length: $l_{k\_cb} := 4mm$

1.2 Screw properties

1.2.1 DIN 7991 M4 class 8.8

Tightening momentum for μ: $M_{A\_M4} := 4.1N \cdot m$

Max. force: $F_{Mzul\_M4} := 5600N$

Flank lead: $P_{M4} := 0.7mm$

Cross area: $A_{M4} := 8.78mm^2$ Diameter : $d_{M4} := 3.545mm$

Young's modulus: $E_{M4} := 200GPa$

1.2.2 DIN 912 M3 class 8.8

Tightening momentum for μ:	$M_{A\_M3} := 1.2N \cdot m$		
Max. force:	$F_{Mzul\_M3} := 3200N$		
Flank lead:	$P_{M3} := 0.5mm$		
Cross area:	$A_{M3} := 5.03mm^2$	Diameter :	$d_{M3} := 2.6mm$
Young's modulus:	$E_{M3} := 200GPa$		

1.2.3 DIN 912 M5 class 8.8

Tightening momentum for μ:	$M_{A\_M5} := 8.1N \cdot m$		
Max. force:	$F_{Mzul\_M5} := 9100N$		
Flank lead:	$P_{M5} := 0.8mm$		
Cross area:	$A_{M5} := 14.2mm^2$	Diameter :	$d_{M5} := 4.48mm$
Young's modulus:	$E_{M5} := 200GPa$		

1.3 Qualification loads

1.3.1 Lunch

	Longitudinal		Lateral	
Static acceleration:	$a_{RXz} := 20g$	(at launch)	$a_{RXx} := 6g$	(at launch)
Random acceleration (at qualification level):	$a_{randz} := 12g$	(at launch)	$a_{randx} := 12g$	(at launch)
Max. total acc.:	$a_z := a_{RXz} + j_{rand} \cdot a_{randz}$		$a_x := j_{rand} \cdot a_{randx}$	
	$a_z = 549.172 \frac{m}{s^2}$		$a_x = 353.039 \frac{m}{s^2}$	

Difference between operating and assembly temperature: $\Delta T_{launch} := 0K$

1.3.2 Re-entry

	Longitudinal	Lateral
Static acceleration:	$a_{RXzr} := 6g$ (at launch)	$a_{RXxr} := 6g$ (at launch)
Random acceleration (at qualification level):	$a_{randzr} := 1g$ (at launch)	$a_{randxr} := 1g$ (at launch)
Max. total acc.:	$a_{zr} := a_{RXzr} + j_{rand} \cdot a_{randzr}$	$a_{xr} := j_{rand} \cdot a_{randxr}$
	$a_{zr} = 88.26 \frac{m}{s^2}$	$a_{xr} = 29.42 \frac{m}{s^2}$

Difference between operating and assembly temperature: $\Delta T_{entry} := 180K$

2. Load calculation

2.1. Sensor Boom interface

2.1.1 Launch

Bolting radius: $r_{sensors} := 27mm$

Number of bolts: $n_{sensors} := 6$

Axial load: $F_{sensorz} := m_{sensors} \cdot a_z$ $\quad F_{sensorz} = 382.224\ N$

Lateral load: $F_{sensorx} := m_{sensors} \cdot a_x$ $\quad F_{sensorx} = 245.715\ N$

Bending momentum: $M_{sensor} := m_{sensors} \cdot a_x \cdot \left(cog_{sensors_2} - z_{sensors}\right)$ $\quad M_{sensor} = 39.708\ N \cdot m$

Max. axial force on screw:

$$F_{sensors\_ax} := \frac{F_{sensorz}}{n_{sensors}} + \frac{4 \cdot M_{sensor} \cdot r_{sensors}}{n_{sensors} \cdot \left(2 \cdot r_{sensors}^2 - \frac{n_{sensors} \cdot A_{M5}}{\pi}\right)}$$

$F_{sensors\_ax} = 563.213\ N$

Max. lateral force on screw:

$$F_{sensors\_lat} := \frac{F_{sensorx}}{n_{sensors}}$$

$F_{sensors\_lat} = 40.953\ N$

2.1.2 Re-entry

Axial load: $F_{sensorzr} := m_{sensors} \cdot a_{zr}$ $F_{sensorzr} = 61.429\ N$

Lateral load: $F_{sensorxr} := m_{sensors} \cdot a_{xr}$ $F_{sensorxr} = 20.476\ N$

Bending momentum: $M_{sensorr} := m_{sensors} \cdot a_{xr} \cdot \left(cog_{sensors_2} - z_{sensors}\right)$ $M_{sensorr} = 3.309\ N \cdot m$

Max. axial force on screw:

$$F_{sensors\_axr} := \frac{F_{sensorzr}}{n_{sensors}} + \frac{4 \cdot M_{sensorr} \cdot r_{sensors}}{n_{sensors} \cdot \left(2 \cdot r_{sensors}{}^2 - \frac{n_{sensors} \cdot A_{M5}}{\pi}\right)}$$

$F_{sensors\_axr} = 51.864\ N$

Max. lateral force on screw:

$$F_{sensors\_latr} := \frac{F_{sensorxr}}{n_{sensors}}$$

$F_{sensors\_latr} = 3.413\ N$

2.2. Cylinder Cover interface

2.2.1 Launch

Bolting radius: $r_{cover} := 111.5mm$

Number of bolts: $n_{cover} := 16$

Axial load: $F_{coverz} := m_{cover} \cdot a_z$ $F_{coverz} = 1.604 \times 10^3\ N$

Lateral load: $F_{coverx} := m_{cover} \cdot a_x$ $F_{coverx} = 1.031 \times 10^3\ N$

Bending momentum: $M_{cover} := m_{cover} \cdot a_x \cdot \left(cog_{cover_2} - z_{cover}\right)$ $M_{cover} = 35.534\ N \cdot m$

Max. axial force on screw:

$$F_{cover\_ax} := \frac{F_{coverz}}{n_{cover}} + \frac{4 \cdot M_{cover} \cdot r_{cover}}{n_{cover} \cdot \left(2 \cdot r_{cover}{}^2 - \frac{n_{cover} \cdot A_{M3}}{\pi}\right)}$$

$F_{cover\_ax} = 140.102\ N$

Max. lateral force on screw:

$$F_{cover\_lat} := \frac{F_{coverx}}{n_{cover}}$$

$F_{cover\_lat} = 64.43\ N$

2.2.2 Re-entry

Axial load: $F_{coverzr} := m_{cover} \cdot a_{zr}$ $\quad F_{coverzr} = 257.719\ N$

Lateral load: $F_{coverxr} := m_{cover} \cdot a_{xr}$ $\quad F_{coverxr} = 85.906\ N$

Bending momentum: $M_{coverr} := m_{cover} \cdot a_{xr} \cdot \left(cog_{cover_2} - z_{cover}\right)$ $\quad M_{coverr} = 2.961\ N \cdot m$

Max. axial force on screw:
$$F_{cover\_axr} := \frac{F_{coverzr}}{n_{cover}} + \frac{4 \cdot M_{coverr} \cdot r_{cover}}{n_{cover} \cdot \left(2 \cdot r_{cover}^{\ 2} - \frac{n_{cover} \cdot A_{M3}}{\pi}\right)}$$

$F_{cover\_axr} = 19.431\ N$

Max. lateral force on screw:
$$F_{cover\_latr} := \frac{F_{coverxr}}{n_{cover}}$$

$F_{cover\_latr} = 5.369\ N$

2.3. Launch Adapter interface

2.3.1 Launch

Bolting radius: $r_{launch} := 111.5mm$

Number of bolts: $n_{launch} := 16$

Axial load: $F_{launchz} := m_{launch} \cdot a_z$ $\quad F_{launchz} = 1.71 \times 10^3\ N$

Lateral load: $F_{launchx} := m_{launch} \cdot a_x$ $\quad F_{launchx} = 1.099 \times 10^3\ N$

Bending momentum: $M_{launch} := m_{launch} \cdot a_x \cdot \left(cog_{launch_2} - z_{launch}\right)$ $\quad M_{launch} = 142.306\ N \cdot m$

Max. axial force on screw:
$$F_{launch\_ax} := \frac{F_{launchz}}{n_{launch}} + \frac{4 \cdot M_{launch} \cdot r_{launch}}{n_{launch} \cdot \left(2 \cdot r_{launch}^{\ 2} - \frac{n_{launch} \cdot A_{M3}}{\pi}\right)}$$

$F_{launch\_ax} = 266.548\ N$

Max. lateral force on screw:
$$F_{launch\_lat} := \frac{F_{launchx}}{n_{launch}}$$

$F_{launch\_lat} = 68.688\ N$

2.3.2 Re-entry

Axial load: $F_{launchzr} := m_{launch} \cdot a_{zr}$ $\quad F_{launchzr} = 274.753\ N$

Lateral load: $F_{launchxr} := m_{launch} \cdot a_{xr}$ $\quad F_{launchxr} = 91.584\ N$

Bending momentum: $M_{launchr} := m_{launch} \cdot a_{xr} \cdot \left(cog_{launch_2} - z_{launch}\right)$ $\quad M_{launchr} = 11.859\ N \cdot m$

Max. axial force on screw:

$$F_{launch\_axr} := \frac{F_{launchzr}}{n_{launch}} + \frac{4 \cdot M_{launchr} \cdot r_{launch}}{n_{launch} \cdot \left(2 \cdot r_{launch}^{\ 2} - \frac{n_{launch} \cdot A_{M3}}{\pi}\right)}$$

$F_{launch\_axr} = 30.48\ N$

Max. lateral force on screw:

$$F_{launch\_latr} := \frac{F_{launchxr}}{n_{launch}}$$

$F_{launch\_latr} = 5.724\ N$

2.4. REXUS rocket interface

2.4.1 Launch

Bolting radius: $r_{rexus} := 158mm$

Number of bolts: $n_{rexus} := 16$

Axial load: $F_{rexusz} := m_{sensors} \cdot a_z$ $\quad F_{rexusz} = 382.224\ N$

Lateral load: $F_{rexusx} := m_{rexus} \cdot a_x$ $\quad F_{rexusx} = 1.435 \times 10^3\ N$

Bending momentum: $M_{rexus} := m_{rexus} \cdot a_x \cdot \left(cog_{sensors_2} - z_{sensors}\right)$ $\quad M_{rexus} = 231.97\ N \cdot m$

Max. axial force on screw:

$$F_{rexus\_ax} := \frac{F_{rexusz}}{n_{rexus}} + \frac{4 \cdot M_{rexus} \cdot r_{rexus}}{n_{rexus} \cdot \left(2 \cdot r_{rexus}^{\ 2} - \frac{n_{rexus} \cdot A_{M4}}{\pi}\right)}$$

$F_{rexus\_ax} = 207.574\ N$

Max. lateral force on screw:

$$F_{rexus\_lat} := \frac{F_{rexusx}}{n_{rexus}}$$

$F_{rexus\_lat} = 89.716\ N$

2.4.2 Re-entry

Axial load: $F_{rexuszr} := m_{sensors} \cdot a_{zr}$ $F_{rexuszr} = 61.429\ N$

Lateral load: $F_{rexusxr} := m_{rexus} \cdot a_{xr}$ $F_{rexusxr} = 119.622\ N$

Bending momentum: $M_{rexusr} := m_{rexus} \cdot a_{xr} \cdot \left(cog_{sensors_2} - z_{sensors}\right)$ $M_{rexusr} = 19.331\ N \cdot m$

Max. axial force on screw:

$$F_{rexus\_axr} := \frac{F_{rexuszr}}{n_{rexus}} + \frac{4 \cdot M_{rexusr} \cdot r_{rexus}}{n_{rexus} \cdot \left(2 \cdot r_{rexus}^{\ 2} - \frac{n_{rexus} \cdot A_{M4}}{\pi}\right)}$$

$F_{rexus\_axr} = 19.146\ N$

Max. lateral force on screw:

$$F_{rexus\_latr} := \frac{F_{rexusxr}}{n_{rexus}}$$

$F_{rexus\_latr} = 7.476\ N$

2.5 Electronics Box interface

2.5.1 Launch

Bolting distance: $r_{ebox} := 80mm$

Number of bolts: $n_{ebox} := 4$

Axial load: $F_{eboxz} := m_{ebox} \cdot a_z$ $F_{eboxz} = 440.436\ N$

Lateral load: $F_{eboxx} := m_{ebox} \cdot a_x$ $F_{eboxx} = 283.138\ N$

Bending momentum: $M_{ebox} := m_{ebox} \cdot a_x \cdot \left(cog_{ebox_2} - z_{ebox}\right)$ $M_{ebox} = -16.64\ N \cdot m$

Max. axial force on screw:

$$F_{ebox\_ax} := \frac{F_{eboxz}}{n_{ebox}} + \frac{-M_{ebox}}{2 \cdot r_{ebox}}$$

$F_{ebox\_ax} = 214.107\ N$

Max. lateral force on screw:

$$F_{ebox\_lat} := \frac{F_{eboxx}}{n_{ebox}}$$

$F_{ebox\_lat} = 70.784\ N$

2.5.2 Re-entry

Axial load: $F_{eboxzr} := m_{ebox} \cdot a_{zr}$ $F_{eboxzr} = 70.784\ N$

Lateral load: $F_{eboxxr} := m_{ebox} \cdot a_{xr}$ $F_{eboxxr} = 23.595\ N$

Bending momentum: $M_{eboxr} := m_{ebox} \cdot a_{xr} \cdot \left(cog_{ebox_2} - z_{ebox}\right)$ $M_{eboxr} = -1.387\ N \cdot m$

Max. axial force on screw: $F_{ebox\_axr} := \dfrac{F_{eboxzr}}{n_{ebox}} + \dfrac{-M_{eboxr}}{2 \cdot r_{ebox}}$

$F_{ebox\_axr} = 26.363\ N$

Max. lateral force on screw: $F_{ebox\_latr} := \dfrac{F_{eboxxr}}{n_{ebox}}$

$F_{ebox\_latr} = 5.899\ N$

2.6 Camera Box interface

2.6.1 Launch

Surface width: $r_{cbox} := 30mm$

Number of bolts: $n_{cbox} := 2$

Axial load: $F_{cboxz} := m_{cbox} \cdot a_z$ $F_{cboxz} = 54.917\ N$

Lateral load: $F_{cboxx} := m_{cbox} \cdot a_x$ $F_{cboxx} = 35.304\ N$

Bending momentum: $M_{cbox} := m_{cbox} \cdot a_x \cdot \left(cog_{cbox_2} - z_{cbox}\right)$ $M_{cbox} = -0.55\ N \cdot m$

Max. axial force on screw: $F_{cbox\_ax} := \dfrac{F_{cboxz}}{n_{cbox}} + \dfrac{-M_{cbox}}{r_{cbox}}$

$F_{cbox\_ax} = 45.805\ N$

Max. lateral force on screw: $F_{cbox\_lat} := \dfrac{F_{cboxx}}{n_{cbox}}$

$F_{cbox\_lat} = 17.652\ N$

2.6.2 Re-entry

Axial load: $F_{cboxzr} := m_{cbox} \cdot a_{zr}$ $F_{cboxzr} = 8.826\ N$

Lateral load: $F_{cboxxr} := m_{cbox} \cdot a_{xr}$ $F_{cboxxr} = 2.942\ N$

Bending momentum: $M_{cboxr} := m_{cbox} \cdot a_{xr} \cdot \left(cog_{cbox_2} - z_{cbox}\right)$ $M_{cboxr} = -0.046\,N \cdot m$

Max. axial force on screw: $$F_{cbox\_axr} := \frac{F_{cboxzr}}{n_{cbox}} + \frac{-M_{cboxr}}{r_{cbox}}$$

$$F_{cbox\_axr} = 5.942\ N$$

Max. lateral force on screw: $$F_{cbox\_latr} := \frac{F_{cboxxr}}{n_{cbox}}$$

$$F_{cbox\_latr} = 1.471\ N$$

3. Safety factor calculation

3.1. Sensor Boom interface

3.1.1 Launch

R2 min. fixation force: $$F_{KQ\_sb} := \frac{F_{sensors\_lat}}{q_{F\_sb} \cdot \mu_G}$$ $F_{KQ\_sb} = 204.763\ N$

$F_{KA\_sb} := F_{sensors\_ax}$ $F_{KA\_sb} = 563.213\ N$

$F_{Kerf\_sb} := \max\left(F_{KQ\_sb}, F_{KA\_sb}\right)$ $F_{Kerf\_sb} = 563.213\ N$

R4 settling- and thermal expansion force losses:

f_z is taken from table 5.4/1 of VDI 2230 $f_z := 0.001mm$

$$F_{Z\_sb} := \frac{f_z}{\frac{l_{k\_sb}}{E_{M5} \cdot A_{M5}} + \frac{l_{k\_sb}}{E_{Alu} \cdot 3 \cdot A_{M5}}}$$ $F_{Z\_sb} = 242.439\ N$

(Washer area = 2 * screw area)

$$\Delta F_{th\_sbl} := \frac{(\alpha_{St} - \alpha_{Alu}) \cdot \Delta T_{launch} \cdot l_{k\_sb}}{\frac{l_{k\_sb}}{E_{M5} \cdot A_{M5}} + \frac{l_{k\_sb}}{E_{Alu} \cdot (2 \cdot A_{M5})}} \qquad \Delta F_{th\_sbl} = 0$$

R5 minimum mounting force:

$$F_{Mmin\_sb} := (F_{Kerf\_sb} + F_{sensors\_ax} + F_{Z\_sb}) \cdot j_{ext} \qquad F_{Mmin\_sb} = 1.78 \times 10^{3}\ N$$

R6 maximum mounting force:

$$F_{Mmax\_sb} := \alpha_A \cdot F_{Mmin\_sb} \qquad F_{Mmax\_sb} = 2.847 \times 10^{3}\ N$$

R8 operational load on screw:

$$F_{Smax\_sb} := F_{Mmax\_sb} + F_{sensors\_ax} - \Delta F_{th\_sbl} \qquad F_{Smax\_sb} = 3.41 \times 10^{3}\ N$$

$$\sigma_{Zmax\_sb} := \frac{F_{Smax\_sb}}{A_{M5}} \qquad \sigma_{Zmax\_sb} = 240.173\ MPa$$

$$\tau_{max\_sb} := \frac{F_{Mmax\_sb} \cdot \frac{d_{M5}}{2} \left(\frac{P_{M5}}{\pi \cdot d_{M5}} + 1.155 \cdot \mu_K \right)}{\frac{\pi}{16} \cdot d_{M5}^{3}} \qquad \tau_{max\_sb} = 103.983\ MPa$$

$$S_{F\_sb} := 640 \frac{MPa}{\sqrt{\sigma_{Zmax\_sb}^{2} + 3 \cdot (0.5 \cdot \tau_{max\_sb})^{2}}} \qquad \boxed{S_{F\_sb} = 2.495}$$

R12 safety against gliding:

$$F_{KRmin\_sb} := \frac{F_{Mmax\_sb}}{\alpha_A} - F_{sensors\_ax} - F_{Z\_sb} \qquad F_{KRmin\_sb} = 973.872\ N$$

$$S_{G\_sb} := \frac{F_{KRmin\_sb}}{F_{KQ\_sb}} \qquad \boxed{S_{G\_sb} = 4.756}$$

R13 required tigtening momentum:

$$M_{A\_sb} := F_{Mmax\_sb} \cdot \left(0.16 \cdot P_{M5} + 0.58 \cdot d_{M5} \cdot \mu_G + \frac{1.5 \cdot d_{M5}}{2} \cdot \mu_K \right) \qquad \boxed{M_{A\_sb} = 3.757\ N \cdot m}$$

3.1.2 Re-entry

R4 settling- and thermal expansion force losses:

(Washer area = 2 * screw area)

$$\Delta F_{th\_sbr} := \frac{(\alpha_{St} - \alpha_{Alu}) \cdot \Delta T_{entry} \cdot l_{k\_sb}}{\frac{l_{k\_sb}}{E_{M5} \cdot A_{M5}} + \frac{l_{k\_sb}}{E_{Alu} \cdot (2 \cdot A_{M5})}} \qquad \Delta F_{th\_sbr} = -2.147 \times 10^{3}\ \mathrm{N}$$

R8 operational load on screw:

$$F_{Smax\_sbr} := F_{Mmax\_sb} + F_{sensors\_axr} - \Delta F_{th\_sbr} \qquad F_{Smax\_sbr} = 5.046 \times 10^{3}\ \mathrm{N}$$

$$\sigma_{Zmax\_sbr} := \frac{F_{Smax\_sbr}}{A_{M5}} \qquad \sigma_{Zmax\_sbr} = 355.362\ \mathrm{MPa}$$

$$S_{F\_sbr} := 640 \frac{\mathrm{MPa}}{\sqrt{\sigma_{Zmax\_sbr}^{2} + 3 \cdot (0.5 \cdot \tau_{max\_sb})^{2}}} \qquad \boxed{S_{F\_sbr} = 1.746}$$

R12 safety against gliding:

$$F_{KRmin\_sbr} := \frac{F_{Mmax\_sb}}{\alpha_{A}} - F_{sensors\_axr} - F_{Z\_sb} \qquad F_{KRmin\_sbr} = 1.485 \times 10^{3}\ \mathrm{N}$$

$$S_{G\_sbr} := \frac{F_{KRmin\_sbr}}{F_{KQ\_sb}} \qquad \boxed{S_{G\_sbr} = 7.253}$$

3.2. Cylinder Cover interface

3.2.1 Launch

R2 min. fixation force:

$$F_{KQ\_cc} := \frac{F_{cover\_lat}}{q_{F\_cc} \cdot \mu_{G}} \qquad F_{KQ\_cc} = 322.148\ \mathrm{N}$$

$$F_{KA\_cc} := F_{cover\_ax} \qquad F_{KA\_cc} = 140.102\ \mathrm{N}$$

$$F_{Kerf\_cc} := \max(F_{KQ\_cc}, F_{KA\_cc}) \qquad F_{Kerf\_cc} = 322.148\ \mathrm{N}$$

R4 settling- and thermal expansion force losses:

f_z is taken from table 5.4/1 of VDI 2230

$$F_{Z\_cc} := \frac{f_{z}}{\frac{l_{k\_cc}}{E_{M3} \cdot A_{M3}} + \frac{l_{k\_cc}}{E_{Alu} \cdot 2 \cdot A_{M3}}} \qquad F_{Z\_cc} = 118.353\ \mathrm{N}$$

(Washer area = 2 * screw area)

$$\Delta F_{th\_ccl} := \frac{(\alpha_{St} - \alpha_{Alu}) \cdot \Delta T_{launch} \cdot l_{k\_cc}}{\frac{l_{k\_cc}}{E_{M3} \cdot A_{M3}} + \frac{l_{k\_cc}}{E_{Alu} \cdot (2 \cdot A_{M3})}} \qquad \Delta F_{th\_ccl} = 0$$

R5 minimum mounting force:

$$F_{Mmin\_cc} := (F_{Kerf\_cc} + F_{cover\_ax} + F_{Z\_cc}) \cdot j_{ext} \qquad F_{Mmin\_cc} = 754.784\ \mathrm{N}$$

R6 maximum mounting force:

$$F_{Mmax\_cc} := \alpha_A \cdot F_{Mmin\_cc} \qquad F_{Mmax\_cc} = 1.208 \times 10^3\ \mathrm{N}$$

R8 operational load on screw:

$$F_{Smax\_cc} := F_{Mmax\_cc} + F_{cover\_ax} - \Delta F_{th\_ccl} \qquad F_{Smax\_cc} = 1.348 \times 10^3\ \mathrm{N}$$

$$\sigma_{Zmax\_cc} := \frac{F_{Smax\_cc}}{A_{M3}} \qquad \sigma_{Zmax\_cc} = 267.944\ \mathrm{MPa}$$

$$\tau_{max\_cc} := \frac{F_{Mmax\_cc} \cdot \frac{d_{M3}}{2} \left(\frac{P_{M3}}{\pi \cdot d_{M3}} + 1.155 \cdot \mu_K \right)}{\frac{\pi}{16} \cdot d_{M3}^{\ 3}} \qquad \tau_{max\_cc} = 132.934\ \mathrm{MPa}$$

$$S_{F\_cc} := 640 \frac{\mathrm{MPa}}{\sqrt{\sigma_{Zmax\_cc}^{\ 2} + 3 \cdot (0.5 \cdot \tau_{max\_cc})^2}} \qquad S_{F\_cc} = 2.195$$

R12 safety against gliding:

$$F_{KRmin\_cc} := \frac{F_{Mmax\_cc}}{\alpha_A} - F_{cover\_ax} - F_{Z\_cc} \qquad F_{KRmin\_cc} = 496.329\ \mathrm{N}$$

$$S_{G\_cc} := \frac{F_{KRmin\_cc}}{F_{KQ\_cc}} \qquad S_{G\_cc} = 1.541$$

R13 required tigtening momentum:

$$M_{A\_cc} := F_{Mmax\_cc} \cdot \left(0.16 \cdot P_{M3} + 0.58 \cdot d_{M3} \cdot \mu_G + \frac{1.5 \cdot d_{M3}}{2} \cdot \mu_K \right) \qquad M_{A\_cc} = 0.932\ \mathrm{N \cdot m}$$

EuroLaunch
A DLR and SSC cooperation

3.2.2 Re-entry

R4 settling- and thermal expansion force losses:

(Washer area = 2 * screw area)

$$\Delta F_{th\_ccr} := \frac{(\alpha_{St} - \alpha_{Alu}) \cdot \Delta T_{entry} \cdot l_{k\_cc}}{\frac{l_{k\_cc}}{E_{M3} \cdot A_{M3}} + \frac{l_{k\_cc}}{E_{Alu} \cdot (2 \cdot A_{M3})}} \qquad \Delta F_{th\_ccr} = -760.536\ \mathrm{N}$$

R8 operational load on screw:

$$F_{Smax\_ccr} := F_{Mmax\_cc} + F_{cover\_axr} - \Delta F_{th\_ccr} \qquad F_{Smax\_ccr} = 1.988 \times 10^{3}\ \mathrm{N}$$

$$\sigma_{Zmax\_ccr} := \frac{F_{Smax\_ccr}}{A_{M3}} \qquad \sigma_{Zmax\_ccr} = 395.153\ \mathrm{MPa}$$

$$S_{F\_ccr} := 640 \frac{\mathrm{MPa}}{\sqrt{\sigma_{Zmax\_ccr}^{2} + 3 \cdot (0.5 \cdot \tau_{max\_cc})^{2}}} \qquad S_{F\_ccr} = 1.555$$

R12 safety against gliding:

$$F_{KRmin\_ccr} := \frac{F_{Mmax\_cc}}{\alpha_A} - F_{cover\_axr} - F_{Z\_cc} \qquad F_{KRmin\_ccr} = 617\ \mathrm{N}$$

$$S_{G\_ccr} := \frac{F_{KRmin\_ccr}}{F_{KQ\_cc}} \qquad S_{G\_ccr} = 1.915$$

3.3. Launch Adapter interface

3.3.1 Lauinch

R2 min. fixation force:

$$F_{KQ\_la} := \frac{F_{launch\_lat}}{q_{F\_la} \cdot \mu_G} \qquad F_{KQ\_la} = 343.441\ \mathrm{N}$$

$$F_{KA\_la} := F_{launch\_ax} \qquad F_{KA\_la} = 266.548\ \mathrm{N}$$

$$F_{Kerf\_la} := \max(F_{KQ\_la}, F_{KA\_la}) \qquad F_{Kerf\_la} = 343.441\ \mathrm{N}$$

R4 settling- and thermal expansion force losses:

f_z is taken from table 5.4/1 of VDI 2230

$$F_{Z\_la} := \frac{f_Z}{\frac{l_{k\_la}}{E_{M3} \cdot A_{M3}} + \frac{l_{k\_la}}{E_{Alu} \cdot 2 \cdot A_{M3}}}$$ $$F_{Z\_la} = 27.616\ N$$

(Washer area = 2 * screw area)

$$\Delta F_{th\_lal} := \frac{(\alpha_{St} - \alpha_{Alu}) \cdot \Delta T_{launch} \cdot l_{k\_la}}{\frac{l_{k\_la}}{E_{M3} \cdot A_{M3}} + \frac{l_{k\_la}}{E_{Alu} \cdot (2 \cdot A_{M3})}}$$ $$\Delta F_{th\_lal} = 0$$

R5 minimum mounting force:

$$F_{Mmin\_la} := (F_{Kerf\_la} + F_{launch\_ax} + F_{Z\_la}) \cdot j_{ext}$$ $$F_{Mmin\_la} = 828.887\ N$$

R6 maximum mounting force:

$$F_{Mmax\_la} := \alpha_A \cdot F_{Mmin\_la}$$ $$F_{Mmax\_la} = 1.326 \times 10^3\ N$$

R8 operational load on screw:

$$F_{Smax\_la} := F_{Mmax\_la} + F_{launch\_ax} - \Delta F_{th\_lal}$$ $$F_{Smax\_la} = 1.593 \times 10^3\ N$$

$$\sigma_{Zmax\_la} := \frac{F_{Smax\_la}}{A_{M3}}$$ $$\sigma_{Zmax\_la} = 316.653\ MPa$$

$$\tau_{max\_la} := \frac{F_{Mmax\_la} \cdot \frac{d_{M3}}{2} \left(\frac{P_{M3}}{\pi \cdot d_{M3}} + 1.155 \cdot \mu_K \right)}{\frac{\pi}{16} \cdot d_{M3}^{\ 3}}$$ $$\tau_{max\_la} = 145.985\ MPa$$

$$S_{F\_la} := 640 \cdot \frac{MPa}{\sqrt{\sigma_{Zmax\_la}^{\ 2} + 3 \cdot (0.5 \cdot \tau_{max\_la})^2}}$$ $$S_{F\_la} = 1.877$$

R12 safety against gliding:

$$F_{KRmin\_la} := \frac{F_{Mmax\_la}}{\alpha_A} - F_{launch\_ax} - F_{Z\_la}$$ $$F_{KRmin\_la} = 534.723\ N$$

$$S_{G\_la} := \frac{F_{KRmin\_la}}{F_{KQ\_la}}$$ $$S_{G\_la} = 1.557$$

R13 required tigtening momentum:

$$M_{A\_la} := F_{Mmax\_la} \cdot \left(0.16 \cdot P_{M3} + 0.58 \cdot d_{M3} \cdot \mu_G + \frac{1.5 \cdot d_{M3}}{2} \cdot \mu_K \right)$$ $$M_{A\_la} = 1.023\ N \cdot m$$

3.3.2 Re-entry

R4 settling- and thermal expansion force losses:

(Washer area = 2 * screw area)

$$\Delta F_{th\_lar} := \frac{(\alpha_{St} - \alpha_{Alu}) \cdot \Delta T_{entry} \cdot l_{k\_la}}{\frac{l_{k\_la}}{E_{M3} \cdot A_{M3}} + \frac{l_{k\_la}}{E_{Alu} \cdot (2 \cdot A_{M3})}} \qquad \Delta F_{th\_lar} = -760.536 \text{ N}$$

R8 operational load on screw:

$$F_{Smax\_lar} := F_{Mmax\_la} + F_{launch\_axr} - \Delta F_{th\_lar} \qquad F_{Smax\_lar} = 2.117 \times 10^{3} \text{ N}$$

$$\sigma_{Zmax\_lar} := \frac{F_{Smax\_lar}}{A_{M3}} \qquad \sigma_{Zmax\_lar} = 420.921 \text{ MPa}$$

$$S_{F\_lar} := 640 \frac{\text{MPa}}{\sqrt{\sigma_{Zmax\_lar}^{2} + 3 \cdot (0.5 \cdot \tau_{max\_la})^{2}}} \qquad S_{F\_lar} = 1.456$$

R12 safety against gliding:

$$F_{KRmin\_lar} := \frac{F_{Mmax\_la}}{\alpha_A} - F_{launch\_axr} - F_{Z\_la} \qquad F_{KRmin\_lar} = 770.791 \text{ N}$$

$$S_{G\_lar} := \frac{F_{KRmin\_lar}}{F_{KQ\_la}} \qquad S_{G\_lar} = 2.244$$

3.4. REXUS rocket interface

3.4.1 Launch

R2 min. fixation force:

$$F_{KQ\_r} := \frac{F_{rexus\_lat}}{q_{F\_r} \cdot \mu_G} \qquad F_{KQ\_r} = 448.581 \text{ N}$$

$$F_{KA\_r} := F_{rexus\_ax} \qquad F_{KA\_r} = 207.574 \text{ N}$$

$$F_{Kerf\_r} := \max(F_{KQ\_r}, F_{KA\_r}) \qquad F_{Kerf\_r} = 448.581 \text{ N}$$

R4 settling- and thermal expansion force losses:

f_z is taken from table 5.4/1 of VDI 2230

$$F_{Z\_r} := \frac{f_z}{\frac{l_{k\_r}}{E_{M4} \cdot A_{M4}} + \frac{l_{k\_r}}{E_{Alu} \cdot 2 \cdot A_{M4}}} \qquad F_{Z\_r} = 180.765\ \mathrm{N}$$

(Washer area = 2 * screw area)

$$\Delta F_{th\_rl} := \frac{(\alpha_{St} - \alpha_{Alu}) \cdot \Delta T_{launch} \cdot l_{k\_r}}{\frac{l_{k\_r}}{E_{M4} \cdot A_{M4}} + \frac{l_{k\_r}}{E_{Alu} \cdot (2 \cdot A_{M4})}} \qquad \Delta F_{th\_rl} = 0$$

R5 minimum mounting force:

$$F_{Mmin\_r} := (F_{Kerf\_r} + F_{rexus\_ax} + F_{Z\_r}) \cdot j_{ext} \qquad F_{Mmin\_r} = 1.088 \times 10^3\ \mathrm{N}$$

R6 maximum mounting force:

$$F_{Mmax\_r} := \alpha_A \cdot F_{Mmin\_r} \qquad F_{Mmax\_r} = 1.741 \times 10^3\ \mathrm{N}$$

R8 operational load on screw:

$$F_{Smax\_r} := F_{Mmax\_r} + F_{rexus\_ax} - \Delta F_{th\_rl} \qquad F_{Smax\_r} = 1.948 \times 10^3\ \mathrm{N}$$

$$\sigma_{Zmax\_r} := \frac{F_{Smax\_r}}{A_{M4}} \qquad \sigma_{Zmax\_r} = 221.91\ \mathrm{MPa}$$

$$\tau_{max\_r} := \frac{F_{Mmax\_r} \cdot \frac{d_{M4}}{2} \left(\frac{P_{M4}}{\pi \cdot d_{M4}} + 1.155 \cdot \mu_K \right)}{\frac{\pi}{16} \cdot d_{M4}^{\ 3}} \qquad \tau_{max\_r} = 103.654\ \mathrm{MPa}$$

$$S_{F\_r} := 640 \frac{\mathrm{MPa}}{\sqrt{\sigma_{Zmax\_r}^{\ 2} + 3 \cdot (0.5 \cdot \tau_{max\_r})^2}} \qquad \boxed{S_{F\_r} = 2.674}$$

R12 safety against gliding:

$$F_{KRmin\_r} := \frac{F_{Mmax\_r}}{\alpha_A} - F_{rexus\_ax} - F_{Z\_r} \qquad F_{KRmin\_r} = 699.657\ \mathrm{N}$$

$$S_{G\_r} := \frac{F_{KRmin\_r}}{F_{KQ\_r}} \qquad \boxed{S_{G\_r} = 1.56}$$

R13 required tigtening momentum:

$$M_{A\_r} := F_{Mmax\_r} \cdot \left(0.16 \cdot P_{M4} + 0.58 \cdot d_{M4} \cdot \mu_G + \frac{1.5 \cdot d_{M4}}{2} \cdot \mu_K \right) \qquad \boxed{M_{A\_r} = 1.836\ \mathrm{N \cdot m}}$$

3.4.2 Re-entry

R4 settling- and thermal expansion force losses:

(Washer area = 2 * screw area)

$$\Delta F_{th\_rr} := \frac{(\alpha_{St} - \alpha_{Alu}) \cdot \Delta T_{entry} \cdot l_{k\_r}}{\frac{l_{k\_r}}{E_{M4} \cdot A_{M4}} + \frac{l_{k\_r}}{E_{Alu} \cdot (2 \cdot A_{M4})}} \qquad \Delta F_{th\_rr} = -1.328 \times 10^{3}\ N$$

R8 operational load on screw:

$$F_{Smax\_rr} := F_{Mmax\_r} + F_{rexus\_axr} - \Delta F_{th\_rr} \qquad F_{Smax\_rr} = 3.087 \times 10^{3}\ N$$

$$\sigma_{Zmax\_rr} := \frac{F_{Smax\_rr}}{A_{M4}} \qquad \sigma_{Zmax\_rr} = 351.649\ MPa$$

$$S_{F\_rr} := 640 \frac{MPa}{\sqrt{\sigma_{Zmax\_rr}^{2} + 3 \cdot (0.5 \cdot \tau_{max\_r})^{2}}} \qquad \boxed{S_{F\_rr} = 1.763}$$

R12 safety against gliding:

$$F_{KRmin\_rr} := \frac{F_{Mmax\_r}}{\alpha_A} - F_{rexus\_axr} - F_{Z\_r} \qquad F_{KRmin\_rr} = 888.084\ N$$

$$S_{G\_rr} := \frac{F_{KRmin\_rr}}{F_{KQ\_r}} \qquad \boxed{S_{G\_rr} = 1.98}$$

3.5. Electronix Box interface

3.5.1 Launch

R2 min. fixation force:

$$F_{KQ\_eb} := \frac{F_{ebox\_lat}}{q_{F\_eb} \cdot \mu_G} \qquad F_{KQ\_eb} = 353.922\ N$$

$$F_{KA\_eb} := F_{ebox\_ax} \qquad F_{KA\_eb} = 214.107\ N$$

$$F_{Kerf\_eb} := \max(F_{KQ\_eb}, F_{KA\_eb}) \qquad F_{Kerf\_eb} = 353.922\ N$$

R4 settling- and thermal expansion force losses:

f_z is taken from table 5.4/1 of VDI 2230

$$F_{Z\_eb} := \frac{f_z}{\frac{l_{k\_eb}}{E_{M5} \cdot A_{M5}} + \frac{l_{k\_eb}}{E_{Alu} \cdot 2 \cdot A_{M5}}} \qquad F_{Z\_eb} = 66.824\ \mathrm{N}$$

(Washer area = 2 * screw area)

$$\Delta F_{th\_ebl} := \frac{(\alpha_{St} - \alpha_{Alu}) \cdot \Delta T_{launch} \cdot l_{k\_eb}}{\frac{l_{k\_eb}}{E_{M5} \cdot A_{M5}} + \frac{l_{k\_eb}}{E_{Alu} \cdot (2 \cdot A_{M5})}} \qquad \Delta F_{th\_ebl} = 0$$

R5 minimum mounting force:

$$F_{Mmin\_eb} := (F_{Kerf\_eb} + F_{ebox\_ax} + F_{Z\_eb}) \cdot j_{ext} \qquad F_{Mmin\_eb} = 825.309\ \mathrm{N}$$

R6 maximum mounting force:

$$F_{Mmax\_eb} := \alpha_A \cdot F_{Mmin\_eb} \qquad F_{Mmax\_eb} = 1.32 \times 10^3\ \mathrm{N}$$

R8 operational load on screw:

$$F_{Smax\_eb} := F_{Mmax\_eb} + F_{ebox\_ax} - \Delta F_{th\_ebl} \qquad F_{Smax\_eb} = 1.535 \times 10^3\ \mathrm{N}$$

$$\sigma_{Zmax\_eb} := \frac{F_{Smax\_eb}}{A_{M5}} \qquad \sigma_{Zmax\_eb} = 108.071\ \mathrm{MPa}$$

$$\tau_{max\_eb} := \frac{F_{Mmax\_eb} \cdot \frac{d_{M5}}{2} \left(\frac{P_{M5}}{\pi \cdot d_{M5}} + 1.155 \cdot \mu_K \right)}{\frac{\pi}{16} \cdot d_{M5}^{\ 3}} \qquad \tau_{max\_eb} = 48.225\ \mathrm{MPa}$$

$$S_{F\_eb} := 640 \frac{\mathrm{MPa}}{\sqrt{\sigma_{Zmax\_eb}^{\ 2} + 3 \cdot (0.5 \cdot \tau_{max\_eb})^2}} \qquad \boxed{S_{F\_eb} = 5.524}$$

R12 safety against gliding:

$$F_{KRmin\_eb} := \frac{F_{Mmax\_eb}}{\alpha_A} - F_{ebox\_ax} - F_{Z\_eb} \qquad F_{KRmin\_eb} = 544.378\ \mathrm{N}$$

$$S_{G\_eb} := \frac{F_{KRmin\_eb}}{F_{KQ\_eb}} \qquad \boxed{S_{G\_eb} = 1.538}$$

R13 required tigtening momentum:

$$M_{A\_eb} := F_{Mmax\_eb} \cdot \left(0.16 \cdot P_{M5} + 0.58 \cdot d_{M5} \cdot \mu_G + \frac{1.5 \cdot d_{M5}}{2} \cdot \mu_K \right) \qquad \boxed{M_{A\_eb} = 1.743\ \mathrm{N \cdot m}}$$

3.5.2 Re-entry

R4 settling- and thermal expansion force losses:

(Washer area = 2 * screw area)

$$\Delta F_{th\_ebr} := \frac{(\alpha_{St} - \alpha_{Alu}) \cdot \Delta T_{entry} \cdot l_{k\_eb}}{\frac{l_{k\_eb}}{E_{M5} \cdot A_{M5}} + \frac{l_{k\_eb}}{E_{Alu} \cdot (2 \cdot A_{M5})}} \qquad \Delta F_{th\_ebr} = -2.147 \times 10^{3}\ N$$

R8 operational load on screw:

$$F_{Smax\_ebr} := F_{Mmax\_eb} + F_{ebox\_axr} - \Delta F_{th\_ebr} \qquad F_{Smax\_ebr} = 3.494 \times 10^{3}\ N$$

$$\sigma_{Zmax\_ebr} := \frac{F_{Smax\_ebr}}{A_{M5}} \qquad \sigma_{Zmax\_ebr} = 246.049\ MPa$$

$$S_{F\_ebr} := 640 \frac{MPa}{\sqrt{\sigma_{Zmax\_ebr}^{2} + 3 \cdot (0.5 \cdot \tau_{max\_eb})^{2}}} \qquad \boxed{S_{F\_ebr} = 2.564}$$

R12 safety against gliding:

$$F_{KRmin\_ebr} := \frac{F_{Mmax\_eb}}{\alpha_{A}} - F_{ebox\_axr} - F_{Z\_eb} \qquad F_{KRmin\_ebr} = 732.122\ N$$

$$S_{G\_ebr} := \frac{F_{KRmin\_ebr}}{F_{KQ\_eb}} \qquad \boxed{S_{G\_ebr} = 2.069}$$

3.6. Camera Box interface

3.6.1 Launch

R2 min. fixation force:

$$F_{KQ\_cb} := \frac{F_{cbox\_lat}}{q_{F\_cb} \cdot \mu_{G}} \qquad F_{KQ\_cb} = 88.26\ N$$

$$F_{KA\_cb} := F_{cbox\_ax} \qquad F_{KA\_cb} = 45.805\ N$$

$$F_{Kerf\_cb} := \max(F_{KQ\_cb}, F_{KA\_cb}) \qquad F_{Kerf\_cb} = 88.26\ N$$

R4 settling- and thermal expansion force losses:

f_z is taken from table 5.4/1 of VDI 2230

$$F_{Z\_cb} := \frac{f_z}{\frac{l_{k\_cb}}{E_{M5} \cdot A_{M5}} + \frac{l_{k\_cb}}{E_{Alu} \cdot 2 \cdot A_{M5}}} \qquad F_{Z\_cb} = 292.353\ N$$

(Washer area = 2 * screw area)

$$\Delta F_{th\_cbl} := \frac{(\alpha_{St} - \alpha_{Alu}) \cdot \Delta T_{launch} \cdot l_{k\_cb}}{\frac{l_{k\_cb}}{E_{M5} \cdot A_{M5}} + \frac{l_{k\_cb}}{E_{Alu} \cdot (2 \cdot A_{M5})}} \qquad \Delta F_{th\_cbl} = 0$$

R5 minimum mounting force:

$$F_{Mmin\_cb} := (F_{Kerf\_cb} + F_{cbox\_ax} + F_{Z\_cb}) \cdot j_{ext} \qquad F_{Mmin\_cb} = 554.343\ N$$

R6 maximum mounting force:

$$F_{Mmax\_cb} := \alpha_A \cdot F_{Mmin\_cb} \qquad F_{Mmax\_cb} = 886.949\ N$$

R8 operational load on screw:

$$F_{Smax\_cb} := F_{Mmax\_cb} + F_{cbox\_ax} - \Delta F_{th\_cbl} \qquad F_{Smax\_cb} = 932.754\ N$$

$$\sigma_{Zmax\_cb} := \frac{F_{Smax\_cb}}{A_{M5}} \qquad \sigma_{Zmax\_cb} = 65.687\ MPa$$

$$\tau_{max\_cb} := \frac{F_{Mmax\_cb} \cdot \frac{d_{M5}}{2} \left(\frac{P_{M5}}{\pi \cdot d_{M5}} + 1.155 \cdot \mu_K \right)}{\frac{\pi}{16} \cdot d_{M5}^{\ 3}} \qquad \tau_{max\_cb} = 32.392\ MPa$$

$$S_{F\_cb} := 640 \frac{MPa}{\sqrt{\sigma_{Zmax\_cb}^{\ 2} + 3 \cdot (0.5 \cdot \tau_{max\_cb})^2}} \qquad \boxed{S_{F\_cb} = 8.96}$$

R12 safety against gliding:

$$F_{KRmin\_cb} := \frac{F_{Mmax\_cb}}{\alpha_A} - F_{cbox\_ax} - F_{Z\_cb} \qquad F_{KRmin\_cb} = 216.185\ N$$

$$S_{G\_cb} := \frac{F_{KRmin\_cb}}{F_{KQ\_cb}} \qquad \boxed{S_{G\_cb} = 2.449}$$

R13 required tigtening momentum:

$$M_{A\_cb} := F_{Mmax\_cb} \cdot \left(0.16 \cdot P_{M5} + 0.58 \cdot d_{M5} \cdot \mu_G + \frac{1.5 \cdot d_{M5}}{2} \cdot \mu_K \right) \qquad \boxed{M_{A\_cb} = 1.17\ N \cdot m}$$

EUROLAUNCH
A DLR and SSC cooperation

3.6.2 Re-entry

R4 settling- and thermal expansion force losses:

(Washer area = 2 * screw area)

$$\Delta F_{th\_cbr} := \frac{(\alpha_{St} - \alpha_{Alu}) \cdot \Delta T_{entry} \cdot l_{k\_cb}}{\frac{l_{k\_cb}}{E_{M5} \cdot A_{M5}} + \frac{l_{k\_cb}}{E_{Alu} \cdot (2 \cdot A_{M5})}} \qquad \Delta F_{th\_cbr} = -2.147 \times 10^{3}\ \text{N}$$

R8 operational load on screw:

$$F_{Smax\_cbr} := F_{Mmax\_cb} + F_{cbox\_axr} - \Delta F_{th\_cbr} \qquad F_{Smax\_cbr} = 3.04 \times 10^{3}\ \text{N}$$

$$\sigma_{Zmax\_cbr} := \frac{F_{Smax\_cbr}}{A_{M5}} \qquad \sigma_{Zmax\_cbr} = 214.08\ \text{MPa}$$

$$S_{F\_cbr} := 640 \frac{\text{MPa}}{\sqrt{\sigma_{Zmax\_cbr}^{2} + 3 \cdot (0.5 \cdot \tau_{max\_cb})^{2}}} \qquad \boxed{S_{F\_cbr} = 2.964}$$

R12 safety against gliding:

$$F_{KRmin\_cbr} := \frac{F_{Mmax\_cb}}{\alpha_{A}} - F_{cbox\_axr} - F_{Z\_cb} \qquad F_{KRmin\_cbr} = 256.048\ \text{N}$$

$$S_{G\_cbr} := \frac{F_{KRmin\_cbr}}{F_{KQ\_cb}} \qquad \boxed{S_{G\_cbr} = 2.901}$$

C.3 Electronics Integration

C.3.1 PCDU

REMOS Integration Protocol

General

Assembly: **REMOS PCDU**

Date: 19.-20.09.2010

Integrator: S. Schweikle

QA: R. Wuseni

Used Tools

- ESD certified cutter
- ESD wristband
- ESD gloves
- Bending tool
- Isopropanol
- Flux
- Cleaning utilities
- Spacers for soldering
- Solder (Non RoHS, contains Pb)
- Soldering paste (Non RoHS, contains Pb)
- Hot air soldering system with temperature regulation
- Soldering-iron with temperature regulation
- USB Microscope

- Laptop for Picture recording
- Tweezers set
- Multimeter with RCL measurement
- Solder sucker
- De-soldering cord

Details

Required Parts

Pos	Amount	Name	Value	Housing
1	2	C1,C3	250nF	2,54X5,08_RM2,54
2	3	C2,C6,C9	100µF	2817_ELKO
3	4	C4,C5,C7,C8	10µF	2817_ELKO
4	2	C10,C15	0,1µF	0805
5	4	C11,C12,C13,C14	10µF	1206_ELKO
6	3	D1,D2,D3	1N5819	DO41
7	2	IC1,IC2	MC34063A(DIL 8)	DIL8
8	1	IC3	IRU1117-5	SOT223
9	2	IC4,IC5	MAX603	SO8_SOT96-1
10	1	IC6	MAX6675ISA	SO8_SOT96-1
11	1	K1	Bus-Connector	WANNENSTECKER-16-ST_HEBEL
12	1	K2	Thermocouple	1X02_BUCHSE
13	3	L1,L2,L3	100µH	07HCP
14	5	R1,R4,R7,R8,R9	0R22	R5
15	2	R2,R5	1,21K	0207_MET
16	2	R3,R6	5,6K	0207_MET

Part details

PCB Bottom View

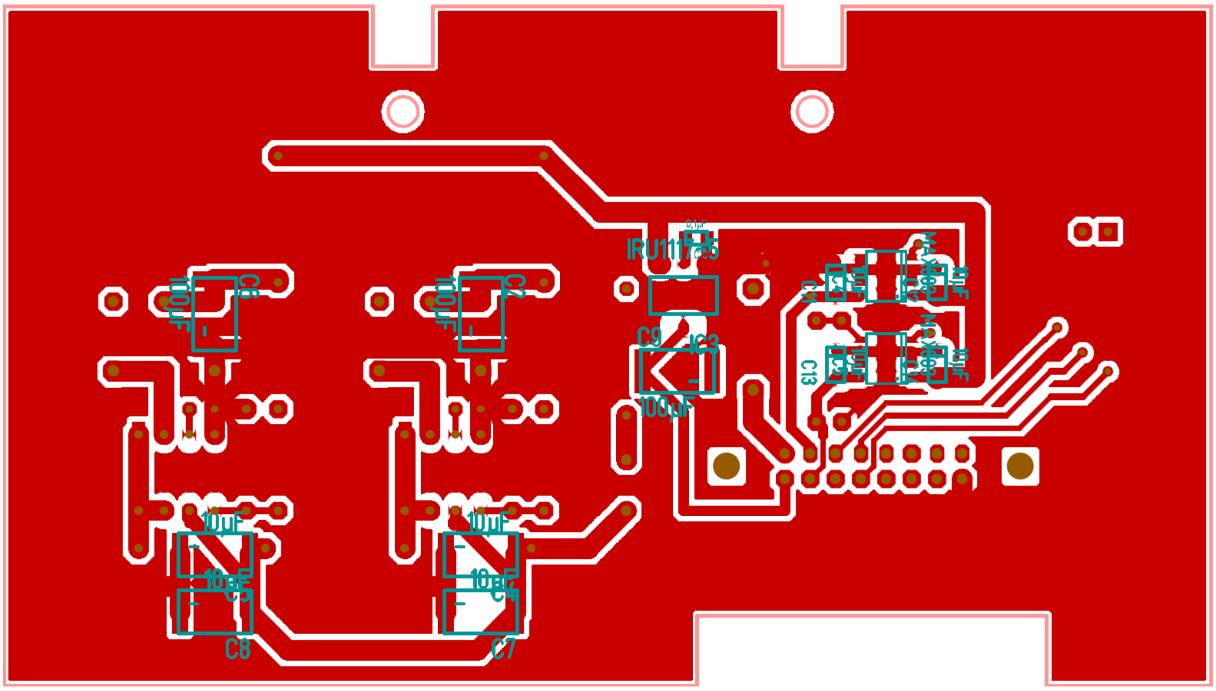

PCB Top View

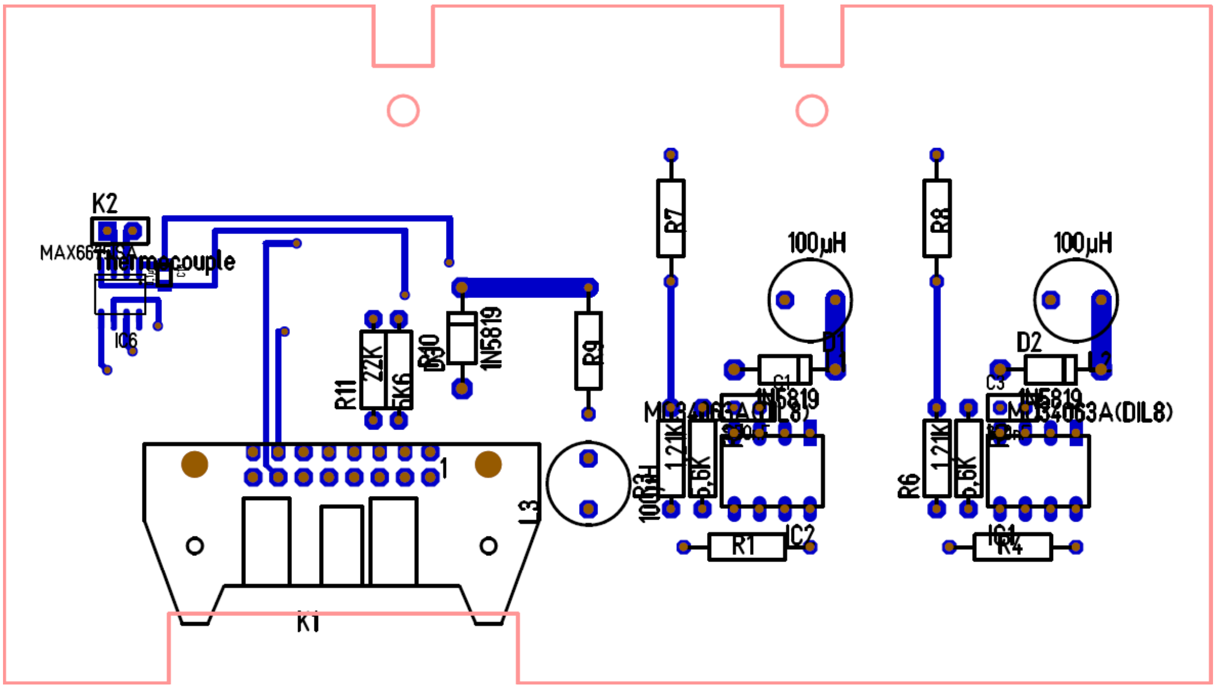

Integration

Positions and Verification of Parts

Nr.	Part	Nom. Value	Housing	X-Pos.	Y-Pos	Side	Measured Value
2	C2	100µF	2817_ELKO	73,200	37,175	bottom	100 µF
4	C4	10µF	2817_ELKO	73,200	13,045	bottom	
5	C5	10µF	2817_ELKO	99,870	13,045	bottom	
6	C6	100µF	2817_ELKO	99,870	37,175	bottom	99 µF
7	C7	10µF	2817_ELKO	73,200	7,330	bottom	
8	C8	10µF	2817_ELKO	99,870	7,330	bottom	
9	C9	100µF	2817_ELKO	53,515	31,460	bottom	97 µF
21	IC3	IRU1117-5	SOT223	52,880	39,080	bottom	-
10	C10	0,1µF	0805	51,610	44,795	bottom	105,1 nF
22	IC4	MAX603	SO8_SOT96-1	32,560	40,985	bottom	-
23	IC5	MAX603	SO8_SOT96-1	32,560	32,730	bottom	-
11	C11	10µF	1206_ELKO	37,640	40,350	bottom	10,28 µF
12	C12	10µF	1206_ELKO	27,480	40,350	bottom	10,34 µF
13	C13	10µF	1206_ELKO	37,640	32,095	bottom	10,29 µF
14	C14	10µF	1206_ELKO	27,480	32,095	bottom	10,13 µF
30	R1	0R22	R5	74,470	13,680	top	0,22 Ω
31	R2	1,21K	0207_MET	70,025	22,570	top	1,199 kΩ
32	R3	5,6K	0207_MET	66,850	22,570	top	5,56 kΩ
33	R4	0R22	R5	101,140	13,680	top	0,21Ω
34	R5	1,21K	0207_MET	96,695	22,570	top	1,200 kΩ

35	R6	5,6K	0207_MET	93,520	22,570	top	5,58 kΩ
36	R7	0R22	R5	66,850	46,700	top	0,22Ω
37	R8	0R22	R5	93,520	46,700	top	0,22Ω
38	R9	0R22	R5	58,595	33,365	top	0,21Ω
39	R10	22K	0207_MET	39,545	31,460	top	21,6 kΩ
40	R11	5K6	0207_MET	37,005	31,460	top	5,58 kΩ
1	C1	150pF	2,54X5,08_RM2,54	74,470	27,650	top	145 pF
3	C3	150pF	2,54X5,08_RM2,54	101,140	27,650	top	146 pF
15	C15	0,1µF	0805	16,050	40,985	top	104 nF
16	D1	1N5819	DO41	78,280	31,460	top	0,195 V
17	D2	1N5819	DO41	104,950	31,460	top	0,196 V
18	D3	1N5819	DO41	45,895	34,635	top	0,203 V
27	L1	100µH	07HCP	80,820	38,445	top	100 µH
28	L2	100µH	07HCP	107,490	38,445	top	101 µH
29	L3	100µH	07HCP	58,595	20,030	top	100,5 µH
25	K1	Bus-Connector	WANNENSTECKER-16-ST_HEBEL	33,830	21,935	top	-
19	IC1	MC34063A(DIL8)	DIL8	103,680	21,300	top	OK
20	IC2	MC34063A(DIL8)	DIL8	77,010	21,300	top	OK
24	IC6	MAX6675ISA	SO8_SOT96-1	11,605	39,080	top	-

Integration Procedures

- The Procedures for soldering are kept as close as possible to “ECSS-Q-ST-70-08C_6March2009_ Manual Soldering”.
- SMD parts are soldered with the hot air soldering system at 250°C
- Through-hole parts are soldered with the soldering iron.
  300°C for connectors, 1W resistors and Capacitors C1 and C3
  270°C for all other parts
- All soldered joints are checked with the USB Microscope

C.3.2 OBC

REMOS Integration Protocol

General

Assembly: **REMOS OBC**

Date: 24.-25.09.2010

Integrator: S. Schweikle

QA: R. Wuseni

Used Tools

- ESD certified cutter
- ESD wristband
- ESD gloves
- Bending tool
- Isopropanol
- Flux
- Cleaning utilities
- Spacers for soldering
- Solder (Non RoHS, contains Pb)
- Soldering paste (Non RoHS, contains Pb)
- Hot air soldering system with temperature regulation
- Soldering-iron with temperature regulation
- USB Microscope
- Laptop for Picture recording
- Tweezers set

- Multimeter with RCL measurement
- Solder sucker
- De-soldering cord

Details

Required Parts

Pos	Amount	Name	Value	Housing
1	1	C12	0,1µF	2,54X5,08_RM2,54
2	3	C3,C4,C5	0,1µF	0805
3	1	R8	0,56K	0805
4	1	D1	1N4148	DO35
5	1	R20	2,7k	0207
6	1	BAT1	3,6V	BATTERIE
7	3	R16,R17,R18	4,7K	0207
8	3	R1,R2,R3	4,7K	0805
9	3	R4,R5,R6	5,36K	0805
10	3	R10,R11,R12	8,5K	0207
11	1	R7	9,53K	0805
12	4	R9,R13,R14, R15	10K	0207
13	3	C7,C8,C9	10nF	2,54X5,08_RM2,54
14	1	C6	10nF	0805
15	2	C10,C11	10µF	0805
16	2	C1,C2	27pF	0805
17	1	IC4	AT45DB161	SOIC8
18	1	IC1	ATMEGA164	DIL40
19	1	K1	Bus Connector	WANNENSTECKER-16-ST_HEBEL
20	1	K4	CAMERA IF	1X06_BUCHSE
21	1	IC3	ISP521-4	DIL16
22	1	R19	KTY23-5	SOT23/3

23	1	IC5	LP2981	SOT23/5
24	1	IC6	M41T93	SO18
25	1	IC2	MAX488CPA	DIL8
26	1	K2	PROGR. IF	2X03_BUCHSE
27	1	Q1	QUARZ_20MHZ	HC49/U
28	1	K3	REXUS IF	1X09_BUCHSE

Part details

PCB Bottom View

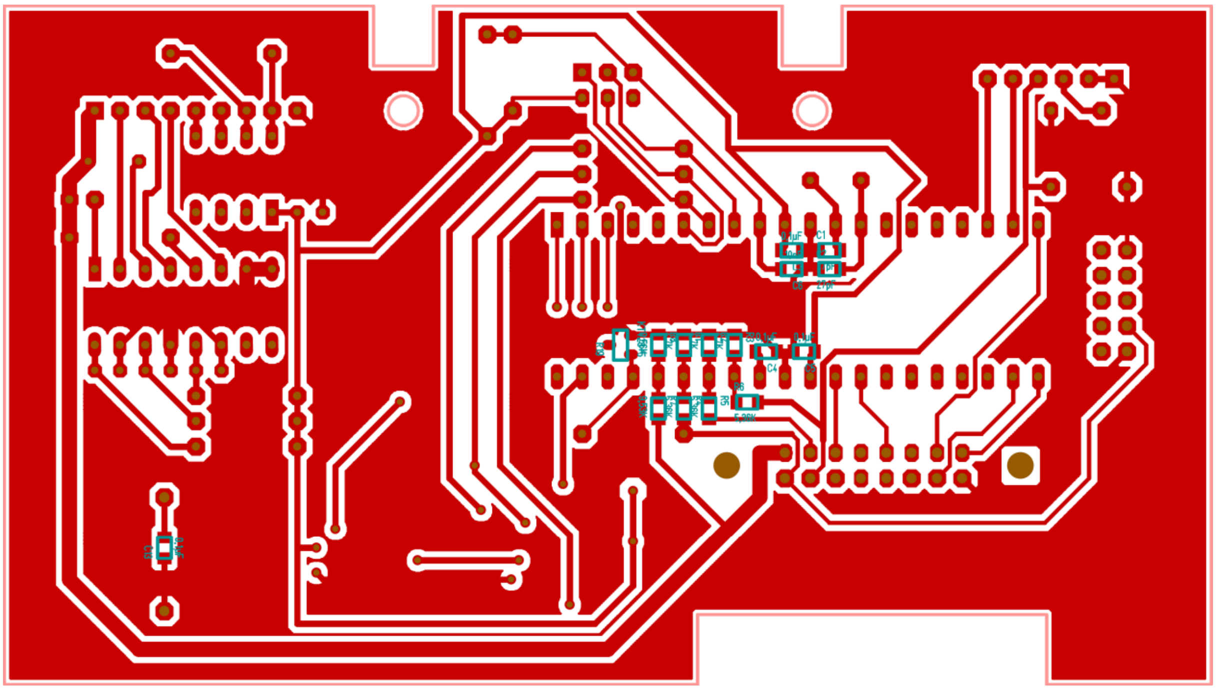

PCB Top View

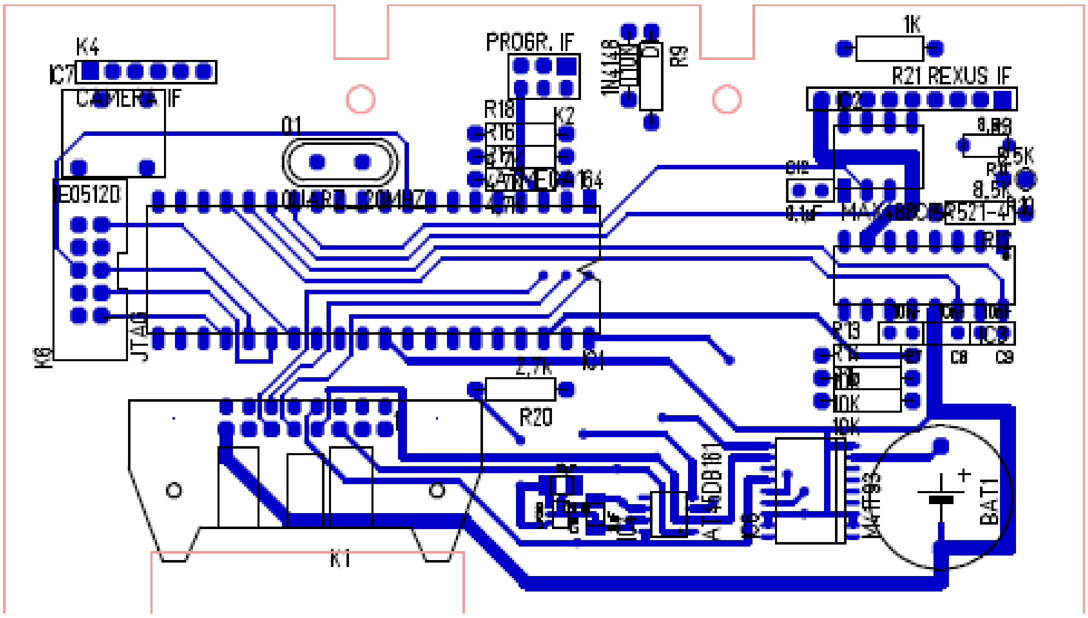

Integration

Positions and Verification of Parts

Nr.	Part	Nom. Value	Housing	X-Pos.	Y-Pos	Side	Measured Value
29	R1	4,7K	0805	52,88	34.000	bottom	4,69 kΩ
30	R2	4,7K	0805	50,34	34.000	bottom	4,69 kΩ
31	R3	4,7K	0805	47,8	34.000	bottom	4,69 kΩ
32	R4	5,36K	0805	52,88	27,65	bottom	5,35 kΩ
33	R5	5,36K	0805	50,34	27,65	bottom	5,34 kΩ
34	R6	10K	0805	46,53	28,285	bottom	9,97 kΩ
35	R7	9,76K	0805	55,42	27,65	bottom	9,69 kΩ
36	R8	0,56K	0805	55,42	34.000	bottom	0,56 kΩ
47	R19	KTY82-110	SOT23/3	59,23	34.000	bottom	0,99 kΩ @22°C
2	C1	27pF	0805	38,275	43,525	bottom	26pF
3	C2	27pF	0805	38,275	41,62	bottom	26pF

4	C3	0,1µF	0805	42,085	43,525	bottom	105,4 nF
5	C4	0,1µF	0805	44,625	33,365	bottom	99,4 nF
6	C5	0,1µF	0805	40,815	33,365	bottom	99,5 nF
7	C6	10nF	0805	42,085	41,62	bottom	9,1 nF
14	C13	0,1µF	0805	104,95	13,68	bottom	101,1 nF
37	R9	10K	0207	72,565	60,035	top	9,9 kΩ
38	R10	8,2K	0207_STEHEN D	113,205	48,605	top	8,17 kΩ
39	R11	8,2K	2,54X5,08_RM 5,08	110,03	52,415	top	8,14 kΩ
40	R12	8,2K	0207	109,395	44,795	top	8,12 kΩ
41	R13	8,2K	0207	96,695	28,92	top	8,14 kΩ
42	R14	8,2K	0207	96,695	26,38	top	8,14 kΩ
43	R15	8,2K	0207	96,695	23,84	top	8,15 kΩ
44	R16	4,7K	0207	57,96	51,145	top	4,67 kΩ
45	R17	4,7K	0207	57,96	48,605	top	4,67 kΩ
46	R18	4,7K	0207	57,96	53,685	top	4,68 kΩ
48	R20	2,7k	0207	57,96	25,11	top	2,69 kΩ
49	R21	1K	0207	99,235	63,21	top	1,01 kΩ
11	C10	10µF	1008	66,215	11,14	top	10,23 µF
12	C11	10µF	1008	62,405	14,315	top	10,34 µF
8	C7	10nF	2,54X5,08_RM 2,54	100,505	31,46	top	9,3 nF
9	C8	10nF	2,54X5,08_RM 2,54	105,585	31,46	top	9,4 nF
10	C9	10nF	2,54X5,08_RM 2,54	110,665	31,46	top	9,4 nF
13	C12	0,1µF	2,54X5,08_RM 2,54	90,345	47,335	top	95,0 nF
23	K1	Bus Connector	WANNENSTE CKER-16-ST_HEBEL	33,83	21,935	top	-
24	K2	PROGR. IF	2X03_BUCHSE	60,5	60,035	top	-

27	K6	JTAG	WANNENSTE CKER-10-ST	9,7	38,445	top	-
15	D1	1N4148	DO35	70,025	61,305	top	-
16	IC1	ATMEGA164	DIL40	41,45	38,445	top	0F4454-1-355C2A-1P1023 e³
17	IC2	MAX488CPA	DIL8	97,965	51,145	top	-
18	IC3	ISP521-4	DIL16	103,045	37,81	top	OK
19	IC4	AT45DB161	SOIC8	74,47	11,14	top	-
20	IC5	LP2981	SOT23/5	62,405	11,14	top	-
21	IC6	M41T93	SO18	90,345	13,709	top	-
22	IC7	IE0512D	NME2412D	12,24	53,685	top	Not required
28	Q1	QUARZ_20M HZ	HC49/U	37,64	50,51	top	-
1	BAT 1	3,3V	BATTERY	104,95	13,045	top	3,29 V

Integration Procedures

- The Procedures for soldering are kept as close as possible to "ECSS-Q-ST-70-08C_6March2009_ Manual Soldering".
- SMD parts are soldered with the hot air soldering system at 250°C
- Through-hole parts are soldered with the soldering iron.
  300°C for connectors
  270°C for all other parts
- All soldered joints are checked with the USB Microscope

C.3.3 CSENSE

REMOS Integration Protocol

General

Assembly: **REMOS C_SENSE**

Date: 21.09.2010

Integrator: S. Schweikle

QA: R. Wuseni

Used Tools

- ESD certified cutter
- ESD wristband
- ESD gloves
- Bending tool
- Isopropanol
- Flux
- Cleaning utilities
- Spacers for soldering
- Solder (Non RoHS, contains Pb)
- Soldering-iron with temperature regulation
- USB Microscope
- Laptop for Picture recording
- Tweezers set
- Multimeter with RCL measurement
- Solder sucker

- De-soldering cord

Details

Required Parts

Pos	Amount	Name	Value	Housing
1	8	C1,C2,C3,C4,C5,C6, C7,C8	0,01µF	2,54X5,08_RM2,54
2	6	C9,C10,C11,C12,C13 ,C14	0,1µF	2,54X5,08_RM2,54
3	4	IC1,IC4,IC5,IC6	TLC556CN	DIL14
4	1	IC2	74HCT138N	DIL16
5	1	IC3	74HC151	DIL16
6	1	K1	CONNECTO R	WANNENSTECKER-16-ST_HEBEL
7	1	K2	K1X08	1X08
8	1	K3	K1X01	1X01
9	4	R1,R3,R5,R7	1M	0207
10	4	R2,R4,R6,R8	1M	0207_STEHEND_MET

Part details

PCB Bottom View

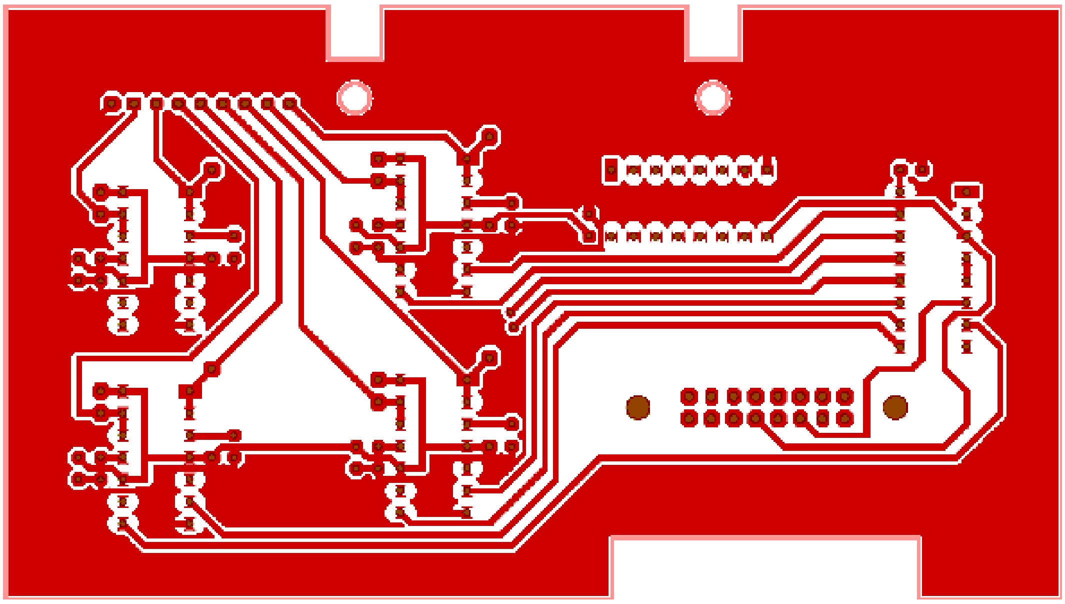

PCB Top View

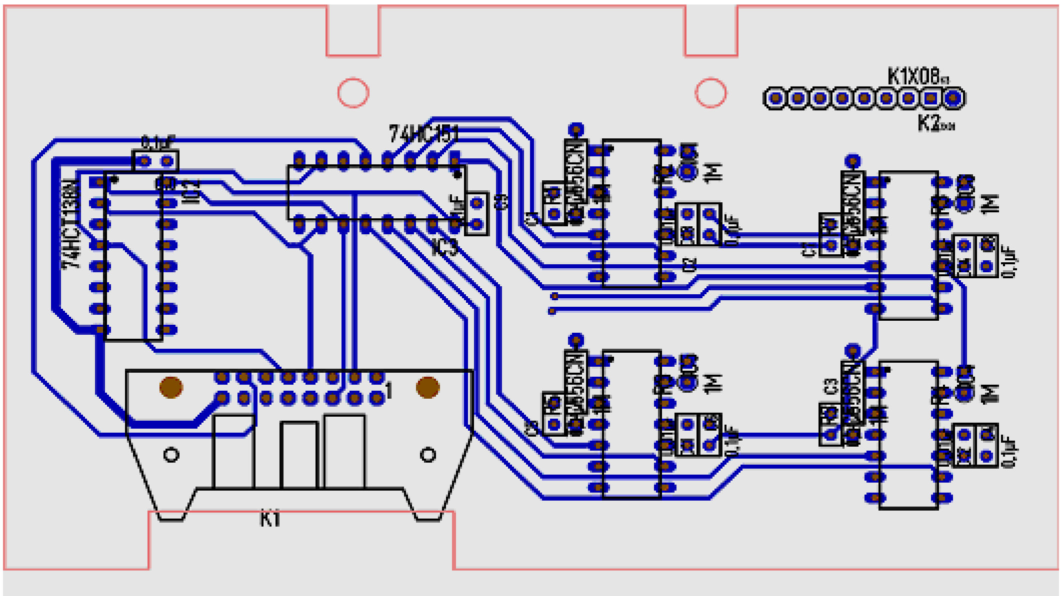

Integration

Positions and Verification of Parts

Nr.	Part	Nom. Value	Housing	X-Pos.	Y-Pos	Side	Measured Value
24	R1	1MΩ	0207	65,58	47,97	Top	0,999 MΩ
25	R2	1M	0207_STEHEND _MET	78,28	49,24	Top	0,999 MΩ
26	R3	1M	0207	97,33	21,3	Top	0,999 MΩ
27	R4	1M	0207_STEHEND _MET	110,03	22,57	Top	0,999 MΩ
28	R5	1M	0207	65,58	22,57	Top	0,999 MΩ
29	R6	1M	0207_STEHEND _MET	78,28	23,84	Top	0,999 MΩ
30	R7	1M	0207	97,33	44,16	Top	0,999 MΩ
31	R8	1M	0207_STEHEND _MET	110,03	45,43	Top	0,999 MΩ
1	C1	0,01µF	2,54X5,08_RM2,	63,04	44,16	Top	9,2 nF

			54				
2	C2	0,01µF	2,54X5,08_RM2,54	78,28	41,62	Top	9,7 nF
3	C3	0,01µF	2,54X5,08_RM2,54	94,79	17,49	Top	9,8 nF
4	C4	0,01µF	2,54X5,08_RM2,54	110,03	14,95	Top	9,7 nF
5	C5	0,01µF	2,54X5,08_RM2,54	63,04	18,76	Top	9,6 nF
6	C6	0,01µF	2,54X5,08_RM2,54	78,28	16,22	Top	9,7 nF
7	C7	0,01µF	2,54X5,08_RM2,54	94,79	40,35	Top	9,8 nF
8	C8	0,01µF	2,54X5,08_RM2,54	110,03	37,81	Top	9,8 nF
9	C9	0,1µF	2,54X5,08_RM2,54	54,15	42,89	Top	96,7 nF
10	C10	0,1µF	2,54X5,08_RM2,54	17,32	49,24	Top	97,4 nF
11	C11	0,1µF	2,54X5,08_RM2,54	80,82	16,22	Top	97,2 nF
12	C12	0,1µF	2,54X5,08_RM2,54	112,57	14,95	Top	97,4 nF
13	C13	0,1µF	2,54X5,08_RM2,54	80,82	41,62	Top	99,2 nF
14	C14	0,1µF	2,54X5,08_RM2,54	112,57	37,81	Top	95,2 nF
21	K1	CONNECTOR	WANNENSTECKER-16-ST_HEBEL	33,83	21,935	Top	-
15	IC1	TLC556CN	DIL14	71,93	42,89	Top	-
16	IC2	74HCT138N	DIL16	14,78	37,81	Top	-
17	IC3	74HC151	DIL16	42,72	45,43	Top	-
18	IC4	TLC556CN	DIL14	103,68	16,22	Top	-
19	IC5	TLC556CN	DIL14	71,93	17,49	Top	-
20	IC6	TLC556CN	DIL14	103,68	39,08	Top	-

Integration Procedures

- The Procedures for soldering are kept as close as possible to “ECSS-Q-ST-70-08C_6March2009_ Manual Soldering”.
- All parts are soldered with the soldering iron.
  300°C for the connectors
  270°C for all other parts
- All soldered joints are checked with the USB Microscope

C.3.4 RTSENSE

REMOS Integration Protocol

General

Assembly: **REMOS RTSENSE**
Date: 22.-23.09.2010
Integrator: S. Schweikle
QA: R. Wuseni

Used Tools

- ESD certified cutter
- ESD wristband
- ESD gloves
- Bending tool
- Isopropanol
- Flux
- Cleaning utilities
- Spacers for soldering
- Solder (Non RoHS, contains Pb)
- Soldering-iron with temperature regulation
- USB Microscope
- Laptop for Picture recording
- Tweezers set
- Multimeter with RCL measurement
- Solder sucker

- De-soldering cord

Details

Required Parts

Pos	Amount	Name	Value	Housing
1	8	R1,R2,R9,R10,R17,R18,R25,R26	1k24	R2
2	8	R5,R6,R11,R12,R19,R20,R27,R28	6k04	R1
3	8	R7,R8,R13,R14,R21,R22,R29,R30	42k2	R1
4	1	R34	100k	0207
5	8	R3,R4,R15,R16,R23,R24,R31,R32	100k	R1
6	7	C5,C6,C11,C12,C13,C14,C15	100nF	3X5R2,54
7	8	C1,C2,C3,C4,C7,C8,C9,C10	150pF	3X5R2,54
8	1	RN1	470K	SIL9
9	2	K4,K5	K1X01_BUCHSE	1X01_BUCHSE
10	2	K2,K3	K1X08	1X08
11	8	IC4,IC5,IC7,IC8,IC10,IC11,IC13,IC14	LM385Z-1.2	TO92
12	1	IC16	LM385Z-2.5	TO92
13	4	IC3,IC6,IC9,IC12	LT1014A	DIL14
14	2	IC2,IC15	MCP3208(DIL16)	DIL16
15	1	IC1	ULN2803	DIL18
16	1	K1	WANNENSTECKER-16-ST_HEBEL	WANNENSTECKER-16-ST_HEBEL

Part details

PCB Bottom View

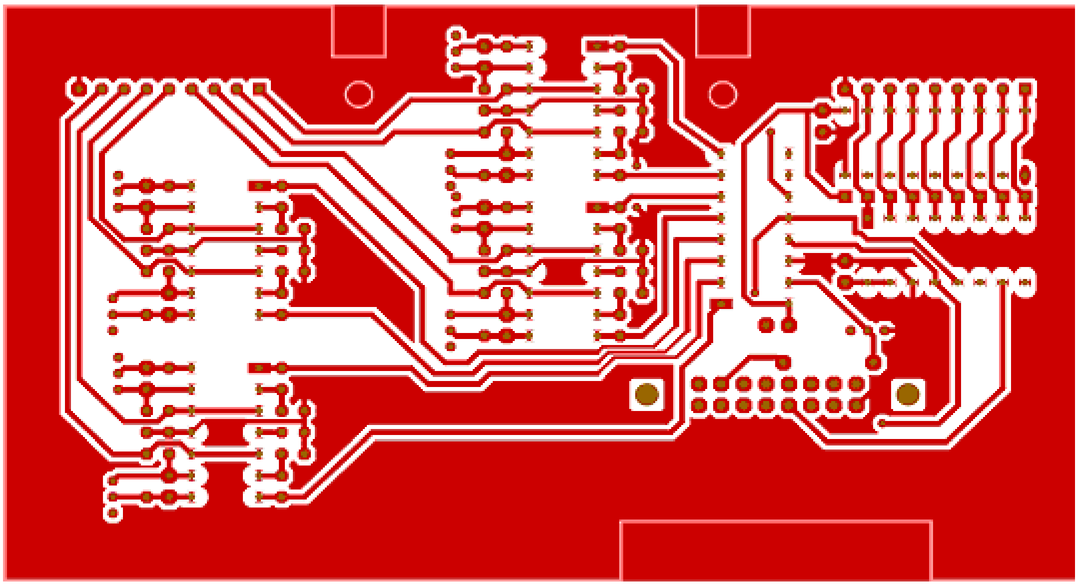

PCB Top View

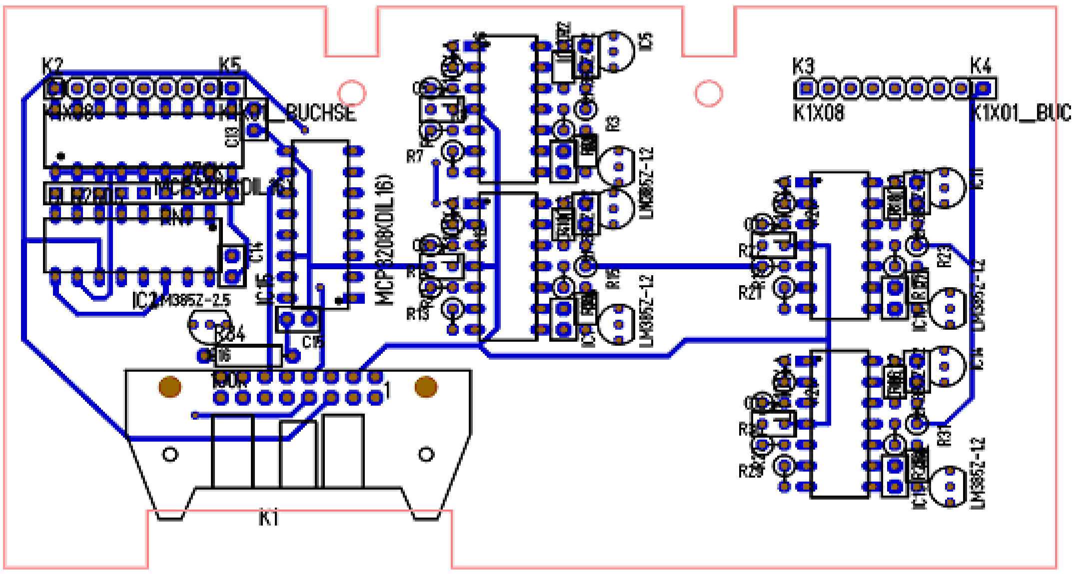

Integration

Positions and Verification of Parts

Nr.	Part	Nom. Value	Housing	X-Pos.	Y-Pos	Side	Measured Value
37	R1	1k24	R2	66,85	50,51	Top	1,24 kΩ
38	R2	1k24	R2	64,31	60,67	Top	1,24 kΩ
39	R3	10k	R1	66,85	56,86	Top	9,98 kΩ
40	R4	10k	R1	64,31	54,32	Top	9,98 kΩ
41	R5	42k2	R1	51,61	49,24	Top	42,2 kΩ
42	R6	42k2	R1	51,61	61,94	Top	42,2 kΩ
43	R7	6k04	R1	50,34	53,05	Top	6,04 kΩ
44	R8	6k04	R1	50,34	58,13	Top	6,04 kΩ
45	R9	1k24	R2	66,85	31,46	Top	1,24 kΩ
46	R10	1k24	R2	64,31	41,62	Top	1,24 kΩ
47	R11	42k2	R1	51,61	30,19	Top	42,2 kΩ
48	R12	42k2	R1	51,61	42,89	Top	42,2 kΩ
49	R13	6k04	R1	50,34	34.000	Top	6,04 kΩ
50	R14	6k04	R1	50,34	39,08	Top	6,04 kΩ
51	R15	10k	R1	66,85	37,81	Top	9,95 kΩ
52	R16	10k	R1	64,31	35,27	Top	9,94 kΩ
53	R17	1k24	R2	104,95	34.000	Top	1,24 kΩ
54	R18	1k24	R2	102,41	44,16	Top	1,24 kΩ
55	R19	42k2	R1	89,71	32,73	Top	42,2 kΩ
56	R20	42k2	R1	89,71	45,43	Top	42,2 kΩ

57	R21	6k04	R1	88,44	36,54	Top	6,04 kΩ
58	R22	6k04	R1	88,44	41,62	Top	6,04 kΩ
59	R23	10k	R1	104,95	40,35	Top	10 kΩ
60	R24	10k	R1	102,41	37,81	Top	9,95 kΩ
61	R25	1k24	R2	104,95	12,41	Top	1,24 kΩ
62	R26	1k24	R2	102,41	22,57	Top	1,24 kΩ
63	R27	42k2	R1	89,71	11,14	Top	42,2 kΩ
64	R28	42k2	R1	89,71	23,84	Top	42,2 kΩ
65	R29	6k04	R1	88,44	14,95	Top	6,04 kΩ
66	R30	6k04	R1	88,44	20,03	Top	6,04 kΩ
67	R31	10k	R1	104,95	18,76	Top	9,95 kΩ
68	R32	10k	R1	102,41	16,22	Top	9,98 kΩ
69	R34	100k	0207	28,115	25,745	Top	99,5 kΩ
70	RN1	100K	SIL9	16,05	45,43	Top	GND-1: 98,5 kΩ - 2: 99,5 kΩ - 3: 98,0 kΩ - 4: 98,6 kΩ - 5: 99,0 kΩ - 6: 98,9 kΩ - 7: 99,3 kΩ - 8: 99,2 kΩ
1	C1	150pF	3X5R2,54	64,31	49,24	Top	146 pF
2	C2	150pF	3X5R2,54	66,85	61,94	Top	141 pF
3	C3	150pF	3X5R2,54	64,31	30,19	Top	144 pF
4	C4	150pF	3X5R2,54	66,85	42,89	Top	141 pF
5	C5	100nF	3X5R2,54	50,34	55,59	Top	94,9 nF
6	C6	100nF	3X5R2,54	50,34	36,54	Top	97,9 nF
7	C7	150pF	3X5R2,54	102,41	32,73	Top	141 pF

8	C8	150pF	3X5R2,54	104,95	45,43	Top	141 pF
9	C9	150pF	3X5R2,54	102,41	11,14	Top	144 pF
10	C10	150pF	3X5R2,54	104,95	23,84	Top	142 pF
11	C11	100nF	3X5R2,54	88,44	39,08	Top	96,6 nF
12	C12	100nF	3X5R2,54	88,44	17,49	Top	95,8 nF
13	C13	100nF	3X5R2,54	28,75	54,32	Top	97,6 nF
14	C14	100nF	3X5R2,54	26,21	36,54	Top	98,3 nF
15	C15	100nF	3X5R2,54	33,83	30,19	Top	96,9 nF
32	K1	WANNENSTECKER-16-ST_HEBEL	WANNENSTECKER-16-ST_HEBEL	33,83	21,935	Top	-
16	IC1	ULN2803	DIL18	16,05	51,78	Top	-
17	IC2	MCP3208(DIL16)	DIL16	14,78	39,08	Top	-
18	IC3	LT1014A	DIL14	57,96	55,59	Top	-
19	IC4	LM385Z-1.2	TO92	70,66	48,605	Top	-
20	IC5	LM385Z-1.2	TO92	70,025	62,575	Top	-
21	IC6	LT1014A	DIL14	57,96	36,54	Top	-
22	IC7	LM385Z-1.2	TO92	70,66	29,555	Top	-
23	IC8	LM385Z-1.2	TO92	70,025	43,525	Top	-
24	IC9	LT1014A	DIL14	96,06	39,08	Top	-
25	IC10	LM385Z-1.2	TO92	108,76	31,46	Top	-
26	IC11	LM385Z-1.2	TO92	108,125	46,065	Top	-
27	IC12	LT1014A	DIL14	96,06	17,49	Top	-
28	IC13	LM385Z-1.2	TO92	108,76	9,87	Top	-
29	IC14	LM385Z-1.2	TO92	108,125	24,475	Top	-

30	IC15	MCP3208(DIL16)	DIL16	36,37	41,62	Top	-
31	IC16	LM385Z-2.5	TO92	23,67	29,555	Top	-

Integration Procedures

- The Procedures for soldering are kept as close as possible to “ECSS-Q-ST-70-08C_6March2009_ Manual Soldering”.
- All parts are soldered with the soldering iron.
  300°C for the connectors
  270°C for all other parts

All soldered joints are checked with the USB Microscope

Appendix D: Test Results

	REMOS Shaker Test	Page1 of13

REMOS Shaker Test

	REMOS Shaker Test	Page2 of13

Table of Content

1. Applicable Documents

- RX-REXUS_user_manual_V7_0-04Dec09.pdf [1]

2. General Overview

The REMOS Experiment is designed to fit into the nosecone section of the REXUS sounding rocket.

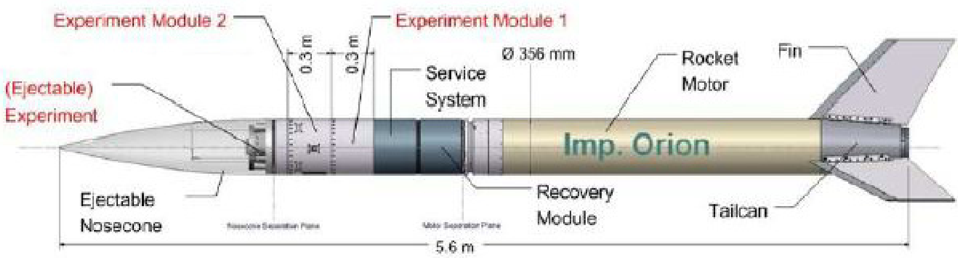

Figure 1: sections of REXUS rocket

3. Tested Object

The REMOS experiment is tested in flight-configuration.

3.1. Object Configuration

- Entire REMOS experiment,
- Including TV-camera
- System mounted on shaker adapter

The upper cover ring and the outer REXUS structure are not tested during this test.

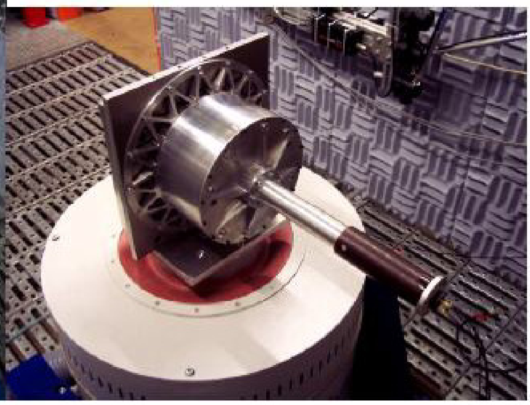

3.2. *Object Properties*

Property	Value	Unit	Comment
Experiment Diameter	328 / 60	mm	Taken from CAD
Experiment Height	452 / 136	mm	Taken from CAD
Experiment Mass	4.8	Kg	Taken from CAD
X/Y Adapter Mass	9.4	Kg	Taken from CAD
Z Adapter Mass	2.1	Kg	Taken from CAD

Table 1: REMOS Properties

4. Test Equipment

- DLR Shaker (DLR)
- HP Regulated Power Supply 50V 0.75A (REMOS)
- REMOS SM simulator (REMOS)
- RS232 null-modem cable (female-female with crossed signals) (REMOS)

- RS232 to USB converter (REMOS)
- USB cable extension (USB A male to USB A female) (REMOS)
- 2x 0.5m Cable with banana jacks (REMOS)
- 3 Acceleration sensors (DLR)
- Laptop with GSE Software (REMOS)
- REMOS shaker adapter (REMOS)

5. Test Setup

The shaker test shall be performed, as described in [1]. In each axis a random vibration shall be applied, while the experiment is operating.

5.1. Load levels

Axes	Frequency	Level	Remark
Longitudinal	(20-2000) Hz	6.0 g_{RMS}	0.018 g^2/Hz
Lateral	(20-2000) Hz	6.0 g_{RMS}	0.018 g^2/Hz

Table 2: Random loads

5-3: load levels

The load has to be applied for 60s at -12dB, -6dB and 0dB level

Sine search runs shall be done at 0.25 g level with a sweep rate of 4 octaves per minute

5.2. Sensors

- A 1D acceleration sensor has to be placed on the base plate of the shaker adapter as reference.
- A 3D-acceleration sensor should be placed on the top of the sensor boom

5.3. Test Timeline

1. Searchrun in x

2. Random in x
3. Random in y
4. Searchrun in z
5. Random in z

6. Test Results

6.1. Sine search run x

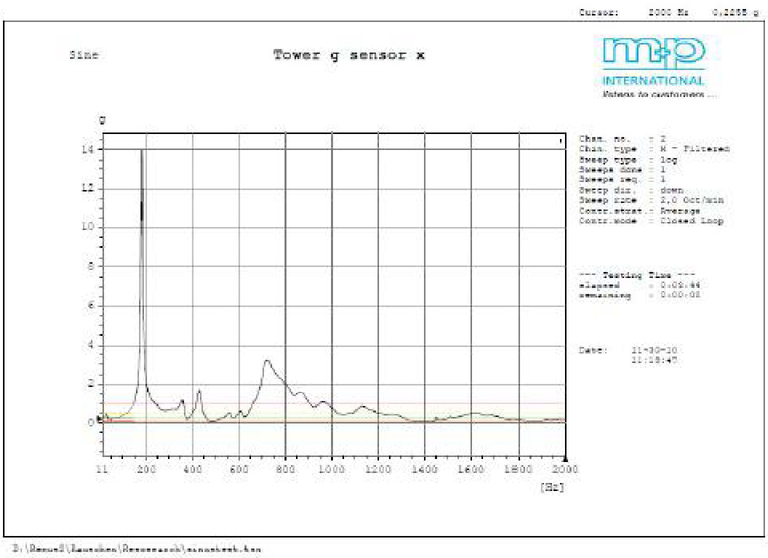

Figure 2: x Sine answer x

EuroLaunch
A DLR and SSC cooperation

	REMOS Shaker Test	Page**7** of**13**

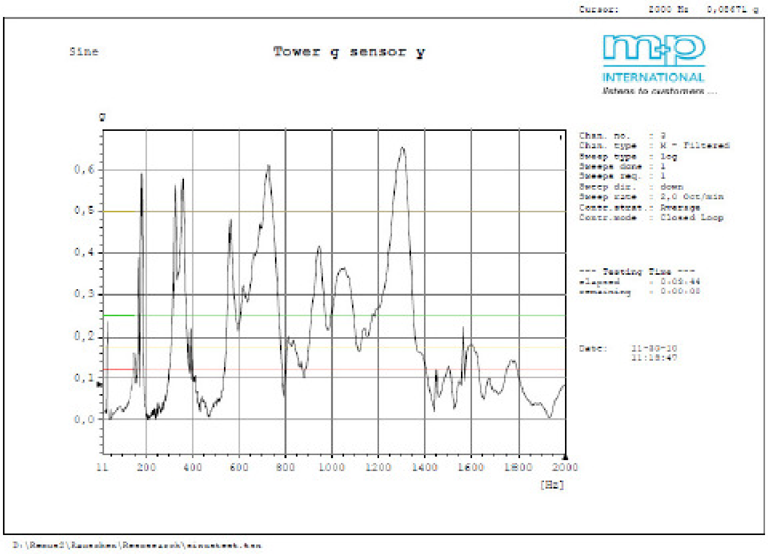

Figure 3: x Sine answer y

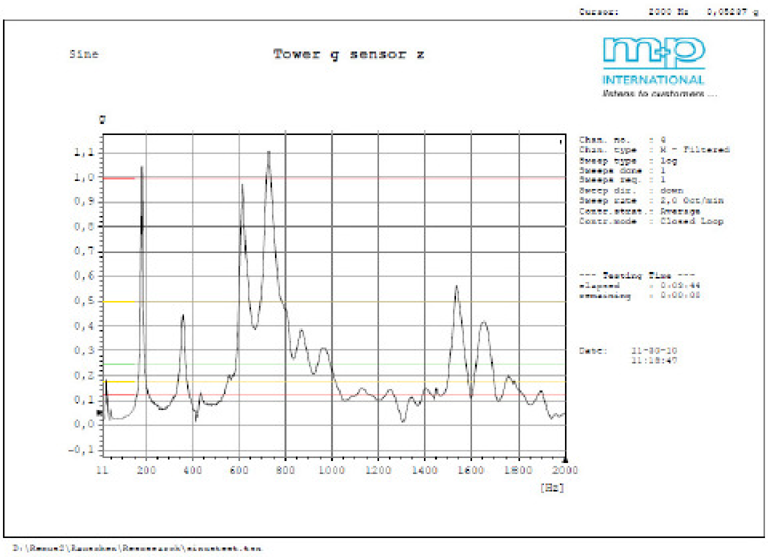

Figure 4: x Sine answer z

6.2. Random x

EUROLAUNCH
A DLR and SSC cooperation

	REMOS Shaker Test	Page8 of13

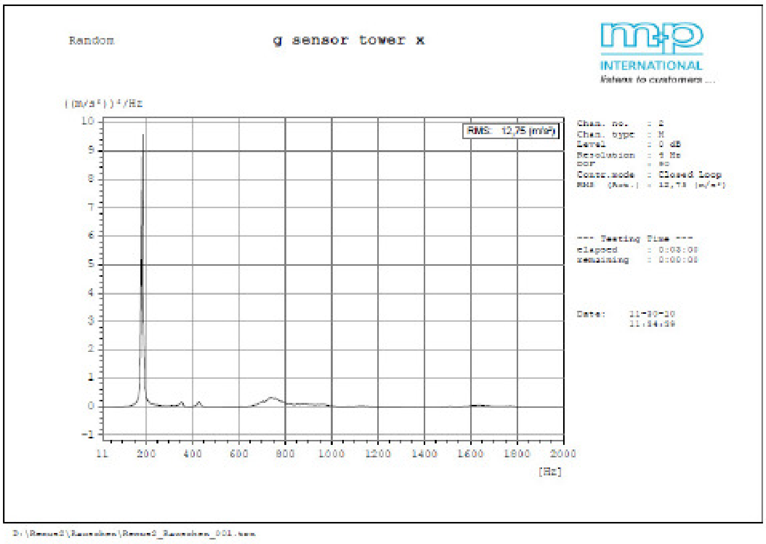

Figure 5: x Random answer x

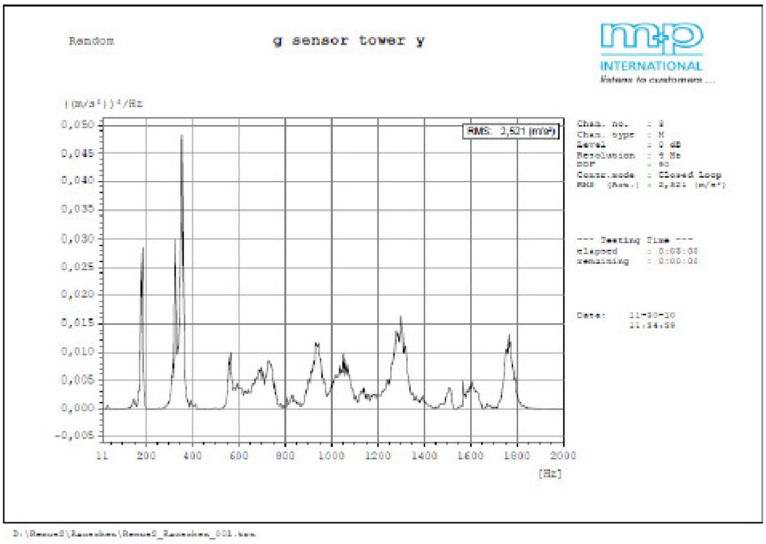

Figure 6: x Random answer y

	REMOS Shaker Test	Page**9** of**13**

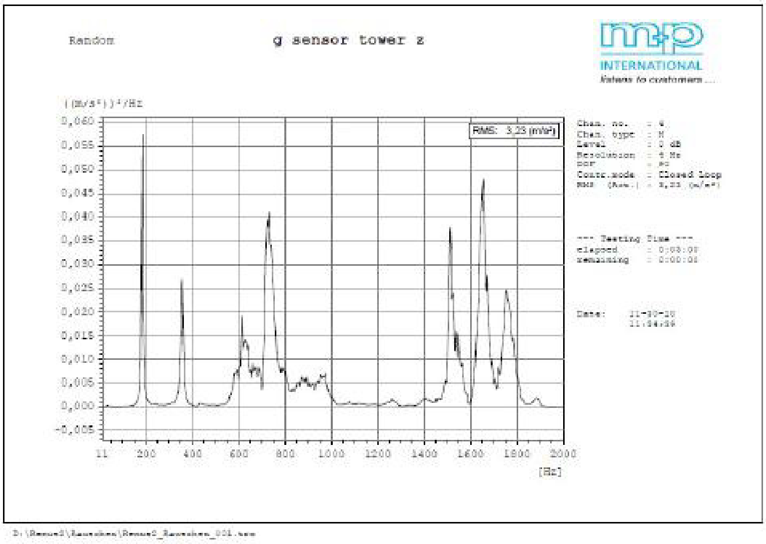

Figure 7: x Random answer z

6.3. Random y

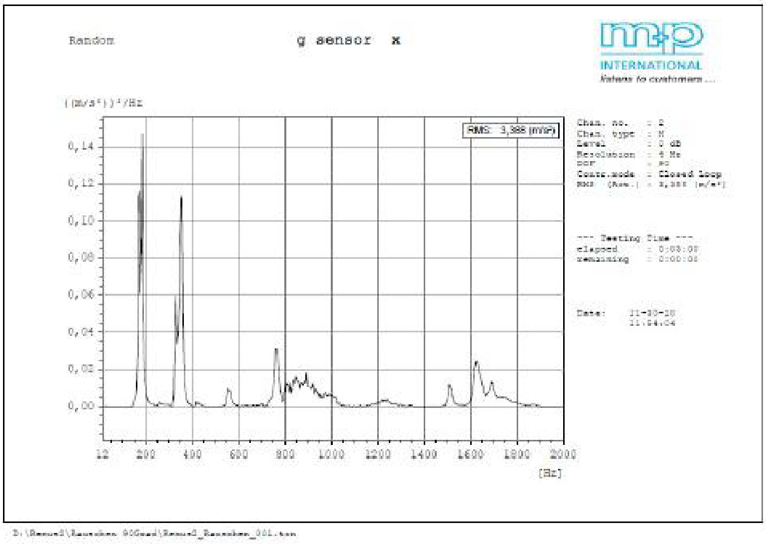

Figure 8: y Random answer x

	REMOS Shaker Test	Page**10** of**13**

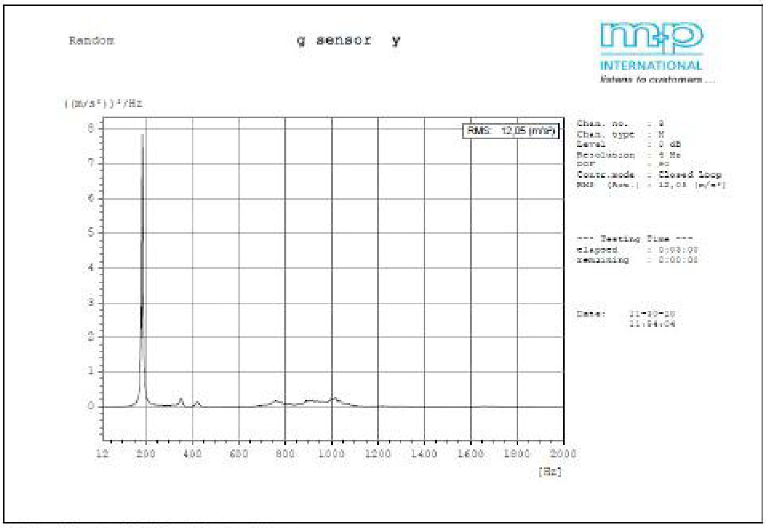

Figure 9: y Answer y

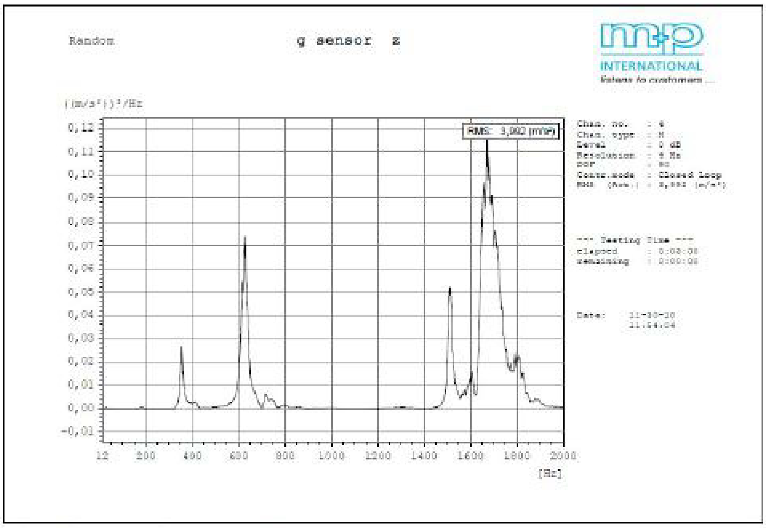

Figure 10: y Answer z

6.4. Sine search run z

	REMOS Shaker Test	Page11 of13

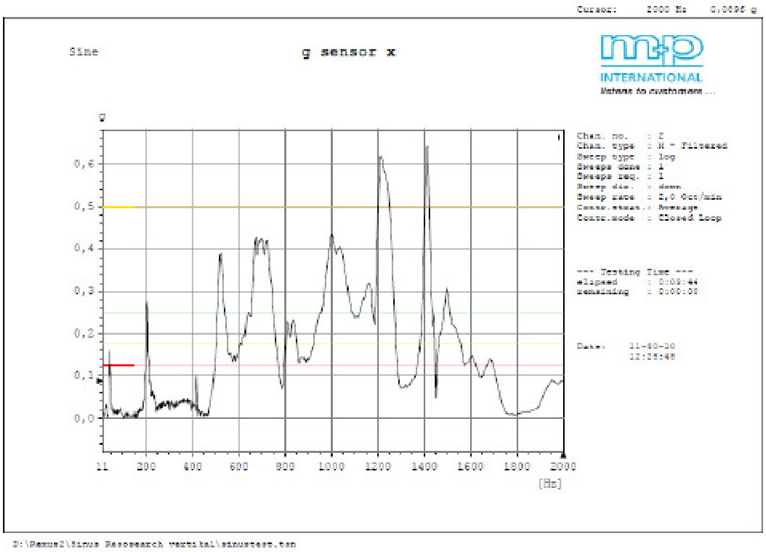

Figure 11: z Sine answer x

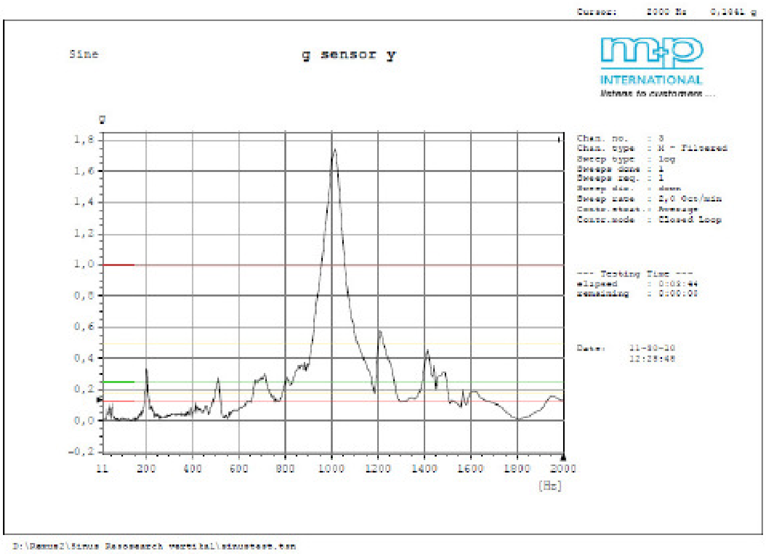

Figure 12: z Sine answer y

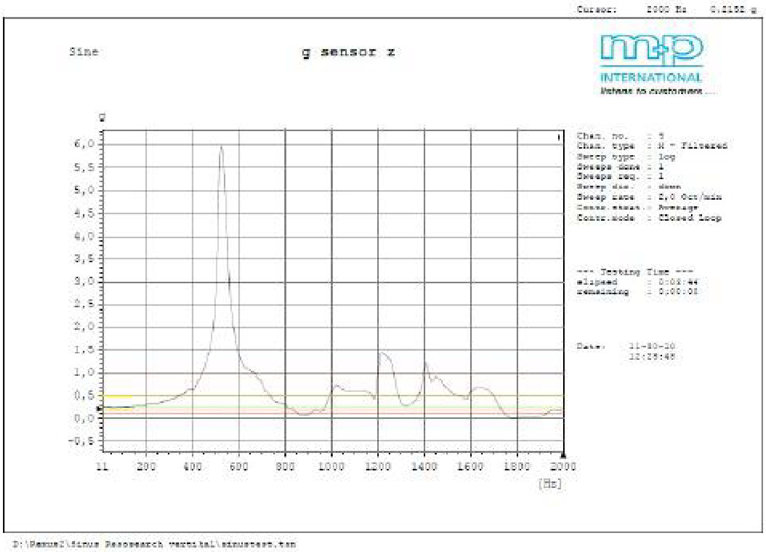

Figure 13: z Sine answer z

6.5. Random z

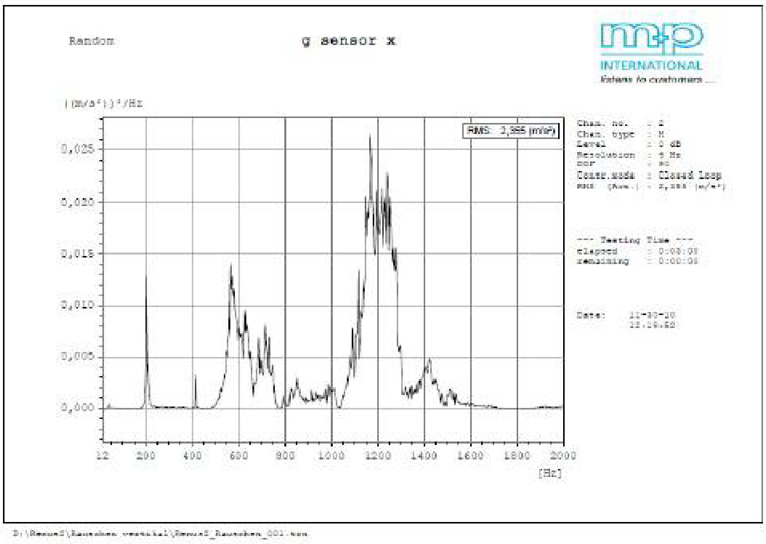

Figure 14: z Random answer x

	REMOS Shaker Test	Page13 of13

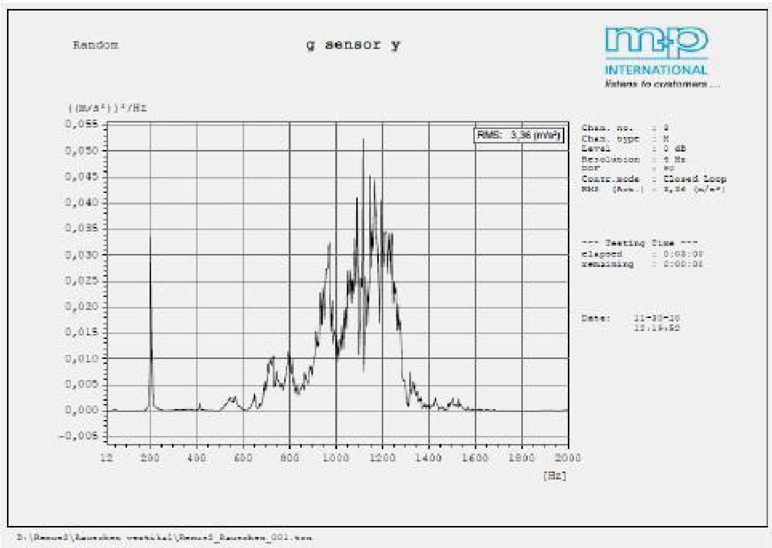

Figure 15: z Random answer y

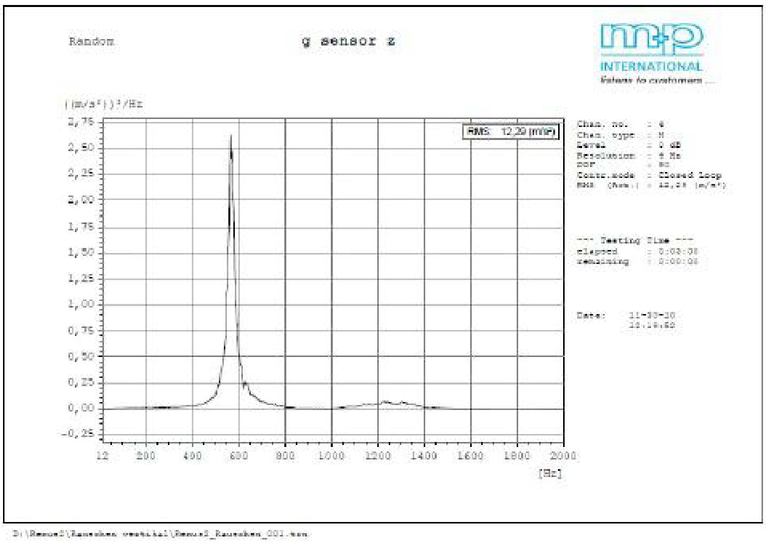

Figure 16: z Random answer z

	REMOS Thermal Vacuum Test	Page1 of7

REMOS Thermal Vacuum Test

	REMOS Thermal Vacuum Test	Page2 of7

Table of Content

1. Applicable Documents

- RX-REXUS_user_manual_V7_0-04Dec09.pdf [1]

2. General Overview

The REMOS Experiment is designed to fit onto nosecone section of the REXUS sounding rocket.

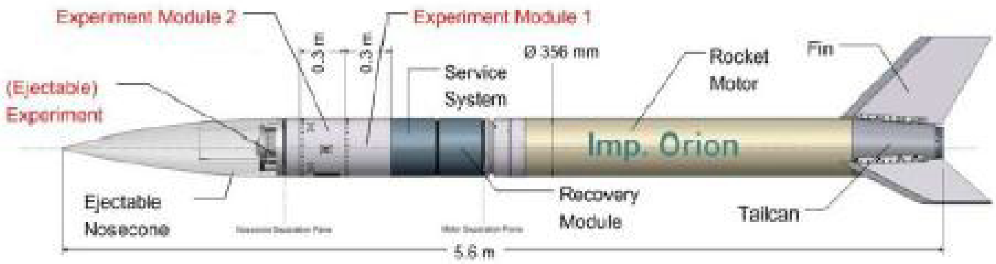

Picture 1: sections of REXUS rocket

3. Tested Object

The entire REMOS experiment is tested in flight-configuration.

3.1. Object Configuration

- REMOS experiment, including
- TV-camera
- REMOS is placed under a thermal insulation.

Picture 2: REMOS in thermal vacuum chamber (left: on interface plate; right: with thermal insulation)

3.2. *Object Properties*

Property	Value	Unit	Comment
Experiment Diameter	356 / 60	mm	Taken from CAD
Experiment Height	452 / 136	mm	Taken from CAD
Experiment Mass	8.380	Kg	Taken from CAD

4. Test Equipment

- IRS Thermal Vacuum chamber
- HP Regulated Power Supply 50V 0.75A
- REMOS SM simulator
- RS232 null-modem cable (female-female with crossed signals)
- RS232 to USB converter
- USB cable extension (USB A male to USB A female)
- 2x 0.5m Cable with banana jacks
- 3x Additional temperature sensors
- Laptop with GSE Software
- Feed through for vacuum chamber

5. Test Procedure

The Vacuum test and the thermal test, as described in [1], are combined in this test.

5.1. Additional Temperature sensors

The sensors shall be placed at the following locations:

1. Interface to cold/hot plate
2. On the voltage regulator for the cameras
3. On the one camera box /cylinder cover

5.2. Test Timeline

- Place experiment in chamber and connect to interface harness
- Evacuate chamber and set cold-plate temperature to -10°C.
- Wait for 24 h
- Evacuate to test conditions, as described in [1].
- Perform a 20min flight simulation
- Heat interface plate to +45°C
- Wait for 2 h.
- Check pressure.
- Perform a 20min flight simulation
- Re-pressurize with operational experiment (5min duration)

6. Test Results

- The experiment operated normal under all tested conditions
- The surrounding temperature could be measured by the experiment itself
- A maximum temperature of 95°C was measured during the hot case on the voltage regulator (max allowed: 125°C).

6.1. *Cold case*

Interface temperature: -10°C

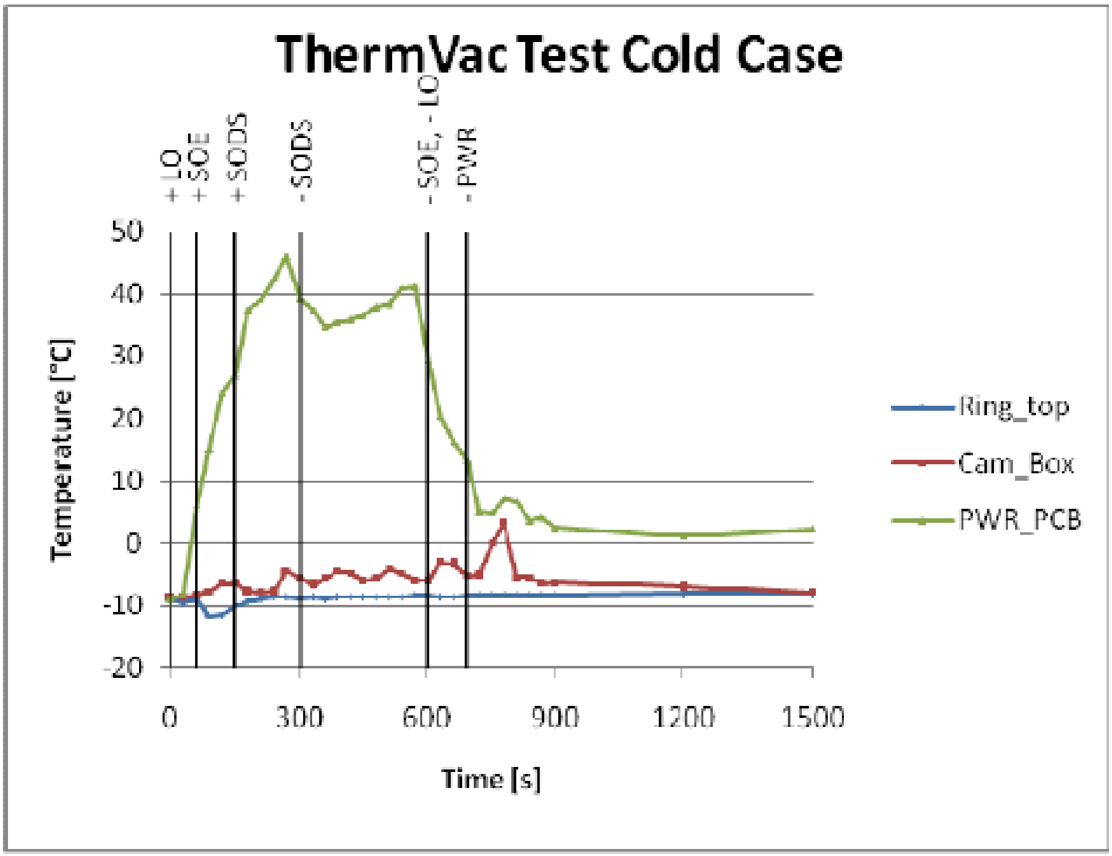

	REMOS Thermal Vacuum Test	Page**7** of**7**

6.2. Hot case

Interface temperature: +45°C

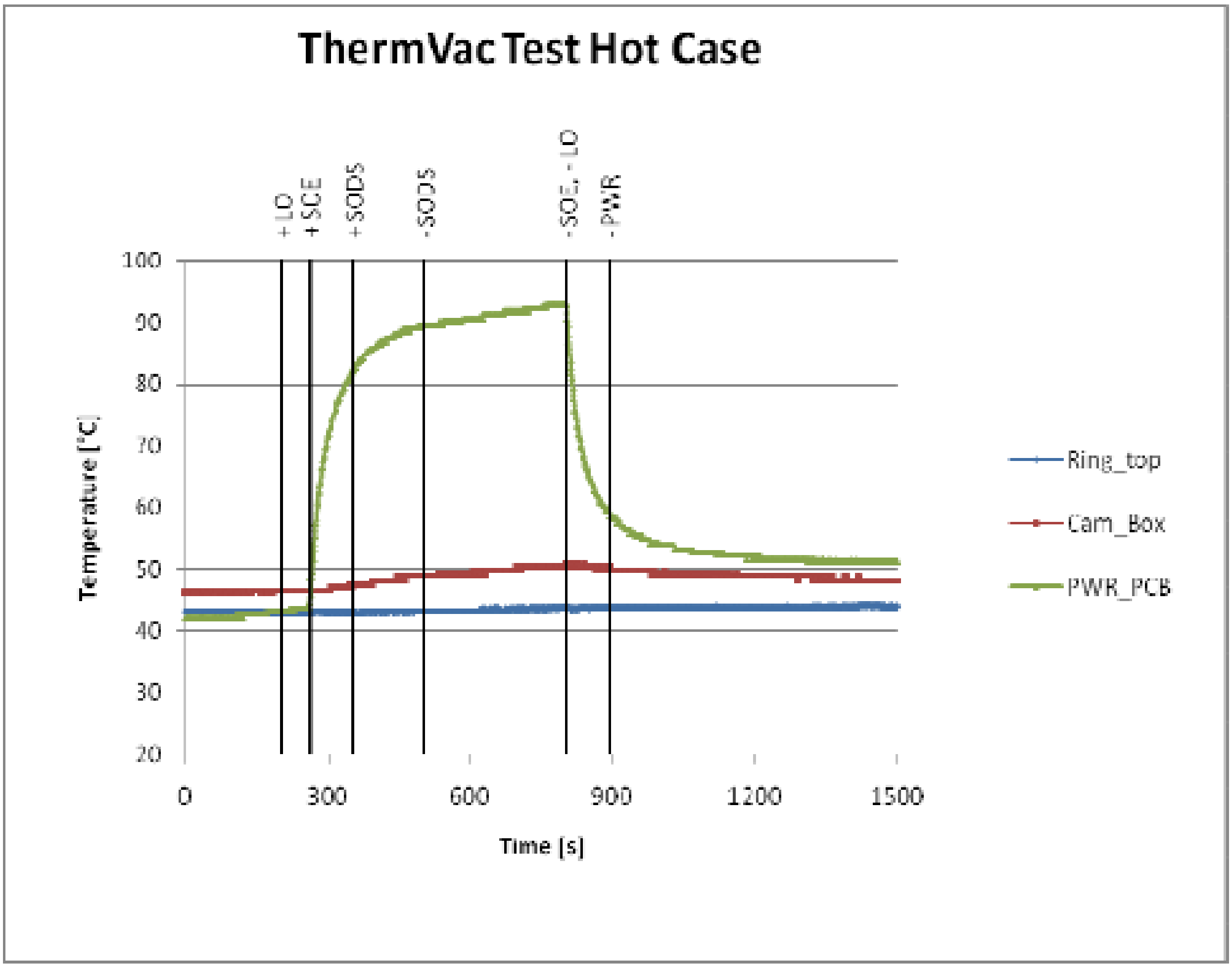

REMOS EMI Test

Table of Content

- # Applicable Documents

- RX-REXUS_user_manual_V7_0-04Dec09.pdf [1]

- # General Overview

The REMOS Experiment is designed to fit into the nosecone section of the REXUS sounding rocket.

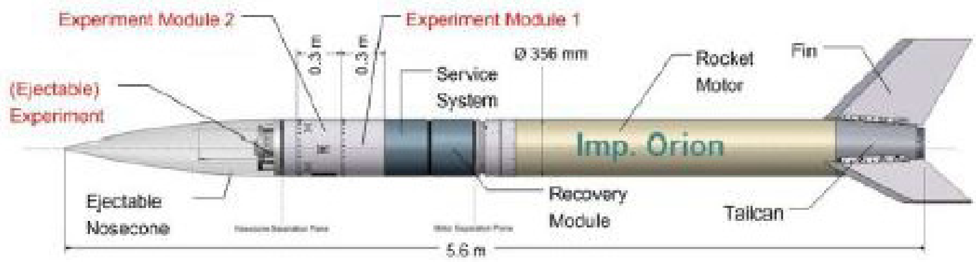

Figure 1: sections of REXUS rocket

- # Tested Object

The REMOS experiment is tested in flight-configuration.

Object Configuration

- Entire REMOS experiment,
- Including TV-camera

Object Properties

Property	Value	Unit	Comment

Experiment Diameter	328 / 60	mm	Taken from CAD
Experiment Height	452 / 136	mm	Taken from CAD
Experiment Mass	4.8	Kg	Taken from CAD

Table 0-1: REMOS Properties

Transmitters	Frequency [MHz]	RF Power [W]	Data type/rate	Polarization	Distance to REMOS [m]
REXUS Downlink	2292,5	5	500 kbit/s PCM	??	0,8
REXUS TV link 1	2338,1	10	8 MHz (BAS/Pal)	??	0,8
REXUS TV link 2	23xx,x	10	8 MHz (BAS/Pal)	??	0,8
Beacon 2 (Payl.)	240.80	0,2	1 KHz (AM)	??	0,8

Table 0-2: Transmitter Properites

- # Test Equipment

- IEH test chamber (DLR)
- HP Regulated Power Supply 50V 0.75A (REMOS)
- REMOS SM simulator (REMOS)
- RS232 null-modem cable (female-female with crossed signals) (REMOS)
- 2x 0.5m Cable with banana jacks (REMOS)
- Computer with GSE Software (REMOS)
- REMOS shaker adapter (REMOS)

Test Setup

- The experiment is placed in the test chamber in the chambers calibrated test position.
- The experiment is connected via the SM-Simulator to a Computer, on which the ground software is running.

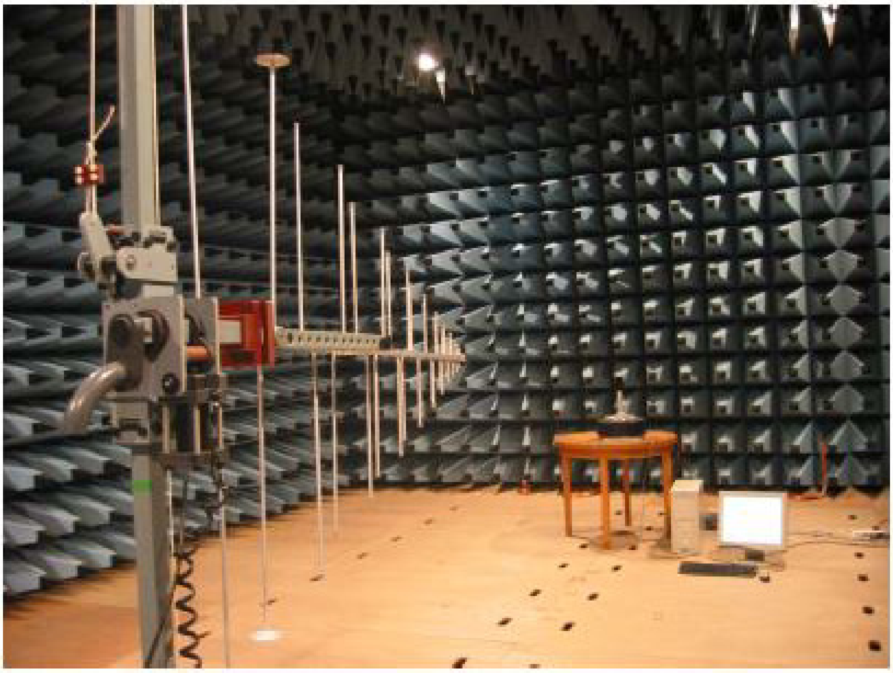

Test Timeline

- Test antenna is polarized horizontally
- REMOS is powered up and brought into RECORD-mode
- Chamber is closed
- Frequency sweep: 80V/m, 800kHz-1000MHz, 3s per step
- REMOS is powered down and recorded data is saved
- Test antenna is polarized vertically
- REMOS is powered up and brought into RECORD-mode
- Chamber is closed
- Frequency sweep: 80V/m, 800kHz-1000MHz, 3s per step
- REMOS is powered down and recorded data is saved

Test Results

Horizontal polarisation

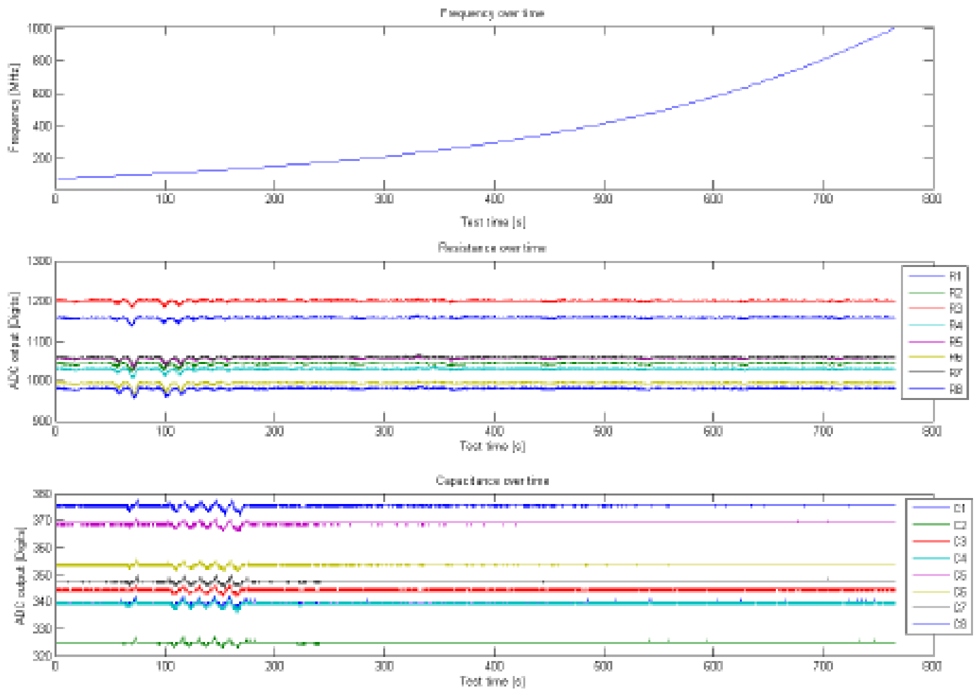

The maximum deviation is 2% at a frequency of 60MHz

Vertical polarization

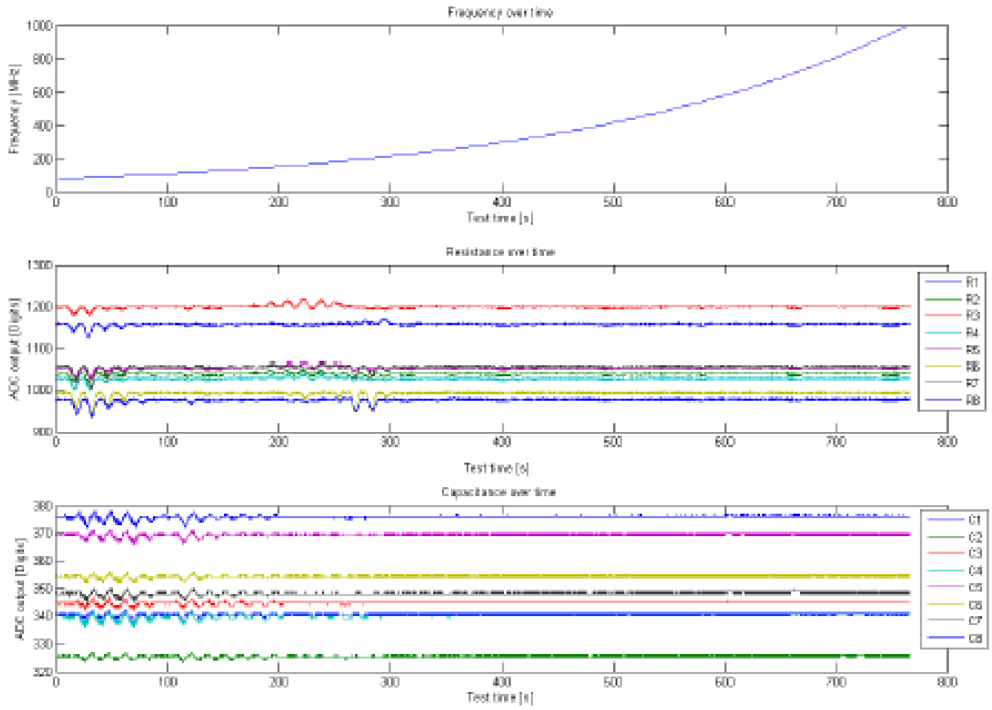

The maximum deviation is 2,5% at a frequency of 60MHz.